SHORT-TERM HYDROLOGICAL RESPONSES OF A FORESTED HILLSLOPE DURING RAINSTORMS, AT PANOLA MOUNTAIN RESEARCH WATERSHED, GEORGIA, USA

Elizabeth B. Ratcliffe

A dissertation submitted for the degree of Doctor of Philosophy
Department of Geography
University of Bristol

December 1996

DECLARATION

This dissertation is the result of my own work and includes nothing which is the outcome of work done in collaboration. It does not exceed the regulations on length and has not been submitted for a degree at any other university.

***Frontispiece**: View of Panola Mountain Research Watershed, Georgia, USA (Top plate)*
View of hillslope plot during growing season (Bottom plate)

DEDICATION

In memory of Mr Tom Stringer and Mr Harry Ratcliffe

And Noah he often said to his wife when he sat down to dine,
"I don't care where the water goes if it doesn't get into the wine"

G.K. Chesterton, 1774 - 1836

Short-term hydrological responses of a forested hillslope during rainstorms at Panola Mountain Research Watershed, Georgia, USA

by

Elizabeth Ratcliffe

A small-scale field experiment was conducted on a hillslope plot within the Georgia Piedmont, USA, with the aim of elucidating the hydrological processes which generate storm runoff and its chemistry. Intensive hydrometric and chemical sampling enabled the collection of detailed observations of hillslope processes during rainstorms. The passage of water was traced through a one-dimensional profile in the hillslope, where rainfall, throughfall, forest floor soil water, soil water at 15, 40, 50 and 70 cm depths, groundwaters and streamwaters were monitored, either manually or automatically. Chemical samples for each water type were also collected.

From analysis of hydrometric data, several hydrological flowpaths were detected that contribute water to storm runoff. Direct channel rainfall is operative in all storms, although its detection is difficult. Overland flow is in operation at some locations on the hillslope, specifically in topographic lows. Macropore and mesopore flow occurred and may lead to groundwater displacement. Groundwater ridging also occurred. Each flowpath was found to vary in its operation, according to a series of controls, namely seasonality, antecedent moisture conditions, rainfall magnitude, duration and intensity, and the timing between rainstorms.

Conservative tracers (chloride and temperature) were employed to investigate the contribution of 'old' and 'new' water to storm runoff. The variation in chloride concentrations in samples collected either sequentially or manually at each flowpath was monitored throughout storms. Rainfall, comprising 'new' water, was found to exhibit a distinct chloride chemistry. Most samples contained < 20 μeq/l Cl^-. A similar trend was observed for samples of throughfall and forest floor soil water. Groundwaters and matrix soil waters contained two to three times greater chloride concentrations than in the 'new' waters, due to evaporative mechanisms. Hence, 'new' water could be distinguished from 'old' water on the basis of chloride chemistry. Similarly, the temperature profile of 'new' and 'old' waters were significantly different. During the summer, rainfall ('new' water) is warmer than groundwater ('old' water), and during the winter, the reverse is true. Hence, both chloride and temperature were instrumental in distinguishing 'old' from 'new' waters.

Direct channel rainfall, overland flow and macropore flow were important flowpaths for the rapid transport of 'new' water through the system during the growing season. Overland flow contributed some 'old' water during the dormant season. Although macropore flow allowed rapid transit of 'new' water to depth, this led to a groundwater displacement mechanism, which ultimately led to the rapid contribution of 'old' water to storm runoff. The combination of hydrometric and tracer data enabled a conceptual hydrological model to be developed of the responses of the hillslope to storm events.

ACKNOWLEDGEMENTS

The work presented in this thesis was completed jointly in the course of a University of Bristol Studentship, supervised by Martyn Tranter; and a W.E.B.B. (Water, Energy and Biogeochemical Budgets) Research Proposal, funded by the Department of the Interior, USA, supervised by Jake Peters.

Data collection took place between January 1994 and May 1995 at Panola Mountain Research Watershed, Georgia, USA; with the financial support of the Water Resources Division, United States Geological Survey, Atlanta, Georgia and W.E.B.B. program. Financial support was also provided by the Department of Geography, University of Bristol.

Advice and assistance on field equipment construction and measurement procedures was provided by Jake Peters (at the Water Resources Division, U.S.G.S. and P.I. of the Panola Project). Assistance in the field was provided by Dana Booker and Tim Pojunas (then with the Panola Project). Chemical analysis of water samples was conducted at the Panola Project Laboratory, Water Resources Division, U.S.G.S, Atlanta, under the supervision of Ed Drake; also with the assistance of Dana Booker and Tim Pojunas, to whom additional gratitude is due to their encouragement and participation of Mexican lunches on fridays. Dissolved organic carbon analyses were performed courtesy of George Aitken (U.S.G.S., Colorado) and oxygen isotope analyses were performed courtesy of Caron Kendal (U.S.G.S., California).

Advice on field procedures and sources of literature was provided by Rosanna Cappellato (then in the Panola Project), who also played a fundamental role in introducing me to the U.S.G.S. and helping me adjust into living in Atlanta. Advice on data storage and manipulation and also assistance in the field was provided by Brent Aulenbach (Panola Project).

Support of Martyn Tranter (at the Department of Geography, University of Bristol) and Jake Peters has been vital to this investigation. Jake Peters provided the enthusiasm, knowledge and help in USA that was required for the study to succeed. He also encouraged a respect for baseball, basketball and Bass beer from an Englishwoman in Atlanta. Additional thanks to this wife, Gwendolyn and children, Jessie and Zak, for making me so welcome, especially in the first month in Atlanta and for their support throughout my study. Martyn Tranter provided continued enthusiasm and encouragement in my project when in Atlanta and in Bristol; and also a respect for English beer, although he did not manage to convert me into a 'Wolves' supporter. Martyn Tranter and Jake Peters read and commented on this thesis.

Thanks to Sue Brooks for enthusiasm in my work and especially for providing an opportunity to contribute to the 'Hillslope Processes' book.

Some less formal, but probably the most important support deserves recognition. I could never have wished for any more support than I have received from my parents, Laurence and Brenda Ratcliffe. They always provide the mental and financial support whenever and wherever I need it. I am deeply grateful to them.

CONTENTS

CHAPTER III: FIELD AND LABORATORY METHODS AND TECHNIQUES

CHAPTER IV: HYDROMETRIC ANALYSIS

APPENDIX

LIST OF FIGURES

CHAPTER VII: HYDROLOGICAL MODEL OF PMRW

LIST OF TABLES

List of Symbols

AT	Air Temperature (°C)
Atb	Area of tipping bucket (m^2)
C	Concentration (μeq/l)
DCR	Direct channel rainfall
DCR_{t1}	Total DCR contribution to storm runoff prior to time t1, where t1 refers to the time of onset of rise in discharge at the lower gage (m^3)
DCR_T	Total DCR for whole storm (m^3)
F	Total flow through tipping bucket (mm)
ff	Forest floor soil water
GQ	Groundwater quality sample
GT	Groundwater temperature (°C)
gt1	Timing at which maximum groundwater height is reached (hr min)
gto	Timing of the onset of groundwater response (hr min)
GW	Groundwater level measurement
GWb	Height of groundwater level during base flow conditions (m below land surface)
GWp	Peak height reached by groundwater (m below land surface)
GWres	Magnitude of groundwater rise (m)
GWt	Timing of groundwater response from the onset of rainfall (min)
H	Depth of zone within saturated zone containing interconnected air-filled pores (Todd, 1980) (m)
Δh	Water level rise by groundwater, caused by air compression effect (Todd, 1980) (m)
(H-m)	Depth by which air-filled pores are compressed by rainfall (Todd, 1980) (m)
i	Initial sample
I	Interception by canopy (mm)
$I_1(t)$	Infiltration of water into the soil matrix from soil surface (Germann, 1980)
$I_2(t)$	Infiltration of water into the soil matrix from the walls of macropores (Germann, 1980)
lg	lower gage streamwater monitoring site
Ma	Million years ago
MCPF	Macropore flow (mm)
n	initial sample (chemical data)
n	No. of tips of tipping bucket (hydrometric data)
O(t)	Overland flow (Germann, 1980)
OVLF	Overland flow (mm)
p	Probability factor associated with correlations and regressions
PE	Event rainfall (mm)

PI	Rainfall intensity (mm/min)
PMRP	Panola Mountain Research Project
PMRW	Panola Mountain Research Watershed
PPO	Rainfall total prior to response at specific node (mm)
PPT	Sequential rainfall (mm)
PPT1hr	Total rainfall in initial hour of storm (mm)
PPT_{tl}	Total rainfall prior to time t1 (mm)
PPT_T	Total rainfall for storm (mm)
P(t)	Total rainfall (Germann, 1980)
PPTTllg	Lag time between max. flow rate of rainfall and throughfall (min)
Pwk	Total rainfall in the week prior to the storm (mm)
Qg	Groundwater flow
Qt	Throughflow
r	Correlation coefficient
RG1	Rain gage
RG	Groundwater response rate (cm/min)
RT	Rate of flow through specific node (cm/min)
$S_1(t)$	Seepage into macropores at soil surface (Germann, 1980)
$S_2(t)$	Flow within macropores (Germann, 1980)
SF	Stemflow (mm)
SMS	Soil moisture status
SMSi	Initial soil moisture status, during base flow conditions
SMSp	Peak soil moisture status reached during storm
SMSran	Rise in soil moisture content
SMStn	Soil moisture content at time (tn), where 'tn' refers to time of passage of wetting front through a specific depth
ST	Streamwater temperature (°C)
SW	Streamwater
t	time (min)
TDR	Time domain reflectometry
TFT	Throughfall temperature (°C)
TI	Sequential throughfall (mm)
TIVI-15lg	Lag time between max. flow rate in throughfall and 15 cm soil water flow (min)
to	Timing of onset of rainfall (hr min)
Tot.	Cumulative total (mm)
tw_{15}	Rate of movement of wetting front from 0 to 15 cm depth (cm/min)
tw_{40}	Rate of movement of wetting front from 15 to 40 cm depth (cm/min)
tw_{50}	Rate of movement of wetting front from 15 to 50 cm depth (cm/min)

tw_{70}	Rate of movement of wetting front from 40 to 70 cm depth (cm/min)
ug	Upper gage streamwater monitoring site
V	Volume (m^3)
VI	Sequential soil water
VI-50VI-15lg	lag time between max. flow through 15 and 50 cm depths (min)
Vtb	Volume of tipping bucket (m^3)
VWM	Volume weighted mean concentration (μeq/l)
XSA	Cross-sectional area (m^2)
XSC	Cross-sectional area of channel (m^2)

Chapter I
INTRODUCTION AND LITERATURE REVIEW

I.1A Introduction

Storm response is greatly controlled by the hydrology of a watershed both during and between rainstorms (McDonnell,. 1990). Flowpaths followed by rainfall within a watershed are of interest to hydrologists in predicting the timing and magnitude of storm runoff, as well as estimating the chemical composition of lakes and streamwaters (Cosby *et al*, 1985; Woolhiser *et al*, 1985; Kennedy *et al*, 1986; Christophersen *et al*, 1990; Eshleman *et al*, 1993). Over the past 15 years, considerable progress has been made in defining the mechanism which generate storm flow in small catchments from the application of a variety of techniques (Mulholland, 1993). However, much controversy still exists as to which flowpaths and mechanisms are responsible for variations in source waters contributing to storm runoff (Pearce *et al*, 1986; Mulholland, 1993). Over the past two decades, changes have occurred in the approaches adopted in hillslope investigations. Source waters to storm runoff have been assessed using distributed computer models (Billet and Cressler, 1992; Robson *et al*, 1994; Kirchner, 1992), hydrograph separations (Fritz *et al*, 1976; Sklash and Farvolden, 1979; Hooper and Shoemaker, 1986; Pearce *et al*, 1986; Sklash *et al*, 1986), end-member mixing models (Dewalle *et al*, 1988; Hooper and Christophersen, 1990; Hooper *et al*, 1993;), tracer investigations (Shanley and Peters, 1988; Neal and Rosier, 1990; O'Brien *et al*, 1996) and small-scale field studies (Bishop *et al*, 1990; Mulholland *et al*, 1990; Mulholland *et al*, 1993; Jenkins *et al*, 1994). Each approach has problems associated with the assumptions that are made, and often results and conclusions are site-specific. Apparent contradiction in results has been generated within specific catchments when different approaches have been applied (Pilgrim *et al*, 1978; Mosley, 1982; Bishop *et al*, 1990; McDonnell *et al*, 1990). Hence, 'storm runoff generation still remains a controversial topic' (Pearce *et al*, 1986) and there is still considerable uncertainty about the flowpaths that water takes from the time it strikes the land surface until it appears as stream flow (Mulholland *et al*, 1993). One solution to these problems lies in the collection of detailed observations of hillslope processes during rainstorms. Despite the importance of appropriate field data, comprehensive datasets are still relatively scarce (Bishop *et al*, 1990; Wheater *et al*, 1991; Mulholland, 1993; Robinson *et al*, 1995).

I.1B Prediction of hydrological flowpaths

(I.1Ba) Computer modelling of hillslope processes

Computer modelling of hillslope hydrology has traditionally adopted a black-box approach, where chemical and hydrological data are combined to predict the responses of catchments. Data is input into the model to produce simulations of the hydrology of a catchment, but the processes in operation are not identified. Typical catchment simulation models are complex and are calibrated to reproduce observed trends in data by adjusting free coefficients in order for simulated results to match actual results closely (Kirchner, 1992; Robinson *et al*, 1995). Many models have been developed, which are often site and process-specific (Robinson *et al*, 1995). Examples of computer models include the Birkenes Model, which is a site-specific, concentration-discharge mode and considers the soil as a two-component system (Billet and Cressler, 1992). The ANSWERS (Areal Non-point Source Watershed Environmental ResponSe) model has been used to reproduce runoff events in forested catchments (Thomas and Beasley, 1986). The model changes several sub-processes; e.g. interflow components of seepage, pipe flow, infiltration, interception, surface storage, in order to reproduce actual runoff events accurately. TOPMODEL is a physically-based semi-distributed model developed for predicting and understanding rainfall-runoff mechanisms. The movement of water through the catchment is founded on a simple representation of physical processes (Robson *et al*, 1993). The RHESSys (Regional Hydroecological Simulation System) model combines a forest ecosystem process model (Running and Couglan, 1988) with TOPMODEL (Beven and Kirkby, 1979) to investigate the distributed feedbacks between ecological and hydrological processes at a watershed scale.

These models have been successful to a certain degree in modelling hillslope processes, but all have various inadequacies and problems in their application. Most of the models are developed with the characteristics of a specific catchment, and hence they cannot be applied successfully to all geographical locations without major recalibration (Robinson *et al*, 1995). A large number of assumptions are involved in their structures and hence a high degree of uncertainty is introduced into predictions (Kirchner, 1992). Until recently, models were becoming more complicated and were using more parameters in their structure, causing their validity became more difficult to test as more detailed data was required. The difficulties of determining water pathways and fluxes have made identification of the hydrological parameters in models problematic (Bishop *et al*, 1990). Although the Birkenes model uses a simple two reservoir approach to simulate the hydrology of the system (Billet and Cresslet, 1992), Hooper *et al* (1990) concluded that it needed to be simplified even further to model the system effectively. Recently, the simplification or omission of hydrological frameworks has become a trend in computer modelling (Cosby *et al*, 1985). Hence, further means are sought to elucidate the hydrological processes which generate runoff and its chemistry (Bishop *et al*, 1990), and one key to this is the development of comprehensive hydrological and chemical datasets from small-scale field investigations (Bishop *et al*, 1990; Mulholland, 1993; Jenkins *et al*, 1994).

(I.1Bb) Small-scale field investigations

There has been a shift from using computer simulations to using data from small-scale field investigations as the basis of hydrological models of hillslope responses during storms (Bishop *et al*, 1990; Mulholland *et al*, 1990; Mulholland, 1993; Jenkins *et al*, 1994). This approach allows a more thorough investigation of the flowpaths, and changes in hydrochemistry within those flowpaths, that contribute to storm runoff during rainstorms. Recently, several studies have been conducted involving intensive temporal and spatial sampling along selected flowpaths. For example, one of the most intensive sampling structures that have been employed in a study to date was at the Allt a Mharcaidh Catchment, Scotland (Jenkins *et al*, 1994). Rainfall, streamwater, groundwater and runoff flow rates were all monitored during storms. Chemical samples were also collected from each flowpath at intervals ranging from 20 min to 1 hr. High intensity temporal hydrometric sampling was combined with high intensity chemical sampling. At the Walker Branch Experimental Watershed, streamwater, soil waters and groundwaters were monitored at 15 to 30 min intervals and automatic chemical sampling of streamwaters occurred using ISCO collectors (Mulholland, 1993). At the Svartberget Forest Research Station, Sweden, water chemistry and hydraulic potentials were monitored along a 50 m hillslope transect, orientated parallel to the presumed flowpath of water. Zero-tension lysimeters, groundwater tubes and tensiometers were employed in a series of 'nests' at varying distances from the stream channel. They output data at 3 - 4 hr intervals (Bishop *et al*, 1990). Each of these approaches was successful in elucidating important flowpaths within each site.

Small-scale investigations provide insight into the links between different flowpaths, which assists in the elucidation of the hydrological processes which generate runoff (Bishop *et al*, 1990). Data collected does not contain the uncertainties that are associated with data output from computer models (Robinson *et al*, 1995). However, some problems do exist in the interpretation of data generated from field investigations. For example, at the Allt a Mharcaidh catchment, the interpretation of a relatively simple hydrological pattern was complicated by the chemical data, which implied that there were source waters to storm runoff that had not been hypothesised nor sampled (Jenkins *et al*, 1994). Wheater et al (1991) warn of the ambiguous interpretation of field data, where data may be limited or is influenced by heterogeneity of flow through the canopy or soil. In a small, apparently uniform hillslope near Stanford, California, ambiguous interpretation of field responses yielded a range of possible mechanisms to explain the observed trends (Pilgrim *et al*, 1978).

The interaction of source areas and flowpath processes in time and space forms the crux of process-orientated hydrochemical modelling. Hopefully, the problem of resolving these classes of process can be rendered more tractable in their study by isolating the output from a single reach. Chemical data can also help to constrain the hydrological system, which physical data alone is unable to do. Very few field investigations to date employ similar temporal resolutions in sampling of hydrometric and chemical data. To reduce the uncertainty concerning the flowpaths that water takes when it hits the land surface, a field investigation that samples hydrology and chemistry intensively is required.

Jenkins *et al* (1994) conclude that without such investigations ' it remains questionable if reliable process-based short-term predictive models of hydrochemistry are achievable'.

I.1C Prediction of chemical variations within hydrological flowpaths

(I.1Ca) Solute Investigations

Streamwater is comprised of a mixture of components that have followed different flowpaths (Hooper *et al*, 1990; Hooper and Christophersen, 1990; Christophersen *et al*, 1990). Changes in the composition of streamwater are determined by changes in the flowpaths and the concomitant changes in component water chemistry (Bishop *et al*, 1990; Mulholland *et al*, 1990; Shanley and Peters, 1993). Traditionally, modelling of streamwater chemistry during hydrological events has concentrated on 'new' and 'old' water contributions only (Sklash *et al*, 1986; McDonnell *et al*, 1990; Pearce *et al*, 1986). 'New' water is current rainfall and 'old' water is that which has been resident within the hillslope since the previous storm. Classical hydrograph separation adopts a two-component separation into 'old' and 'new' water, based on the equations representing conservation of the mass of water and a 'conservative' chemical species (e.g. Cl^- or $\delta^{18}O$) (Sklash and Farvolden, 1979; McDonnell *et al*, 1990; Maule and Stein, 1990). More recently, three-component mixing-models have been developed, in which a soil-water component is added to explain chemical variations in streamwater chemistry (Dewalle and Sharp, 1988; Hooper *et al*, 1990). These approaches model the streamwater chemistry quite well, but ambiguities can be introduced into the interpretation of their results, since only two or three flowpaths (i.e. rainfall, soil water and groundwater) are monitored. Intensive field investigations (Mulholland, 1993; Jenkins *et al*, 1994) have shown that the hillslope is more complicated that this somewhat simplistic view. Hewlett (1982) proposed that *"No graphical or mathematical operation performed on a hydrograph will reveal the source or pathway of streamflow"*.

Approaches similar to those outlined above have lead to apparent contradictions in hydrological evaluations of the same site. For example, studies using $\delta^{18}O$, Cl^- and Si suggest that streamflow at the M8 catchment, New Zealand, can be generated primarily from water in the soil prior to the event, which is displaced by rainfall by way of a piston-like mechanism (Sklash and Farvolden, 1986; Kennedy *et al*, 1986; Dewalle *et al*, 1988), whereas, studies using hydrometric data and dye tracing techniques suggest that streamflow can be generated by the rapid passage of water through the soil via natural pipes (Mosley, 1979; 1982; Wilson and Smart, 1984). More recent studies which monitor the chemistry and hydrology of all flowpaths within the system have reconciled the apparent contradiction in these investigations (McDonnell, 1990; Luxmoore *et al*, 1993), since the combinations of both types of data allows a more complete insight into dominant hydrological mechanisms. Hence, hydrograph separation and mixing model techniques potentially generate inaccurate results since only a small proportion of all flowpaths are considered.

Another problem in their application results from assumptions in their structure. As rainfall passes through the hillslope, there are many possible processes that might affect the water chemistry en route (Best and Monk, 1975; Cryer, 1986; Ryan *et al*, 1989; Lindberg *et al*, 1990; Probst *et al*, 1992). For

example, in the canopy, leaching and washoff may occur (Peters and Driscoll, 1991; Lindberg *et al*, 1990) and adsorption reactions may occur in the soil (Mulholland *et al*, 1990; Van Genuchten, 1991; Jenkins *et al*, 1994; Huntington *et al*, 1994). The extent and magnitude of these and similar reactions are likely to vary throughout the storm, as solute sources are exhausted and new hydrological flowpaths become operative (Martinec, 1974; Bishop *et al*, 1990; Hooper and Christophersen, 1990; Maule and Stein, 1990; Mulholland, 1993). The major assumption of some hydrograph separations and end-member mixing analyses is that the chemistries of end-members are invariant in time and space (Hooper *et al*, 1990). Hence, the predictions made from these approaches contain inaccuracies. The transient nature of reactions and flow routing have thus been acknowledged in the literature (Wigington *et al*, 1990; Jenkins *et al*, 1994), but have received little investigation to date. A possible solution to these problems could be achieved by monitoring the chemistry of all flowpaths throughout storms. To achieve the desired resolution of temporal and spatial sampling, this would necessitate that the studies were small-scale. Also, use of conservative tracers and solutes such as Cl^- and Si may be preferable to using other solutes as tracers of water movement, since they show minimal variation in content with respect to storm duration

(1.31Cb) Tracer Investigations

Hydrochemical tracers are ubiquitous and exhibit differential behaviour during hydrological processes (Barnes and Allison, 1988). Their advantage as tracers lie in the fact that they do not modify the characteristics of the media in which they are transported (Bonta and Rao, 1994). Their use is based on the premise that 'new' water (i.e. rainfall) and 'old' water (i.e. groundwater) have distinct signatures (Dincer *et al*, 1970; Martinec *et al*, 1974; Fritz *et al*, 1976; Shanley and Peters, 1988; Leaney *et al*, 1993). Stable isotopes ($\delta^{18}O$ and $\delta^{2}H$) are frequently used in flowpath identification studies (Pearce *et al*, 1986) and chloride has also been used widely as a water tracer (Johnston, 1989; Rasher *et al*, 1987; Williamson *et al*, 1987; Peters and Driscoll. 1989; Roth *et al*, 1991; Leaney *et al*, 1993). Cl^- has been used as a water tracer during rainstorms in many studies (Neal *et al*, 1990; Leaney *et al*, 1993) and also in the identification of source waters to streamwater (Rasher et al, 1987).

Temperature has been used as a tracer of water movement in the unsaturated and saturated zone (Stallman, 1960; Bredehoeft and Popodopulus, 1965; Sorey, 1970; Andrews and Andrews, 1979; Shanley and Peters, 1988; Arai, 1993; Sinokrot and Stefan, 1993). Temperature has been used a tracer of source waters to storm runoff (Shanley and Peters, 1993), however, its use is limited in the monitoring of short-term mechanisms in the unsaturated and saturated zone. Previous investigations have acknowledged the contrast in the temperature of 'old' and 'new' waters (Arai, 1993; Sinokrot and Stefan, 1993) and hence, it is postulated that temperature may be useful in the tracing of 'new' water through the hillslope during rainstorms.

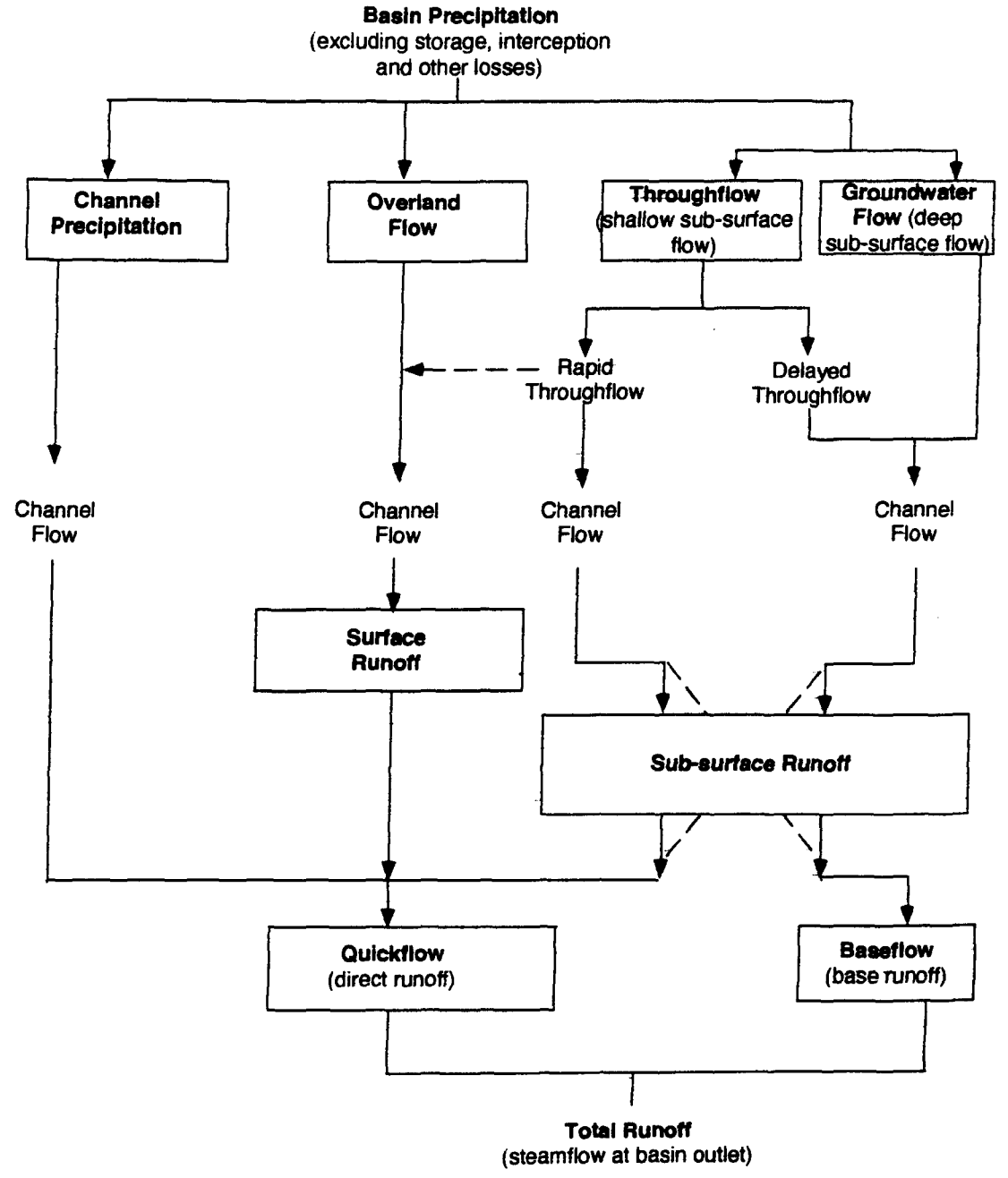

***Figure 1.1**: Diagrammatic representation of the runoff process (after Ward, 1989)*

(I.1D) Hillslope Flowpaths: Previous studies

Current thinking in hillslope hydrology is well described by Ward (1989). Figure 1.1 summarises the most important routes that contribute to storm runoff. The four most dominant routes that water can take once entering the catchment are channel rainfall (Rawitz *et al*, 1970; Shanley and Peters, 1988), overland flow (Horton, 1933; Hewlett and Hibbert, 1967; Kirkby and Chorley, 1967; Eshleman *et al*, 1993), throughflow (interflow) (Rode, 1969; Mosley, 1979, 1982; Beven and Germann, 1982; Kennedy *et al*, 1986; Huntington et al, 1994) and groundwater flow (Todd, 1980; Sklash *et al*, 1986; McDonnell, 1990). Channel rainfall, overland flow and rapid sub-surface flow can all contribute 'new' water to total runoff, whereas delayed sub-surface flow and groundwater flow can contribute 'old' water. Many studies have been conducted into assessing flow and chemistry of the flowpaths discussed above. However, some flowpaths still prove to be 'grey' areas in hillslope hydrology in terms of determination of rates of flow, the proportion of 'old' vs. 'new' water and the controls on flowpath operation. A brief overview is provided of the operation of each flowpath, the type of water contributed to storm flow via that flowpath and examples of previous investigations in which each flowpath was assessed.

(I.1Da) Channel rainfall

Direct channel rainfall is that proportion of water that falls onto the stream channel; hence the process excludes storage or interception by the canopy (Ward, 1989). This is a route by which 'new' water can contribute to storm runoff. The contribution of water via this mechanism is typically considered to be low, but the amount varies according to storm magnitude and intensity (Shanley and Peters, 1988). In high magnitude and high intensity rainstorms, a high proportion of storm magnitude might be derived from this mechanism (Rawitz *et al*, 1970).

(I.1Db) Overland Flow

Several forms of overland flow have been documented, all of which describe the routing of water over the land surface. Horton (1933) proposed that a constant value of infiltration capacity of soil is attained throughout a watershed. If rainfall falls at a more rapid rate than the soil can absorb, and surface runoff results. If Hortonian overland flow occurs, then the water contributed to storm runoff will be 'new'. Since Hortonian overland flow assumes a constant infiltration capacity throughout a catchment, it was suggested to be a widespread phenomenon. However, recent investigations have found that Hortonian overland flow is generally limited in its spatial extent (Wheater *et al*, 1991; Eshleman et al, 1993).

The variable source area concept of overland flow was developed by Hewlett (1982). The assumption is made that infiltration is seldom a limiting factor and that only under special conditions does rainfall intensity exceed infiltration capacity. Variable source areas become quickly saturated (e.g. lower valley sides and intermittent channels). Thus, variable source area overland flow is not widespread,

but tends to be site specific in its operation. This form of overland flow will also deliver 'new' water to storm runoff.

Saturation overland flow (Kirkby and Chorley, 1967; Betson and Marius, 1969; Eshleman *et al*, 1993; Bonta and Rao, 1994) differs from the other forms markedly, in that it can contribute 'old' water to storm runoff. The mechanism typically results from rainfall of low intensity and long duration (Eshleman et al, 1993). This mechanism has also been observed where saturated flow converges due to undulations in bedrock topography. When the soil becomes saturated and the rainfall intensity is greater than the increase in throughflow across a section of the hillslope, then the excess rainfall can not enter the soil, but must flow over the surface (Eshleman *et al*, 1993). Throughflow that intercepts the soil surface flows over the land surface, and hence the return flow of 'old' water may be incorporated in overland flow. Hence, saturation overland flow can contribute a mixture of 'old' and 'new' water. The areas of saturation expands and contracts both seasonally and during events (Hewlett and Hibbert, 1967; Betson and Marius, 1969). Few studies exist that have attempted to quantify the amount of 'new' and 'old' water in overland flow.

(I.1Dc) Throughflow

Throughflow is shallow sub-surface flow in the unsaturated zone and is divided into two components, 'rapid throughflow (otherwise known as macropore flow (Mosely, 1979, 1982; Beven and Germann, 1982; Leaney *et al*, 1994)) and delayed flow (otherwise known as matrix flow, Beven and Germann, 1982). Macropore flow and matrix flow can occur in either lateral or vertical directions (Whipkey, 1969; Kirkby and Chorley, 1969; Beven and Germann, 1982; Nielsen *et al*, 1986; McLord and Stephens, 1987; Valocchi, 1990; Van Genuchten, 1991). Lateral flow tends to occur where the lateral hydraulic conductivity in the surface horizons of the soil is substantially greater than the overall vertical conductivity through the soil profile (Mulholland et al, 1990)

(i) Matrix flow (or delayed throughflow)

Flow in the soil matrix is subject to the forces of gravity and capillarity. Flow is considered to be conventional Darcy-based unsaturated flow. Water in the matrix is able to move in all directions due to capillary action (Beven and Germann, 1982). Matrix soil water moves slowly through a large pore-volume and has a long residence time, in contrast to macropore flow water. Hence, matrix water is predominantly 'old' water.

(ii) Macropore flow (or rapid throughflow)

Macropores are voids and channels > 750 μm in diameter (Clothier and White, 1981; Beven and Germann, 1982; Bouma, 1981). Conditions that promote pipe development relate to shallow soil depths, underlying permeable bedrock and root growth and decay (McDonnell, 1990). Flow through a macropore is subject to the force of gravity only and water moves rapidly though relatively small volume fractions (Germann and Beven, 1986). The effects of macropores are dependent on the spacing between large pores, the pattern of rainfall intensities and the hydraulic characteristics of the soil matrix (Jones, 1987). Luxmoore (1981) designated three classes of pores; macro- (> 1000 μm),

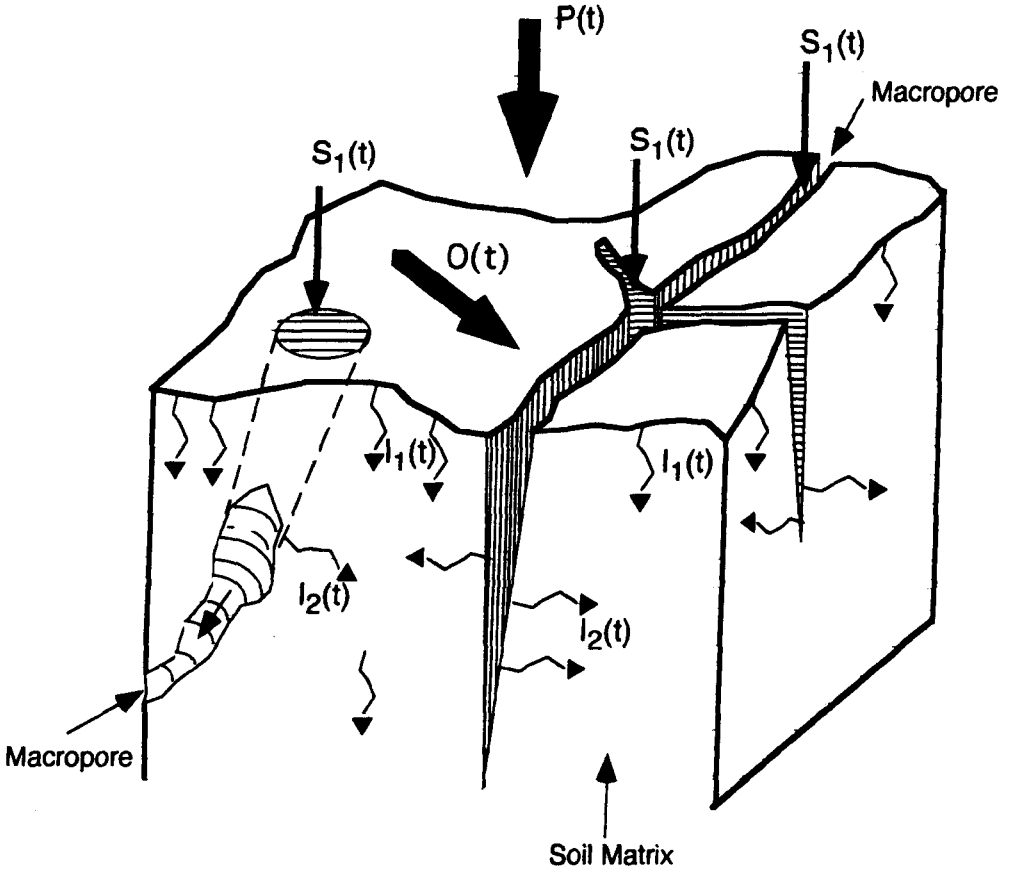

Figure 1.2: *Definition diagram for water flows during infiltration into a block of soil with macropores. P(t), overall input (rainfall); $I_1(t)$, infiltration into the matrix from the surface; $I_2(t)$, infiltration into the soil matrix from the walls of the macropores; $S_1(t)$, seepage into the macropores at the soil surface; $S_2(t)$, flow within the macropores; O(t), overland flow (afterGermann, 1980)*

meso- (10 - 1000 μm) and micro- (< 10 μm). Mesopores contribute more to rapid infiltration than macropores, in that rainfall is often insufficient to initiate channelling in macropores while being sufficient to initiate preferential flow in mesopores (Omoti and Wild, 1979). Luxmoore et al (1993) suggest that there are major interactions between macropores, mesopores and micropores, allowing storage and/or release of water between and during rainstorms, respectively.

Figure 1.2 displays a definition diagram for water flow during infiltration into a block of soil with macropores (Germann, 1990; Beven and Germann, 1982). Flow in the unsaturated zone is described in three stages, where rainfall is assumed to be the sole contributor of water to the system. In the first stage, all water that arrives at the soil surface is absorbed by the matrix (i.e. micropore flow). Hence, the infiltration capacity of the soil ($I_1(t)$) exceeds rainfall input (Pt). As rainfall continues, seepage into the macropores at the soil surface occurs ($S_1(t)$). With time, this process magnifies and flow within the macropore occurs ($S_2(t)$). As the infiltration of the surface soil is exceeded, overland flow (O(t)) may be initiated. Macropore flow still occurs at this point, although it may be reduced slightly due to lateral losses into the surrounding soil matrix ($I_2(t)$).

Even a small amount of macroporosity can influence the water flux through a saturated soil by more than one order of magnitude in soils of low to moderate conductivity (Beven and Germann, 1982). Beven and Germann (1982) found differences in flow velocities of between 100 to 400 times amongst matrix and macropore drainage. Macropores and pipes have also been documented to speed up drainage in hillslopes to rates comparable with and exceeding overland flow (Jones, 1987).

(iii) Macropore flow: a 'grey' area

Macropore flow is a 'grey' area of hillslope hydrology, especially in terms of the type of water (i.e. 'old' or 'new') transported. The direct measurement of by-pass flow is rather difficult because of the tremendous spatial and temporal variability in water movement in the field soil (Roth *et al*, 1991; Flury *et al*, 1994). There is strong circumstantial evidence for rapid flow, via preferred pathways, in soils, in many forested areas (Pearce *et al*, 1986). However, field evidence for macropore flow is sparse in the environments where it is considered important (Beven and Germann, 1982). Few investigations have been able to quantify the 'new' or 'old' water contribution in macropores. Mosley (1979, 1982) used dye tracing and sub-surface flow measurements to conclude that macropores transported 'new' water to storm runoff at the M8 catchment, New Zealand. Leaney *et al* (1993) used Cl^- and δ^2H as tracers of water movement in the Onkaparinga catchment, S. Australia. Mean Cl^- concentrations of throughflow closely resembled that of rainfall rather than pre-existing soil waters. Hence, they conclude that during the initial stages of rainfall, infiltrating water by-passes much of the soil matrix.

Pearce *et al* (1986) and Skalsh *et al* (1986) used natural, stable isotopes and chemical tracers at the M8 catchment and concluded that throughflow during storm events was predominantly 'old' water. Dewalle *et al* (1988) concluded that a piston flow mechanism was in operation at Fish Run, Appalachians, USA, where stored soil water was displaced to the stream by infiltrating 'new' water.

Hence, macropores have been found to contribute both 'old' and 'new' waters, depending on sample site and the method used in the analysis. In none of these studies is the proportion of either water type quantified. Little discussion is available concerning the mechanisms that control macropore operation or seasonal variations in macropore flow.

(I.1Dd) Groundwater flow

Freeze (1974), indicated that recharge of groundwater by infiltrating rainfall was likely to be greater for long duration, low-intensity rainstorms, following wet antecedent moisture conditions (assuming homogeneous, isotropic soils). Where the unsaturated zone above a water table has a moisture content less than that of specific retention, the water table will not respond from rainfall until this deficiency has been satisfied. A near-instantaneous response of shallow water levels to rainfall is occasionally noted (Todd, 1980). Todd explains this observation by the pressure increases of air trapped in the zone of aeration when rainfall seals surface pores and infiltrating water compresses the underlying air. For shallow water tables, the rise can be an order of magnitude larger than the depth of the infiltrating rainfall.

This phenomenon has been explored in other investigations, where the reasons for its occurrence are different to those suggested by Todd (1980). Skalsh *et al* (1986) investigated groundwater responses in the Maimai Catchments, New Zealand, using δ^2D, electrical conductivity and Cl^- data. They suggest that the physical response at Maimai is entirely consistent with the concept of groundwater ridging. According to this concept, a disproportionately large rise in the water table is caused by the conversion of a tension-saturated capillary fringe into phreatic water by infiltrating rain. Saturated wedges on the lower slopes and groundwater ridges on the valley bottoms convert the tension-saturated zone into phreatic water. This conversion rapidly increases the hydraulic gradient to the stream and promotes the gravity drainage of groundwater. When the rainfall rate cannot sustain the groundwater discharge rate, the phreatic zone thins, the hydraulic gradient to the stream diminishes and the stream hydrograph begins to recede. Sklash and Farvolden (1979) suggest that groundwater ridging effects occur in regions where the capillary fringe is at or near the ground surface. These zones are most likely to occur in the lower slopes and valley bottoms than in the upslope areas.

Another mechanism that has been identified as a cause of groundwater response is groundwater displacement (McDonnell, 1990). This mechanism is another 'grey' area of hillslope hydrology and hence requires more detailed research. In the few investigations where the mechanism is proposed as being in operation, the infiltration of 'new' water to depth via macropores is suggested to prompt the displacement of groundwater downslope. Thus, the operation of macropore flow is concurrent with groundwater response. In all groundwater response mechanisms, 'old' water is contributed to storm runoff.

(I.1De) Summary

The development of a conceptual hillslope model that defines all major flowpaths during storms and which is applicable to all geographical locations is impossible. The studies outlined in the above section were conducted at numerous locations, where the mechanisms detected as being dominant in storm runoff were different in each. This is, in part, due to the bias of most studies towards the analysis of a particular flowpath, and also to the fact that all catchments respond differently (Wheater *et al*, 1990). It is clear that information about some flowpaths, e.g. overland flow and matrix water flow, is much more detailed than for the 'grey' area flowpaths, namely macropore flow and groundwater displacement. The lack of field investigations that sampled intensively mean that sparse datasets are available for these flowpaths. Field experiments that sample at 1 hr and even 30 min intervals do not possess the necessary temporal resolution to identify quick flow mechanisms, such as macropore flow. In the majority of tracer experiments, Cl^- or stable isotopes have been employed in the hydrochemical assessment of flowpaths. The sampling resolution of chemical data is typically greater than hydrometric data, which explains why no quantitative calculations are available of 'old' and 'new' water contributions to macropore water. The only solution to gaining more knowledge about short-term flow processes is to implement very intense hydrometric and chemical sampling programmes. Ideally a tracer is sought that can be sampled as intensively as hydrometric equipment. From the initial discussion of previous tracer studies in section (1.3B), temperature seems to be the ideal tracer to do this.

I.2 AIMS AND APPROACHES OF THE STUDY

I.2A General Principles

The purposes of this study are two-fold:

- to identify the major flowpaths followed by water in a hillslope during rainstorms
- to assess the magnitude of 'old' vs. 'new' water in those flowpaths

The study aims to examine the variation in quantity, quality and routing of rainfall as it passes through a hillslope system. The hillslope is regarded as a one-dimensional transect, from the tree canopy to the saturated zone, through which flow is pre-dominantly in a vertical direction. The influence of seasonality, storm magnitude, rainfall intensity and antecedent conditions on flow and chemical composition of waters in the various locations along the one-dimensional transect are assessed. The flowpaths investigated generally fall within the categories described in Section I.1D. Emphasis is placed on determining the contribution of 'new' vs. 'old' waters within specific flowpaths. A recurrent theme is comparison with other process-specific and small-scale field investigations.

I.2B Specific aims and questions

The study seeks to address the following questions:

- What are the major flowpaths in operation in the hillslope environment during rainstorms?
- What is the characteristic flow regime of each flowpath?
- Do those flow regimes vary seasonally?
- What other controls influence the flow regimes of individual flowpaths?
- How do the flow regimes of adjacent flowpaths vary?
- Can Cl^- and temperature be used to distinguish between 'old' and 'new' waters?
- What is the predominant water type (i.e. 'old' or 'new') in each flowpath?
- What are the controls on the magnitude of 'old' vs. 'new' water contribution to each flowpath?
- Can the contribution of 'old' vs. 'new' water be quantified?
- Can a conceptual model of hillslope response to rainstorms be developed?

The way in which these questions are addressed is broken down as follows:

Hydrometric Analysis (Chapter IV)

The passage of rainfall is traced through a one-dimensional profile through the hillslope, assessing each flowpath in turn. Flowpaths outlined in Section I.1D are assessed in terms of their flow regimes during storms. The controls on those flow regimes are investigated,. (e.g. controls of antecedent moisture conditions, storm magnitude and intensity and seasonality). The flow regimes within each adjacent flowpath in that profile are compared. In this way, mechanisms that affect flow in all sections of the hillslope can be assessed. Results from the current study are compared with previous studies into forest nutrient cycling, hydrological flowpaths and controls on flow throughout. Analysis of flow regimes in the unsaturated zone will be undertaken, in order to investigate the phenomena of macropore flow.

Chloride Tracer Analysis (Chapter V)

Cl^- has been successfully applied as a tracer of 'old' vs. 'new' water in some studies (Neal *et al*, 1990; Leaney *et al*, 1993). Hence, its applicability of a tracer at the field site is investigated. Ideally the concentration of 'new' water (i.e. rainfall) should display a significantly different Cl^- signature to 'old' water (i.e. groundwater). Once its applicability has been determined, the Cl^- concentrations of collection sequences along specific flowpaths throughout rainstorms allows the assessment of the general type of water carried within each flowpath. Implementation of mixing models of forest floor soil water and mobile soil waters is proposed as a method for quantification of the contribution of each water type to overland flow and macropore flow, respectively.

Temperature Tracer Analysis (Chapter VI)

Temperature has been used to monitor base flow conditions in groundwater (Sinokrot and Stallam, 1993). The temperature of 'new' and 'old' water have also been shown to vary significantly (Arai, 1993). Hence, it is used to trace the movement of 'new' water through the hillslope profile, which is a method that is not found in previous investigations. The use of temperature in this way will assist in the exploration of the grey areas of hillslope hydrology, namely macropore flow and groundwater displacement.

Conceptual hydrological model (Chapter VII)

The development of a conceptual hydrological model of the hillslope environment is achieved by the combination of hydrometric data and the results of the tracer investigations. Models are developed for growing season and dormant season conditions, where quantitative assessments are made of the losses and gains of water within each section of the hillslope. With the addition of tracer data, some assessment is made of the general 'old' or 'new' water content of each flowpath, and in some cases this is quantified. The model aims to identify all major hydrological flowpaths in operation within the hillslope, and emphasis is placed on elucidating the operation of macropore flow and groundwater displacement mechanisms, for which general field information is lacking at present.

In Chapters II and III, descriptions of the field site and field and laboratory methodologies are presented. In Chapter VIII, the conclusions to these and answers to the questions above are provided.

Chapter II
FIELD SITE DESCRIPTION

II.1 INTRODUCTION

The Panola Mountain Research Project (hereafter PMRP) has been in operation since 1985 and is run by the Water Resources Division, United States Geological Survey (U.S.G.S.), Atlanta. In the nine years prior to the current investigation, the PMRP has accumulated some 20,000 samples, on which full chemical analyses have been performed. The catchment has also been intensively instrumented for hydrometrical observations. Thus, large hydrometric and chemical databases exist, which were available for corroboration of data generated in this study.

This chapter commences with a brief outline of the watershed as a whole and is followed by a more detailed description of the sampling site. A discussion of previous investigations and available data from the PMRP which are applicable to this investigation follows.

II.2 PANOLA MOUNTAIN RESEARCH WATERSHED: CATCHMENT DESCRIPTION

II.2A Site

Panola Mountain Research Watershed (hereafter, PMRW) is located within the Panola State Conservation Park, Stockbridge, Georgia, 25 km to the south-east of Atlanta (Figure 2.1). The watershed (84°10'W, 33°37'N) is within the Piedmont Physiographic Province. Annual rainfall averages 120 mm, ranging from 760 to 1580 mm, from 1985 to the present (Peters, 1993). The annual temperature averages 15°C. Rainstorms are typically convective in summer, characterised by high intensities and short durations. Winter rainstorms are typically frontal and are of lower intensity and duration (Shanley and Peters, 1988). The major geomorphological feature of the watershed is the granite outcrop in the headwaters of the catchment.

II.2B Geology

Most of the catchment is underlain by Panola Granite, of granodiorite composition. The Panola granite was emplaced 320 Ma in a host rock of the Clairmont Formation, which contains units of amphibolite and muscovite schist (Higgins *et al*, 1988).

II.2C Soils

The regolith is greater than 7 m deep and is typically deepest (approx. 10 m) in the valley bottom. It thins to about 1 m on the ridges. Bedrock is at or near the surface in the vicinity of the valley outlet. Several soil types are present: Entisols occupy the region close to the base of the granite outcrop, whereas the remaining area is comprised of Inceptisols of the Ashlar series, and Ultisols of the

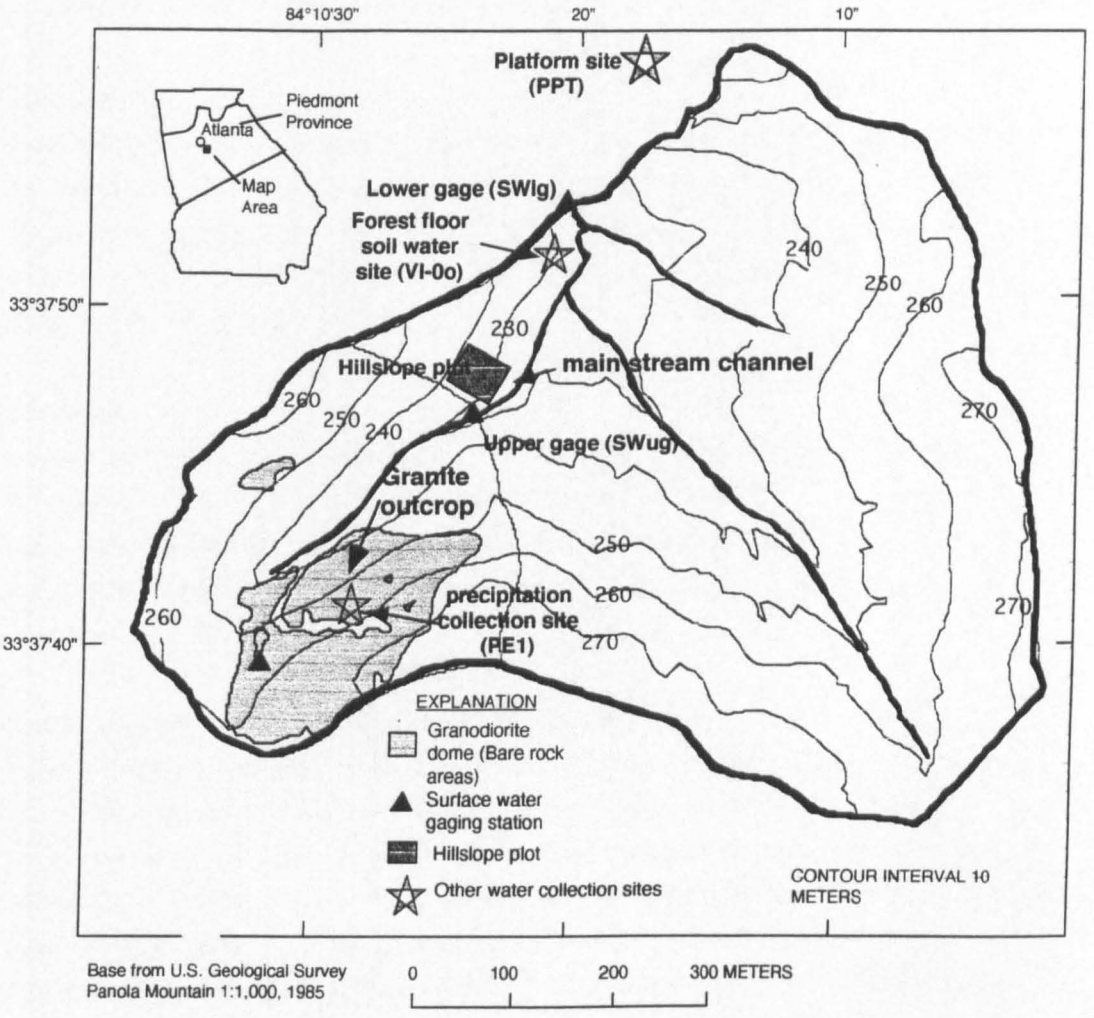

Figure 2.1: Location map of Panola Mountain Research Watershed (PMRW)

Gwinnett and Pacolet series (Shanley, 1993). These soils are sandy loams, which vary from 60 to 100 cm in depth, and are extensively weathered on hillslopes and ridges (Shanley, 1989) The average inclination of the hillslopes is 40° and soil creep is evident.

II.2D Vegetation

94% of the catchment is covered by forest, except for a 3 ha lichen- and moss-covered bedrock outcrop at the headwaters. Approximately 70% of the forest comprises mixed deciduous stands, dominated by 70 to 100 yr. old stands of Southern Red Oak (*Quercus falcata)* and mockernut hickory (*Carya glabra*), and younger stands of tulip poplar (*Liriodendron tulipfera*), black oak (*Quercus glabra*) and white oak (*Quercus alba*) (Carter, 1978).

II.2.E Runoff

The upper reach of the stream is ephemeral. The stream becomes perennial approximately 250 m downstream from the base of the granite outcrop. Streamflow at PMRW has a distinct seasonal baseflow component with highest baseflow during the late winter and spring (e.g. 6 - 10 l/s for March and April storms), and lowest during the summer and early fall (e.g. typically 2 l/s for June and July storms).

Runoff is highly variable at PMRW, but averages 20 - 30% annually (Peters, 1994). Primary factors causing rapid runoff are the 3 ha lichen- and moss-covered bare rock area, other smaller rock outcrops and thin soils in the headwaters (Shanley and Peters, 1988; Shanley and Peters 1993). Depending on the antecedent moisture conditions, a flood wave from a 2 - 4 cm intense rainstorm in the outcrop area takes from 20 to 40 min to move through the watershed. The wetter the soils, the faster the water is transported through the watershed (Peters and Ratcliffe, in prep). Streamflow is flashy and the time from maximum rain intensity to peak streamflow is typically less than 40 min (Shanley, 1989). Discharge at the lower gage can reach over 100 l/s.

II.3 PREVIOUS INVESTIGATIONS OF FLOWPATHS AT PMRW

A number of methods have been employed at PMRW to identify significant flowpaths within the catchment. A number of different models and tracers have been employed, all of which produce somewhat different results (Shanley and Peters, 1988; Christophersen *et al*, 1990; Hooper *et al*, 1990; Hooper and Christophersen, 1992; Shanley, 1992). However, all outline the major control of antecedent moisture conditions, rainstorm duration and intensity on the contributions from identified flowpaths. Three of these approaches are particularly relevant to the current investigation and pertinent observations are detailed below.

II.3A Using temperature as a tracer

Temperature has been used as a conservative tracer in order to assess source water contributions to runoff (Shanley and Peters, 1988). Rainwater may be warmer than streamwater and groundwater during the summer base flow conditions. Thus, the change in streamwater temperature during rainstorms can be used to infer contributions from either rainfall or groundwater sources. All rainstorms analysed were found to produce a spectrum of temperature responses, which were governed by antecedent moisture conditions. The major storm runoff components were channel interception, groundwater displacement and macropore flow

II.3B Application of EMMA and MAGIC

Hooper *et al* (1990) performed an end-member mixing analysis (EMMA) at PMRW in order to assess the zones of the watershed that contributed most to the hydrochemistry of streamwater. Streamwater arises from a mixture of soil water end-members, which, to a first approximation, are considered to be invariant in time and space. Christophersen *et al* (1990) have shown that if streamwater is comprised of a mixture of soil waters, then at least three soil solutions are necessary to encompass the streamwater observations. Hooper *et al* (1990) chose organic horizon, hillslope and groundwater end-members, each of which has a distinct chemical composition. The analysis showed that the organic horizon was the critical zone in determining streamwater chemical response during the summer. However, the hillslope component dominated during the winter. It was concluded that antecedent moisture conditions and seasonality had major impacts on the source areas of storm runoff.

The Model of Acidification of Groundwater in Catchments (MAGIC) is a soil-oriented charge balance model and was applied to PMRW by Hooper and Christophersen (1992). The analysis also concluded that the organic horizon is the critical zone in determining the streamwater chemical response and future streamwater chemistry trends.

II.3C Aqueous sulphate chemistry investigations

Several investigations into SO_4^{2-} dynamics have been performed at PMRW and have enabled major flowpaths within the system to be identified. Shanley (1992) found that during base flow, SO_4^{2-} retention by Fe^{3+} and Al^{3+} oxides in the mineral soil limits SO_4^{2-} concentrations in groundwaters and streamwaters to < 10 μeq/l, despite the SO_4^{2-} concentration in rainfall of approx. 100 μeq/l. During rainstorms, streamwater SO_4^{2-} concentrations increase to 100 μeq/l, reflecting increased flow through shallow soils where SO_4^{2-} is poorly retained. In fact for some rainstorms, SO_4^{2-} concentrations were observed to increase by a factor of 20 from their concentrations under base flow conditions. This suggests that significant quantities of high SO_4^{2-} waters were entering the stream as a combination of channel interception, macropore flow and rapid sub-surface return flow.

In a later investigation, Shanley and Peters (1993) discovered that soil waters from upper (15 cm) and lower (50 cm) soil horizons displayed similar median SO_4^{2-} concentrations (200 μeq/l). However, total SO_4^{2-} concentrations in the deep soil varied between 0 - 1000 μeq/l. Concentrations in the upper soil

layers did not display such a range. This pattern was attributed to the rapid transit to depth of throughfall and stemflow waters via macropores. The spikes in SO_4^{2-} concentrations at depth typically followed dry antecedent moisture conditions, which promotes macropore flow (Mosley, 1982).

Thus, previous investigations at PMRW have identified important flowpaths during rainstorms, namely channel rainfall, rapid sub-surface flow through the organic horizon, macropore flow and groundwater displacement. However, no investigations to date have investigated the variation in chemistry or flow rates through individual flowpaths throughout rainstorms. By contrast, Hooper *et al* (1990) assume no chemical variation in soil water composition. Investigations have also tended to concentrate on individual flowpaths and not to assess the hydrology of the system as a whole. This investigation attempts to identify all major flowpaths within the forested hillslope system and to assess how their chemistry and flow rates vary through time. Previous investigations suggest that antecedent moisture conditions, seasonality and storm duration and magnitude are critical factors.

II.4 FIELD PLOT SITE

A site was chosen that was representative of the hillslope geomorphology of the 10 ha sub-catchment, occupied by the granite outcrop. To minimise spatial heterogeneity in chemistry and flow rates within the study location, the site had uniform soil type and geology. A site where previous investigations had been conducted was preferred as instrumentation was already available, as was hydrological and chemical data from previous rainstorms. Hence a site was selected on the hillslope adjacent to the upper gage streamwater monitoring site (Figure 2.2) which met all the above requirements.

II.4A Field Plot Description

(a) *Site*

A 20 m x 20 m forested hillslope plot was chosen for instrumentation (Figure 2.2). The site is located adjacent to the upper gage streamwater monitoring site (SWug), which monitors the ephemeral proportion of the stream reach. The lower portion of the plot is within the riparian zone of the stream channel, and is 2 m away from the stream channel itself. The plot is 200 m downstream of the granite outcrop, 250 m upstream from the lower gage streamwater monitoring site (SWlg), and 400 m upstream from the site where rainfall was monitored ('platform site' or PPT). The maximum elevation of the plot was 231 m above sea level, and the plot extended to the riparian zone, which was 229 m above sea level (survey by Ratcliffe and Aulenbach, 1995). The slope of the plot was 10° and it faced in a south-east direction.

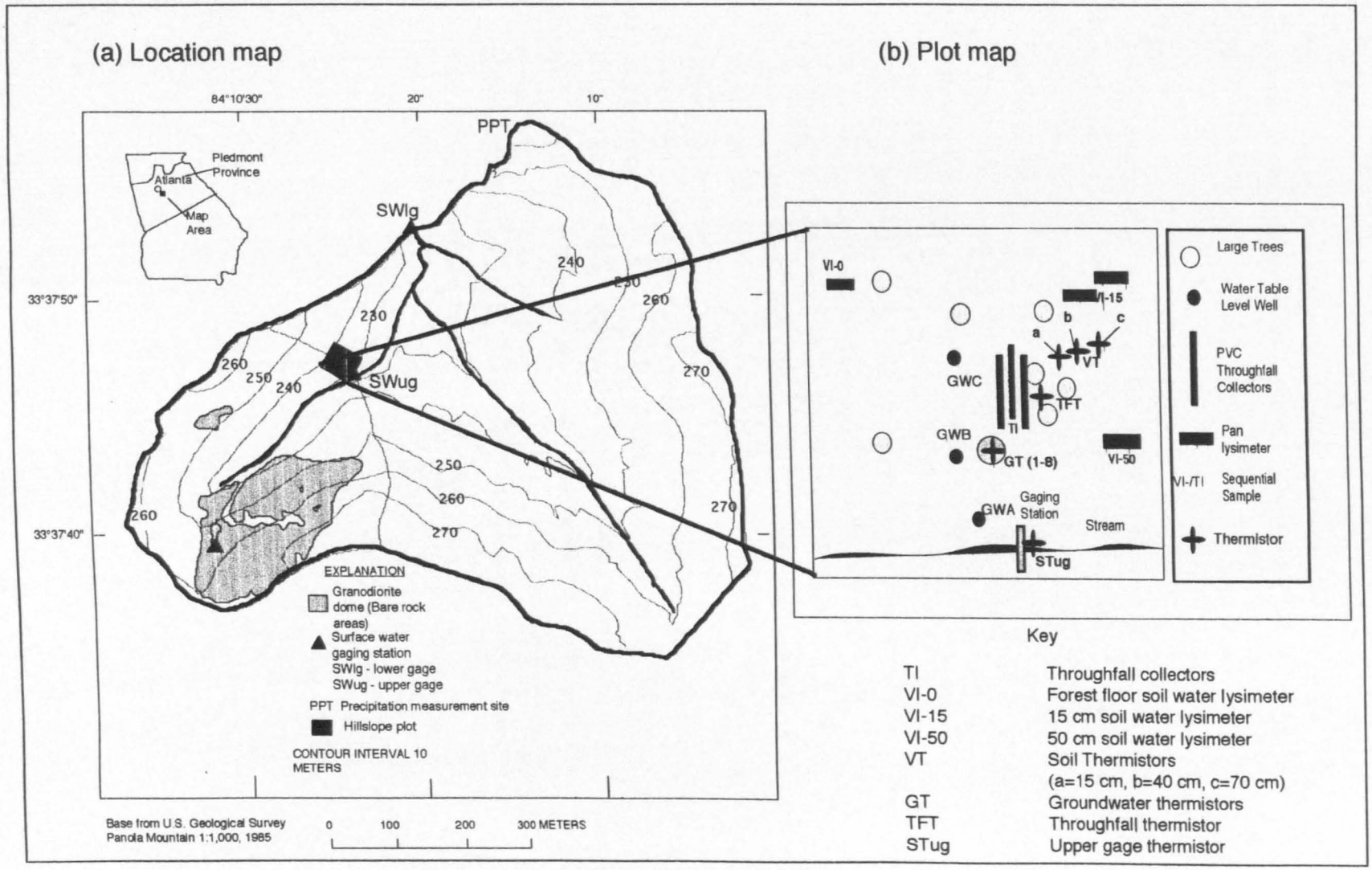

Figure 2.2: *Panola Mountain Research Watershed map, showing position of hillslope plot, and major hydrometric sampling equipment within plot*

Throughfall collection equipment, tension lysimeters and zero-tension lysimeters existed at the site prior to the current investigation (see below). All hydrometric and chemical sampling equipment employed in this investigation were located within the plot. Exceptions to this were rainfall monitoring equipment, located at PPT; forest floor soil water monitoring and collection equipment, located 200 m downstream (VI-0o); streamwater monitoring equipment at the lower gage, 250 m downstream (SWlg) and rainfall collection equipment on the granite outcrop (PE1) and outside the watershed (RG1) (Figure 2.2).

(b) Physical features

The site is underlain by Panola Granite. Soil and saprolite depths are highly variable throughout the watershed, but the regolith averages from 1 to 2 m thick on hillslopes underlain by Panola Granite, with thicker deposits near the stream channels. Soils developed in colluvium and residuum are mainly ultisols and become more characteristic of inceptisols in the portions of the hillslope that are highly eroded. Soils are generally from the Ashlar Wake Complex, where the dominant clay mineral is kaolonite (MacIntosh *et al*, in prep.). They are characterised by a very dark grey, greyish-brown sandy loam surface layer at 7 cm and a yellowish brown sandy loam subsoil. Material underlying the sub-soil is typically brown, sandy loam to approximately 66 cm, followed by a soft bedrock layer of strongly weathered granite and a hard bedrock layer at 86 cm. Soils from the Ashlar series are permeable and drainage is rapid throughout these soils (Huntington *et al*, 1993). Many large tree roots also penetrate to depth (MacIntosh et al, in prep.) Hence, with a combination of the presence of plant roots and a permeable structure, rapid flow via macropores is anticipated in these soils. For soil profile diagram, see Figure 4.12 (Chapter IV).

The hillslope is vegetated by deciduous species (Table 2.1). Two of a series of vegetation plots selected by Cappellato (1993) were located within close proximity to the hillslope plot (Site 559 and Site 652). The results of the investigation performed in 1992 are presented in Table 2.1, providing information on basal diameters, biomass and basal area for dominant species. Within the hillslope plot, the most dominant species are Southern red oak (*Quercus falcata*) and Northern red oak (*Quercus rubra*). Other species that were present were Pignut hickory (*Carya glabra*), Mockernut hickory (*Carya tomensota*) and Dogwood (*Cornus florida*).

Site	Species	Basal diameter (cm)	Biomass (kg/yr)	Basal area (cm^2)
599	QF	47	1600	1700
599	QR	40	1100	1300
599	QV	32	610	800
599	CG	15	90	170
599	COVL	31	610	760
599	CT	21	290	400
599	LT	na	na	na
599	Other	na	na	na
652	QF	na	na	na
652	QR	24	310	460
652	QV	39	980	1200
652	CG	41	1300	1300
652	COVL	21	430	490
652	CT	37	1700	1400
652	LT	16	90	200
652	Other	16	90	190

***Table 2.1**: Vegetation analyses at plots located close to the field plot (sites 599 and 652), displaying basal area, biomass and basal diameters for dominant species (after Cappellato, 1993). QF = Quercus falcata (Southern red oak), QR = Quercus rubra (Northern red oak), QV = Quercus vetulina (Oak), CG = Carya glabra (Pignut hickory), CT = Carya tomensota, LT = Liriodendron tupilfera (Dogwood), Other = other species*

(c) Hydrological overview during study period

Annual rainfall during the study period (April 1994 - May 1995) was high at 1500 mm. Individual rainstorms ranged from 0.2 to 179 mm. The summer of 1994 was the wettest on record and was caused by Tropical Storm 'Alberto' and subsequent high magnitude rainstorms.

II.4B Summary of previous investigations and equipment installation

A number of studies have been performed investigating the variations in flow and chemistry along specific flowpaths within the field plot.

(a) *Canopy processes*

Weekly collection of throughfall samples from a Aerochem Metrics wetfall - dryfall collector (TW) have been carried out at this site for several years, as have the measurement of throughfall flow volumes from a 25 cm o.d. tipping bucket gage (TI2) (see Chapter III for more detail). Cappellato (1991) performed an investigation into throughfall and stemflow chemistry at a series of sites throughout the watershed (see Chapter IV for details). Two of these sites were located within the hillslope plot (Table 2.1). This data will be used to assess the accuracy of the throughfall volumes recorded in the current investigation. Comparison of the data series may provide insight into the spatial heterogeneity of throughfall within the deciduous canopy. Interception losses may also be estimated using throughfall volumes collected in the current study and the stemflow volumes recorded in the previous investigation.

(b) *Soil waters*

An investigation of sulphur dynamics within the hillslope region (Shanley, 1992) necessitated the installation of 15 cm (VI-15o) and 50 cm (VI-50) depth pan lysimeters. These lysimeters were used in the present investigation, and chemical data was available at both sites for a four year period.

Cappellato (1993) installed a series of zero-tension lysimeters and tension lysimeters at three sites (VA, VB and VC) within the hillslope plot (see Chapter III for details). These were used in this study. They had been installed three years prior to the initiation of the investigation and thus, it is likely that the equipment had attained chemical equilibrium with the soil prior to this investigation.

(c) *Streamwaters*

Stage monitoring has been performed for several years at the upper gage (Peters, 1993), and water samples have been collected both manually and automatically. In the current investigation, samples of streamwater from the upper gage were only collected on a manual basis. If the chemistry of these samples are similar to the samples collected manually at the upper gage prior to the study, then it is postulated that the automatically collected samples may have similar chemical signatures. Thus 'past' samples may be useful in assessing current hydrochemical patterns in streamwater at the upper gage.

Chapter III
FIELD AND LABORATORY METHODS AND TECHNIQUES

III.1 INTRODUCTION

Sequential chemistry and flow rates were examined for the following water types during selected storms from April 1994 to May 1995 (Figure 3.1):

- Precipitation
- Throughfall
- Soil waters
- Groundwaters
- Streamwaters

This chapter describes the full range of field and laboratory techniques that were employed. The first section gives an overview of sampling strategy and the fundamentals of the sampling methodology. The following sections relate to the details of sampling for each water type. The chapter concludes with the chemical procedures that were adopted.

III.2 SAMPLING STRATEGY

It was not possible to sample all storms over the period of the study for logistical and pragmatic reasons. Sampling of approximately one storm per month was implemented, with the aim of investigating seasonal effects on storm chemistry. A series of storms with differing intensities were selected (Table 3.1).

The aim of the sampling strategy was to monitor the variation in flow rates and chemistry of the major hydrological flowpaths throughout rainstorms. Thus, intensive sampling on a temporal scale was required. An imaginary vertical transect through the hillslope was chosen as the basis of the sampling structure. It extended from above the canopy level to the saturated zone (Figure 3.2). Each sampling point along the one-dimensional profile through the hillslope is henceforth referred to as a node and relates to an important flowpath within the system. The nodes sampled were as follows:

- Precipitation
- Throughfall
- Forest floor soil water
- 15 cm soil water
- 40 cm soil water
- 50 cm soil water
- 70 cm soil water
- Groundwater screened 30 cm below water table
- Groundwater screened 120 cm below water table
- Streamwater

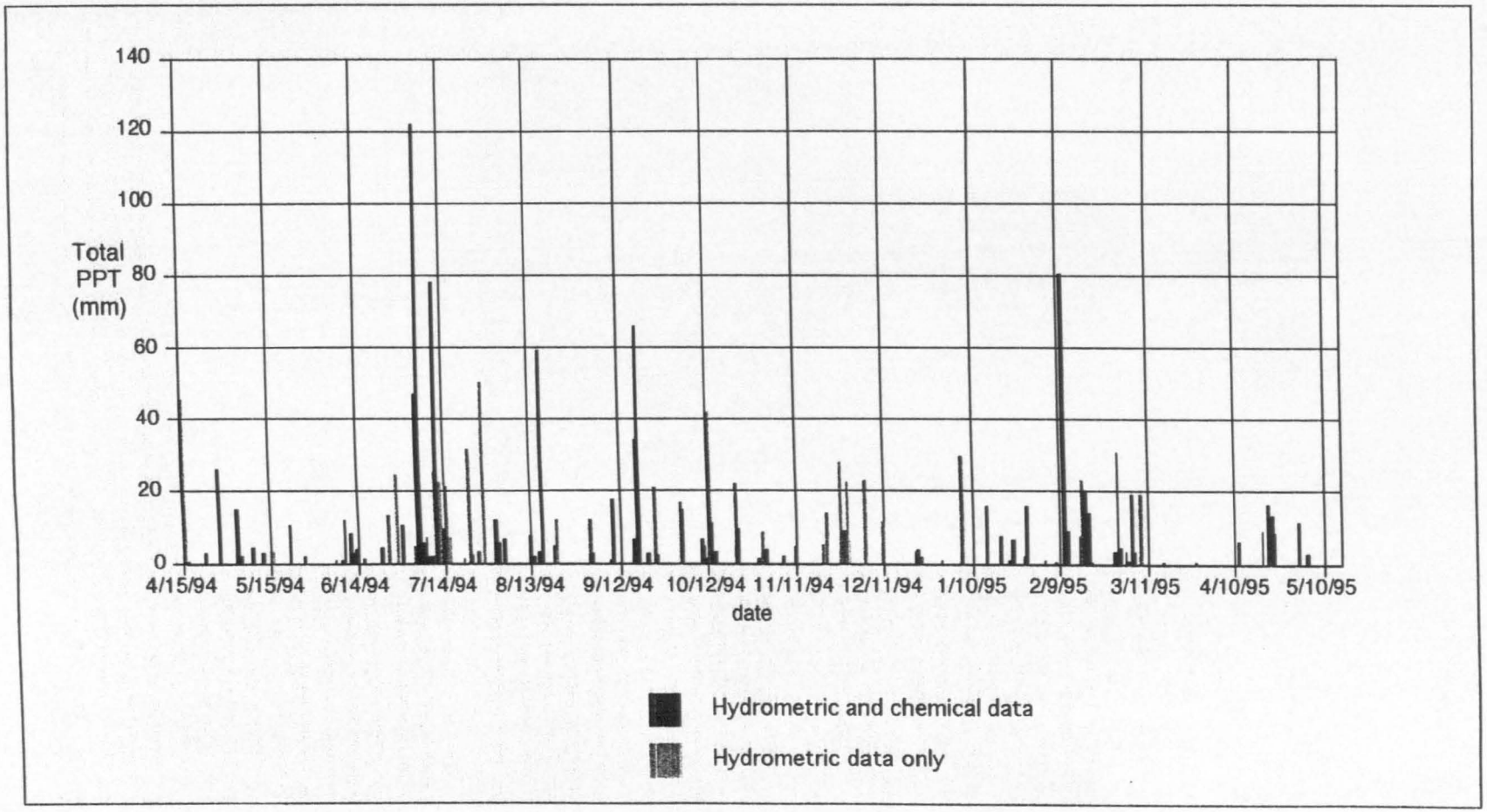
140
120
100
Total PPT (mm)
80
60
40
20
0
4/15/94
5/15/94
6/14/94
7/14/94
8/13/94
9/12/94
10/12/94
11/11/94
12/11/94
1/10/95
2/9/95
3/11/95
4/10/95
5/10/95
date
Hydrometric and chemical data
Hydrometric data only

Figure 3.1

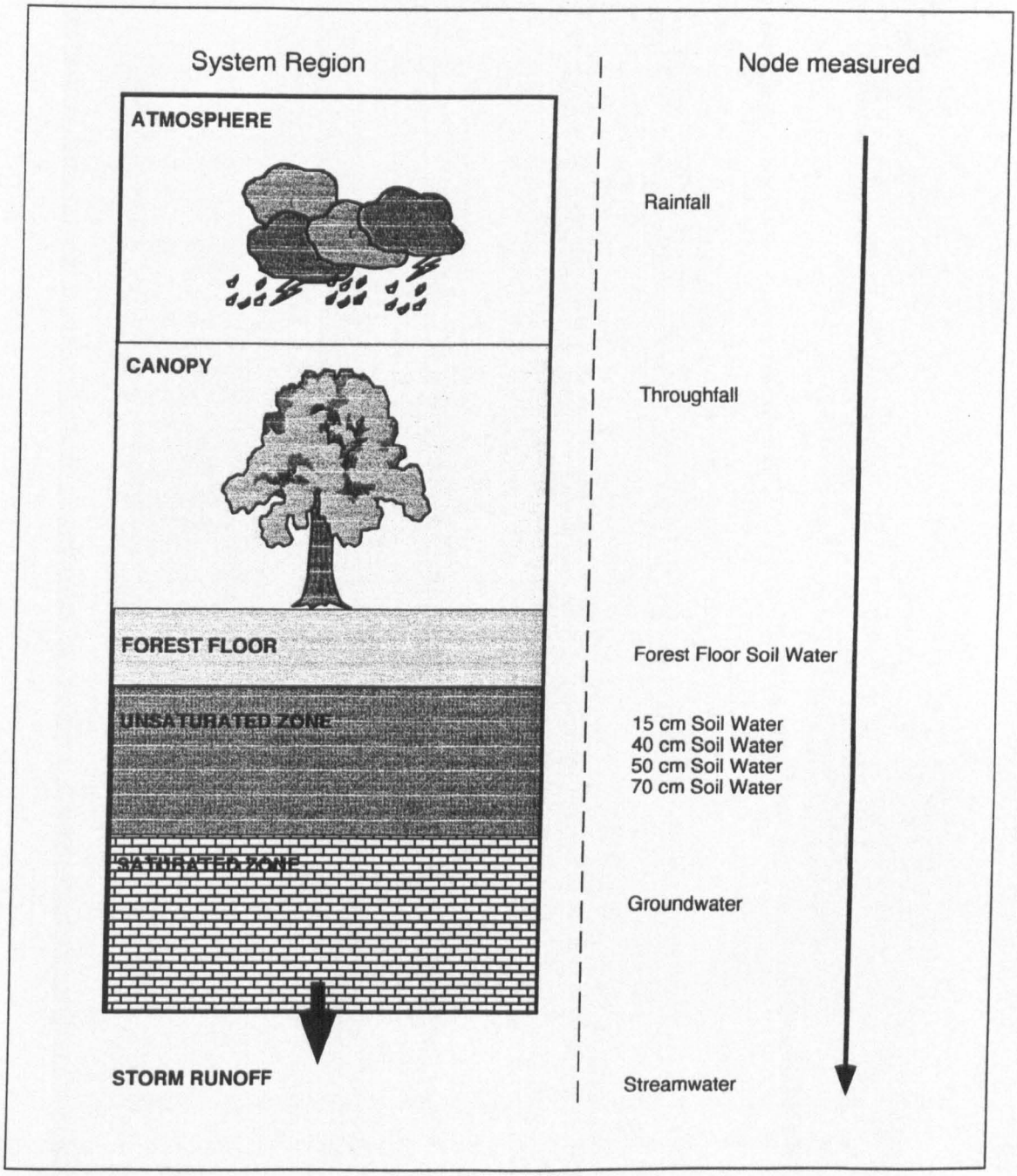

***Figure 3.2**: One-dimensional vertical transect, showing nodes chosen for hydrometric and chemical sampling*

Storm Date	Total Rainfall (mm)	Rainfall Duration (hr min)	Total Rainfall in previous week (mm)
15 April 1994	42	14 hrs 34	7
3 May 1994	15	10 hrs 31	26
9 June 1994	12	1 hr 57	2
24 June 1994	13	0 hr 57	4
27 June 1994	12	7 hrs 02	18
3 July 1994	175	290hrs 42	35
10 July 1994	26	3 hr 17	190
11 July 1994	78	10 hrs 45	211
12 July 1994	22	3 hr 46	242
14 July 1994	22	3 hr 40	146
22 July 1994	32	10 hr 03	9
27 July 1994	50	16 hr 21	38
16 August 1994	60	14 hrs 39	12
21 August 1994	12	5 hr 37	67
1 September 1994	12	2 hr 10	0
9 September 1994	18	6 hr 50	4
16 September 1994	36	36 hrs 24	18
23 September 1994	23	16 hr 39	110
2 October 1994	32	33 hr 17	6
11 October 1994	46	36 hrs 19	7
13 October 1994	11	16 hrs 51	55
21 October 1994	22	1 hr 19	3
20 November 1994	19	12 hr 09	0
26 November 1994	37	4 hr 01	19
29 November 1994	23	20 hr 13	65
4 December 1994	23	5 hr 00	30
6 January 1995	29	16 hr 36	1
14 January 1995	16	16 hrs 36	0
19 January 1995	7	4 hrs 02	16
27 January 1995	17	17 hrs 32	8
10 February 1995	85	26 hrs 27	2
16 February 1995	23	7 hr 00	97
27 February 1995	38	38 hrs 16	0
8 March 1995	19	9 hr 04	26
11 April 1995	6	6 hrs 21	0
19 April 1995	9	3 hrs 50	1
21 April 1995	17	3 hr 44	9
22 April 1995	13	4 hr 04	26
23 April 1995	9	10 hr 00	39
1 May 1995	12	2 hr 46	0

***Table 3.1**: Storm characteristics: Total rainfall, storm duration and total rainfall in the week prior to the onset of the rainstorm. N.B. A gap of 6 hr in which no rainfall occurred was used as a criteria for distinguishing one storm from another. Thus, in some of the storms, there are 'dry periods' of less than 6 hr.*

At each node, a collection of hydrometric equipment was installed in order to monitor the short-term hydrological variations throughout rainstorms. Collection of water samples at each node allowed the short-term variations of the biogeochemistry along each flowpath to be monitored.

III.2A HYDROMETRIC SAMPLING METHODS

Three types of equipment were frequently employed during this investigation, namely tipping bucket gages, Time Domain Reflectometry (TDR) and stage measurement equipment.

(a) Tipping bucket gages

Tipping buckets were used to monitor the timing and flux of water movement. The tipping bucket mechanism consists of a two-sided bucket. When the volume capacity of the bucket is reached, it tips, allowing the other side to fill. All tipping buckets were monitored with Campbell Scientific Model CR21X and CR10 dataloggers (Peters, 1994).

The amount of water passing through the mechanism can be determined easily from the following expression:

$$F = \frac{n\,Vtb}{Atb} \qquad \text{Eqn 3.1}$$

where

F	=	Total flow	(cm)
n	=	number of tips	
Vtb	=	volume of tipping bucket	(cm^3)
Atb	=	area of collector	(cm^2)

Flow rate, Rt, can also be calculated, since the timing between the tips is known. Hence:

$$Rt = \frac{Vtb}{Atb \times t} \qquad \text{Eqn 3.2}$$

where

Rt	=	Flow rate	(cm/s)
t	=	time between tips	(s)

Two types of tipping bucket were employed in this investigation. For rainfall and throughfall collection, Sierra Misco 25 cm o.d. bucket gages were used, housed in a stainless-steel 25 cm o.d. cylinder. These tipping bucket gages were constructed in such a way that one tip of the bucket was equivalent to 0.1 inch (0.25 cm) precipitation. Rainwise tipping buckets were employed for throughfall and soil water collection. The volumes of water required to cause each side of the bucket to tip varied according to the tip-mechanism on individual tipping buckets. Four types of rainwise tipping buckets were employed, whose volumes varied from 11 ml to 14 ml. Collection equipment was connected by 2.0 cm o.d. silastic tubing. Water entered the box via a drain in the lid, directing water onto the centre of the tipping bucket mechanism.

False tips were induced on the equipment on a monthly basis. Known quantities of water (500 ml) were introduced to the equipment to ensure that it recorded the correct volumes. Both the Sierra Misco housing and the plexiglass boxes were measured with a spirit level to ensure that they were level and to ensure that there was no volume bias on either side of the tipping bucket.

(b) Time Domain Reflectometry

Time Domain Reflectometry (TDR) is a method of measuring soil moisture content (Topp *et al*, 1982). It allows continuous, real time, accurate measurements of soil moisture at multiple sites in a soil profile (Herkelrath *et al*, 1991). TDR uses the step voltage pulse propagated along parallel transmission lines, consisting of two parallel, 30 cm long stainless-steel rods attached to a twin-lead cable (Figure 3.3a and b). The propagation velocity of electromagnetic waves is a function of the dielectric constant of the medium in which the wave is propagating (Ledieu et al, 1986), which for a given soil is a function of the free water content (see Chapter IV for a more detailed description of the theory of TDR operation).

(c) Stage measurement

Groundwaters and streamwaters were both monitored using a potentiometer and a float-counterweight system. Stage potentiometers were monitored with Campbell Scientific Model CR21X and CR10 dataloggers (Peters, 1994).

III.2B CHEMICAL SAMPLING METHODS

Collection of water samples was performed either manually or sequentially. In the case of most manual sampling, a single sample was taken during the rainstorm. However, sequential samples were collected remotely, and in excess of 20 samples might be collected from each node, depending on the magnitude of the rainstorm. The sampling strategy that was employed to collect sequential samples is illustrated in Figure 3.3c. Water is allowed to exit the plexiglass box housing the Rainwise tipping bucket via a drain in the base of the box. Water then travels along 2.0 cm o.d. silastic tubing and reaches a series of polyethylene bottles, which collect on a fill-spill principle (Peters, 1994). The total number of bottles required to collect the entire sequence of flow at each node can be calculated from the consideration of previous storm amounts and comparison of these amounts with the area of the collector. For example, consider the following hypothetical case:

Storm magnitude = 7.5 cm
Area of collector = 1970 cm^2
Size of bottle = 1000 ml (cm^3)

During storm, the total volume of water passing to bottles = 7.5 x 1970
= 14,775 ml

Thus, number of bottles required = $\frac{\text{total volume of water}}{\text{vol. of bottle}}$ Eqn 3.3

= $\frac{14,775}{1000}$

= 15 (14.8) bottles

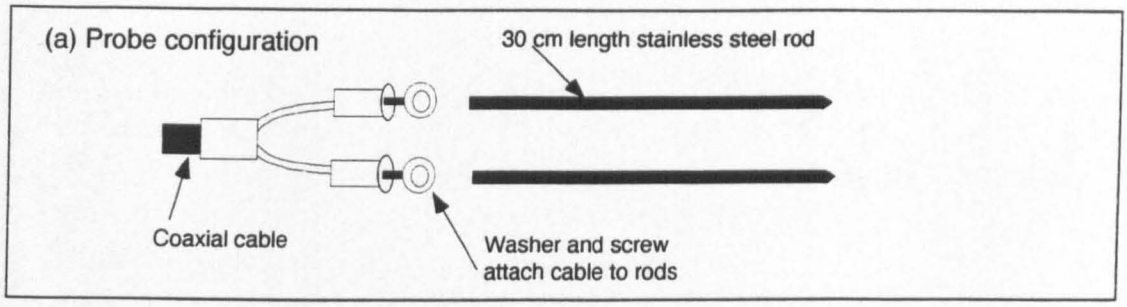

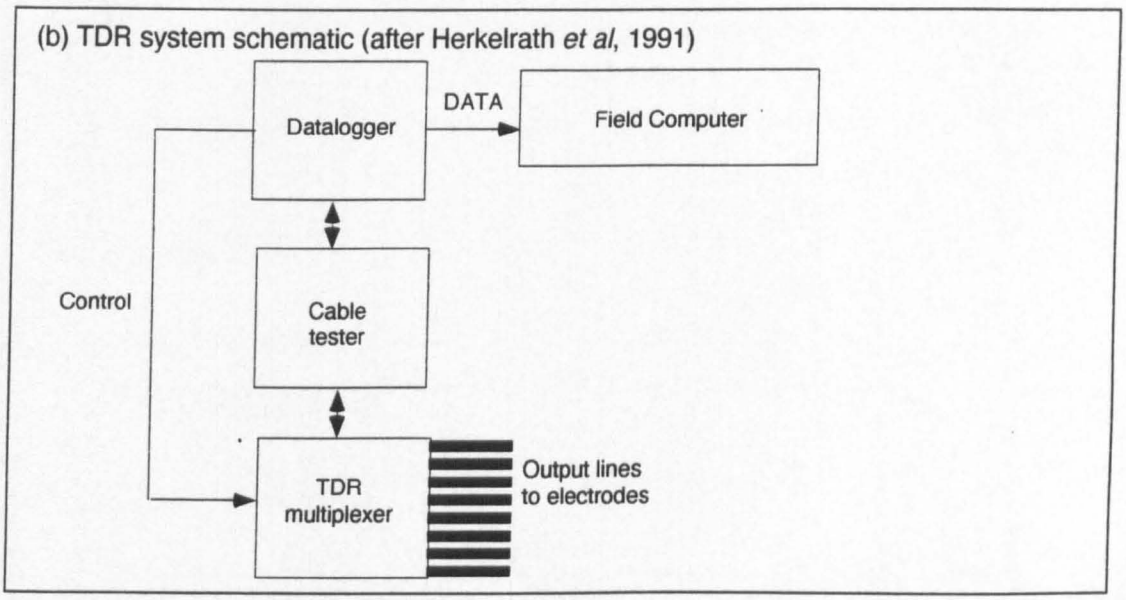

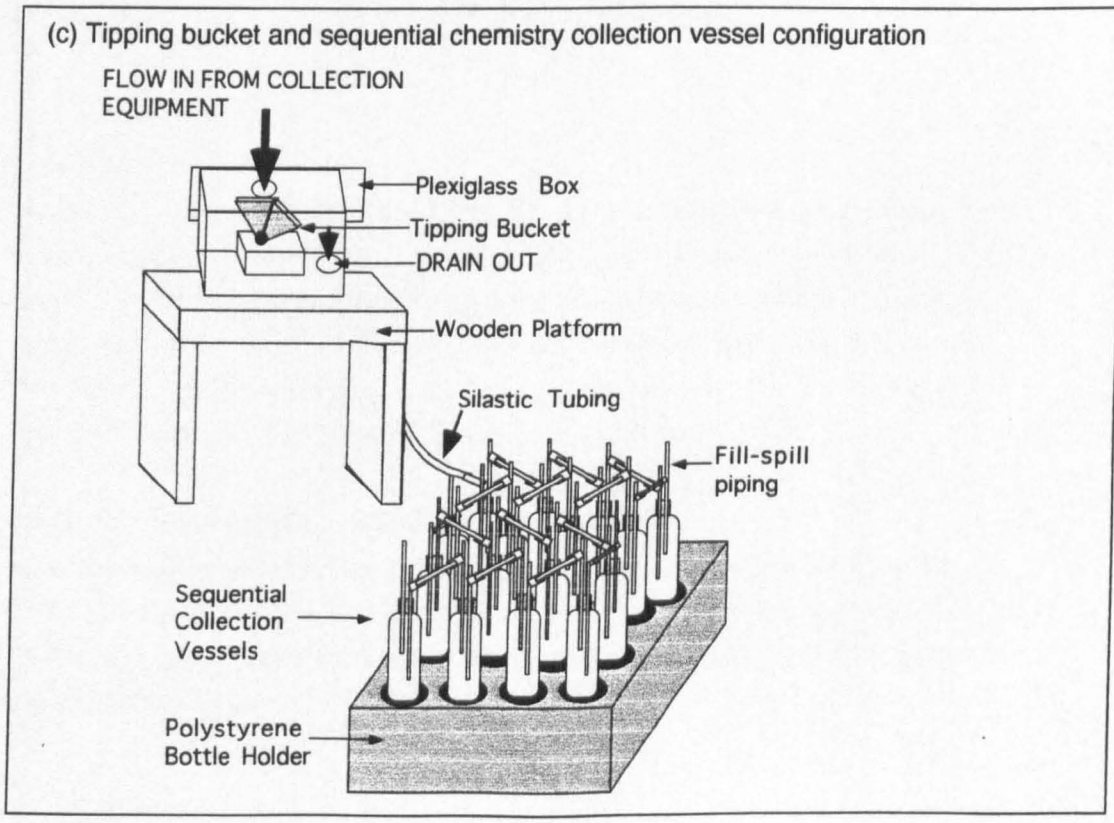

***Figure 3.3**: Hydrometric equipment : Time Domain Reflectometry apparatus and Rainwise tipping bucket configuration*

Thus, 15 bottles of 1000 ml volume would be required to collect all water passing through a node with a collector of area 1970 cm^2 during a storm of 7.5 cm magnitude. The total volume of water collected in individual bottles will represent different proportions of the total flow at that node, depending on the magnitude of the storm and the response of the node. Table 3.2 shows the bottle volumes used for water collection at each node and the magnitude of flow they represent.

Node	Bottle volume (ml)	Flow (mm)
Rainfall (PPT)		
	125	2.0
	250	4.0
	500	8.0
Throughfall (TI)		
	500	2.5
	1000	5.1
Forest Floor soil water (VI-0)		
	500	6.2
15 cm soil water (VI-15)		
	500	1.2
	1000	2.3
50 cm soil water (VI-50)		
	500	0.63
	1000	1.25

***Table 3.2**: Bottle volumes in sequential collection sequences at various nodes, and corresponding flow volumes*

III.2.C TRACERS

The passage of water through the canopy and hillslope was investigated using chloride and temperature as conservative tracers. Chloride determinations were carried out on all samples (see Section III.4). BETETHERM Model 5K3D39 thermistors were installed to monitor the temperature of throughfall, soil waters, groundwaters and streamwaters. The thermistors were monitiored by Campbell Scientific CR21X dataloggers. Temperature variations were related to water movement and were used in the assessment of the source of waters to each node (i.e. 'old' or 'new' waters).

III.3 COLLECTION OF DIFFERENT WATER TYPES

The sampling site, the related hydrometric and chemical collection equipment employed and the tracer used to monitor water movement will be described next for each water type that was examined. Table 3.3 provides a summary of the water types and the methodology employed. Figure 3.4 displays the location of all collection equipment on the hillslope plot.

	Collector	Hydrometric Equip	Samples	Tracer
RAINFALL				
PPT 'platform site' 400 m from hillslope	Aerochem Metrics wet fall - dry fall collector	Sierra Misco tipping bucket gage	Sequential collection equipment	Cl^-
PE1 'granite outcrop site 200 m from hillslope	Aerochem Metrics wet fall - dry fall collector	Sierra Misco tipping bucket gage	Single storm sample (manual)	Cl^-
THROUGHFALL				
TI 10 m upslope at hillslope	3 x 7.5 o.d. 1 m long PVC troughs	Rainwise tipping bucket gage	Sequential collection equipment	Cl^-
TW weekly throughfall 2 m upslope at hillslope	Aerochem Metrics wet fall - dry fall collector		Single storm sample (manual)	Cl^-
TI2 5 m upslope at hillslope		Sierra Misco tipping bucket gage		
TFT 2 m upslope at hillslope	Thermistor in bottle housed in tipping bucket structure			throughfall temperature
FOREST FLOOR SOIL WATER				
VI-0o 200 m downstream from hillslope	1 m^2 stainless-steel pan lysimeter	Rainwise tipping bucket gage	Sequential collection equipment	Cl^-
VI-0 15 m upslope at hillslope	0.08 m^2 polyethylene pan lysimeter	Rainwise tipping bucket gage	Sequential collection equipment	Cl^-
VAo, VBo 15 m upslope at hillslope	0.08 m^2 polyethylene pan lysimeters		1 to 2 manual samples per storm	Cl^-
SOIL WATERS				
VI-15 12 m upslope at hillslope	2 x 0.23 m^2 stainless-steel pan lysimeter	Rainwise tipping bucket gage	Sequential collection equipment	Cl^-
VI-50 20 m upslope at hillslope	1 m^2 stainless-steel pan lysimeter	Rainwise tipping bucket gage	Sequential collection equipment	Cl^-
VA, VB, VC 15 m upslope at hillslope	Tension lysimeters installed at 15, 40 and 70 cm depths		1 to 4 manual samples per storm	Cl^-
TDRA, TDRB, TDRC (2 m, 10 m and 15 m upslope at hillslope)	30 cm long, 5 mm diameter probes inserted horizontally at 15, 40 and 70 cm depths	Soil moisture variations every 5 min		
VT 10 m upslope at hillslope	Thermistors inserted in soil at depth of 15, 40 and 70 cm			Soil temperatures at 15, 40 and 70 cm
GROUNDWATER				
GWA, GWB, GWC riparian zone, 5 m and10 m upslope at hillslope	5.1 cm o.d. wells	Potentiometer and float-counterweight assembly		
GQA,GQB, GQCs, GQCd GQD (riparian one, 5 m, 8 m 8 m and 15 m upslope	5.1 cm o.d. wells (depths of 150 cm, 260 cm, 400 cm, 430 cm and 660 cm		1 to 4 manual samples per storm	Cl^-
GT 5 m upslope at hillslope	Thermistors inserted in well at depths of 2.12, 2.29, 2.44, 2.59, 2.74, 3.36, 3.96 and 4.6 m			Groundwater temperatures at 8 depths (GT1 .. GT8)
STREAMWATER				
SWlg 'lower gage' 200 m downstream at watershed outlet	V-notch weir	Potentiometer and float-counterweight assembly	Sequential samples from ISCO (SWlg) and manual grab samples (SWlgm)	Cl^-, temp (STlg)
SWug 'upper gage' adjacent to hillslope plot	V-notch weir	Potentiometer and float-counterweight assembly	manual grab samples (SWug)	Cl^-, temp (STug)

Table 3.3 *Water types sampled : site description, hydrometric equipment, sampling strategy and tracer investigations*

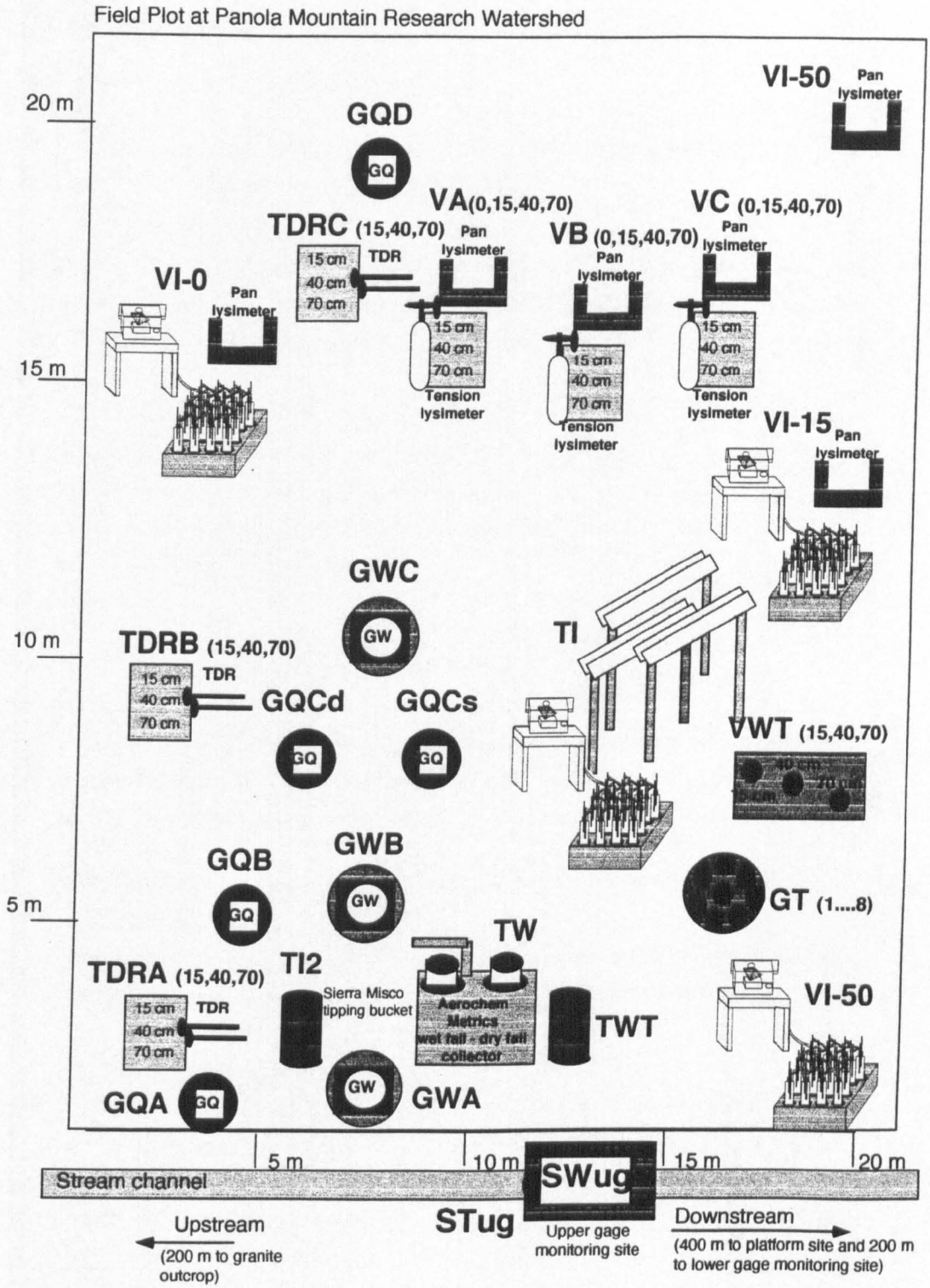

***Figure 3.4**: Hydrometric and chemical sampling equipment installed within the 20 m x 20 m hillslope plot at Panola Mountain Research Watershed (see Figure 2.1. for site location and Table 3.3 for equipment descriptions)*

III.3A PRECIPITATION

Rainfall was collected at three sites, PPT, PE1and RG1

(a) PPT : This site was located 400 m downstream from the hillslope plot, just outside the watershed. This location is also referred to as 'the platform site' (Figure 2.2.).

Hydrometric Equipment

Rainfall was collected in a 13 cm o.d. polyethylene bucket within the 'wet' collection side of an Aerochem Metrics wet fall - dry fall collector, to minimise contamination of the rainfall (wet deposition) sample by dry deposition. Rainfall flow rates were measured from a Sierra Misco tipping bucket gage.

Collection of samples for chemical determinations

Sequential samples of rainfall were collected at this site. Water was directed from the bucket on the 'wet' collection side of the Aerochem Metrics wet fall - dry fall collector via 2 cm o.d. silastic tubing into sequential collection bottles. Eight 150 ml bottles, two 250 ml bottles and two 500 ml bottles were employed in a fill-spill configuration.

Tracer study

(i) Chloride

Chloride determinations were performed on all samples (see Section III.4).

(ii) Temperature

The temperature of incoming rainfall was not recorded. However, air temperature was monitored from a BETATHERM Model 5K3D39 thermistor installed on a mast 3 m above the ground, at site PPT. Temperature was recorded at 5 min intervals by a Campbell Scientific Model CR10 datalogger.

(b) PE1: This site was located on the bedrock outcrop, 200 m from the hillslope plot (Figure 2.1).

Hydrometric equipment

Rainfall was collected by the same method used at site PPT (i.e. via an Aerochem Metrics wet fall - dry fall collector). A Sierra Misco tipping bucket gage also provided measurement of rainfall flow rates.

Collection of samples for chemical determinations

Manual collection of rainfall was performed at this site. A single sample of rainfall for each rainstorm was obtained. The dry weight of the collection bucket was known and the weight of rainfall was determined by subtracting the dry weight of the bucket from the wet weight. Once this measurement had been determined, a 250 ml sample was taken.

Tracer Study

(i) Chloride

Chloride determinations were performed on all samples (see Section III.4).

(c) RG1: This site was located 450 m downstream from the hillslope plot and outside the watershed (Figure 2.2).

Hydrometric equipment

Rainfall was collected in a 2.5 cm o.d. polyethylene rain gage, positioned 1.5 m above the land surface. The volume of rainfall was recorded, and used to corroborate the volumes recorded from the Sierra Misco tipping bucket gages at sites PPT and PE1.

III.3B THROUGHFALL

Throughfall was monitored at four positions on the hillslope plot, TI, TW, TI2 and TFT (Figure 3.4):

(a) TI : This site was located 10 m upslope (Figure 3.4). Event throughfall collection was conducted at this site using three 7.5 cm o.d. 1 m long PVC trough collectors, erected at heights of 1 m, lying parallel to the ground surface. The passage of particulate matter into collection vessels was reduced by attaching an elbow collector to the end of each trough with a mesh across it. This arrangement allowed water to pass through to the drain at the end of the trough, but prevented any large particles from moving through.

Hydrometric equipment

Throughfall flow rates were determined from a Rainwise tipping bucket, housed in a plexiglass box. Water was directed from the trough collectors via 2.0 cm o.d. silastic tubing.

Collection of samples for chemical determinations

Sequential collection of throughfall was performed at this site. Water was collected in 500 ml and 1000 ml polyethylene bottles, arranged in a fill-spill configuration.

Tracer study

(i) Chloride

Chloride determinations were performed on all samples (see Section III.4)

(b) TW :This site was located 2 m upslope (Figure 3.4). Weekly collection of samples was performed. No hydrometric sampling was undertaken at this site.

Sample collection for chemical determinations

Throughfall was collected in a 13 cm o.d. polyethylene bucket within the 'wet' collection side of an Aerochem Metrics wet fall - dry fall collector (as described for rainfall collection at site, PE1).

Tracer Study

(i) Chloride

Chloride determinations were performed on all samples (see Section III.4).

(c) TI2 :This site was located 5 m upslope on the hillslope plot (see Figure 3.4).

Hydrometric Equipment

Throughfall flow rates were measured from a Sierra Misco tipping bucket.

(d) TFT : This site was located 2 m upslope on the hillslope plot (Figure 3.4). The temperature of incoming water was measured by routing throughfall, via a funnel, into a 250 ml bottle containing a BETATHERM Model 5K3D39 thermistor (Figure 3.5.a). When the bottle filled, water spilled out to allow new water in. The short-term variation in temperature that was measured was assumed to be caused by the incoming throughfall. Temperature data was recorded at 5 min intervals by a Campbell Scientific Model CR21X datalogger.

III.3C FOREST FLOOR SOIL WATERS

Forest floor soil water was collected from four sites, VI-0o, VI-0, VAo and VBo:

(a) VI-0o :This site was located outside the hillslope plot, 200 m downstream (Figure 2.1). Water was collected in a 1 m^2 stainless-steel pan lysimeter. The site was used from April 1994 to 11 July 1994.

Hydrometic equipment

Soil water flow rates were monitored using a Rainwise tipping bucket, housed in a plexiglass box. Water was directed from the drain on the lysimeter to the plexiglass box via 2.0 cm o.d. silastic tubing.

Sample collection for chemical determination

Sequential samples were collected using 500 ml and 1000 ml polyethylene bottles in a spill-fill configuration.

Tracer Study

(i) Chloride

Chloride determinations were performed on all samples (see Section III.4)

(b) VI-0 :This site was located 15 m upslope (Figure 3.4). Samples were collected for all storms after 11 July 1994 (i.e. when VI-0o was decommisioned). Water was collected in a 0.08 m^2 polyethylene pan lysimeter.

The same equipment was used for hydrometric monitoring and sample collection as used at site VI-0o. The same tracer studies were performed at this site

(c) VAo, VBo :These sites were located 15 m upslope (Figure 3.4). Sampling methods were the same at each site. Water was collected from 0.08 m^2 polyethylene pan lysimeters.

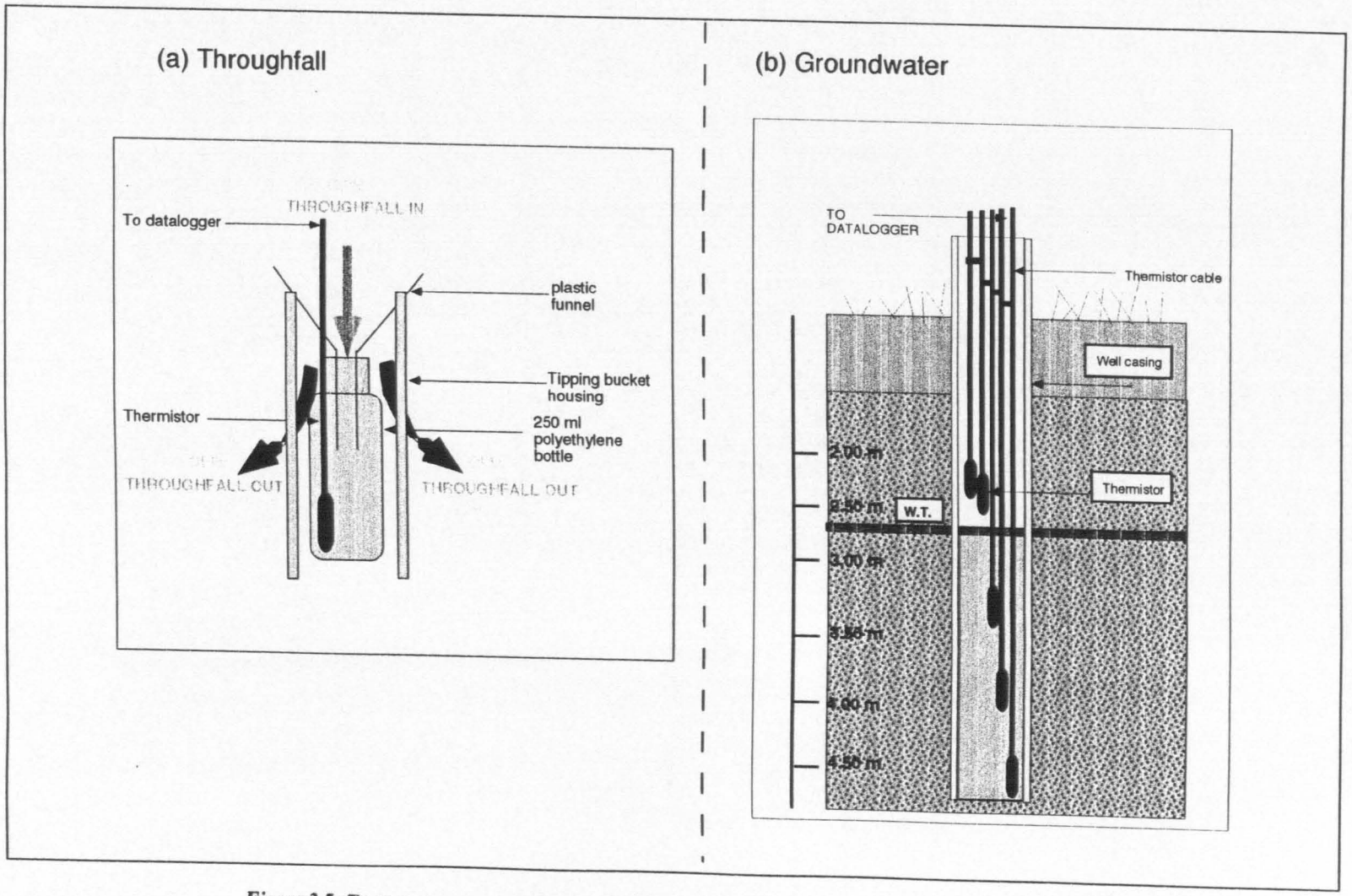

Figure 3.5: Temperature measurement equipment for th

Sample collection for chemical determinations

Each lysimeter was drained via a 2.0 cm o.d. silastic tube to a 1000 ml polyethylene bottle. Thus, up to 12 mm of forest floor soil water could be collected by each lysimeter. During some storms, the bottles were removed when full, and replaced with another so that a furthur manual sample could be taken.

Tracer study

(i) Chloride

Chloride determinations were performed on all samples (see Section III.4).

III.3D 15 cm SOIL WATERS

Soil water was monitored at 15 cm depth at eight sites, VI-15, VA_{15}, VB_{15}, VC_{15}, $TDRA_{15}$, $TDRB_{15}$, $TDRC_{15}$ and VT15 (Figure 3.4).

(a) VI-15 :This site was located 12 m upslope (Figure 3.4). Water was collected from two 0.23 m^2 stainless-steel pan lysimeters.

Hydrometric equipment

Flow was monitored using a Rainwise tipping bucket, housed in a plexiglass box. Water was directed from the drains in each lysimeter via PVC pipe, which was joined by an elbow connector, and was then directed to the lid of the plexiglass box via 2.0 cm o.d. silastic tubing.

Samples collected for chemical determination

Sequential samples were collected using 500 ml and 1000 ml polyethylene bottles in a fill-spill configuration.

Tracer Study

(i) Chloride

Chloride determinations were performed on all samples (see Section III.4).

(b) VA_{15}, VB_{15}, VC_{15} :

These sites were located 12 m upslope on the hillslope plot (Figure 3.4).

Sample collection for chemical determinations

Prior to each storm, lysimeters were filled with de-ionised water. The water was extracted using the sampling apparatus (a foot pump, a conical flask and associated tubing), so rinsing all equipment thoroughly. Twenty-four hours prior to rainfall , a negative pressure of 80 cb was applied to each lysimeter. Samples were collected 2 to 24 hours after rainfall ceased. In some cases, samples were collected during the storm and pressure was applied again in order to collect a series of samples. Samples were taken in 250 ml polyethylene bottles. The total amount of water collected by each lysimeter was recorded.

Tracer study

The same determinations were carried out as for VI-15.

(c) $TDRA_{15}$, $TDRB_{15}$, $TDRC_{15}$:

These sites were located 2 m (TDRA), 10 m (TDRB) and 15 m (TDRC) upslope.

Hydrometric equipment

Two 30 cm long, 5 mm o.d. stainless-steel probes were installed into the soil profile at each site, parallel to one another, at a distance of 25 cm apart. The pairs of rods were connected to an oscilloscope by coaxial cable with a constant impedance (Figure 3.5.a). The rods were installed laterally into the profile at a depth of 15 cm. The oscilloscope was interrogated by a Campbell Scientific Model CR10 datalogger at 5 min intervals.

(d) VT15

This site was located 10 m upslope. A rod was pushed into the soil surface to 15 cm depth, removed and a BETATHERM Model 5K3D39 thermistor installed in the space. The site was then back-filled with extracted material. Temperature data was recorded at 5 min intervals by a Campbell Scientific Model CR21X datalogger.

III.3E 40 cm SOIL WATERS

Soil water was monitored at 40 cm depth at seven sites, VA_{40}, VB_{40}, VC_{40}, $TDRA_{40}$, $TDRB_{40}$, TDRC40 and VT_{40} (Figure 3.4).

(a) VA_{40}, VB_{40}, VC_{40}

All chemical and tracer investigations are the same as those performed at sites VA_{15}, VB_{15}, VC_{15}.

(b) $TDRA_{40}$, $TDRB_{40}$, $TDRC_{40}$

All hydrometric investigations are the same as those performed at sites $TDRA_{15}$, $TDRB_{15}$, $TDRC_{15}$.

(c) VT40

This site was located 10 m upslope. A rod was pushed into the soil surfce to 40 cm depth, removed and a BETHATHERM Model 5K3D39 thermistor installed in the space. The site was then backfilled with extracted material. Temperature data was recorded from 40 cm depth at 5 min intervals by a Campbell Scientific CR21X datalogger.

III.3F 50 cm SOIL WATERS

Soil water was monitored at 50 cm depth at a single site, VI-50, located 20 m upslope at the hillslope plot (Figure 3.4). Water was collected from a 1 m^2 stainless-steel pan lysimeter.

(a) VI-50

Hydrometric equipment

Flow was monitored using a Rainwise tipping bucket, housed in a plexiglass box. Water was directed from the drain of the lysimeter along PVC pipe. The location of the tipping bucket was 2 m upslope. thus the water from the lysimeter travelled a distance of 18 m down the pipe before reaching the tipping bucket.

Sample collection for chemical determinations

Sequential collection of 50 cm depth soil water was performed at this site, using 500 ml and 1000 ml polyethylene bottles.

Tracer Study

(i) Chloride

Chloride determinations were performed on all samples (see Section III.4).

III.3G 70 cm SOIL WATERS

Collection Sites

Soil water was monitored at 70 cm depth in the soil at seven sites, VA_{70}, VB_{70}, VC_{70}, $TDRA_{70}$, $TDRB_{70}$, $TDRC_{70}$ and VT70

(a) VA_{70}, VB_{70}, VC_{70}

All chemical and tracer investigations are the same as those performed at sites VA_{15}, VB_{15}, VC_{15}.

(b) $TDRA_{70}$, $TDRB_{70}$, $TDRC_{70}$

All hydrometric investigations are the same as those performed at sites $TDRA_{15}$, $TDRB_{15}$, $TDRC_{15}$.

(c) VWT70

This site was located 10 m upslope. A rod was pushed into the soil surfce to 70 cm depth, removed and a BETHATHERM Model 5K3D39 thermistor installed in the space. The site was then backfilled with extracted material. Temperature data was recorded from 70 cm depth at 5 min intervals by a Campbell Scientific CR21X datalogger.

III.3H GROUNDWATERS

Groundwater was monitored from nine wells installed at the hillslope plot (Figure 3.4). Groundwater stage was monitored from three wells, located in the riparian zone (GWA), 5 m upslope (GWB) and 10 m upslope (GWC). Groundwater quality was monitored from four wells, screened 30 cm below the water table, at Sites GQA, GQB, GQCs and GQD, located in the riparian zone, 5 m upslope, 8 m upslope and 15 m upslope respectively. Groundwater quality was monitored from one well, screened 120 cm below the water table, at Site GQCd, located 8 m upslope. Finally, groundwater temperatures were monitored in well GT, located 5 m upslope.

(a) GWA, GWB and GWC

Hydrometric equipment

Groundwater stage was monitored at each of these sites using a potentiometer and a float-counterweight system. The groundwater stage potentiometers were monitored from Campbell Scientific Model CR21X and CR10 dataloggers (Peters, 1994). The dataloggers were programmed to record groundwater stage every 5 min.

(b) GQA, GQB, GQCs, GCd, GQD

The wells were constructed from 5.1 cm o.d. pipe, installed by hand auger to specified depths. Four of the wells were fitted with 30 cm long screens at the bottoms: GQA (150 cm below land surface), GQB (260 cm below land surface), GQCs (400 cm below land surface) and GQD (660 cm below land surface). Well GQCd (430 cm below land surface) was fitted with a 120 cm long screen.

Sample collection for chemical determinations

These wells were sampled during and after rainstorms using a portable peristaltic pump, extracting groundwater via a 2.0 cm o.d. silastic sampling tube. The wells were pumped dry and sampled after the well recharged, which was typically within a few minutes. Samples were taken in 250 ml polyethylene bottles.

Tracer study

(i) Chloride

Chloride determinations were performed on all samples (see Section III.4).

(c) GT1,....GT8

Tracer study

A 4.6 m deep well (GT) was drilled by hand auger and BETATHERM Model 5K3D39 thermistors were positioned in the well at depths of 2.1 m (GT1), 2.3 m (GT2), 2.4 m (GT3), 2.6 m (GT4), 2.7 m (GT5), 3.4 m (GT6), 4.0 m (GT7) and 4.6 m (GT8) (Figure 3.5b). Temperature data was recorded at 5 min intervals by a Campbell Scientific Model CR10 datalogger.

III.3I STREAMWATERS

Streamwater was monitored at the watershed outlet (lower gage, SWlg) and at a location within the drainage area containing the granite outcrop (upper gage, SWug), adjacent to the hillslope plot (Figures 2.1, 3.4). At each site, streamwater was monitored using a compound, sharp-crested 90° V-notch weir.

(a) SWlg - lower gage

Hydrometic equipment

Streamwater stage was measured using a potentiometer and a float-counterweight assembly. Discharge was determined from a stage-discharge rating using a Campbell Scientific Model CR21X datalogger (Peters, 1994).

Sample collection for chemical determination

Grab samples of streamwater **(SWlgm)** were collected at the V-notch weir. The bottles were rinsed with streamwater immediately before collection.

Streamwater samples were also collected sequentially with an ISCO model 2900 sampler **(SWlg)** (Peters, 1993). The ISCO was programmed to collect samples once stage height had risen by a user-selected increment over a specified time interval. The ISCO was capable of holding 24 x 1 litre bottles and thus able to automatically take up to 24 samples per storm.

Tracer study

(i) Chloride

Chloride determinations were performed on all samples (see Section III.4).

(ii) Temperature

A BETATHERM Model 5K3D39 thermistor was installed in the V-notch weir **(STlg)**, in the part of the stream reach that was perennial. Temperature was recorded at 5 min intervals by a Campbell Scientific Model CR21X datalogger.

(b) SWug - upper gage

Hydrometric equipment

Streamwater stage was measured using a potentiometer and a float-counterweight assembly. Discharge was determined from a stage-discharge rating (Peters, 1994) using a Campbell Scientific Model CR21X datalogger.

Sample collection for chemical determination

Grab samples of streamwater **(SWug)** were collected at the V-notch weir. The bottles were rinsed with streamwater immediately before collection.

Tracer study

(i) Chloride

Chloride determinations were performed on all samples (see Section III.4).

(ii) Temperature

A thermistor was installed in the V-notch weir (**STug**). The stream reach was ephemeral and the thermistor was not always immersed. Thus, for part of the study period, this thermistor was above the water surface and measured air temperature. Temperature was recorded at 5 min intervals by a Campbell Scientific Model CR21X datalogger.

III.4 LABORATORY ANALYSIS

All samples were stored in 250 ml polyethylene bottles and refrigerated at 4°C. A 90 ml aliquot was filtered through 0.45 μm cellulose acetate filter, of which 40 ml was shipped on ice within a day to a USGS laboratory in Boulder, Colorado, for determinations of dissolved organic carbon (DOC) and UV absorbance at a wavelength of 254nm . The remaining 50 ml aliquot was acidified with 200 μl nitric acid for analysis using direct current plasma (DCP) for Na^+, K^+, Mg^{2+}, Ca^{2+} and Si. The unfiltered aliquots were analysed for pH and specific conductance within 24 hours of collection using a Cole-Palmer 5800-05 solution analyser and then refrigerated. The refrigerated filtered samples were typically analysed within a couple of weeks for NO_3^-, SO_4^{2-} and Cl^- by ion chromatography, within a few days for NH_4^+ by colorimetry using a complexation reaction with nitroferricyanide and within a few days for alkalinity by Gran titration. Chemical analyses were performed in the Panola Laboratory, U.S.G.S., Atlanta, under the supervision of Ed Drake. With the excpetion of filtering, pH and conductivity analysis, all other chemical analyses were conducted by Ed Drake, with the assistance of Tim Pojunas and Dana Booker.

Data relating to the precision of analyses is provide in Appendix 3.1. In each set of analyses, reference standards were employed in order to assess the precision of determinations. The average and standard deviation concentrations of determinations of standards for all solutes employed by U.S.G.S. are shown in Appendix 3.1. The data shows that the lower the average concentration (and hence closer to the dectection limit), the greater the standard deviation of the determinations (hence the lower the precision of the analysis).

Chapter IV
HYDROMETRIC DATA ANALYSIS

IV.1 BACKGROUND

The movement of water through the various compartments of a hillslope control the timing and magnitude of streamwater response (Cosby *et al*, 1985; Woolhiser *et al*, 1985; Kennedy *et al*, 1986; Eshleman, 1988; Christophersen *et al*, 1990). Major flowpaths followed by rainfall were identified in Chapter I as: direct channel rainfall (Rawitz *et al*, 1970), throughfall and stemflow (Goudie *et al*, 1985; Tanaka *et al*, 1992; Crockford *et al*, 1996); overland flow (Horton, 1933; Hewlett and Hibbert, 1967; Dunne and Black, 1970); macropore flow (Beven and Germann, 1982; Mosley, 1979, 1982; Neilsen *et al*, 1986; Jones, 1987); matrix flow (Beven and Germann, 1982) and groundwater displacement and ridging (Sklash *et al*, 1986; McDonnell *et al*, 1990). Flowpaths followed by water have also been suggested to vary throughout a rainstorm's duration. For example, Mosley (1982) graphically presented possible pathways (matrix and macropore) for sub-surface flow and concluded that the actual pathways taken by water change over the duration of storm hydrographs and that hydrographs *'show little of the differences in relative importance of flowpaths over time'*. This view is echoed by that of Beven (1989). He illustrates problems arising with hydrograph separation techniques in their inability to attribute components of streamflow to geographical source areas to account for realistic runoff generation and declares that:

'In many circumstances, we must consider such detailed descriptions of the surface and sub-surface characteristics of a watershed to be essentially unknowable from a modelling perspective'.

Thus, the application of traditional hydrograph separation techniques often result in inaccurate predictions of the source waters to storm runoff, since the approach tends to ignore important flowpaths in the system altogether (Jenkins *et al*, 1994), and fails to incorporate variations in the relative importance of flowpaths in the model structure. A more robust approach may be achieved with small scale investigations, which use intensive sampling configurations. The transit of rainfall through the hillslope location at PMRW was monitored along a one-dimensional pathway (Chapter III). Individual flowpaths followed by rainfall could be rigorously monitored using this sampling structure. The employment of intensive hydrometric sampling allowed calculation of the times of flow onset, maximum flow and flow cessation. Dominant flowpaths in the system could thus be assessed, so could the variation in their contribution throughout the storm. Comparison of response times at all nodes in the system allowed consideration of source waters to storm runoff.

The overall aim of Chapter IV is to identify which flowpaths are important for transport of water in terms of its magnitude and the rapidity of flow. Each flowpaths' contribution is assessed throughout a rainstorm. The factors that may influence the operation of the flowpath throughout the storm duration are also assessed, e.g. rainfall intensity, antecedent moisture conditions, rainfall magnitude and duration.

IV.2 AIMS

The aim of this analysis is to assess the operation of the following flowpaths in the transport of rainwater at PMRW:

(a) Throughfall and canopy processes
(b) Overland flow
(c) Macropore flow
(d) Matrix flow
(e) Groundwater displacement/ridging

The following section provides hypotheses of trends expected in the data and the calculations employed to provide a more quantitative description of the flowpath. Finally, the actual results are outlined and discussion follows, assessing whether the observed patterns corroborate the expected patterns. Several case study storms are presented, illustrating storms where the expected and observed patterns match well, and in some cases where this flowpath is found to be unimportant.

Thus, flowpaths that are important for water transport at the hillslope situation at PMRW are presented. Comparison of their response times and magnitude is made and thus some assessment is made of their interaction with one another.

IV.3 STORMS AND DATA

IV.3A Storms

Between one and two storms were sampled per month (Chapter III). Hydrometric and chemical data were collected for storms of varying intensities and durations (Appendix 4.1). The influence of antecedent moisture conditions (Appendix 4.2), rainfall intensities (Appendix 4.3) and the effects of seasonality on both flow rates and chemistry along flowpaths were assessed. Figure 3.1 shows the selected rainstorms.

The investigation was carried out over a 13 month period, from April 1994 to May 1995. Forty storms were sampled hydrometrically over this time frame. An array of rainstorms were sampled, with varying magnitudes, durations and antecedent moisture conditions. Rainfall totals ranged from 6 mm (11 April 1995) to 175 mm (4 July 1994) (Appendix 4.1). The watershed experienced two tropical storms during the study period; The first (Tropical Storm Alberto: 175 mm) occurred on 4 July 1994, and was followed by numerous, smaller magnitude storms during the following week. The second (Tropical Storm Beryl: 60 mm) occurred on 16 August 1994.

Four of the 40 rainstorms exceeded 60 mm in magnitude (high magnitude rainstorms). Seventeen of the remaining rainstorms were between 20 and 60 mm (medium magnitude rainstorms) and the

remaining 19 were below 20 mm (low magnitude rainstorms) (Appendix 4.1). Rainfall intensities varied greatly: maximum 5 min rainfall intensities exceeded 5 mm in only seven storms, and for over half of the rainstorms, maximum 5 min rainfall intensities did not exceed 2 mm (Appendix 4.3). High intensities were encountered in low, medium and high magnitude rainstorms and no seasonal trend was apparent.

The rainfall seasons are divided into two categories: the 'growing' season (from April through September) and the 'dormant' season (from October through March). Twenty-four rainstorms occurred during the growing season and 16 occurred during the dormant season (Appendix 4.1).

Antecedent moisture conditions also varied greatly amongst storms. Several measures were used to express antecedent conditions, e.g. the total rainfall occurring in defined intervals prior to the onset of the rainstorm (Appendix 4.2). If the example of total rainfall in the previous week is used, the range of values for the rainstorms sampled is 0 mm (1 September 1994) to 242 mm (12 July 1994).

It will be appreciated that a wide range of conditions were encompassed by the choice of storms, and thus the operation of each flowpath can be assessed for a series of storms with different hydrological characteristics.

IV.3B Comparison of 1994 - 1995 water year with previous years

Water year	All storms	Growing season storms	Dormant season storms
1986 - 1987	113	36	77
1987 - 1988	77	36	41
1988 - 1989	101	59	42
1989 - 1990	170	89	81
1990 - 1991	104	52	52
1991 - 1992	132	85	47
1992 - 1993	153	73	80
1993 - 1994	96	32	64
1994 - 1995	155	95	60

Table 4.1: *Total rainfall (cm) at PMRW for (a) yearly (April to March), (b) Growing season, (c) Dormant season storms, between 1986 and 1995 (data from PMRP database).*

Table 4.1 shows total rainfall at PMRW over the past 10 years. Rainfall totals are provided on a yearly basis (from April through March of the following year). The study period (April 1994 to March 1995) was one of high yearly rainfall (155 cm). The growing season was the wettest on record (95 mm), due to the occurrence of the two tropical storms. The dormant season experienced moderate rainfall (60 cm), compared with other years.

Figure 4.1 displays rainfall amounts over the 10 year period. The diagram shows the high rainfall amount that occurred in the growing season of 1994. This is due to high rainfall during July 1994 (46 cm). Rainfall during the dormant season was average, compared with other years. However, relatively high rainfall occurred in February 1995 (19 mm) compared to the dry conditions experienced in previous two months (5 and 8 cm for December and January, respectively). The occurrence of very high rainfall in the summer, when conditions would 'normally' be drier, has a

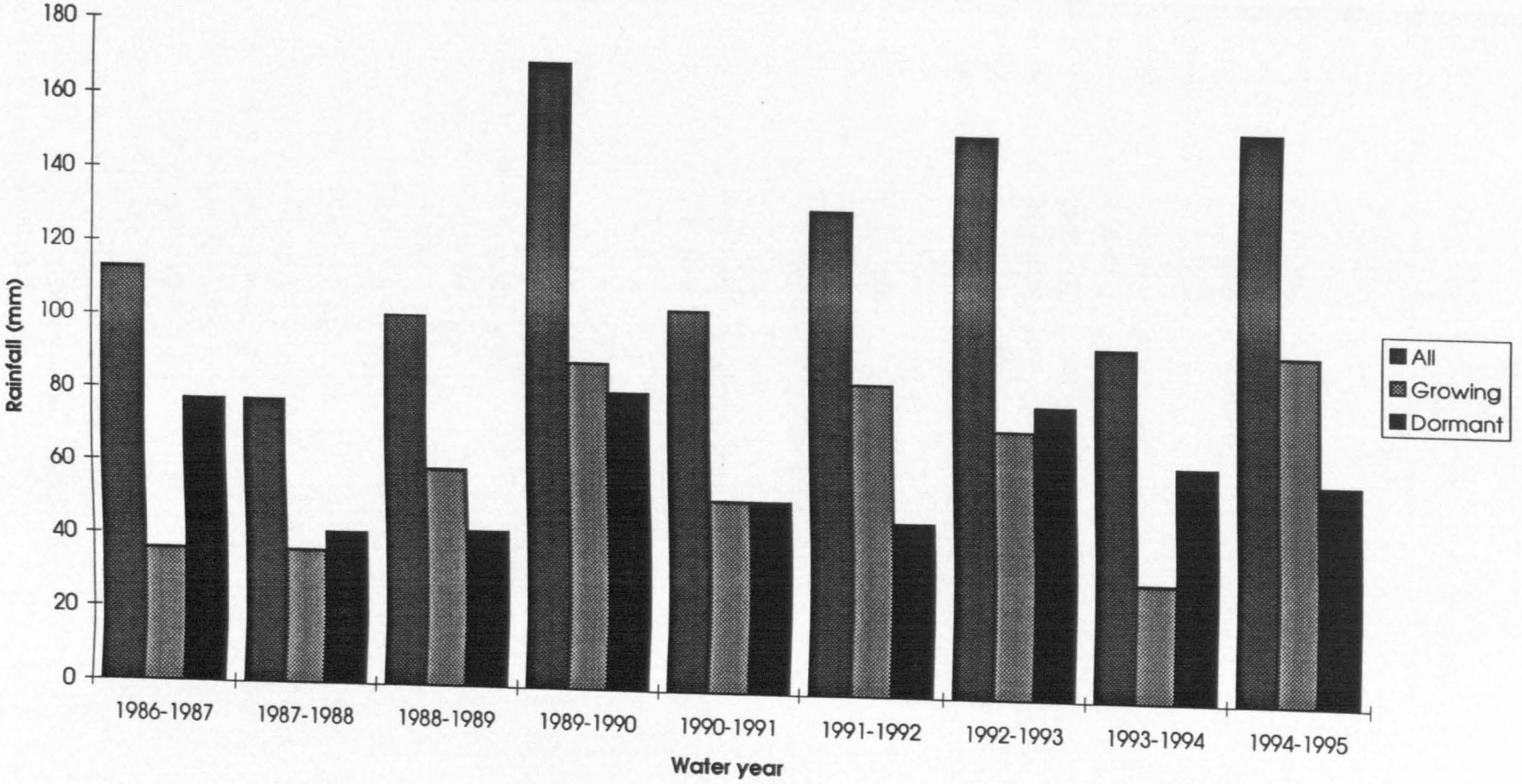

Figure 4.1: Total rainfall during all storms, growing season storms and dormant season storms for water years from 1986 - 1995 (water year is taken from April to March, inclusive).

major effect on the hydrology of the site, and the results of the investigation might therefore be atypical of the hydrology of the site during the growing season.

IV.3C Data Collection

Twenty-one of the 40 rainstorms were sampled both hydrometrically and chemically (Appendix 4.4), whereas the remaining 19 storms were only sampled hydrometrically.

IV.3D Data Format

Data was obtained from a selection of apparatus (Chapter III), all of which output information to dataloggers at different time intervals. In order for response times at various nodes to be compared, output from each piece of equipment will be presented at 5 min intervals. Cumulative flow at each node (i.e. tipping bucket data) was output every 5 min. 'Instantaneous' values were output every 5 min for streamwater and groundwater stage. TDR values were averaged over 5 min. Although the resolution of the data was reduced in some instances, it facilitated the comparison of flow at all nodes.

IV.4 FLOWPATH INVESTIGATION

IV.4A Introduction

The following section is divided into segments, each segment dealing with a specific flowpath or node. The segments are as follows:

- Canopy processes: throughfall, stemflow and interception
- Forest floor soil water flow and overland flow
- Matrix flow
- Macropore flow
- Groundwater responses

Answers are sought, where possible, for the following general questions:

(i) Can the operation of the flowpath be identified at the hillslope?

(ii) Is there spatial heterogeneity in the flowpath?

(iii) Is there temporal heterogeneity in the flowpath?

(iv) What are the controls on the flowpath operation?

Each segment will now be considered in turn:

IV.4B THROUGHFALL AND CANOPY PROCESSES

The following questions will be addressed in this section:

(i) What quantity of rainfall is translated to throughfall?

(ii) Is there a seasonal pattern to throughfall volumes?

(iii) Can spatial heterogeneity in throughfall be detected?

(iv) Can temporal variability in throughfall be detected?

(v) What parameters control the spatial and temporal variability in throughfall?

(vi) Can interception loss be calculated?

(IV.4Bb) Hypothesised patterns

(i) Conversion of rainfall to throughfall

In general, the correlation between cumulative throughfall and rainfall would be expected to be close to 1.0. The deviation from this relationship is controlled by a series of factors, (which will be discussed in detail in following sections) for example, abundance of leaves, development of drip points and rainfall intensity. Previous study at PMRW (Cappellato, 1991) suggests that the amount of throughfall measured will approximate 95% of rainfall. Analysis of data collected in some studies produced a similar estimate (e.g. Neal *et al*, 1990), whereas others produced a lower figure of 70 to 80% (Gash *et al*, 1980; Loustau *et al*, 1992; Robson *et al*, 1994). Thus, throughfall volumes are expected to approximate between 70 and 95% of total rainfall. Significant variation between results obtained in the current and previous studies (Cappellato, 1991) at PMRW would suggest significant spatial heterogeneity in throughfall.

(ii) Seasonal pattern of throughfall

Previous study at PMRW (Cappellato, 1991) found higher throughfall volumes in the dormant season than during the growing season. This trend has been observed in other studies (Neal *et al*, 1990; Loustau *et al*, 1992). The higher leaf cover in the growing season results in higher interception losses and hence less throughfall. A similar trend in anticipated in the current data.

(iii) Spatial heterogeneity of throughfall

High spatial heterogeneity has been found in numerous throughfall studies (Gash, 1979; Herwitz, 1987; Neal *et al*, 1990; Loustau *et al*, 1992; Robson *et al*, 1994), and hence some degree of spatial heterogeneity would be expected at PMRW.

Comparison of throughfall volumes with those collected in the previous investigation (Cappellato, 1991) for similar magnitude storms may provide some indication of the spatial heterogeneity in throughfall at PMRW. Variability will depend on tree type, tree density, penetration of the canopy by wind and the height of the lowest branches which drain intercepted water. The occurrence of 'drip points' and 'sheltered areas' in the canopy have also been found to affect throughfall variability (Herwitz, 1987; Neal *et al*, 1992; Robson *et al*, 1994).

(iv) Temporal variability of throughfall

The temporal variability of throughfall and rainfall are expected to be similar, with periods of intense throughfall corresponding to periods of intense rainfall. Variation between patterns may be due to variations in the spatial distribution of rainfall or vegetative cover between the site where rainfall is monitored (PPT) and where throughfall is monitored (TI).

(v) Controls on temporal and spatial variability of throughfall

Rainfall magnitude has been found to influence the form of throughfall that dominates (Loustau *et al*, 1992). In small storms, 'free throughfall' (i.e. direct transmission of rainfall to the ground) dominates, due to reduced influence of rain splash mechanisms. In larger storms, 'sensu stricto throughfall' (i.e. water dripping from the canopy) dominates (Gash, 1979; Loustau *et al*, 1992). Rainfall intensity has been found to influence the operation of drip points. In more intense rainstorms, the efficiency of drip points increases (Herwitz, 1987; Neal *et al*, 1992; Loustau *et al*, 1992; Robson *et al*, 1994).

Variations in rainfall intensity over an area may explain variations of throughfall and rainfall, since the two nodes were monitored at different locations within the watershed. Throughfall volumes have also been shown to vary with distance from the trunk (Robson *et al*, 1994). Low input areas correspond to regions most distant from the tree trunk (Robson *et al*, 1994). A combination of these factors explains heterogeneity in throughfall.

(vi) Calculation of interception loss

Interception loss is that fraction of rainfall that is held in the canopy and is subsequently evaporated (Goudie *et al*, 1985; Crockford *et al*, 1996). Interception is generally 25 - 30% of rainfall (Gash *et al*, 1980). However, in a previous study at PMRW (Cappellato, 1991), interception loss was found to be negligible. This figure appears inaccurate, since high interception loss would be anticipated from a deciduous canopy in a warm, temporal sub-tropical climate (Ball, 1994). Interception loss can be calculated as the difference between total rainfall and total throughfall plus total stemflow.

(IV.4Bc) Equipment and Calculations

(i) Equipment

In the current study, throughfall was monitored at two locations on the hillslope site; at TI using a rainwise tipping bucket (collecting from troughs of surface area 2250 cm^2) and TI2, using a Sierra Misco tipping bucket (of surface area 177cm^2). Rainfall was monitored at Site PPT (see Chapter III), from a Sierra Misco tipping bucket (of surface area 177 cm^2). In the previous study at PMRW (Cappellato, 1991), throughfall and stemflow were measured in four plots within the deciduous forest (Sites 551, 652, 661 and 662). At each plot, four throughfall collectors were installed randomly, consisting of 16.8 cm o.d. funnels connected to 1 litre density polypropylene bottles. Stemflow was collected by installing polypropylene collars (20 cm) at breast height on two duplicates of the six most important tree species (Chapter II). Stemflow was collected in 220 litre plastic containers. Rainfall was collected from Site PE1 (located on the granite outcrop) from an Aerochem wet fall - dry fall collector.

(ii) Throughfall and rainfall data

Rainfall and throughfall volumes were output at 5 min intervals. The 5 min data was cumulated for rainfall and throughfall to provide totals for all rainstorms. To provide an estimate of the amount of

rainfall that passes through the canopy, a simple linear regression was performed between cumulative rainfall and cumulative throughfall totals for a sub-set of storms. The assumptions made in the application of a simple linear regression are recognised. A similar approach was used in a previous investigation at PMRW (Cappellato, 1991), and thus, in order to compare the results of this and the current investigation, the use of regression is merited. This approach also allows calculation of the amount of canopy interception (see (iii))

(iii) Interception calculation

Interception (I) can be calculated by subtracting total throughfall plus stemflow from total rainfall. i.e.

$$I = \text{Tot PPT} - (\text{Tot TI} + \text{Tot SF})$$

Eqn 4.1a

Another procedure is to use the intercept term in the regression plot of throughfall on rainfall, since the intercept corresponds to the amount of rainfall required before throughfall is initiated, i.e. the amount of rainfall that does not penetrate the canopy.

(IV.4Bd) Results and discussion

(i) **Conversion of rainfall to throughfall**

Data from a total of 30 storms were analysed in this section (Appendix 4.5). The cumulative data for throughfall and rainfall is presented graphically in Figure 4.2a. The graph illustrates a positive relationship between throughfall and rainfall, as would be expected. The relationship between throughfall and rainfall in previous studies has been shown to tend to rainfall=throughfall, although in most studies, throughfall usually comprises between 70 - 95% rainfall (Gash *et al*, 1980; Neal *et al*, 1990). In Figure 4.2a, several outliers have been identified, where the amount of throughfall that was recorded exceeded rainfall. This is physically impossible, and may be explained by factors including positioning of equipment beneath drip points in the canopy, or perhaps due to variations in rainfall intensity across the catchment. These factors will be discussed in more detail, when assessing the degree of spatial heterogeneity in throughfall (in section iii).

When these outliers are removed from the analysis, and hence where data that is only physically possible is presented (in Figure 4.2b), a similar positive relationship is observed. If a simple linear regression is applied to the data, the equation that is obtained is as follows:

$$\text{Cum TI} = -1.7 + 0.8\ \text{Cum PPT}$$

Eqn 4.1b

An R^2 of 0.95 and a p-value of < 0.0001 are obtained, suggesting that the result is statistically significant. Hence, the equation indicates that throughfall approximates 78% rainfall, which lies within the range of values obtained during other investigations (Gash *et al*, 1980; Loustau *et al*, 1992; Robson *et al*, 1994). The intercept term of - 1.7 provides a value for the degree of interception; indicating that a total of 1.7 mm of rainfall is lost to this mechanism (or 1.7 mm of rainfall must occur before throughfall is initiated).

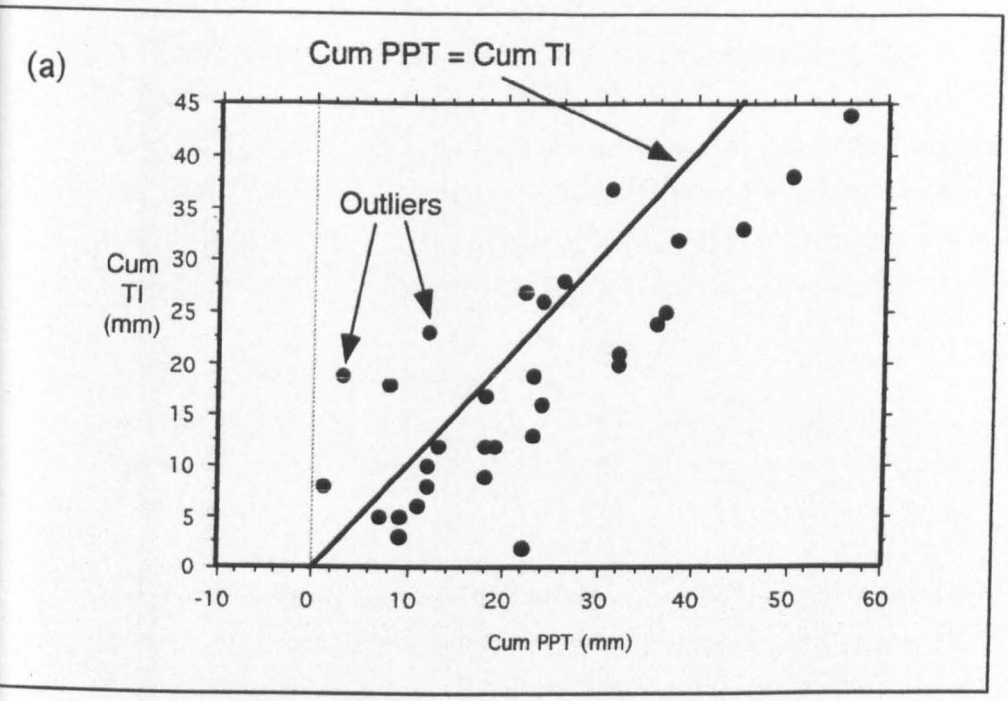

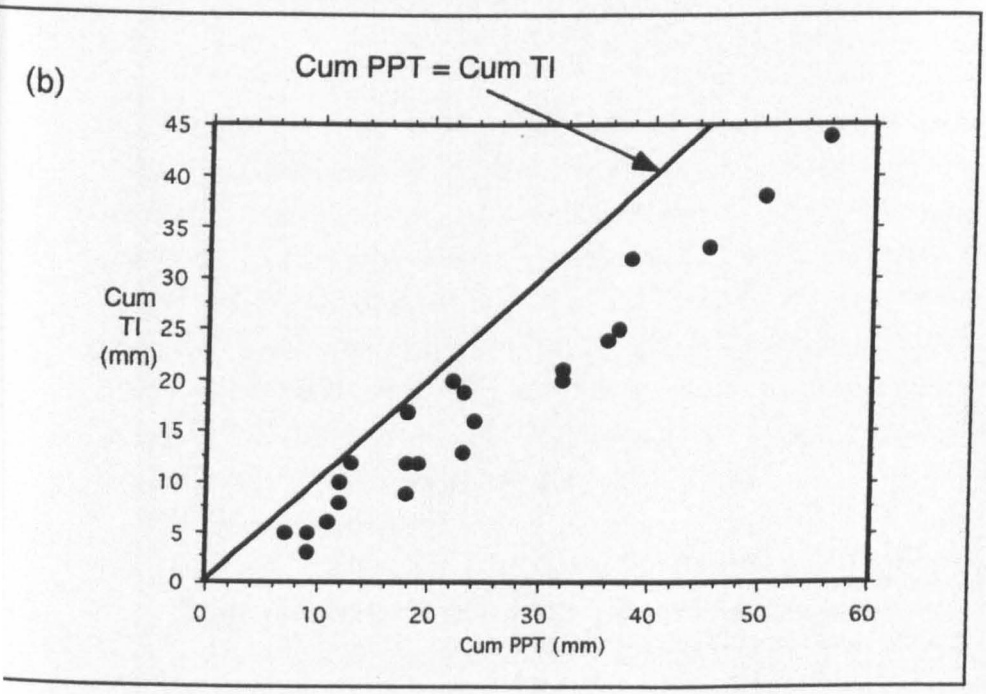

***Figure 4.2**: Cumulative throughfall vs cumulative rainfall for (a) All storms; (b) Storms for which data is physically realistic (i.e. outliers removed)*

In a previous investigation into the relationship between rainfall and throughfall at PMRW by Cappellato (1991), a similar statistical procedure was applied to the data (and hence merits the use of simple linear regression in the current investigation). In that case, a regression equation was obtained which suggested that throughfall was equivalent to 95% of rainfall. Hence, the previous study at the same catchment indicated a much greater amount of rainfall was able to penetrate the canopy as throughfall, a result that is attributed to high spatial heterogeneity of throughfall (see section iii).

(ii) **Seasonal pattern of throughfall**

The storms analysed in the current and previous study were divided into those occurring during the growing season (April to September, inclusive) and those occurring in the dormant season (October to March, inclusive).

Dormant season storms

In the analysis of dormant season storms, only those storms where physically realistic data is available are used. The data is shown in Figure 4.3a and a linear regression was again applied to the data in order to make some assessment of the amount of interception and the relationship between rainfall and throughfall during this season. The equation of the regression line is as follows:

$$\text{Cum TI} = -0.5 + 0.8\ \text{Cum PPT}$$

Eqn 4.1c

An R^2 of 0.95 and p-value of < 0.0001were obtained, which again suggests that the relationship is statistically significant. The equation suggests that throughfall is equivalent to 79% rainfall. The intercept term provides a value for the amount of interception that occurs, which is 0.5 mm. A low value for interception would be expected during the dormant season, due to absence of leaves.
The previous investigation (Cappellato, 1991) generates a different regression equation of throughfall on rainfall for dormant season storms (10 storms in total). The equation suggests that throughfall is equivalent to 95% rainfall. Hence, during the dormant season, the amount of rainfall that penetrates the canopy in the current study was found to be substantially less than in the previous investigation, a result that is again attributed to spatial heterogeneity of throughfall.

Growing Season Storms

Only storms for which the data is physically possible have been used in the analysis of growing season storms. The data is presented in Figure 4.3b. The number of storms for which data is available are small, due to the large number of outlier storms in Figure 4.2a occurring during the growing season. The graph shows that for smaller magnitude storms (< 15 mm rainfall), slightly more rainfall penetrates the canopy than for the larger storms (> 15 mm rainfall), which is probably due to variations in rainfall intensity. Although only 9 storms are used in the analysis, a regression line was drawn through the data in order to obtain some indication of the amount of interception. The equation obtained for the regression is:

$$\text{Cum TI} = -2.5 + 0.8\ \text{Cum PPT}$$

Eqn 4.1d

(a)

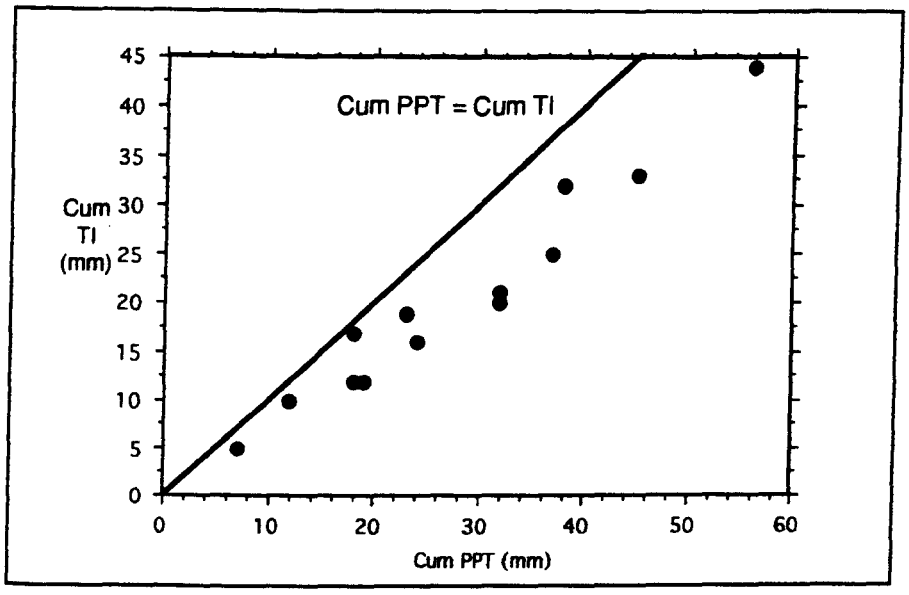

(b)

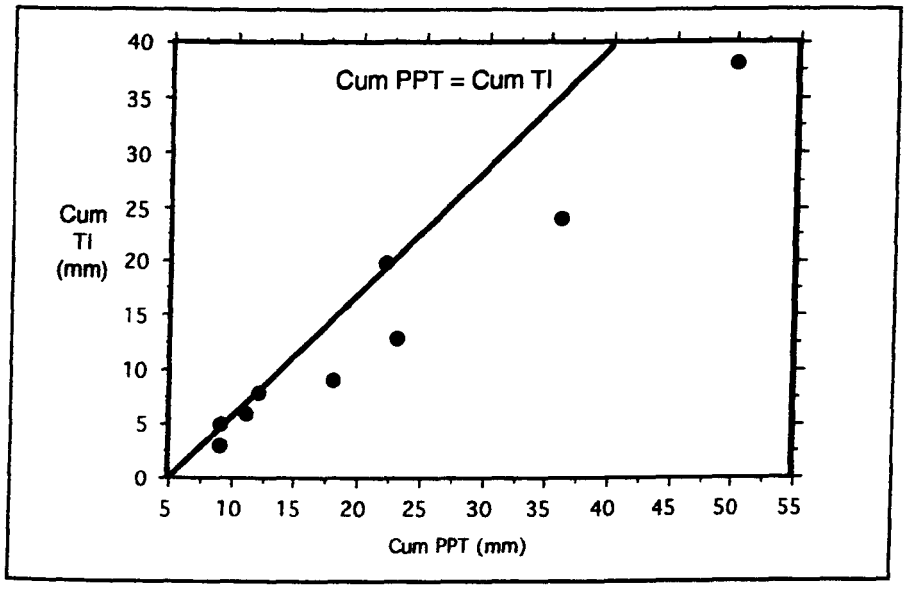

***Figure 4.3**: Cumulative rainfall vs. cumulative throughfall for (a) dormant season storms; (b) growing season storms*

An R^2 of 0.96 and a p-value of < 0.0001 were obtained, suggesting that the relationship was statistically significant. The equation suggests that throughfall is equivalent to 78% rainfall, but it must be recognised that this relationship has been calculated from only 9 storms. A more valuable result from the regression is the intercept term of - 2.5, suggesting that during the growing season, interception by the canopy is equivalent to 2.5 mm rainfall. As expected, interception is much greater during the growing season than during the dormant season (due to presence of the canopy).

In the previous investigation at PMRW, during the growing season, total throughfall was found to be equivalent to 96% rainfall.

Thus, seasonality in throughfall was not significant. Throughfall totals were slightly higher during the dormant season, which is consistent with the hypothesised trends. Seasonality was shown in interception losses, which were almost 5 times higher in the growing season than the dormant season.

The % values of throughfall in terms of rainfall calculated for the current investigation were substantially lower than those calculated by Cappellato (1991) in the previous study at PMRW. A reason for this variation may be spatial heterogeneity in throughfall which will be considered in greater detail in the following section. The reason why greater throughfall totals than rainfall totals were recorded for some storms will also be discussed in a following section.

(iii) Spatial heterogeneity of throughfall

The results of the previous sections suggest that there may be significant spatial heterogeneity in throughfall in the deciduous canopy at PMRW. The regression analyses performed on the data from Cappellato (1991) used the average throughfall volume collected from 16 sites for each storm (Appendix 4.6). This approach suppresses any spatial heterogeneity that exists in the data. Hence, to explore this in more detail, all throughfall volumes were retrieved for all sites for 28 storms, and individual regressions of throughfall on rainfall were calculated for all sites.

Figure 4.4 displays a scattergraph of throughfall volumes at all sites for all storms. Rainfall total is also shown. A great deal of variability is visible in the data, which suggests that even though average throughfall from all sites correlates well with total rainfall for individual storms, the location where throughfall is measured has a major control on the volume obtained. Regression analyses were performed on total throughfall and total rainfall for each Site (Table 4.2). When each equation was solved (i.e. when PPT = 100%), the total throughfall ranges from 83% to 93% of rainfall, which is broadly the spectrum of figures encountered in all other investigations (Gash *et al*, 1980; Loustau *et al*, 1992; Robson *et al*, 1994).

Hence, when the sites are investigated on an individual basis, for some locations the amount of throughfall collected approached the average value of 78% obtained in the current investigation. When the average throughfall value was recalculated from data collected in the previous study, the figure that was obtained was 87%, not 95%, which is reported by Cappellato (1991). This also seems a more reasonable figure, since it allows for some interception loss.

Thus, the inter-comparison of the current throughfall volumes with throughfall volumes collected at 16 sites for storms between October 1987 and December 1989 provide evidence of high spatial

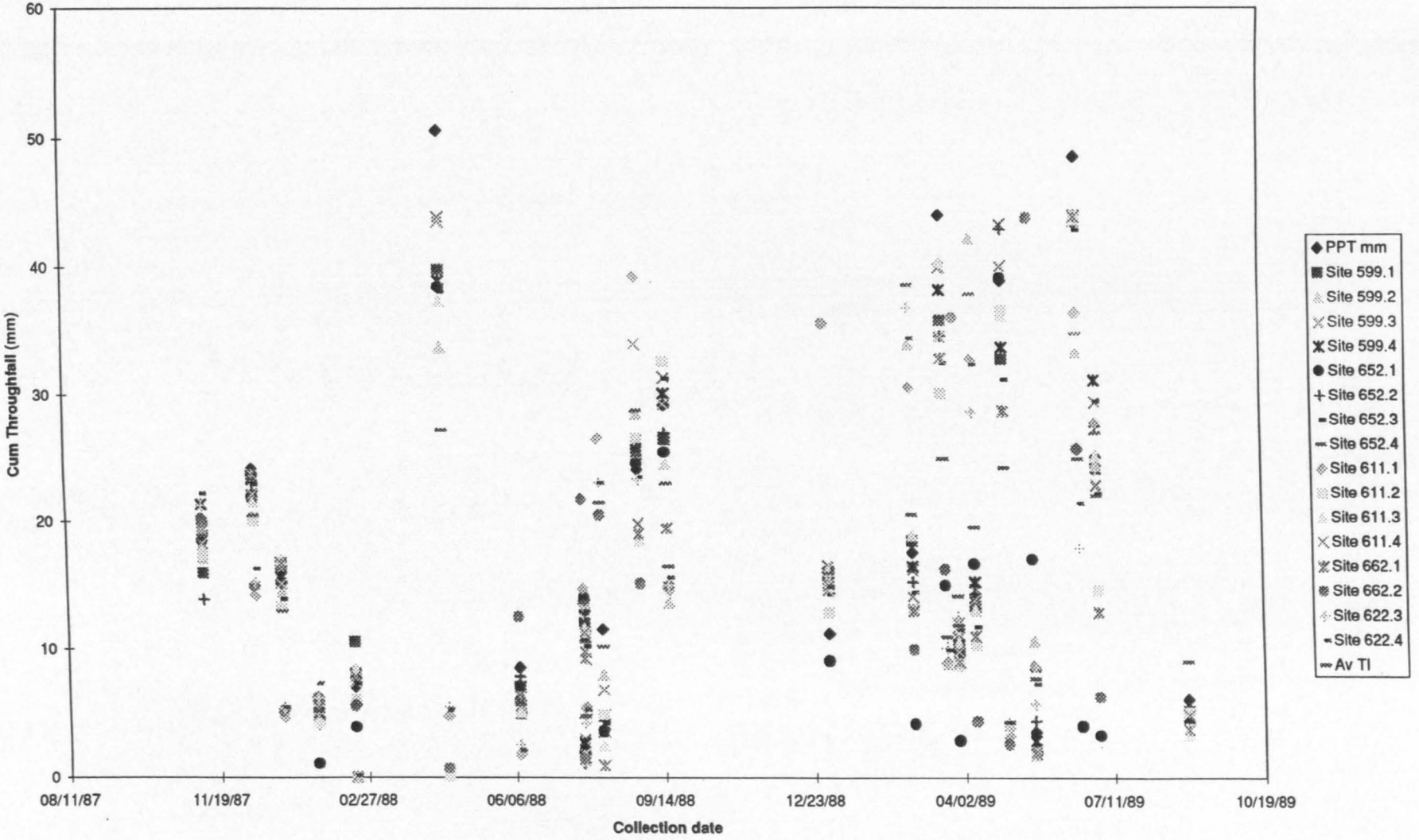

***Figure 4.4** : Throughfall and rainfall volumes collected during 1987 to 1989 (Cappellato, 1991), from sixteen positions within the deciduous region of PMRW.*

heterogeneity in throughfall at this location. The factors that control the degree of spatial heterogeneity will be explored further in the next sections.

Site	Regression Equation	r^2(adj)	r	p	TI (% tot PPT)
511.1	TI = 1.36 + 0.84 PPT	95.3	0.98	0.00	87
511.2	TI = 0.17 + 0.93 PPT	87.0	0.94	0.00	93
511.3	TI = -0.229 + 0.93 PPT	95.1	0.98	0.00	93
511.4	TI = 1.28 + 0.87 PPT	93.6	0.97	0.00	90
652.1	TI = 1.03 + 0.82 PPT	93.4	0.97	0.00	84
652.2	TI = 0.88 + 0.88 PPT	92.1	0.96	0.00	90
652.3	TI = 0.42 + 0.82 PPT	94.6	0.97	0.00	83
652.4	TI = 0.48 + 0.90 PPT	95.3	0.98	0.00	91
661.1	TI = 0.25 + 0.89 PPT	87.1	0.94	0.00	90
661.2	TI = - 1.23 + 0.90 PPT	85.8	0.93	0.00	87
661.3	TI = 0.11 + 0.88 PPT	92.8	0.97	0.00	88
661.4	TI = 6.88 + 0.76 PPT	27.1	0.55	0.01	90
662.1	TI = - 0.39 + 0.80 PPT	91.0	0.96	0.00	79
662.2	TI = - 0.20 + 0.87 PPT	94.0	0.97	0.00	87
662.3	TI = - 0.30 + 0.88 PPT	94.2	0.97	0.00	87
662.4	TI = 0.42 + 0.88 PPT	95.0	0.98	0.00	89
Average	TI = 0.83 + 0.85 PPT	95.5	0.98	0.00	87

***Table 4.2** : Relationships between total throughfall and total rainfall for rainstorms from October 1987 to September 1989, collected at 16 Sites within the deciduous forest area at PMRW (after Cappellato, 1991). Regression equations, r2, r and p values are provided. Throughfall is expressed as a % of total rainfall by solving each regression equation*

(iv) Temporal variability between throughfall and rainfall

The temporal variability in throughfall was hypothesised to be similar to that of rainfall during rainstorms. In general, 35% of storms experienced throughfall within 15 min of the onset of rainfall, and most storms experienced throughfall within 40 min of the onset of rainfall. Storms that took longer than this for throughfall to be detected typically received very low rainfall initially, too low to initiate throughfall and in which the intercepted rainfall was lost to interception (e.g. 23 September 1994). 40% of the storms experienced throughfall up to an hour after rainfall had ended, and for the remainder of the storms, throughfall was detected for longer time periods, even though throughfall was very low intensity. Examples of two case study storms (4 December 1994 and 16 September 1994) follow, which display the similarity in temporal patterns of throughfall and rainfall.

Case study storm: 4 December 1994

This storm occurred in the dormant season storm and is marked by having periods of both high and low intensity rainfall (Figure 4.5.a). Rainfall begins at 1:50 on 4 December and throughfall begins some 35 min later. Initially, rainfall is gentle, but then becomes rapid at 9:10 on 4 December. Throughfall responded 5 min later. Rainfall then proceeds to be less intense until 11:35, which is again mimicked by the throughfall pattern, where intense flow occurs at 11:35. The intense period of rainfall ceases at 17:35, with a total cumulative volume of 23 mm. The intense period of throughfall ceases 15 min after rainfall at 17:50, with a total cumulative volume of 16 mm. However, throughfall

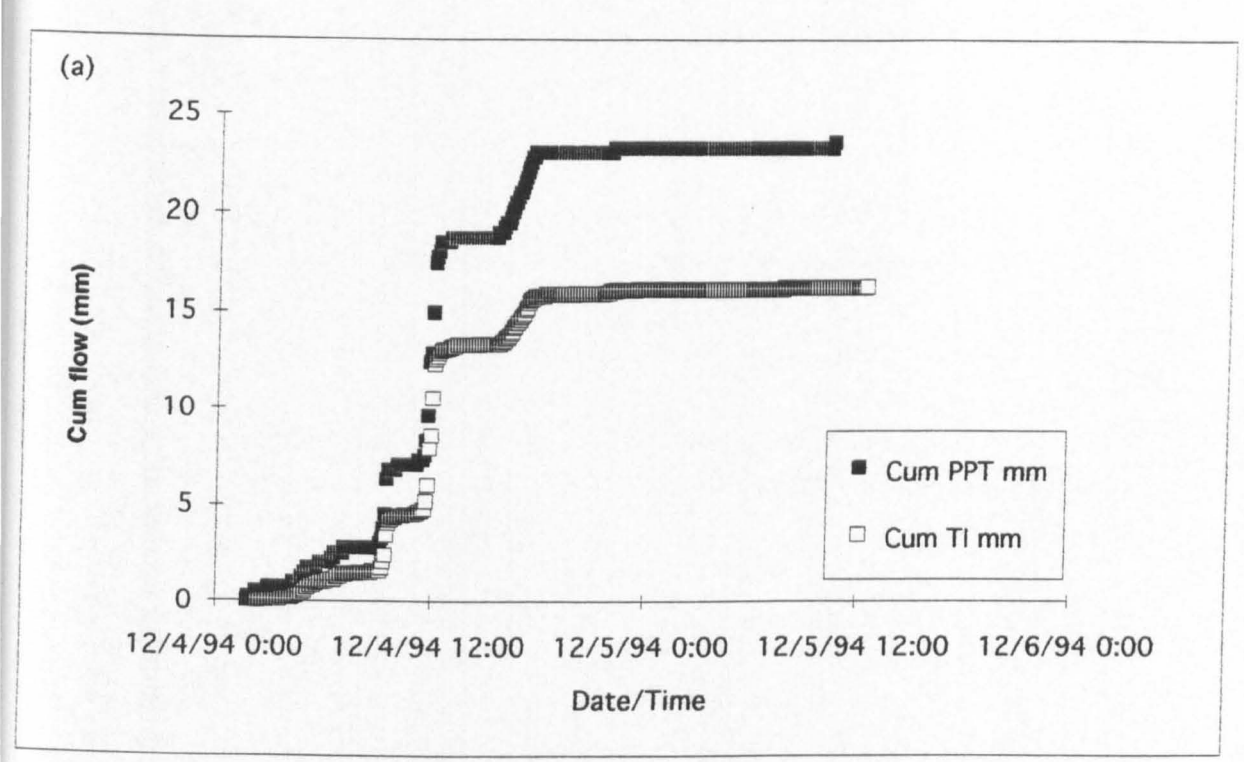

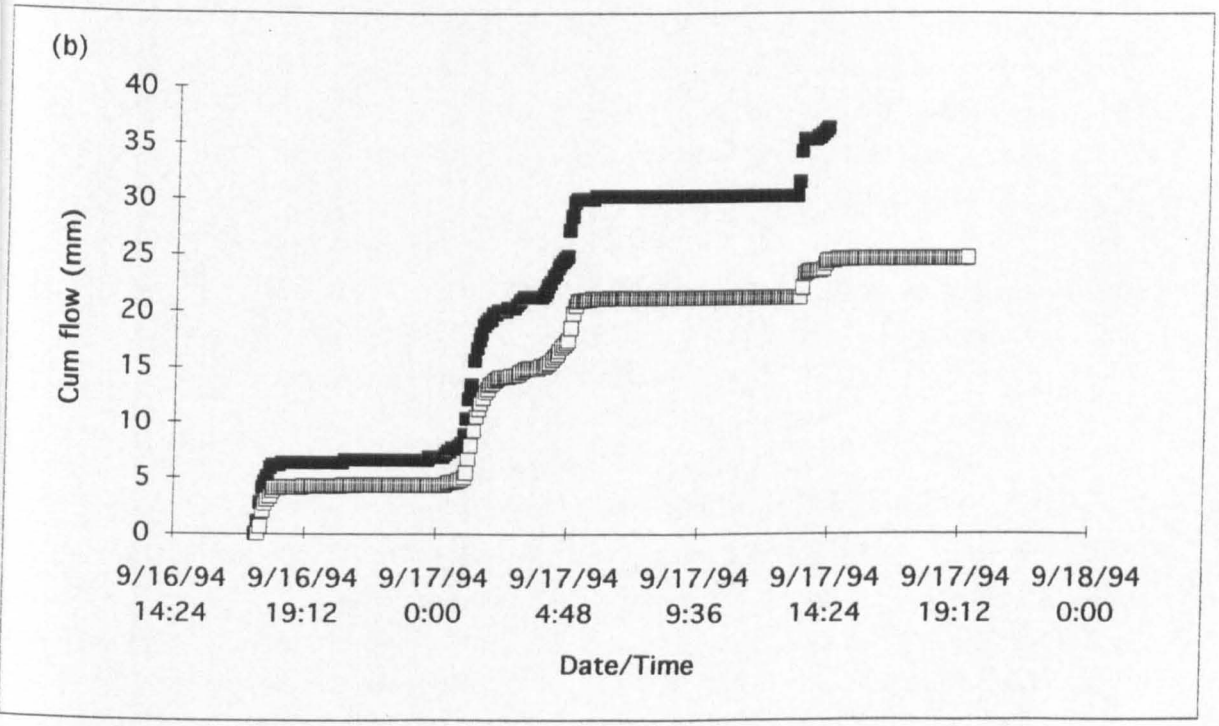

Figure 4.5. Relationship between cumulative rainfall (PPT) and cumulative throughfall (TI) on (a) 4 December 1994 and (b) 16 September 1994

continues to drain with a steady flow of 0.058 mm per hour until it finally ceases at 23:35, with a total cumulative volume of 16 mm. The storm throughfall was 70% of the rainfall.

Case study storm: 16 September 1994

This occurred in the growing season, and is marked by a long duration, having periods of both high and low intensity (Figure 4.5b.). Rainfall begins at 17:30 on 16 September and throughfall begins 5 min later. Initially rainfall is intense, as is throughfall. The second major burst of rainfall occurs at 00:20 on 17 September. Throughfall becomes intense at the same time (00:20). Rainfall then becomes lighter and the final period of intense rainfall starts at 13:10 on 17 September, which is mimicked 10 min later by throughfall. Rainfall ceases at 14:10 on 17 September, with a cumulative total flow of 36 mm. The higher intensity throughfall stops at 14:35, but flow eventually ceased at 19:25, totalling 25 mm. Throughfall was 68% of total rainfall.

Appendix 4.6 displays the timing of maximum flow at all nodes in the system. Maximum flow has been calculated as the greatest volume of flow at a specific node per 5 min interval. All times of maximum flow have been reported in storms where greater than one maximum is observed. The column PPT-TIlg shows the time lag that is calculated between the maximum flow rates of rainfall and the corresponding maximum flow rate of throughfall. In some storms a negative value is obtained, suggesting that maximum flow rates of throughfall were recorded prior to those of rainfall (5 to 50 min in advance). This observation provides evidence for variability in rainfall intensity over the study area. The largest time interval by which rainfall maximum intensities lag throughfall maximum intensities is 50 min (during Tropical Storm Alberto), which was associated with high wind speeds, causing rain to fall as squalls. For the majority of storms, the time of the maximum throughfall intensity was concurrent with the time of maximum rainfall intensity.

The similarity in timing of onset of intense rainfall and throughfall, and similar patterns in cumulative plots at both nodes suggest that temporal synchroneity between throughfall and rainfall is high, and shows the significant control of rainfall on throughfall volumes.

(v) Controls on spatial and temporal variability of throughfall

Calculations in previous sections suggest that the spatial heterogeneity of throughfall is high and that the temporal synchroneity of throughfall and rainfall is high and is controlled to a great degree by rainfall intensity. Several controls on throughfall heterogeneity have been suggested: rainfall magnitude (Loustau *et al*, 1992); rainfall intensity (Herwitz, 1987; Neal *et al*, 1992; Loustau *et al*, 1992, Robson *et al*, 1994); storm type (Neal *et al*, 1992); distance of measurement from the tree trunk (Robson *et al*, 1994); tree type, tree density, penetration of the canopy by wind and the height of the lowest branches which drain intercepted water. Several of these factors will now be considered in more detail.

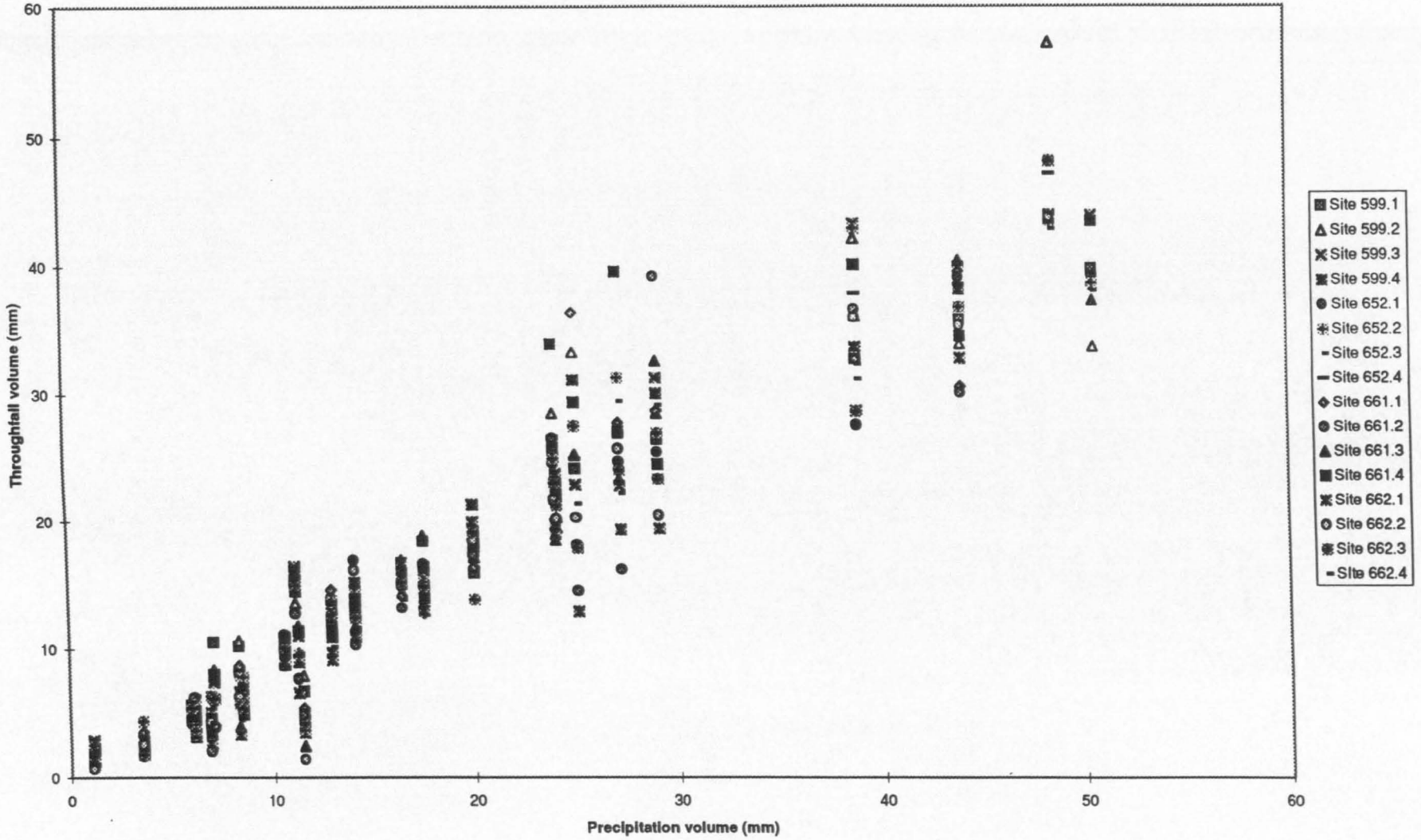

***Figure 4.6** : Rainfall and throughfall volumes for storms occurring between 1987 and 1989 (Cappellato, 1991), collected from 16 positions within the deciduous region of PMRW*

Storm magnitude

Figure 4.4 displays throughfall and rainfall totals for storms between 1987 and 1989 (Cappellato, 1991). There is a general trend of increasing spatial heterogeneity with increasing magnitude of rainfall. This trend is displayed in Figure 4.6, where there is a major increase in the variability of throughfall once rainfall exceeds 20 mm. Hence, throughfall variability is influenced to some extent by storm magnitude.

Rainfall intensity

In the current investigation, it seems possible that spatial heterogeneity in throughfall may be attributed to variations in rainfall intensity. In a sitka spruce plantation in Dumfrieshire, patterns of throughfall intensity were less marked when incident rainfall was heavy or light, rather than intermediate (Ford and Deans, 1978). In some storm cases e.g. 9 June, 27 June, 10 July, 12 July and 22 July, throughfall totals were greater than rainfall totals (from 8 to 50% greater) (Appendix 4.5). Rainfall was intense during these storms, which may result in greater penetration of rainfall through the canopy. Most of the storms experienced periods of rainfall that exceeded 3 mm per 5 min. Also, storms following Tropical Storm Alberto (4 July 1994) (i.e. 10, 12 July) were accompanied by high wind speeds. It was during these storms that higher throughfall than rainfall volumes were recorded. Higher wind speeds might lead to:

- lower accuracy of rainfall measurements by rain gages
- variations in rainfall intensity over the area. Rainfall fell as squalls, and thus may have led to variations between throughfall measurements at the hillslope site (TI) and rainfall measurements at the platform site (PPT), 450 m downstream.

Distance from trunk

Data is not available on the distance of the collection vessel to the nearest tree trunk and hence no proper consideration of the control of this parameter on throughfall variability can be made. Areas between trees apparently experience lower throughfall volumes than areas near to the tree trunk (Ford and Deans, 1978; Robson *et al*, 1994). Thus, the sites where higher throughfall amounts are consistently measured (e.g. Sites 661.1 and 661.4) may have been located in near-trunk areas. The troughs employed in the current study were positioned in order to take account of this factor and were located at varying distances away from the trunk. Output from all troughs were connected and hence an average throughfall volume from all troughs was measured. The lower overall throughfall volumes measured in this study might be explained because the throughfall volumes that the troughs collect are less biased by this control.

Tree and canopy structure

Data is not available to relate canopy cover or structure to throughfall volumes. However, its control on throughfall may be significant and hence the findings of previous studies merit mention. As an inclined branch is wetted, many of the flowlines terminate at 'drip points'. These drip points do not remain in the same position for long, since the flowlines are gradually extended down the slope of the branch. However, once the flowlines coalesce and the undersides of the branches become thoroughly

wetted, the drip points that do develop tend to be relatively stationary in position because they correspond to a particular point on the branch surface (Herwitz, 1987). Robson *et al* (1994) attribute the high variance and non-normal distribution of throughfall volumes to drip points. Neal *et al* (1990) attribute collection of higher throughfall amounts than rainfall amounts to the occurrence of drip points and shielded areas at the canopy level and along stems and branches.

The placement of the collectors directly beneath large trees may have lead to some focusing of flow, whereby water may be routed along branches and then fall to the ground, where a trough may collect this accumulated flow. This 'focusing' effect may depend on the magnitude of rainfall, and the pathways taken by the water would depend on the change of the structure of the canopy. Thus, if water was routed along branches, this may explain why such high throughfall totals were measured during some storms (i.e. the 'outlier' storms in section (i)).

(vi) Interception calculation

Two ways of calculating interception loss were outlined in Section IV.4Bciii, the first by subtracting total throughfall plus stemflow from total rainfall; and the other from the intercept of the regression of throughfall on rainfall. The first approach requires an estimation of stemflow volumes. In a previous investigation at PMRW (Cappellato, 1991), the regression of total rainfall on total throughfall plus total stemflow (Tot SF) produced the following regression equation:

$$\text{Tot PPT} = -0.11 + 0.98\,(\text{Tot TI} + \text{Tot SF}),\ R^2 = 0.97 \qquad \text{Eqn 4.1e}$$

Thus, the amount of water collected as stemflow plus throughfall would be equivalent to 102% PPT. This suggests that all the rainwater transits the canopy as throughfall and stemflow. Hence, calculation of stemflow plus throughfall for storms from 1987 to 1989 exceeded total rainfall. This is attributed to the difficulty in assessing the contributing area to stemflow, and hence inaccurate stemflow determinations. The higher amount than total rainfall suggests that water must be focused onto the collector, which might also suggest the over-estimation of throughfall totals by the previous investigation

The other approach for estimation of interception was favoured in this investigation, where an estimate of average interception loss can be obtained from the intercept of the regression of throughfall on rainfall (Figure 4.2 and 4.3). The intercept corresponds to the amount of rainfall that has to occur in order for throughfall to be initiated i.e. the amount of rainfall that does not make it through the canopy. In the regression for all storms, the intercept is - 1.7, hence interception is comprised 1.7 mm rainfall.

A seasonal trend was evident in the amount of interception loss. In the growing season (from Eqn 4.1d), interception comprises 2.5 mm, and the dormant season (from Eqn 4.1c), 0.5 mm. Thus, the hypothesised seasonal pattern was obtained, whereby greater interception was noted, on average, during the growing period.

(IV.4Be) Summary

At the hillslope location at PMRW, throughfall was found to comprise approximately 78% rainfall for most storms. This value is similar to that of other investigations (e.g. Moore 1989 (73%)). However, much greater variations have been found in some studies, e.g. throughfall was equivalent to between 9 and 97% incident rainfall in a sitka spruce plantation, Dumfrieshire (Ford et al, 1978). It was also found to closely follow the pattern of rainfall throughout the storm duration. In some cases, throughfall was found to be greater than rainfall, a trend that is attributed to variation in rainfall intensity or the formation of drip points in the canopy amongst monitoring sites. Seasonal trend in throughfall volumes was insignificant although slightly more throughfall occurred in the dormant season (on average 79% of rainfall) with sparse vegetation cover compared to the growing season (on average 78% rainfall).

Significant spatial heterogeneity in throughfall volumes was found at PMRW. This is attributed to a number of factors, including rainfall magnitude, rainfall intensity, distance from the tree trunk and canopy structure. Spatial patterns of throughfall depend on tree type, tree density, penetration of the canopy by wind, or the height of lowest branches which drain the intercepted water. Ford *et al* (1978) conclude that the canopy can generate distinct patterns of water flux to the forest floor. Canopy interception can concentrate rainfall so that it arrives at the soil surface at only a few drip points (Armstrong and Mitchell, 1988).

The area of the collector may have been insufficient to account for spatial heterogeneity of throughfall. Previous investigations have shown that inherent complexities in canopy structure can cause large differences in throughfall over distances of a few metres (Edwards *et al*, 1989). Lawrence and Fernandez (1993) collected throughfall from polyethylene (342 cm^2) at the Howland Integrated Forest Study. For plots of area 40 x 50 cm, they concluded that between 43 to 221 collectors were required to obtain a sample of throughfall that was statistically representative of the 'population'. In this study, throughfall volumes were collected at two locations on the hillslope and volumes correlate well. However, the study by Cappellato (1991) shows the high degree of spatial heterogeneity in throughfall in the deciduous cover at PMRW. Hence, even with close correlation of throughfall volumes collected at two sites within the hillslope plot, those volumes can not necessarily be extrapolated to the deciduous hillslope as a whole. Greater exploration into spatial heterogeneity of throughfall in the current field programme is restricted by the sampling configuration.

(IV.4C) OVERLAND FLOW

(IV.4Ca) Aims and Questions

Overland flow involves the routing of 'new' water to the stream channel across the land surface (Horton, 1933). The type of overland flow that occurs and the controls on its development have been outlined in Chapter I. The following questions will be addressed in the following section:

(i) Does overland flow occur at PMRW?

(ii) Can total overland flow be calculated?

(iii) Does overland flow vary seasonally?

(iv) Can temporal variability between overland flow and throughfall be detected?

(v) What are the controls on overland flow?

(vi) What type of overland flow dominates at PMRW?

(vii)

(IV.4Cb) Hypothesised patterns

(i) Detection of overland flow at PMRW.

Several mechanisms have been identified as causing overland flow. For Hortonian overland flow to occur, rainfall intensities are in excess of the infiltration capacity of the soil (a parameter which varies over a small area). Partial-area overland flow occurs on those parts of a catchment where rainfall rates exceed the soil saturation and the upper parts of the soil profile become saturated from the top downward. The excess rainfall becomes available for surface detention and flow over the ground surface. Saturation overland flow is generated by rain that falls directly onto saturated areas near stream channels or in valley floors. Water tables rise to the surface in these areas (initially fed by the infiltrating rainfall, but also fed by the outflow of rainfall that has infiltrated upslope of the runoff source area) soon after rainfall begins, and further rainfall generates flow over the surface (Eshleman et *al*, 1993). Hence, different mechanisms may control the operation of overland flow, but the results are the same: the lateral flow of water over the surface.

The measurement of overland flow is difficult. In this study, pan lysimeters were installed to collect forest floor soil water. They were installed at two locations (VO-0o and VI-0o). In each situation, the lysimeters were installed horizontally into the profile. At Site VI-0o, a 1 m^2 stainless steel lysimeter was installed at a site 200 m downstream of the hillslope plot. At Site VI-0, a polyethylene (0.08m^2) pan lysimeter was installed on a steep section of the hillslope plot. This lysimeter was located in a topographic low. Although both lysimeters were designed to collect only vertically moving water (i.e. throughfall), it is possible that during large and high intensity storms, overland flow (laterally moving water) was also collected. Neither lysimeter had a 'lip' preventing water from higher on the slope from entering the vessel.

Hence, there are two scenarios for water collection by the lysimeters during storms (Figure 4.7). In storms of low magnitude and intensity and following dry antecedent conditions, rainfall is

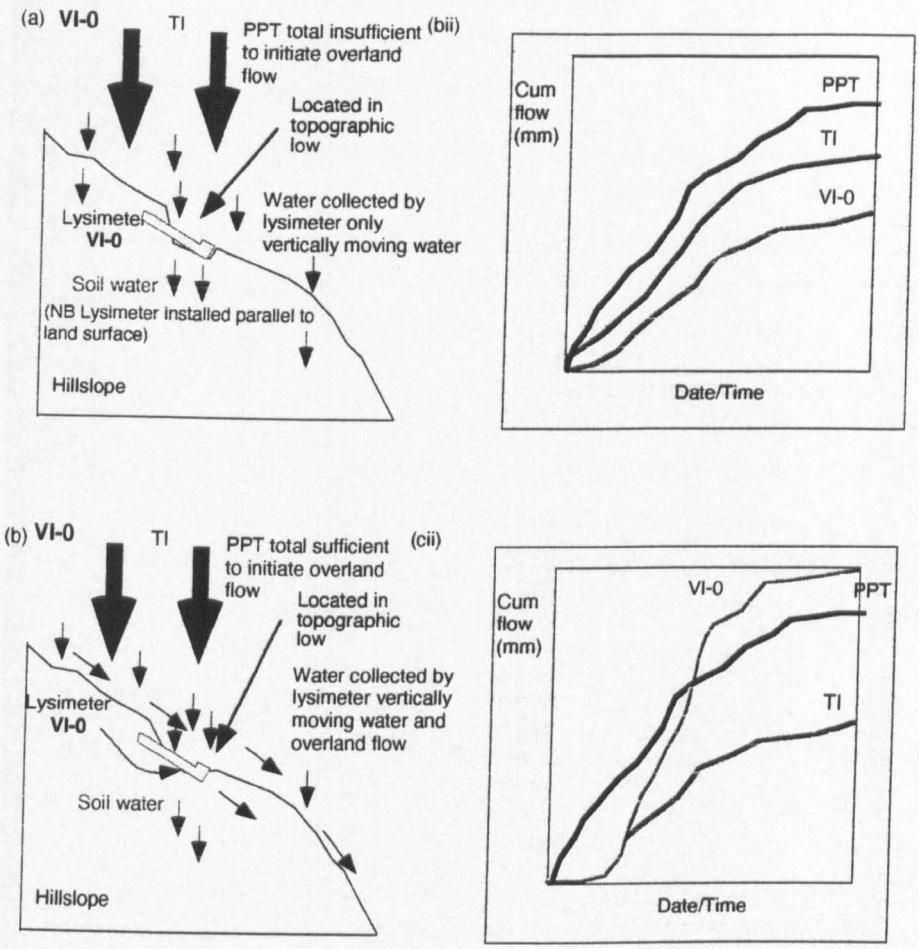

Figure 4.7 *Diagram to show expected flow patterns for rainfall (PPT), throughfall (TI), and forest floor soil water (VI-0)for particular field set-ups for lysimeter VI-0 (at hillslope plot) during storms with (a) insufficient PPT to initiate overland flow and (b) sufficient PPT to initiate overland flow*

insufficient to initiate overland flow. Hence, the water collected by the lysimeter is only vertically moving water, i.e. throughfall (Figure 4.7a). In more intense storms, especially following wet antecedent conditions, rainfall may be sufficient to initiate overland flow and hence the water collected by the lysimeter may be a combination of vertically (throughfall) and laterally (overland flow) moving water (Figure 4.7b). The positioning of the VI-O lysimeter in the topographic low might also encourage the collection of saturation overland flow.

Tipping bucket data provides information on total cumulative flow and also the rate of flow of the forest floor soil water. Calculation of whether or not overland flow is occurring can be made by comparison of cumulative forest floor soil water with cumulative throughfall totals. If total forest floor soil water exceeds total throughfall, then all water that contributed to the lysimeter cannot have fallen vertically and some of the water must have moved to the equipment laterally (i.e. in the form of overland flow).

This is a very simplistic approach to collection and 'quantification' of overland flow. The overall quantification of overland flow is difficult since the source area of the water is impossible to define accurately. In the following section, the area that is used in the calculation of the 'depth' of water collected by the lysimeter is the cross-sectional area of the lysimeter. In reality, the water comes from a wider area than this and hence the absolute quantification of overland flow in this study is not possible.

Similar problems arise in the current approach when the type of overland flow is investigated. The type of overland flow (i.e. Hortonian vs. Saturation) can easily be identified if it is known whether the soil is saturated or not. (The soil must be saturated for saturation overland flow to occur, but not for Hortonian overland flow to occur). This information could be obtained from use of the TDR rods if they had been calibrated and if porosity measurements of the soil has been conducted. However, in the current investigation, neither parameters were calculated (see Chapter VIII for future recommendations for research). However, full chemical analyses were performed on forest floor soil water, 15 cm soil water and throughfall samples, and some assessment of the type of overland flow that occurred can be made using this data. These results are presented in Chapter V.

(ii) Quantification of overland flow

In storms where total forest floor soil water exceeds total throughfall, the excess water must come from overland flow. Hence, the difference between the totals gives total overland flow. There are potential errors in this calculation. The source area of the overland flow is not known and hence the totals that are calculated are not absolute. Problems in calculations arise due to spatial heterogeneity in throughfall. The input volume recorded at one position (i.e. where TI is collected) may not necessarily be the same as the input volume above where forest floor soil water is collected. The high temporal resolution of sampling reduces the resolution of spatial sampling that can occur in this field programme.

(iii) Seasonal variations in overland flow

Previous studies suggest that overland flow may vary on a seasonal basis (Dunne and Black, 1970). A major control on overland flow is the infiltration capacity of the soil (Horton, 1933). Higher temperatures and plant activity in the growing season may lead to substantial extraction of water from the soil and a lower soil moisture content and hence the higher infiltration capacities. Thus, higher overland flow might be expected in the dormant period, when soil moisture content of the soil is higher. However, during the growing season of the study period, the occurrence of two tropical storms may also reduce the infiltration capacity of the soil and high overland flow may result.

(iv) Temporal variability in throughfall and forest floor soil water flow.

The temporal variability in overland flow and throughfall is expected to be similar. Periods of high intensity throughfall would be expected to promote periods of rapid overland flow, especially since the excess of rainfall intensity over infiltration capacity is recognised as a major control of development of overland flow (Horton, 1933; Hewlett and Hibbert, 1967; Betson and Marius, 1969; Bonta and Rao, 1994). However, the antecedent moisture conditions will significantly affect this relationship (see section v).

(v) Controls on overland flow

Antecedent moisture conditions have been found to influence overland flow (Kirkby and Chorley, 1967; Dunne and Black, 1970; Eshleman *et al*, 1993). Saturation overland flow occurs preferentially where soils are most readily saturated (Kirkby and Chorley, 1967) and hence overland flow would be more prevalent following wet antecedent conditions. Since infiltration capacity of the soil is a major control on Hortonian and partial area overland flow (Horton, 1933; Hewlett and Hibbert, 1967), wet antecedent conditions favour low infiltration capacity and high overland flow.

Storm magnitude has been found to influence overland flow (Starosolszky, 1987). During small, moderate storms, overland flow occurs only on impermeable surfaces. Thus, storm magnitude influences the area that contributes water. Dunne and Black (1970) have suggested that the operation of saturation overland flow is also dependent on storm duration.

Rainfall intensity is recognised as a major control on overland flow operation (Horton, 1933; Hewlett and Hibbert, 1967; Betson and Marius, 1969; Eshleman *et al*, 1993; Betson, 1994). Overland flow occurs where rainfall intensities or throughfall rates exceed the infiltration capacity of the soil.

Finally, the microtopography of the land surface and location on the hillslope will be of influence. Kirkby and Chorley (1967) suggest that saturation overland flow appears preferentially in areas of thin or less permeable soils, in areas of flow concentrations provided by surface profile concavity or contour curvature, and in areas adjacent to streams, which tend to be wettest. McLord and Stevens (1987) showed that when flow converges on a topographic low, water moves to and flows over the land surface. Vegetative cover will also limit the operation of overland flow. Pearce *et al* (1986)

concluded that on humid, well vegetated areas, soil hydraulic conductivities and infiltration capacities often exceeded rainfall rates.

(vi) Dominant type of overland flow

Previous investigations at PMRW have not reported large-scale overland flow (Shanley and Peters, 1988; Hooper *et al*, 1990; Peters, 1994. The position of the two forest floor soil water collectors enable some estimation of the type of overland flow that occurs. Saturation overland flow is hypothesised to occur in topographic lows, where sub-surface flowpaths intersect the surface (Betson and Marius, 1969; Dunne and Black, 1970). Thus any overland flow at Site VI-0 (positioned in the topographic low) is likely to be saturation overland flow.

(IV.4Cc) Equipment and Calculations

Forest floor pan lysimeters, VI-0o and VI-0, monitored forest floor soil water flow rates, which were output at 5 min intervals. These rates were cumulated to provide total forest floor soil water. The forest floor collected may have been a combination of throughfall and overland flow. However, in the calculation of the 'depth' of forest floor soil water (see Chapter III, Eqn 3.1), the cross-sectional area of the lysimeter was used as the source area of water. This assumption had to be made since measurement of the source area of overland flow was impossible.

Throughfall was monitored at Site TI (see Chapter III) and data was also output at 5 min increments. Total throughfall was calculated by cumulating the data. In the calculation of overland flow, 100% collection of throughfall (TI) by the lysimeter is assumed, and excess water collected by the lysimeter is assumed to be from overland flow (OVLF):

$$\text{Tot OVLF} = \text{Tot VI-0} - \text{Tot TI} \qquad \text{Eqn 4.2a}$$

Tot OVLF	= Total overland flow (mm)
Tot VI-0	= Total forest floor soil water (mm)
Tot TI	= Total throughfall (mm)

(IV.4Cd) Results and discussion

(i) Detection of overland flow at PMRW

Total cumulative forest floor soil water (VI-0) was compared with total cumulative throughfall for all storms in Figure 4.8.a. For the majority of storms in which forest floor soil water was collected at the hillslope site, total flow through the forest floor exceeded throughfall and rainfall totals (i.e. all storms lie about the throughfall = forest floor soil water line). Thus, a combination of throughfall (or rainfall) and overland flow may have contributed to total flow through the forest floor lysimeter.

(a)

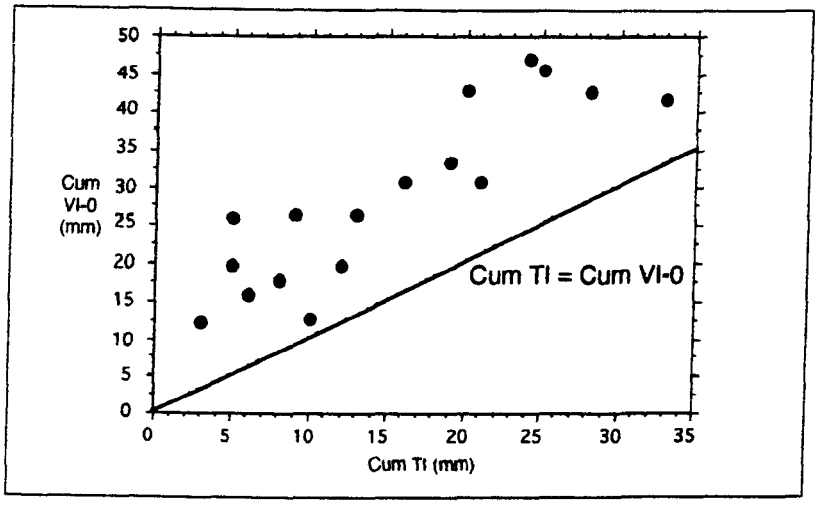

(b)

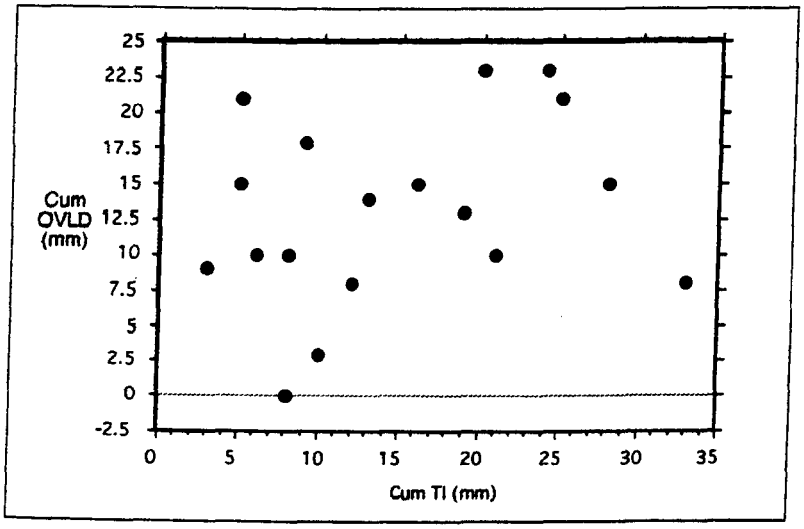

Figure 4.8: Plots of (a) total forest floor soil water flow (Cum VI-0) against total throughfall (TI), for all storms; (b) total overlandflow (cum OVLD) against total throughfall for all storms NB. The data used for forest floor soil water was collected at sites VI-0o and VI-0.

(ii) Quantification of overland flow

Table 4.3 shows the differences between total forest floor soil water and total throughfall. These values give a rough estimation of total overland flow. The final column of the table provides a calculation of the amount of overland flow as a percentage of throughfall and shows that the amount of water contributed as overland flow as a percentage of throughfall varies greatly, from 0% (where total throughfall is greater than total forest floor soil water) to over 400% throughfall. Hence, in some storms, the difference between total forest floor soil water and total throughfall is very large, and hence, the additional water can not be explained on the basis of spatial variability of throughfall. Water must be derived from another source, which is probably overland flow. The high percentages that are calculated are also a result of the inaccuracy that is introduced into the calculation on account of the actual vs. assumed source area of overland flow.

Figure 4.8b plots total throughfall against total overland flow. The pattern is random.

STORM	PPT (mm)	TI (mm)	VI-0 (mm)	OVLF (mm)	OVLF (%TI)
24 June 1994	13	8	5	0	0
10 July 1994	26	28	43	15	46
21 Aug 1994	12	8	18	10	125
9 Sept 1994	18	9	27	18	200
16 Sept 1994	36	24	47	23	96
23 Sept 1994	23	13	27	14	108
2 Oct 1994	32	21	31	10	48
11 Oct 1994	45	33	41	8	24
13 Oct 1994	12	10	13	3	30
21 Oct 1994	32	20	43	23	115
20 Nov 1994	18	12	20	8	67
26 Nov 1994	37	25	46	21	84
28 Nov 1994	23	19	32	13	68
4 Dec 1994	24	16	31	15	94
19 Jan 1995	7	5	20	15	300
11 Apr 1995	9	3	12	9	300
19 Apr 1995	9	5	26	21	420
1 May 1995	11	6	16	10	167

***Table 4.3** : Total precipitation (PPT), total throughfall (TI), total forest floor soil water (VI-0) and total overland flow (OVLF), expressed in mm and as a % of throughfall, assuming 100% collection of throughfall by forest floor lysimeter (VI-0o and VI-0)*

(iii) Seasonal variation of overland flow

Dormant season storms

Figure 4.9a shows the relationship between total throughfall and total forest floor soil water for dormant season storms. All storms lie about the line representing throughfall=forest floor soil water. A vaguely linear relationship is obtained between the two parameters, where larger storms (i.e greater throughfall) experience greater forest floor soil water flow. Figure 4.9b shows the relationship between total throughfall and total overland flow. A random pattern is obtained. However, most storms experience lower overland flow than throughfall (i.e. most storms lie below the line of throughfall = overland flow). The two storms (21 October 1994 and 19 January 1995) where overland

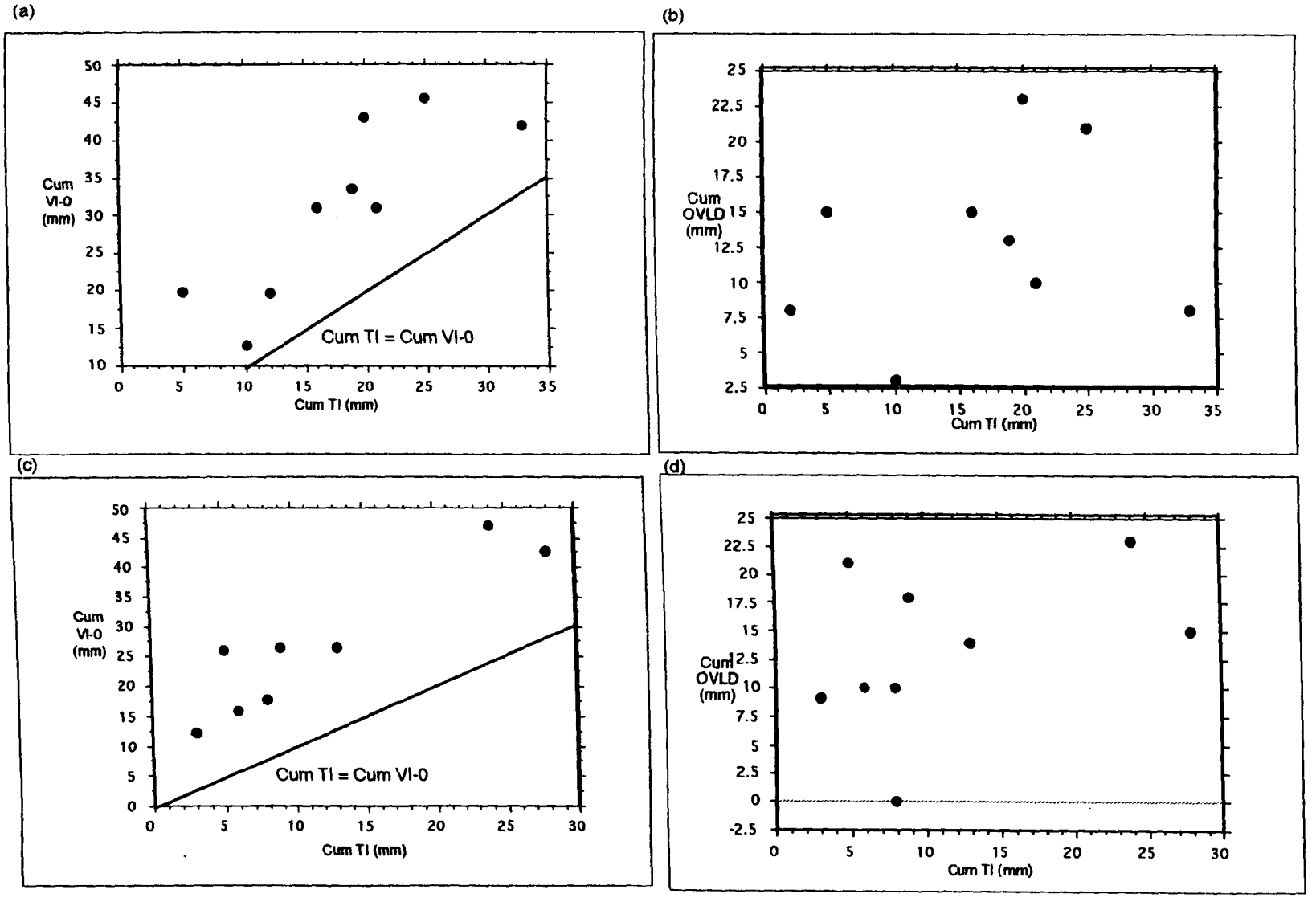

Figure 4.9: *Relationship between (a) Cumulative throughfall and cumulative forest floor soil water in dormant season storms; (b) cumulative throuhfall and cumulative overland flow in dormant season storms' (c) cumulative throughfall and cumulative forest floor soil water in growing season storms; (d) cumulative throughfall and cumulative overland flow in growing season storms*

flow is greater than thoughfall both experience high rainfall (and throughfall) intensity in the first hour of the storm).

The average cumulative overland flow for dormant season storms was 13 mm , compared with an average cumulative throughfall of 18 mm.

Growing season storms

Figure 4.9c shows the relationship between total throughfall and total forest floor soil water for growing season storms. Again, all storms lie above the line of throughfall=forest floor soil water, indicating that all water collected by the lysimeter is not vertically moving. The relationship between the two parameters is again linear, where larger storms experience greater forest floor soil water flow. Figure 4.9d displays the relationship between total throughfall and total overland flow. A random pattern is obtained. However, for most storms, cumulative overland flow is greater than cumulative throughfall (i.e. most storms above under the line representing throughfall = overland flow). During two of these storms, forest floor soil water was collected at site VI-0o. These are the only storms during which forest floor soil water was collected at this site. The lower amounts of overland flow might be explained by the operation of a different form of overland flow compared to the other site. However, without further measurement of other parameters (e.g. porosity, hydraulic conductivity), the verification of this hypothesis is not possible.

The average cumulative overland flow for growing season storms was 13 mm, compared with an average cumulative throughfall of 12 mm. Hence, the relative amount of overland flow is greater in the growing season than the dormant season.

(iv) Temporal variability in forest floor soil water flow and throughfall

The temporal variability of forest floor soil water was hypothesised to be similar to that of throughfall during rainstorms. In Appendix 4.6, the timing of maximum flow rates through the forest floor and for throughfall are shown. The maximum flow rate is the maximum volume of water per 5 min interval at each node. Several maximum flow rates are provided for storms where more than one high intensity period existed. The column, TIVI-0lg refers to the time lag between the maximum flow periods of throughfall and forest floor soil water. For the majority of storms, the time lag is below 5 min, illustrating the similar temporal variability in flow at each node. In some cases, the maximum flow rate through the forest floor precedes that of throughfall, which may be explained by the spatial heterogeneity of throughfall.

Overland flow occurrence was calculated as the time at which cumulative forest floor soil water flow exceeded cumulative throughfall, which is displayed in the plots that follow for three case study storms (on 16 September 1994, 2 October 1994 and 4 December 1994).

Case study storm: 16 September 1994

This storm occurred during the growing season, and overland flow occurred (Figure 4.10a). Plots are presented for rainfall, throughfall and overland flow. Rainfall began at 17:30 on 16 September and flow at VI-0 (i.e. forest floor soil water) began at 17:35. Throughout the storm, cumulative VI-0

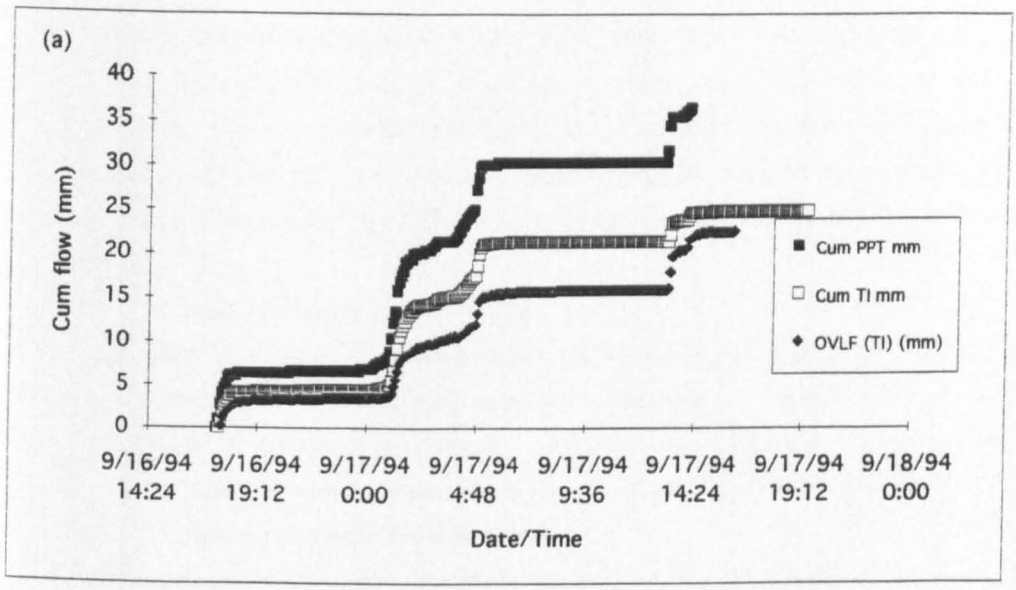

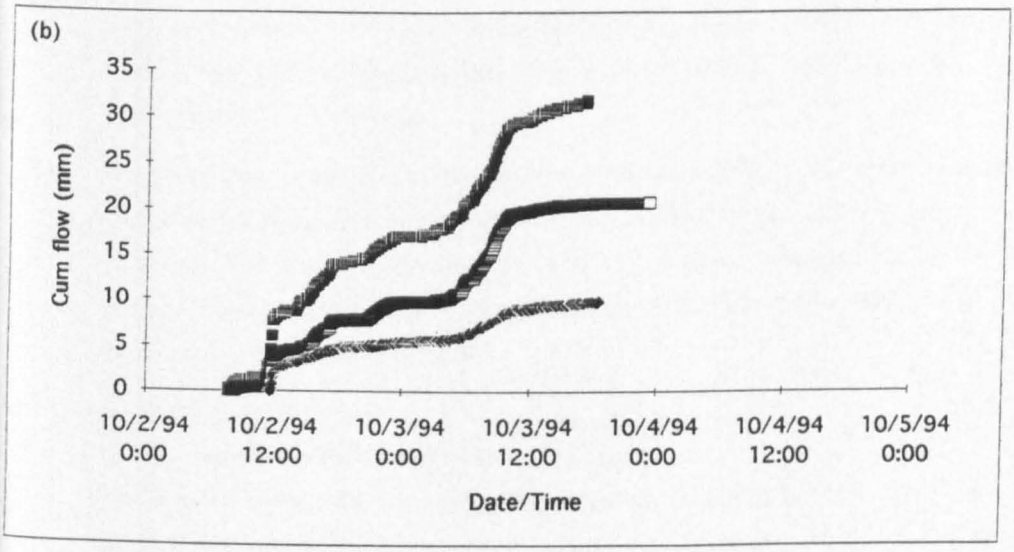

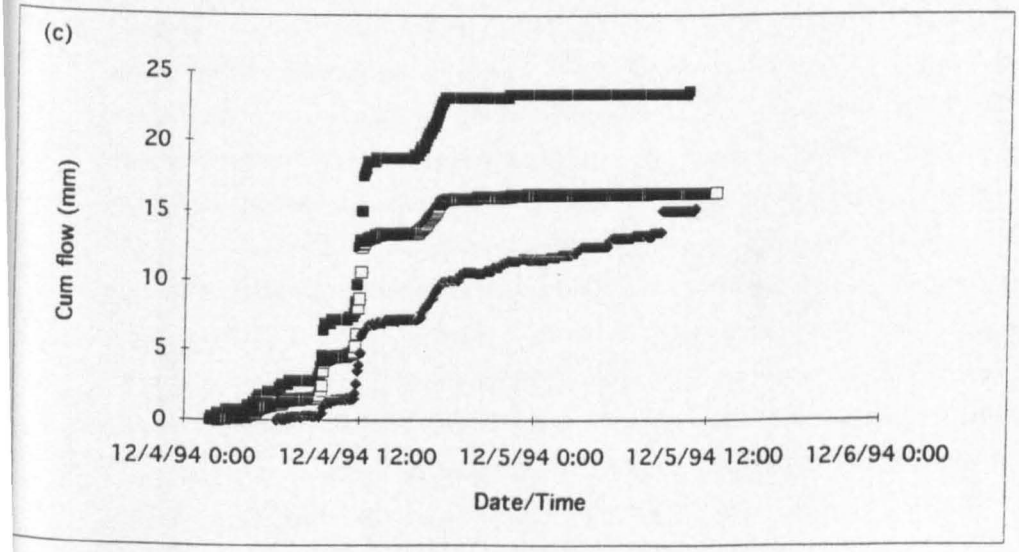

Figure 4.10: Relationship between cumulative precipitaiton (PPT), cumulative throughfall (TI), cumulative overland flow (OVLF(TI)), for (a) 16 September 1994; (b) 2 October 1994; (c) 4 December 1994

exceeded cumulative throughfall. Thus, if the overland flow is calculated as the difference between total throughfall and total forest floor soil water flow, then overland flow was seen to occur throughout the storm. Periods of intense rainfall (four in all) coincided with periods of rapid overland flow. Rainfall ended at 14:10 on 17 September, with a cumulative total of 36 mm, whereas the forest floor continued to drain for another 2 hr, with a cumulative total flow of 47 mm. Total overland flow was 23 mm.

Case study storm: 2 October 1994

This storm occurred in the dormant season (Figure 4.10.b). The graph displays the similarity in temporal variability of flow at each node. Rainfall began at 7:50 on 2 October, but did not become 'continuous' until 11:15. Forest floor soil water flow was detected within 5 min. Rainfall ceased at 17:10 on 3 October, with a cumulative total flow of 32 mm. Cumulative overland flow was 10 mm.

Case study storm: 4 December 1994

This storm occurred during the dormant season (Figure 4.10.c). Rainfall began at 1:50 on 4 December, but rainfall intensity was very low in the first hour (0.51 mm). Overland flow began 4 hr after and after 1.27 mm of rainfall had occurred. Rainfall ceased at 10:25, with a cumulative total of 24 mm. Total overland flow was 15 mm.

These case study examples show the similarity in the temporal variations of flow at each node. When intense rainfall occurs, intense throughfall and overland flow are observed, lagging that of rainfall by 5 to 10 min. This suggests that throughfall (or rainfall) intensity is an important factor which controls overland flow magnitude, supporting evidence found in other studies (Betson and Marius, 1969; Eshleman, 1988; Bonta and Rao, 1994).

(v) Controls on overland flow

Antecedent moisture conditions

Figure 4.11a displays the relationship between cumulative overland flow and antecedent moisture conditions (as total rainfall in week prior to storm). The pattern appears random, however, trends are observed when the relationship is broken down on a seasonal basis. Figure 4.11b displays the relationship for growing season storms. The graph displays two distinct trends. For storms that experienced between 0 - 20 mm rainfall in the previous week, there is a trend of increasing overland flow with wetter antecedent moisture conditions. For storms that experienced greater rainfall (> 60 mm) in the previous week, there is also a trend of greater overland flow, although the increase is not as rapid. Thus, the hypothesis that overland flow is greater following wet antecedent conditions is not true, since storms experiencing relatively dry antecedent conditions have significant overland flow. In Figure 4.11c, the relationship between overland flow and antecedent moisture conditions are shown for dormant season storms. The relationship is random, but shows that during storms that followed periods of high rainfall (> 50 mm in the previous week), overland flow was relatively low.

This suggests that a combination of parameters control overland flow (e.g. storm intensity, water table elevations, soil physical properties), including antecedent moisture conditions.

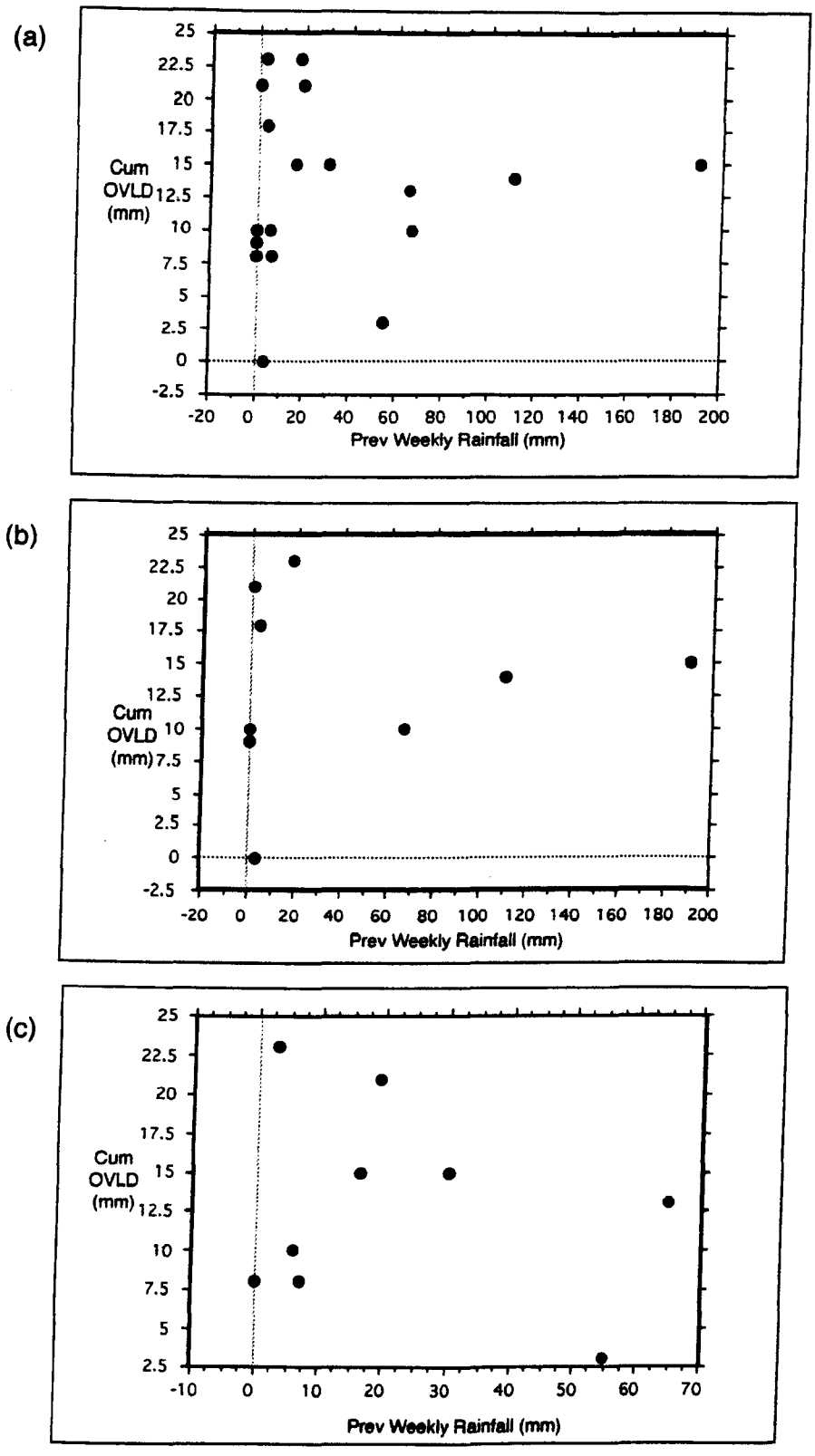

***Figure 4.11**: Cumulative overland flow (Cum OVLD) vs. antecedent moisture conditions (previous rainfall in week prior to storm) for (a) all storms; (b) growing season storms; (c) dormant season storms*

Rainfall characteristics

A parameter found to be significant in influencing overland flow is the amount of rainfall that occurred prior to the onset of overland flow, and this was found to vary seasonally.

Growing season

Analysis of rainfall total and time at which cumulative flow through the forest floor exceeds cumulative rainfall, shows that for all growing season storms (excluding those during which forest floor soil water was measured at VI-0o), cumulative rainfall is between 6.1 and 6.9 mm (on average 6.4 mm) when overland flow occurs, i.e. when cumulative forest floor soil water exceeds cumulative rainfall. The timing is more variable, with overland flow occurring from the onset of the storm to periods exceeding 300 min after the onset of rainfall (on average 85 min after the storm onset). However, this variation in timing can be explained by antecedent moisture conditions and rainfall intensities. Both storms where overland flow was instant (on 21 August 1994 and 1 May 1995) followed wet antecedent conditions and periods of high rainfall intensity respectively.

Dormant season

For dormant season storms, cumulative rainfall total was between 5.8 and 18.5 mm (on average 12.5 mm) when overland flow began. Thus, on average, twice as much rainfall is required to initiate overland flow during dormant season storms compared to growing season storms. Also, the timings from the onset of rainfall at which overland flow occurs range from 40 to 160 min (on average 290 min). Thus, during the dormant season, it appears that overland flow occurs much later on during a storm, and that more rainfall is required to initiate its occurrence than in the growing season. The occurrence of overland flow in the dormant season also appeared to be controlled by antecedent moisture conditions and rainfall intensity.

Microtopography

Site location was the final control on overland flow that was identified in this study. Where data was collected at VI-0, on the hillslope plot, total forest floor soil water exceeded throughfall in all storms by a higher magnitude than when collected at Site VI-0o. Hence, positioning of the equipment in a topographic low was successful in the collection of overland flow water. The control of microtopography on overland flow occurrence was thus localised.

(vi) Dominant type of overland flow at PMRW.

The microtopography of the site was found to control the occurrence of overland flow, supporting the conclusions of Pearce *et al* (1986). If topography is a major control on overland flow, this suggests that the mechanism by which it occurs is due to the convergence of flowpaths in the topographic low (Betson and Marius, 1969; Dunne and Black, 1970), in other words saturation overland flow (Bonta and Rao, 1994). Hursh (1936) recognised that a significant component of saturation overland flow may be due to the convergence of lateral flow. Lateral flow is generally considered to occur as a result of surface or sub-surface runoff over horizons of low permeability. McLord and Stephens (1987) suggest that during infiltration and subsequent redistribution, a zone of increased moisture occurs at some depth below the land surface. This creates a zone of relatively high conductivity parallel to the

sloping land surface and moisture flowpaths may converge in this zone. When flow converges on a topographic low, water may surface and flow over the land surface.

The total amount of rainfall that needed to have occurred in order to initiate overland flow was very different between storms occurring in the growing season and storms occurring in the dormant season. During the growing season, rainfall totals of 6.4 mm (on average) were required to initiate overland flow, and usually occurred within 85 min of the onset of the rainstorm. However, for dormant season storms, the rainfall total was much higher, at 12.5 mm (on average) to initiate overland flow. The timing at which this occurred was also much later, at over 200 min after the onset of the rainstorm.

The current investigation aimed to measure the vertical movement of water through the soil profile. From observation of the large amount of forest floor soil water flow that was recorded, it was apparent that overland flow was an important mechanism in this environment. In future investigations at the site, parameters such as porosity, hydraulic conductivity and suction gradients should be measured and calculated in order to make a more rigorous assessment of overland flow mechanisms. In Chapter 5, Cl^- is used as a tracer in order to make some assessment of the form of overland flow that operates at the hillslope. If overland flow is partial area overland flow, then the chemical signature of the forest floor soil water should be similar to that of 'new' water (i.e. throughfall). If the overland flow is saturation overland flow, then the water comprises a component of return flow or sub-surface flow. Hence, the chemical signature of the water should resemble that of a mix between 'new' and 'old' water. The hydrometric results that have been presented herein do not allow the identification of the type of overland flow. However, the results do suggest that overland flow occurs on the hillslope (even though it may be confined to specific regions), which have not been reported in any other documents to date.

(IV.4Ce) Summary

Overland flow was detected in 85% of the storms analysed. When overland flow was calculated by subtracting total throughfall from total forest floor soil water flow, overland flow totals ranged from 3 to 23 mm. Overland flow totals in relation to rainfall and throughfall totals were not found to correlate well, and there was a seasonal pattern to this relationship. In general, total flow through the forest floor was related to throughfall. This is not unexpected, since just over half of the water collected as forest floor soil water was actually throughfall. However, overall storm magnitude was not found to influence overland flow operation to a high degree.

Greater collection of forest floor soil water than total throughfall might also be attributed to spatial heterogeneity of throughfall. Throughfall inputs have been shown to vary spatially, and hence, sites where forest floor soil water were collected might receive greater throughfall input than where throughfall was measured. Again, the basis of the investigation on sampling intensively on a temporal scale reduced the resolution of spatial sampling. However, in some storms, the amount of water input in excess of throughfall was very high (up to 400% throughfall) and it seems that this is too great a

variation to be attributed to spatial variability in throughfall alone, but must be due to input from another water source, which may be overland flow.

In general, a seasonal pattern was found in the relationship between total throughfall and total forest floor soil water flow and with total overland flow. Greater overland flow in relation to throughfall totals was experienced during the growing season. This was expected due to the presence of Tropical Storm Alberto and subsequent storms. Each storm was moderate to high magnitude and they followed soon after each other. Hence, the soil was (probably) close to saturation since it was not given sufficient time to drain before the onset of the next storm. This also explains the onset of overland flow soon after the onset of growing season storms and with lower amounts of rainfall than for the dormant season storms.

The amount of overland flow that occurred was found to vary throughout the storm. The temporal variability of overland flow was similar to those of rainfall and throughfall. Thus, periods of intense rainfall prompted rapid overland flow.

The occurrence of overland flow was directly related to where forest floor soil water was collected. Where forest floor soil water was monitored in a topographic depression (at VI-0), overland flow was found to operate in all storms. Thus, the positioning of the equipment in a topographic low on the hillslope was successful in the collection of overland flow water. When samples were collected at Site VI-0o, total forest floor soil water was found to exceed total throughfall in only one storm (10 July 1994), which might suggest that overland flow was occurring. This is possible, since the storm was of particularly high intensity. However, other reasons exist which may explain this observation. One reason is that the area experienced flooding during this storm, and the excess water may infact be streamwater. The other reason is that, due to the high intensity of the rainfall, the rate of introduction of water to the tipping bucket assembly may have been greater than the rate of drainage from the plexiglass box. Thus, water may have welled up in the plexiglass box, and caused the tipping mechanism to float on the water surface and hence record false tips.

Thus overland flow was found to be in operation in a topographic low on the hillslope plot. However, it is possible that the occurrence of overland flow was localised in occurrence and hence was not a major process at PMRW on a whole. The aim of this section was to show that overland flow occurs at PMRW. In the calculation of overland flow totals, a major assumption had to be made that the source area of the forest floor soil water was the cross sectional area of the pan lysimeter. In reality, the source area of the overland flow would have been much greater than this. However, this was the only approach by which comparisons between overland flow totals and other parameters could be made. Hence, this section provides a 'picture' of the overland flow mechanisms at PMRW, but the results described should not be taken as absolute.

(IV.4D) SHALLOW SUB-SURFACE FLOW

(IV.4Da) Aims and Questions

The following questions will be considered at major soil nodes.

(i) What quantity of water from the adjacent node, higher in the profile, is translated to this node?

(ii) Is there a seasonal pattern to water flow through that node/depth?

(iii) Is there temporal variability in flow patterns between adjacent nodes?

(iv) Is there spatial heterogeneity in flow rates at a specific node?

(v) What are the controls on flow?

(IV.4Db) Hypothesised patterns

(i) Transfer of water from the upper adjacent node

The vertical movement of water through the profile might be expected to decrease with respect to depth due to the mechanisms of storage, overburden pressure, decreasing porosity, water uptake by plants, evaporation and lateral flow (Atkinson, 1980) In Chapter II, description of the soil profile was provided, which is also presented in Figure 4.12. The upper 7 cm of the soil is a grey sandy loam, which is underlain to 66 cm by a brown sandy loam. Macintosh *et al* (1997) report that soils on the hillslopes tend to be underlain by kaolonite clay, and that the clay content of the soil increases with depth, especially below 40 cm Many tree roots penetrate to depth in this soil, although their concentration is greatest in the shallowest horizons. Figure 4.12 illustrates the soil profile; there is litter and a partly organic A horizon at the surface, underlain by a sandy loam soil, with greater clay content below 40 cm depth. Below this is a soft bedrock layer of strongly weathered granite. Due to the decrease in pore size and macropore activity with depth and to the increase in clay content and overburden pressure with depth, the hydraulic conductivity might be expected to decrease exponentially with depth. If this is so, then flow magnitude and rapidity would also decrease with depth.

Under dry conditions, flow through the soil matrix in the upper horizons may be initially slow, since empty pores are still available to fill. Smaller pores must be filled before larger pores are filled. However, larger pores are able to transmit water much more efficiently in relation to their cross-sectional area than smaller pores. Hence, the movement of water through the soil profile is controlled by a combination of pore size and the proportion of pores that are already filled (i.e. antecedent soil moisture status). Due to the greater concentration of roots near the surface, macropore activity might be expected to be greater in the shallow horizons, which allows rapid transport of water to depth.

If the deeper soil horizons are saturated, then the percolation of more water may raise the level of the saturated zone directly, especially is the clay swells and acts as an impeding layer. If this process continues for long enough, then the saturated layer may build up to the surface, producing overland

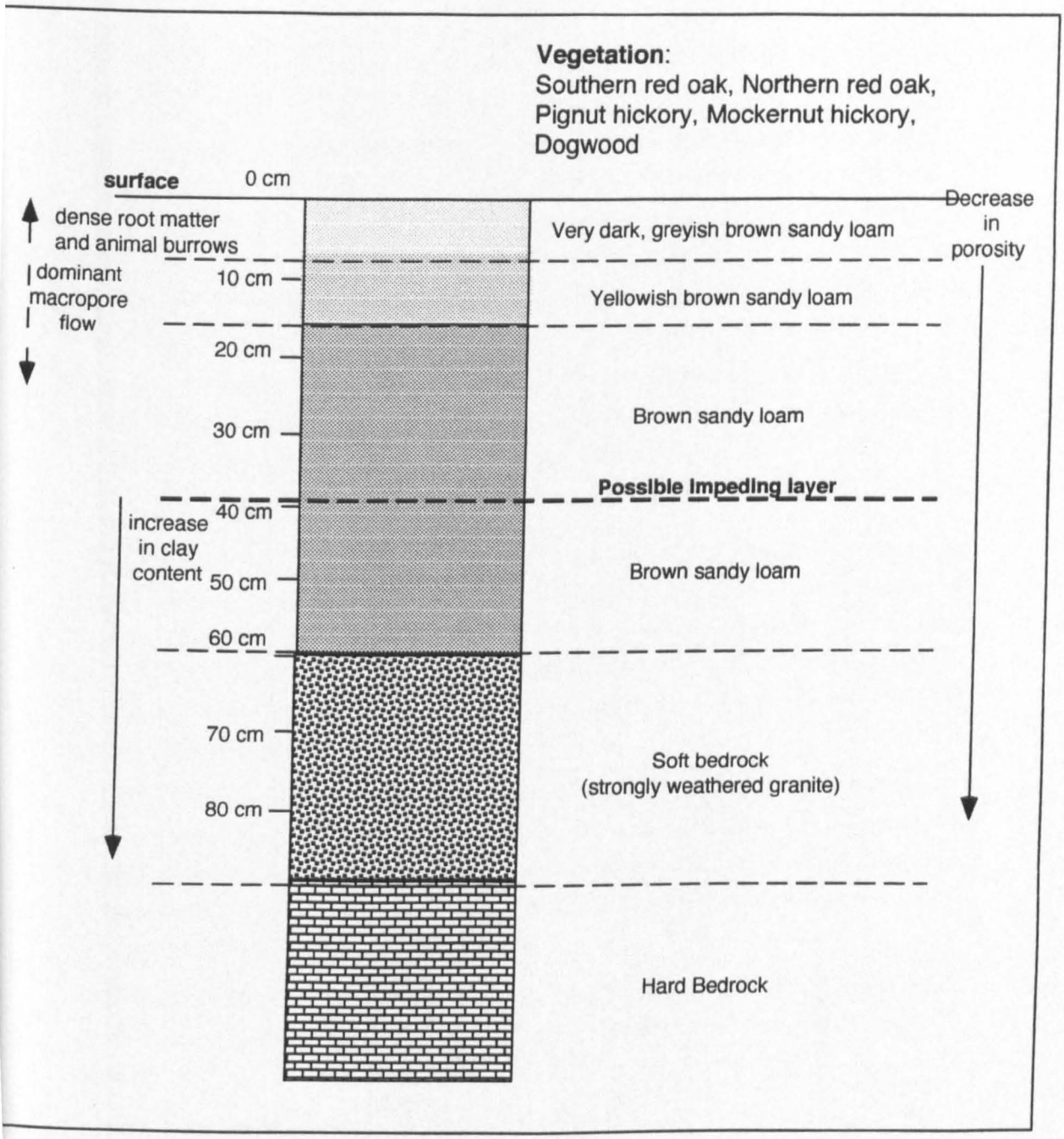

Figure 4.12: *Schematic of typical soil profile on hillslope plot*

seepage of previously subsurface flow, and also prevents the entry of further rainfall, which therefore runs off directly as saturation overland flow.

Hence, the amount of rapidity and magnitude of flow is hypothesised to be greater in the upper soil horizon (< 40 cm). Flow magnitude and rate is expected to be reduced with depth, since the increase in clay content of the soil, and the greater overburden weight reduces the porosity of the soil and hence reduced the hydraulic conductivity. If greater flow rates are seen at depth, then this must be attributed to macropore flow. If greater flow magnitude is recorded at depth, then this may also be attributed to the addition of water than does not move in a vertical direction, but which must flow laterally.

The exact contribution in time and space from each soil compartment will depend on antecedent moisture conditions, rainfall intensity and duration and spatial distribution of rainfall within the catchment (Kennedy *et al*, 1986; Reynolds and Pomeroy, 1988).

(ii) Seasonal pattern of water flow

The operation of evaporation and water uptake by plants is prevalent in the growing season, leaving the soil moisture content depleted and hence, the infiltration capacity higher. Hence, during the growing season, storms that follow dry antecedent moisture conditions may experience low flow rates initially, as this water is stored. In low magnitude storms, flow at depth may be low, if all water is stored in the upper soil horizons. Only in larger storms, where small and large pores are filled, will flow be significant at depth.

During the dormant season, lower temperatures and negligible water uptake by plants causes a general high soil moisture content of the soil. Such conditions allow rapid initial flow, since small pores are already full at storm onset and water is transmitted via larger pores. However, the higher soil moisture status may also contribute to rapid saturation of the soil, leading to saturation overland flow and an overall reduction in the amount of flow at depth.

The seasonal variations in flow volumes depend significantly on the antecedent moisture status of the soil and also the rainfall characteristics (i.e. small or high magnitude storms, and high or low intensity rainfall).

(iii) Temporal variability in flow patterns between nodes

The patterns of flow at each node will be controlled by a variety of factors, e.g. rainfall duration and intensity, antecedent moisture conditions (Kennedy *et al*, 1986). In high intensity storms, and under wet antecedent conditions approaching saturation, if water flow through the soil is assumed to be vertical, then similar flow patterns might be expected at each node, since storage would be minimal and the rainfall was of sufficient intensity to translate water to depth. In less intense storms, following dry antecedent conditions, high temporal variability of flow between nodes would be expected, as water takes longer to transit the soil and higher storage reduces the overall volume of water that reaches the lower node. Hence, these factors influence the timing of the passage of the wetting front through each depth and also the general flow pattern that is observed throughout the storm.

(iv) Spatial heterogeneity of flow within nodes

Huge variations in flow patterns are found from catchment to catchment, and to a lesser extent between plots in a single catchment, and from time to time in a single plot (Whipkey, 1967). At some sites, subsurface flow may be generated due to a discontinuity in the soil, below which the soil is relatively impermeable. At other sites, the main location of subsurface flow varies with antecedent moisture conditions. The rate of movement, the path of movement and quantity of water depends on rainfall rates and duration as well as on the hydraulic properties of the soil (Whipkey,1967). The position of measurement sites on the hillslope is a major factor determining the amount of flow that is observed. Downslope sites tend to give greater measured flow (Jamison and Peters, 1967; Whipkey, 1967). The spatial distribution of vegetation cover on the surface will have a major impact on flow, since it is a control on soil moisture content. Thus, some degree of spatial heterogeneity is hypothesised in this study, although the degree of variation in flow patterns is expected to decrease with respect to depth.

(v) Controls on flow

Sections (i) to (iv) have already outlined the large number of parameters that influence subsurface flow. Storm magnitude and duration will control the amount of water that is available for infiltration into the soil (Kennedy *et al*, 1986). Rainfall intensity will influence flow patterns, especially with respect to the timing of maximum flow at each node (Kennedy *et al*, 1986; Reynolds and Pomeroy, 1988). The hydraulic properties of the soil (i.e. texture and clay content) will influence the amount and the rapidity of infiltration (Whipkey, 1967; Jones, 1971). Antecedent moisture conditions will play a major role in rates and volumes of sub-surface flow (Kennedy *et al*, 1986). Finally, the position of the monitoring site will have some influence on sub-surface flow (Weyman, 1970; Harr, 1977; Mosely, 1979; Bonta and Rao, 1994).

(IV.4Dc) Equipment and Calculations

(i) Operation of Time Domain Reflectometry (TDR)

Matrix water movement was monitored using Time Domain Reflectometry (TDR) (see Chapter III). The rationale for using electromagnetic techniques to measure soil water content lies in exploitation of the large contrast between the dielectric properties of liquid water and those of dry soil, at microwave frequencies. The large dielectric constant of water results from the fact that it is a polar molecule which is free to rotate along the direction of the applied electric field. The dielectric constant of water at microwave frequencies is approximately 80, compared to 3 to 5 for dry soils. As a result, the dielectric constant of wet soils can range from 10 up to 30 or more (Topp *et al*, 1980; Schmugge, 1985).

TDR measurements relate to the propagation constants of electromagnetic waves, e.g. velocity and attenuation to in situ soil properties, e.g. water content and electrical conductivity (Topp *et al*, 1980, 1985, 1988). The TDR technique uses a step voltage pulse propagated along parallel transmission

lines. These parallel rods, or wires, serve as conductors while the soil serves as a dielectric medium. After propagation as a plane wave through the soil, the signal is reflected from the end of the transmission line and returns back to the TDR receiver. The volumetric water content is related to the propagation velocity and thus to the real part of the dielectric constant. The TDR approach has proven reliable for a wide range of mineral soils with accuracies of +/- 2% in estimating volumetric water content (Topp *et al*, 1988).

(ii) Matrix flow movement

The movement of water through the unsaturated zone was monitored using lysimeter and tipping bucket gages (VI-15 and VI-50). TDR probes were installed horizontally into the upslope face of a soil pit at depths of 15, 40 and 70 cm at three Sites (TDRA, B and C). TDRA was located at the base of the hillslope, TDRB was located 5 m upslope and TDRC was located 10 m upslope (see Figure 3.4). After probe installation, each soil pit was back filled with earth extracted from the pit. Each rod pair was interrogated at 5 min intervals. As water flows vertically through the soil, its movement can be traced by monitoring the movement of the wetting front through the soil (i.e. changes in volumetric soil moisture content with depth and time). As the wetting front passes through each depth (i.e. 15 to 40 to 70 cm), increases in soil moisture contents are recorded. The rate of the movement of the wetting front can be calculated from 0 to 15 cm depths, 15 to 40 cm depths and 40 to 70 cm depths. Figure 4.13.a. shows a hypothetical storm case for flow at 15, 40 and 70 cm, derived from TDR data Figure 4.13.ai shows the field installation of the TDR rods at 15, 40 and 70 cm depths in the soil. Rainfall begins at time (to), and at time (t1), the wetting front reached 15 cm depth. This is reflected in the associated soil moisture graph (Figure 4.13aii), where the first increase in soil moisture is noted at 15 cm depth at time (t1). Thus, the initiation of the rising limb of the soil moisture graph signals the time at which the wetting front passes through 15 cm depth. Soil moisture content then continues to rise until a peak is reached. Movement of matrix water in the example is assumed to be in a vertical direction only, and thus, the next response is noted at 40 cm depth (time (t2)) and then at 70 cm depth (time (t3)). Thus, if the times at which the wetting front passes each depth, t1, t2 and t3 (at 15, 40 and 70 cm respectively) are compared, then the rate of movement of the wetting front can be calculated through the soil profile, assuming that all matrix flow is vertical.

The movement of the wetting front can also be traced using tipping bucket gage data at 15 cm depth (VI-15) and at 50 cm depth (VI-50) (Figure 4.13b.). Any rapid flow that is recorded shortly after the onset of a rainstorm, followed by periods of low flow or cessation of flow, is attributed to macropore flow (Phase 1 in Figure 4.13.bii). When flow begins after this or resumes, the second movement of water is attributed to the matrix flow, and the timing at which matrix flow occurs is considered to be the time at which the wetting front passes through that depth. Thus, timing of the passage of the

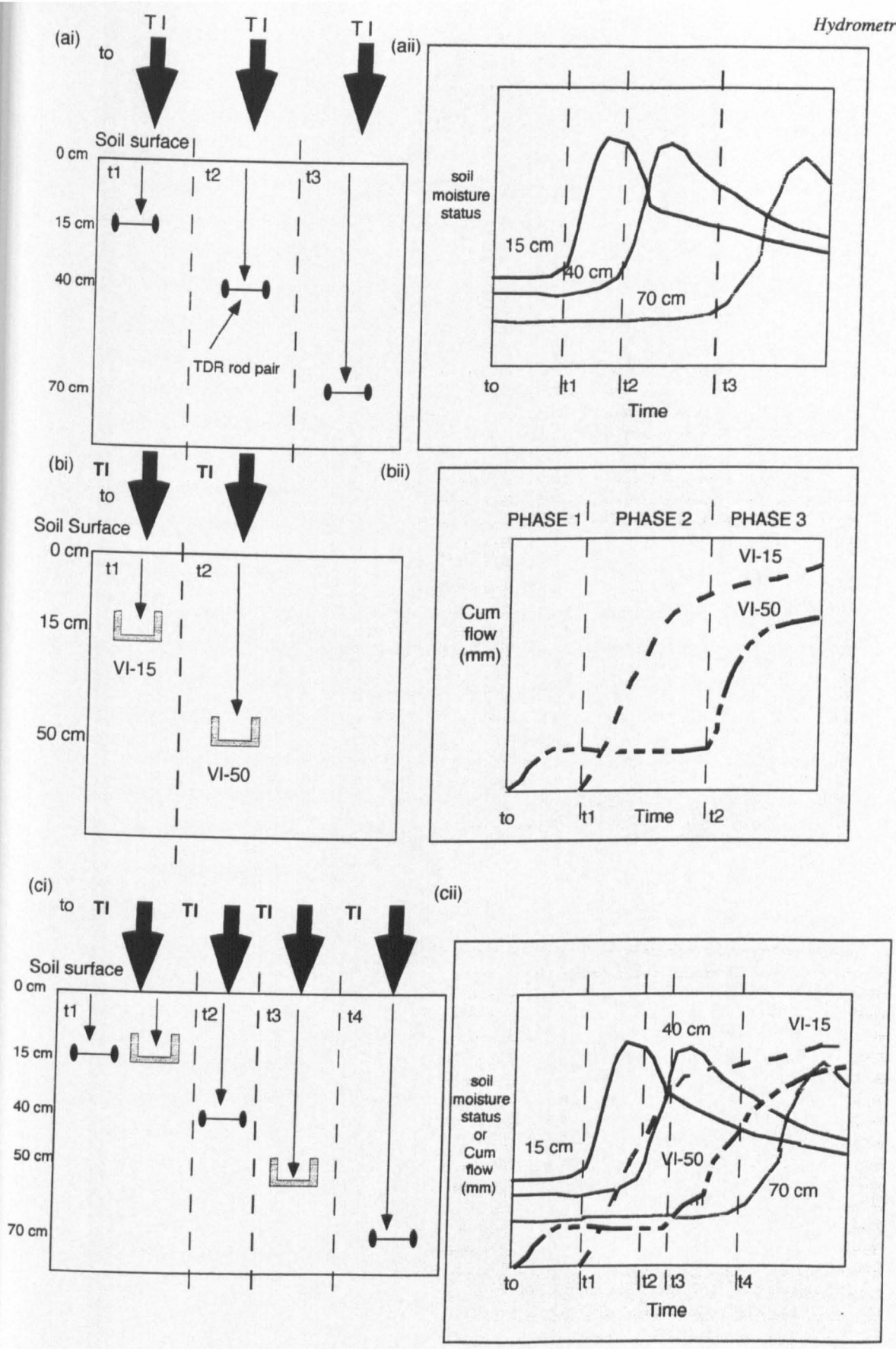

***Figure 4.13**:Field equipment setup and associated responses to storms for (a) TDR rods installed at 15, 40 and 70 cm depths, (b) lysimeters installed at 15 cm (VI-15) and 50 cm (VI-50) depths, (c) TDR rods at installed at 15, 40 and 70 cm and the 15 and 50 cm depth lysimeters*

wetting front through 15 cm using tipping bucket gage data could be corroborated from TDR data at 15 cm from three sites on the hillslope (time (t1)). TDR probes were not installed at 50 cm depth, but some corroboration of the timings derived from the 50 cm lysimeter (VI-50) could be obtained from TDR probes installed at 40 cm depths at the same three Sites.

Figure 4.13.bi, shows the field location of lysimeter VI-15 (15 cm depth) and lysimeter VI-50 (50 cm depth). In diagram (bi), the wetting front reaches the 15 cm lysimeter at time (t1), which is reflected in the flow graph (ii) in phase 2, as the time flow occurs at 15 cm depth. The wetting front reaches 50 cm depth at time (t2), which is reflected in phase 3 of the associated flow graph (ii), when rapid flow is noted at 50 cm depth.

Figure 4.14 displays hypothetical storm examples, where responses in the unsaturated zone are illustrated for pan lysimeters and TDR equipment. In the following section, two major characteristics of flow through individual nodes are calculated; the timing of the passage of the wetting front through a specific depth, and the rate of flow from one depth to another.

Passage of wetting front

Lysimeter data: Figure 4.14a shows responses at 15 and 50 cm depths. The timing of the passage of the wetting front is taken as the time of rapid flow on the cumulative plot, i.e. for 15 cm flow this is time (t1) and for 50 cm flow (t2). (N.B. any flow prior to this at either node is regarded as macropore flow (see Section IV.4E)

TDR data: Figure 4.14b displays soil moisture response at 15 cm. In this case, the timing of the wetting through that depth is regarded as the time of the initiation of the rise in the soil moisture curve (i.e. at time, t1 in the example given).

Calculation of flow rates

Both TDR and lysimeter data are used in the calculation of flow rates. TDR data allows calculation of flow rates between 0 - 15, 15 - 40 and 40 - 70 cm depth. Lysimeter data allows calculation of flow rates from 0 to 15 and 15 to 50 cm depths.

Lysimeter data: In Figure 4.14a, rainfall begins at time to, and the wetting front passes through 15 cm at time t1 and 50 cm at time t2. The rate of movement of the wetting front from 0 to 15 cm (twf_{15}) can be calculated from:

$$twf_{15} = \frac{(t1 - to)}{z}$$

Eqn 4.3a

where z = distance traveled by the wetting front (i.e. 15 cm)

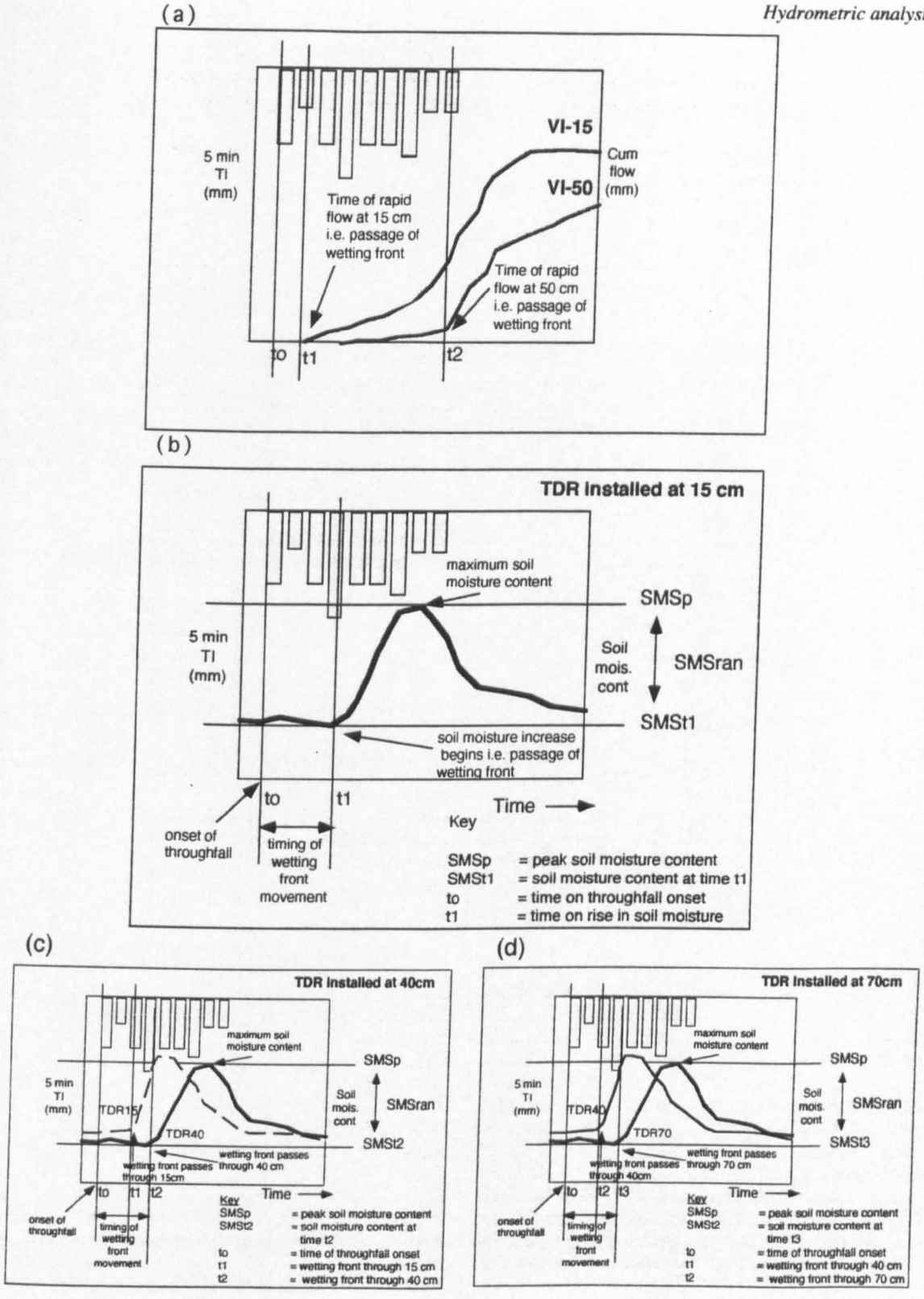

***Figure 4.14**: Soil water response for a hypothetical storm, outlining parameters used in equations (see text), using TDR data (at depths of 15, 40 and 70 cm) and tipping bucket data from lysimeters at 15 cm (VI-15) and 50 cm (VI-50) depths*

The equation is adapted for calculation of the rate of movement of the wetting front from 15 to 50 cm, twf_{50}:

$$twf_{50} = \frac{(t2 - t1)}{z}$$

Eqn 4.3b

where z = distance traveled by the wetting front (i.e. 35 cm)

TDR data: in Figure 4.14b, c and d, rainfall begins at time, to, and the wetting front passes through 15 cm at time, t1 (Figure 4.14b), through 40 cm at time, t2 (Figure 4.14c) and through 70 cm at time, t3 (Figure 4.14d). Hence, similar equations to those above can be used to calculate the rate of movement of the wetting front from TDR data ($TDRwf_{15}$, $TDRwf_{40}$ and $TDRwf_{70}$, respectively).

Calculation of 0 - 15 cm rate of wetting front movement

$$TDRwf_{15} = \frac{(t1 - to)}{z}$$

Eqn 4.3c

where z = distance traveled by the wetting front (i.e. 15 cm)

Calculation of 15 - 40 cm rate of wetting front movement

$$TDRwf_{40} = \frac{(t2 - t1)}{z}$$

Eqn 4.3d

where z = distance traveled by the wetting front (i.e. 25 cm)

Calculation of 40 - 70 cm rate of wetting front movement

$$TDRwf_{70} = \frac{(t3 - t2)}{z}$$

Eqn 4.3e

where z = distance traveled by the wetting front (i.e. 30 cm)
In all of the above equations, the assumption is made that flow is in a vertical direction only.

Other calculations

Lysimeter data: flow volumes at 15 and 50 cm (i.e. Vl-15 and Vl-50) were output at 5 min intervals. This data was cumulated in order to obtain total flow volumes through each depth.

TDR data: TDR rods were not calibrated, hence the soil moisture contents that are reported are not absolute. However, they are relative to each other and are therefore useful in looking at timing and magnitude of soil water content responses. In this section, the following nomenclature will be employed:

$$SMSran = SMSp - SMStn \qquad \text{Eqn 4.3f}$$

where:

SMSran = Rise in soil moisture content during storm

SMStn = soil moisture content at time (n), where n refers to the passage of the wetting front at that depth

SMSp = peak soil moisture content

(IV.4Dd) Results and Discussion

(i) 15 cm and 50 cm soil water flow characteristics

- 15 cm soil water: transfer of water from upper adjacent node

Figure 4.15a displays the relationship between cumulative throughfall and cumulative 15 cm soil water flow for all storms. A positive relationship is observed, where higher magnitude storms (and hence storms experiencing greater throughfall) generate greater flow at 15 cm depth. The graph illustrates some interesting trends that should be explored in some detail.

The first observation is that throughfall must exceed 10 mm before any flow at 15 cm is noted. Hence, in smaller magnitude storms, the upper 15 cm of the soil may be capable of storing this water, providing that the soil is not saturated or near-saturation prior to the storm For storms that follow closely after one another, near-saturated conditions may occur, and in such cases, flow might not be observed at 15 cm depth since throughfall is unable to penetrate to depth and flows over the land surface instead (as saturation overland flow). Another potential mechanism by which negligible flow is recorded at 15 cm depths is when water by-passes the matrix, and flows to depth via macropores.

The second trend to note from the graph is that as storms get larger in magnitude, the total soil water flow at 15 cm does not increase proportionately. As storms get larger, the cumulative increase in flow decreases. For storms that exceed 35 mm in magnitude, there appears to be a considerable decrease in the amount of flow noted at 15 cm. This observation might be attributed to the saturation of the soil, and routing of throughfall via overland flow, or greater connectivity of meso- and macropore channels under wetter conditions and greater transport of water via by-pass flow. In the following section that discusses macropore flow, and in Chapter V, the problems of measuring macropore flow are addressed. It would appear that the 15 cm pan lysimeter does not intersect macropores and only collects matrix water. Hence it is possible that lower flow rates at 15 cm are being measured in some storms since macropore flow is not recorded at this site.

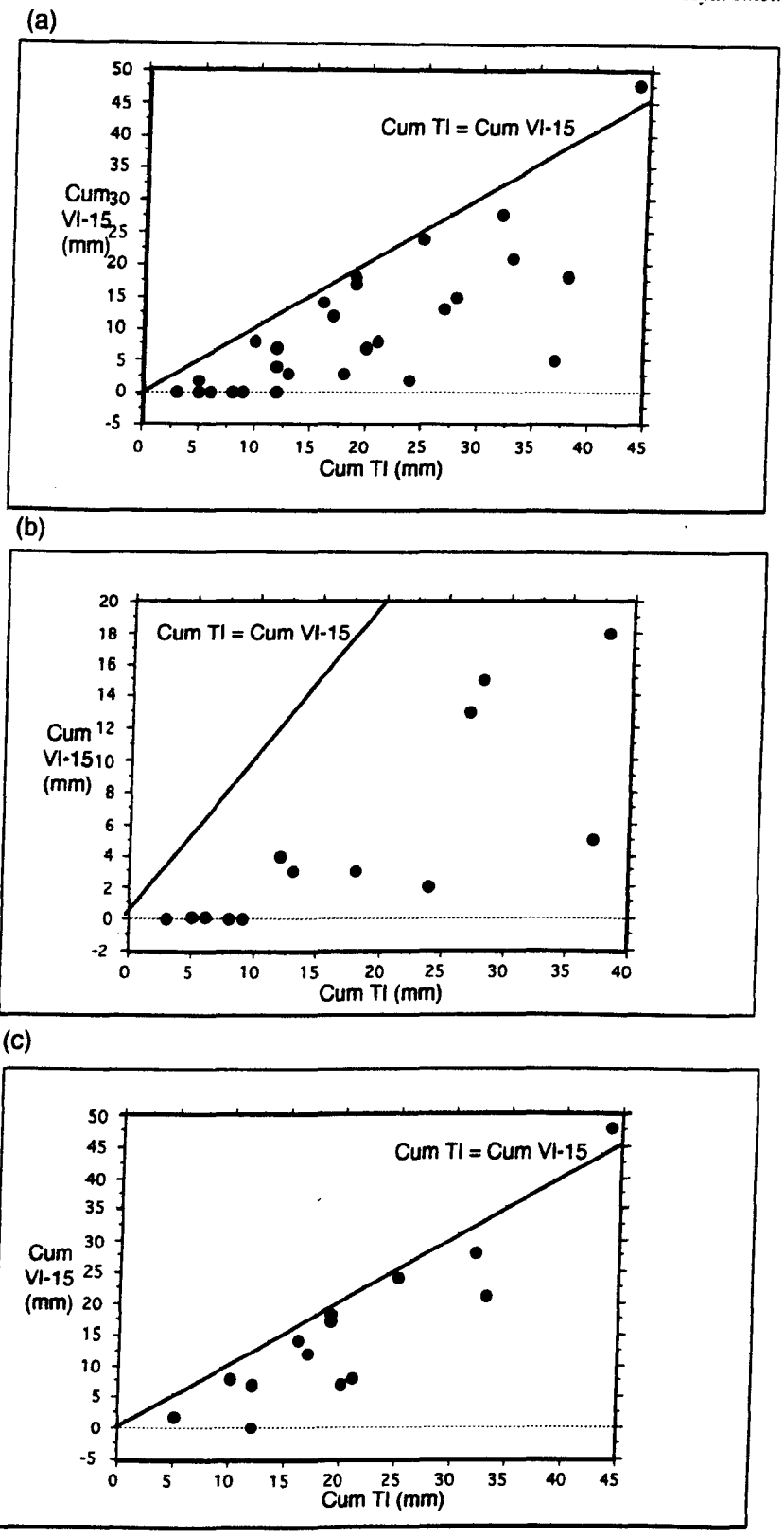

Figure 4.15: *Plots of cumulative 15 cm soil water flow (Cum VI-15) and cumulative throughfall (Cum TI), for (a) all storms; (b) growing season storms; (c) dormant season storms*

Some of the points addressed in the previous section can be considered in greater deal if the storms are divided on a seasonal basis.

Growing season storms

Figure 4.15b displays cumulative throughfall and cumulative 15 cm soil water flow for storms occurring during the growing season (April through September, inclusive). Throughfall clearly has to exceed 10 mm before flow at 15 cm is observed. For storms during which negligible flow was measured (i.e. those in which cumulative throughfall < 10 mm), rainfall during the previous 4 days was < 4 mm (Appendix 4.2). Hence, with low rainfall and warm temperatures leading to depletion of soil moisture via evaporative mechanisms, the soil moisture content of the upper 15 cm of the soil was low. Thus, the hypothesis that low flow was noted at 15 cm due to storage of incoming water by the soil also appears reasonable.

The diagram shows that for storms whose magnitude ranges between 10 and 25 mm, the amount of flow measured at 15 cm does not increase proportionally with storm magnitude, but instead remains around 2 - 4 mm. Infact, it seems that for significant (i.e. > 10 mm) flow at 15 cm to be noted, storm magnitude must exceed 25 mm. For storms of between 10 -15 mm magnitude, half received below 5 mm rainfall in the previous 4 days, whereas the others received between 25 - 30 mm in the previous 4 days. The low flow measured at 15 cm depths during these storms and smaller magnitude storms is best explained as a combination of storage mechanisms and/or macropore flow. Indeed, in many previous investigations, the operation of macropore flow was prevalent during the growing season.

The storms in which high flow was noted at 15 cm, were higher magnitude storms and followed closely after other storms. The storms in which > 10 mm flow occurred all experience > 35 mm rainfall in the previous week and within 5 days of the previous storm. Hence, it would appear that the wetter conditions allow greater transport of water to depth, since hydraulic conductivity would be high. Also, since there is a general increase in flow with respect to storm magnitude, it would appear that saturated conditions has not yet been achieved in the upper 15 cm of the soil, (since for a given head under saturated conditions, vertical flow should be constant). Hence, it would appear that during the growing season, the upper 15 cm of the soil did not become saturated at this location, which provided evidence that saturation overland flow may indeed be confined to the topographic low.

In the high magnitude storm where lower flow at 15 cm was noted (4 mm soil water flow), rainfall during the previous week was < 9mm, and the time lag from the previous storm was also over a week. Hence, under drier conditions and with a longer time lag for evaporative mechanisms to operate under the high summer temperatures, the soil moisture content of the soil would be reduced and hence greater storage capacity of the soil would account for the overall lower 15 cm soil water flow.

Application of standard descriptive statistics on the data show that average flow at 15 cm during the growing season was 6.7 mm (and a standard deviation of 6.5 mm)

Dormant Season Storms

Figure 4.15c displays cumulative throughfall and 15 cm soil water flow for all dormant season storms. Only one small magnitude storm (i.e. < 10 mm) was sampled where low flow was noted at 15 cm depth. Negligible rainfall occurred during the 4 days prior to the storm, hence, a combination of low throughfall and low soil moisture content of the soil may have allowed for storage to occur.

The relationship between soil water flow and throughfall during the dormant season differs greatly from that during the growing season in that there appears to be a much closer relationship between the two parameters The increase in flow at 15 cm increases almost proportionately with the increase in throughfall. It also appears that during the dormant season, there is considerably greater flow per throughfall total than during the growing season. This would be expected, since soil moisture status is generally higher in the dormant season than growing season, allowing for lower storage and greater hydraulic conductivity.

Application of standard descriptive statistics on the data show that average flow at 15 cm during the dormant season was 15.6 mm (and a standard deviation of 12 mm). Hence, on average, flow was over twice as great during the dormant season compared to the growing season.

- Trends in 15cm soil water flow

In an unsaturated soil, the temporal variability of soil water flow might be expected to follow that of throughfall closely. The initial response noted at 15 cm would depend on the soil moisture content of the soil prior to the rainstorm. The hydraulic conductivity of a soil of low soil moisture content is lower than for a soil of high soil moisture content. In a soil that has low soil moisture content, flow through 15 cm would initially be slow, as incoming water filled empty soil pores. In the previous section, it was found that for hydraulic conductivity of the soil to increase significantly, and for flow to be noted at 15 cm, 10 mm of throughfall must occur. Once past this threshold, the temporal variability of soil water flow might be expected to closely follow that of throughfall, i.e. rapid soil water flow accompanies intense throughfall periods. However, once saturation of the soil has occurred, then a steady state of soil water flow would be expected, and hence greater variability might be observed between soil water flow and throughfall flow.

Two case study storms (on 27 July 1994 and 13 October 1994) provide examples of the similarity in the temporal variability of 15 cm soil water flow and throughfall, which suggests that in both storms, saturation of the upper 15 cm of the soil did not occur.

Case study storm: 27 July 1994

Cumulative rainfall, throughfall and flow at 15 cm depth (VI-15) are shown for a storm on 27 July 1994 in Figure 4.16a. Rainfall begins at 5:40 on 27 July and throughfall begins 5 min later (forest floor soil water flow was not recorded during this storm). Flow begins at 15 cm depth at 6:15 on 27 July, and the rate increases at 7:10, which is probably the time at which the wetting front passes through this depth. The graph shows that there are three periods of intense rainfall, which, although delayed somewhat, also occur in throughfall and 15 cm soil water. The close association between temporal flow patterns at each node suggest that flow at 15 cm may be controlled to a high degree by

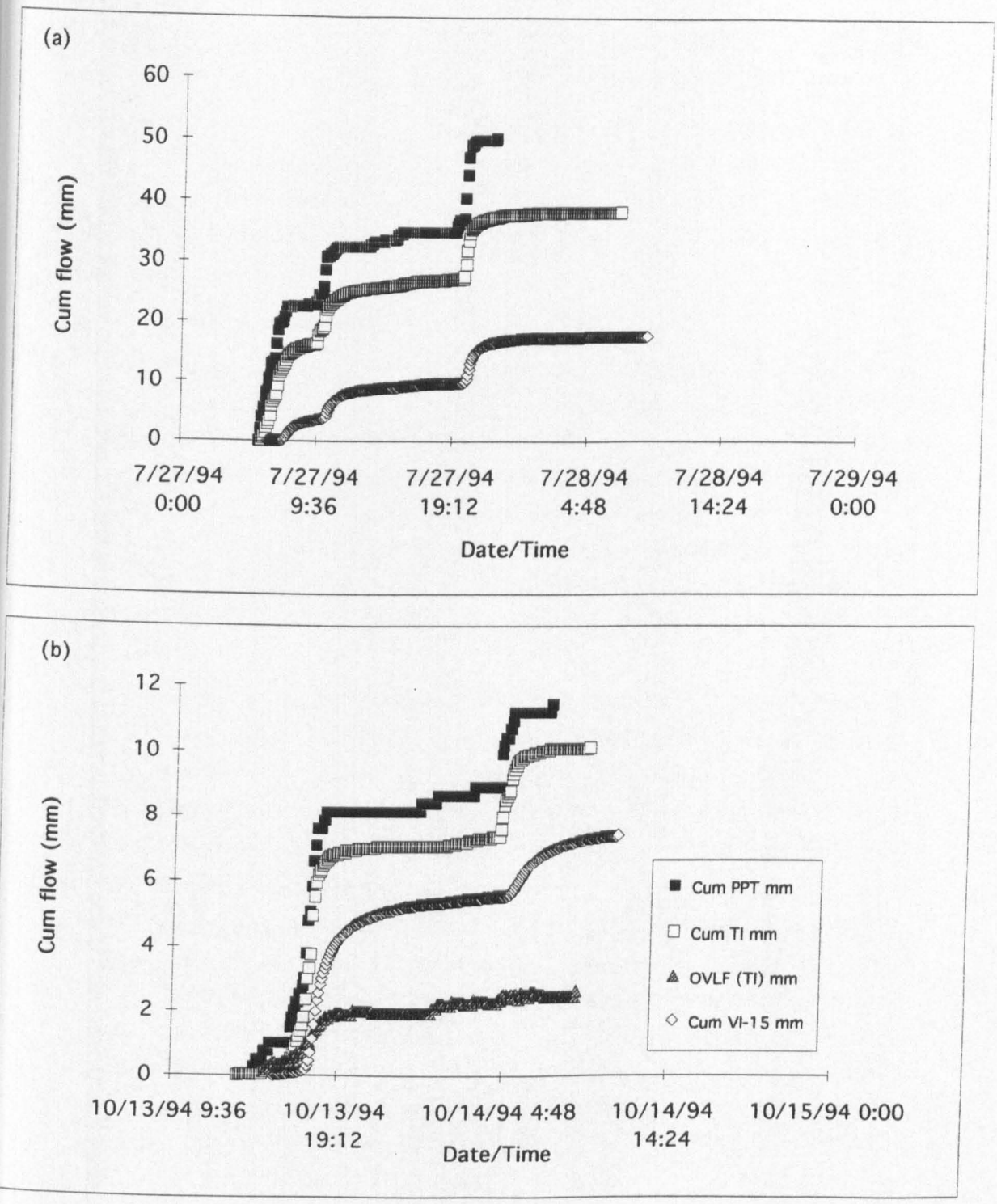

Figure 4.16: Relationship between precipitation, throughfall, overland flow and 15 cm soil water flow for storm occurring on (a) 27 July 1994 and (b) 13 October 1994

rainfall intensity and magnitude. Cumulative rainfall at the end of the first hour of the storm was 16 mm. However, after the first hour of flow at 15 cm depth, cumulative flow was only 2.6 mm.

Rainfall ends at 22:00 on 27 July, with a cumulative total of 50 mm. Throughfall ends at 9:00 on 28 July, with a cumulative total of 38 mm. Flow at 15 cm depth ends at 7:00 on 28 July, with a cumulative total of 18 mm. Total flow at 15 cm depth was 36 % rainfall and 47 % throughfall. Flow at 15 cm during this storm was much greater (18 mm) than the average of all growing season storms (6.7 mm).

Case study storms: 13 October 1994

Figure 4.16b also illustrates the similarity in the temporal variability between flow at 15 cm and rainfall and throughfall. Flow plots are presented for rainfall, throughfall, overland flow and 15 cm soil water flow for a storm on 13 October 1994. Rainfall begins at 14:25 on 13 October. During this storm, throughfall was found to occur before rainfall, suggesting that there is some spatial variability in rainfall in the watershed. Overland flow begins at 14:45 on 13 October and flow is first detected at 15 cm depth at 15:40. However, initially the flow at 15 cm depth is discontinuous and flow rates are slow. This pattern is attributed to the continued drainage of 'old' water from the previous rainstorm (11 October 1994). Rapid flow at 15 cm depth occurs at 17:20 on 13 October, after 3.8 mm rainfall has occurred.

During the storm, there are two periods of intense rainfall, which coincide with two periods of intense flow by throughfall and 15 cm soil water. Overland flow only occurs during the first period of intense rainfall. Rainfall ends at 7:20 on 14 October, reaching a cumulative total of 11.7 mm. Throughfall ceased at 7:50 with a cumulative total of 10 mm. Overland flow total volume was 3 mm and total flow at 15 cm depth was 8 mm and ceased at 10:30 on 14 October Thus, flow at 15 cm was equivalent to 68% of rainfall and 78% of throughfall.

Periods of maximum throughfall and maximum 15 cm soil water flow were calculated (Appendix 4.7). Maximum flow was calculated as the maximum volume of water that passed that depth per 5 min increment. Several maximum values may be presented in storms where there were several periods of rapid soil water flow. Column TIVI-15lg provides the time lag between the maximum throughfall intensity and the corresponding time of maximum 15 cm soil water flow. The time lags varied from 0 to 170 min. However, the majority of the time lags were within 30 min, which suggests that throughfall intensity (which is directly related to precipitation intensity) greatly influenced flow at 15 cm.

Thus, the analysis of the case study storms show that flow rates at 15 cm depth are governed to a high extent by the 'rainfall signature', since periods of intense rainfall prompt periods of rapid flow at 15 cm depth.

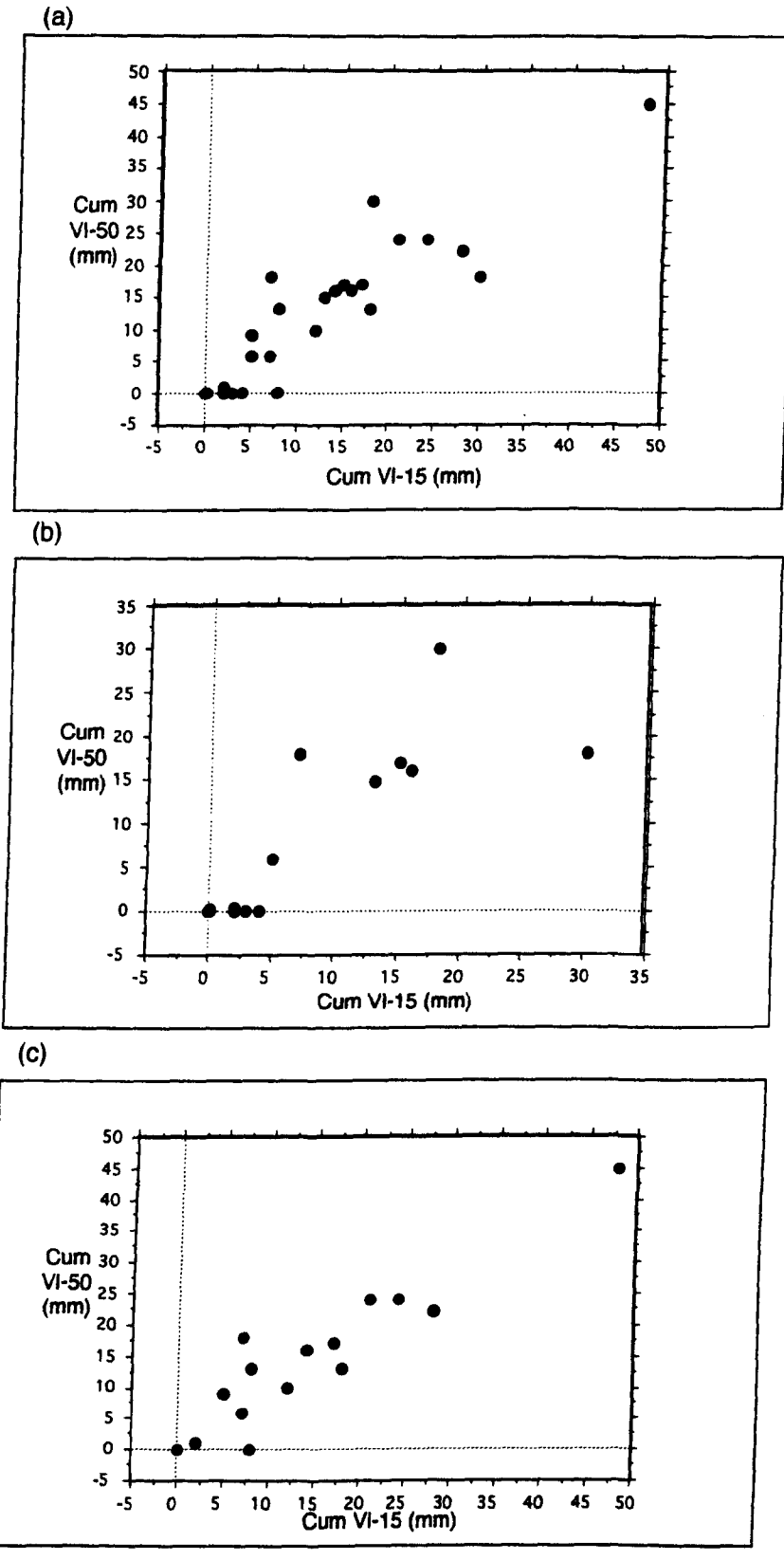

***Figure 4.17**: Plots of cumulative 50 cm (Cum VI-50) and 15 cm (Cum VI-15) soil water flow for (a) all storms; (b) Growing season storms; (c) Dormant season storms*

- 50 cm soil water flow: transfer of water from upper adjacent node

Total flow at 50 cm depth ranged from 0 mm (22 April 1995) to 45 mm (16 February 1995) (Appendix 4.8) Figure 4.17a displays the relationship between cumulative 50 cm soil water (VI-50) and 15 cm soil water (VI-15) flow. The graph shows a general positive relationship between the two parameters. The diagram shows that for flow to be noted at 50 cm depth, the magnitude of flow at 15 cm must exceed 5 mm. When flow through 15 cm exceeds 5 mm, the hydraulic conductivity of the soil increases dramatically, and significant flow is noted at 50 cm (up to 18 mm). In many storms, the total amount of flow that was recorded at 50 cm depth was greater than the total flow recorded at 15 cm depth. Reasons of this observation may include contribution of water to 50 cm via macropore flow or via lateral flow. In the following section, and in Chapter V, results suggest that the 50 cm lysimeter receives macropore water, whereas the 15 cm lysimeter only appears to collect matrix flow.

Hence, the greater soil water volume collected at 50 cm depth may be attributed to the operation of macropore flow, which is not collected by the lysimeter at 15 cm depth.

Once the amount of flow through 15 cm exceeds 10 mm, there appears to be two trends to the flow patterns observed at 50 cm. In some cases, flow at 50 cm continues to exceed that at 15 cm, which is attributed to the same mechanisms as mentioned above. In other storms, there appears to be a decrease in the amount of flow noted at 50 cm depth. This might be due to storage of water or might be because the soil is becoming saturated. However, in the analysis of 15 cm soil water flow, the results suggest that the upper 15 cm of the soil do not become saturated. A possible explanation for the saturation of the 15 - 50 cm soil zone is contribution of water from lateral flow.

Division of storms on a seasonal basis provides a more detailed investigation of these mechanisms:

Growing Season Storms

Figure 4.17b displays cumulative flow through 15 and 50 cm depths for growing season storms. The diagram shows that flow must exceed 5 mm through 15 cm depth to be observed at 50 cm depth. In storms where flow is observed at 50 cm depth, the amount of flow is either equal to or greater than flow through 15 cm. The storm that is an outlier to this pattern occurred on 1 August 1994, where 30 mm flow was recorded at 15 cm depth and 18 mm was recorded through 50 cm depth. The lower flow through 50 cm is attributed to the dry conditions in the week prior to the storm and the warm summer temperatures, leading to depletion of soil moisture content of the soil through evaporative mechanisms.

Dormant Season Storms

Figure 4.17c displays cumulative flow through 15 and 50 cm depths for dormant season storms. A similar pattern is displayed during the dormant season, where flow must exceed 5 mm through 15 cm depth to be detected at 50 cm depth. When flow through 15 cm exceeds 5 mm, there is rapid increase in the amount of flow noted through 50 cm, and in some cases, flow at 50 cm depth was greater than through 15 cm, which is again attributed to lateral or macropore flow. When flow exceeds 10 mm through 15 cm depth, the amount of flow through 50 cm is reduced, since for most storms, the flow through 50 cm is less than through 15 cm. This suggests that near-saturation is occurring between 15 and 50 cm depth.

Similar seasonal patterns were outlined for average 50 cm soil water volumes compared to 15 cm soil water flow volumes. Flow was higher in the dormant season (16 mm on average) than in the growing season (9 mm on average). Hence, during the growing season, average flow at 50 cm (9 mm) is greater than through 15 cm (7 mm), suggesting that either flow regimes at each site are different, or that the additional water at 50 cm is derived from macropore or lateral flow. During the dormant season, the average flow volumes are similar at each depth (both 16 mm).

- 50 cm soil water flow characteristics

The temporal variability between 15 and 50 cm soil water flow was expected to be high, since the hydrological signature of incoming water was likely to be attenuated by greater contact with the soil matrix and the hydraulic conductivity of the soil also decreases with depth, since porosity decreases with depth due to overburden pressure. Times of maximum flow at 50 cm depth were calculated and compared with those through 15 cm (Appendix 4.5). Column VI-50-VI-15lg provides the time lag between corresponding times of maximum flow at 15 and 50 cm depths. The range of time lags was from 15 min to 480 min (although, in some instances, maximum flow rates at 50 cm preceded those at 15 cm, which must be attributed to macropore flow). Thus, the time lags were highly variable, showing that the control of flow intensity at the adjacent node diminishes with respect to depth.

Figure 4.18a and b illustrate the way in which flow at 50 cm depth does not necessarily follow the trends in rainfall, throughfall, overland flow and 15 cm soil water flow. Two storm examples (on 20 November and 13 October 1994) are provided, one in which the pattern of flow at 50 cm depth deviates from those at the other nodes, and the other in which flow patterns at all nodes are similar.

Case study storm: 20 November 1994

Figure 4.18a presents flow plots of rainfall, throughfall, overland flow, 15 cm soil water flow and 50 cm soil water flow. During this storm, flow patterns at 50 cm depth deviate from those at the other nodes. Rainfall begins at 20:10 on 20 November, and throughfall begins 20 min later. Overland flow begins at 22:45. Flow at 15 cm is rapid and sudden, suggesting the passage of the wetting front through this depth at 1:00 on 21 November. This storm is of low duration and high intensity (although rainfall in the first hour is only 0.25 mm). The temporal variations of rainfall, throughfall, overland flow and 15 cm soil water are similar, and differ to that of 50 cm soil water flow. Macropore flow is evident at 50 cm depth during this storm, since flow at 50 cm is noted at 21:30 (which is 3 hr 30 min prior to the passage of the wetting front through 15 cm depth). Flow becomes more rapid at 8:10 on 21 November, which is regarded as the timing of the passage of the wetting front through this depth. The slow response of soil water at 50 cm suggests that significant storage of water occurs in the 15 - 50 cm soil horizon (infact, 18% of water is stored). This storm did follow dry antecedent moisture conditions (0 mm rainfall in the previous week), and flow must be attributed to storage mechanisms. The flow rate increases after 8:10 on 21 November, which suggests that this is the time after which all small pores have been filled and the majority of water movement is through the larger pores.

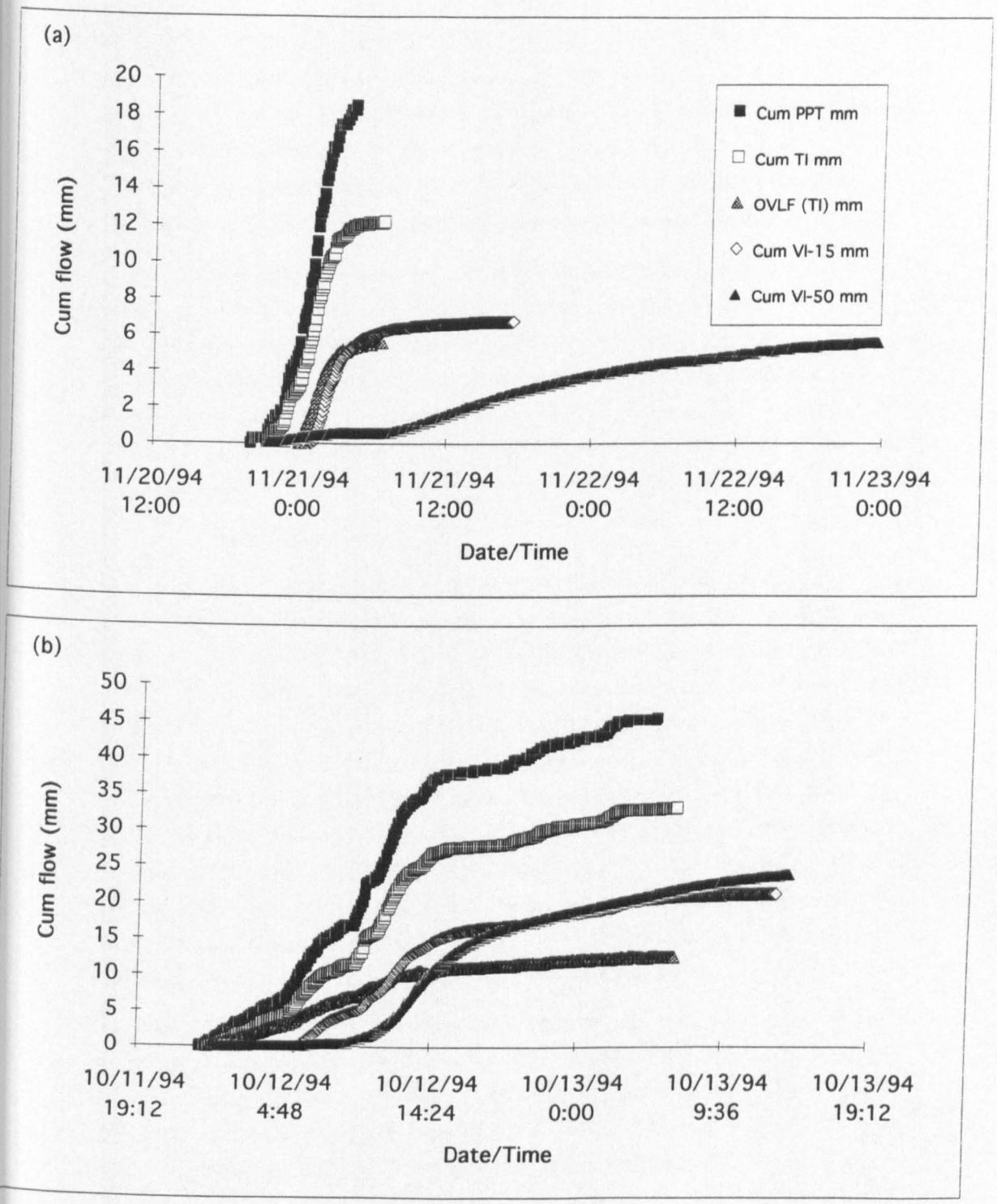

igure 4.18: Relationship between precipitation, (PPT) throughfall (TI), overland flow (OVLF TI), 15 cm soil water flow (VI-15) and 50 cm soil water flow (VI-50) for storms occurring on (a) 20 November 1994 and (b) 11 October 1994

Flow at 50 cm is 5.6 mm, which is equivalent to 15% of total rainfall (37 mm), 22% of total throughfall (25 mm) and 82% of total flow through 15 cm depth (7 mm). This storm followed very dry antecedent conditions (0 mm rainfall in the previous week). It delivered high intensity rainfall, although overland flow was not found to be great (only 8 mm in total). Thus, low flow at 50 cm must be attributed to storage of water in the soil. Throughfall is 25 mm in total, and 8 mm of this is lost to overland flow. In the calculation of overland flow, it is assumed that the forest floor pan lysimeter collects 100% throughfall. Thus, the total water that enters the forest floor is 25 mm. Total flow measured at 15 cm is 7 mm, and thus, 18 mm of this water is lost either to storage in the upper 15 cm of the soil profile or to lateral flow above 15 cm depth. The high storage capacity of the upper 15 cm of the soil is postulated as the cause for the deviation in the temporal trends of rainfall and throughfall with flow at 50 cm depth. The storage capacity of the soil is also linked to antecedent moisture conditions. The slow flow rates at 50 cm also suggest that storage in the soil may be responsible for low flow at depth.

Case study storm: 11 October 1994:

Figure 4.18b shows flow plots of rainfall, throughfall, overland flow, and flow at 15 and 50 cm depths. In this storm, temporal variability of the soil waters are similar. Rainfall begins at 23:25 on 11 October, throughfall begins at 23:55 and overland flow begins at 00:00 on 12 October. Flow at 15 cm is sudden and rapid, which suggests the passage of the wetting front through this depth at 5:25 on 12 October. Flow at 50 cm is noted prior to the response at 15 cm, at 5:35 on 12 October, which may be due to macropore flow. Flow becomes rapid at 50 cm depth at 8:45, which is considered as the time at which the wetting front passes through this depth. The temporal patterns of flow at 15 and 50 cm are quite similar (more so than in the previous example). The storm did not follow especially wet antecedent conditions (only 7 mm rainfall in the previous week), however, it did occur in the dormant season, when soil moisture status is generally higher. Hence, the reason that the flow patterns are more similar is because the soil moisture content of the 15 -50 cm horizon was high, and hence, flow was immediately via larger pores, which are able to transmit water efficiently.

Low intensity rainfall (1 mm) occurs during the first hour of the storm, then becomes more intense and finally becomes light again. Rainfall ends at 4:55 on 13 October, with a cumulative total of 46 mm. Throughfall ends at 6:25 with a cumulative total of 33 mm. Overland flow totals 8 mm, flow at 15 cm depth totals 22 mm, and flow at 50 cm depth totals 24 mm. Thus, total flow at 50 cm depth is equivalent to 53% of total rainfall, 73% of total throughfall and 109% of total 15 cm soil water flow.

The analysis of the case study storms shows how the temporal variability in flow at each node varies. Although some generalisations can be drawn concerning the relationship between flow rates at various nodes, storms will exist where conditions do not adhere to these generalisations. Seasonality, antecedent moisture conditions and rainfall magnitude appear to exert major controls on the flow rates and totals in the unsaturated zone.

(ii) Temporal variability of flow patterns between nodes

The timing of the movement of water through the soil is dependent on a series of factors, including rainfall intensity, timing between rainstorms and soil moisture content. Variations in soil parameters, e.g. soil type, porosity, mineral content, may be responsible for the variation in the time lags recorded at different sampling sites for individual storms.

The passage of the wetting front through 15 cm (monitored at VI-15) occurred from 10 min to 13 hr after the time of rainfall onset (Appendix 4.9). A seasonal control was apparent on wetting front movement. The average wetting front movement time was 120 min for all storms, 69 min for growing season storms and 190 min for dormant season storms. However, it must be recognised that these are average values and that for storms during both seasons, flow was experienced within 15 min of rainfall onset.

The timing of the passage of the wetting front through 50 cm after the onset of rainfall was found to vary seasonally (Appendix 4.9). On average, during the growing season, it reached 50 cm depth after 190 min, and after 252 min during the dormant season (from VI-50 data). These were longer time lags than calculated for the timing of the passage of the wetting front through 15 cm (69 and 190 min for the growing and dormant seasons, respectively).

The time lag of the passage of the wetting front from 15 to 50 cm depths ranged from 15 to 480 min (Appendix 4.11). Time of the wetting front movement from 15 to 40 cm, measured by TDR at Sites A, B and C, are provided in Appendix 4.11. At Site A, the minimum time is 0 min and maximum time is 13 hr. At Site B, the minimum time is 5 min and the maximum time is 10 hr 40 min. At Site C, the minimum time is 1 hr and the maximum time is 12 hr 40 min. Thus, there is considerable variability in the timing of the wetting front movement amongst sites. When negative values are reported, this corresponded to flow detection at 50 cm depth prior to that at 15 cm, which is attributed to macropore flow. At Site A, all lag times were positive, but at Sites B and C, the soil moisture response at 40 cm preceded that at 15 cm by up to 11 hr. This observation is attributed to the occurrence of lateral flow at 40 cm depth. Hence, temporal variability exists in flow at 40 - 50 cm depths.

(iii) Variation of flow patterns within nodes.

The time of wetting front movement for individual storms were found to vary greatly according to where the sampling site was located. In over half of all storms, the onset of soil moisture increase was noted at Site A prior to Site C (with time periods ranging from 5 min to over 11 hr). The soil moisture increase at Site A preceded the onset of flow through lysimeter VI-15 in all storms. This variation in timings suggested two things. The first is that soil characteristics must vary significantly within the 20 m x 20 m plot. The soil is generalised as belonging to the Ashlar Wake Complex (see Chapter II). The upper 7 cm of the soil is greyish-brown sandy loam, underlain by yellowish brown sandy loam, hence rapid movement of water would be anticipated in such well-drained soil. Macintosh *et al* (in prep) describe that soils on the ridgetops of the catchment are from the Madison series, which is

characterised by a yellowish-brown, sandy loam to 15 cm and a strong brown sandy clay loam from 15 - 23 cm, which is underlain by red clay. These soils with a high clay content are less well drained and hence wetting front movement might be expected to be slower. Thus, if there is some variation in soil type within the hillslope plot, where the soils higher up slope have a greater clay content, then the flow characteristics across the plot would be expected to vary. The sandy loams at Site A are well drained and hence wetting front movement would be expected to be most rapid, whereas with distance upslope, and as the clay content of the soil increased, drainage would be excepted to be less rapid.

Another explanation for the observed trend of more rapid water movement through the soil on the lower slope position (Site A) is that the increase in soil moisture may be due to contribution of water from the stream channel to the soils on the lower slope. The response of the upper gage stream hydrograph was compared with the timing of the response of 15 cm TDR at Site A, and in over half of all storms, the stream hydrograph increase preceded the onset of soil moisture increase. Hence, it is possible that during these storms, streamwater contribution may have been responsible for the soil moisture increase.

(iv) Controls on water movement

ANTECEDENT MOISTURE CONDITIONS

The water content of the soil is of paramount importance to transport of water and solutes (Mulholland *et al*, 1990). Soils that are initially dry (i.e. following dry antecedent moisture conditions) may exhibit low flow initially since pores are available to store water. Soils following wet antecedent moisture conditions may allow rapid transport of water via larger pores. However, if conditions are such that the soil is at or close to saturation, this may cause water to be directed via overland flow, since storage and infiltration capacity of the soil is exceeded. Hence, sub-surface flow is reduced (Dewalle *et al*, 1988). However, some studies suggest that antecedent moisture conditions have no effect on flow regimes. For example, in an investigation using brilliant blue FCF to trace water movement in a catchment in Switzerland, initial water content was found to have little or no effect on the flow pattern (Flury *et al*, 1994).

Two parameters were used to investigate the effect of antecedent moisture conditions on flow regimes at the hillslope. The first was the total rainfall in the 48 hrs prior to the storm, the second parameter was total rainfall in the 7 days prior to the storm.

15 cm soil water flow

The relationship between total flow at 15 cm depth and previous rainfall for both intervals are very different between dormant and growing season rainstorms. Figure 4.19 displays scatterplots of total flow at 15 cm vs. previous rainfall during two day and seven days prior to growing season and dormant season rainstorms.

Figure 4.19a and b show two distinct trends in the data. In Figure 4.19a, the first cluster of points shows high flow in the soil following a relatively dry two day period (< 5 mm rainfall). The second cluster relate to storms in which rainfall in the previous two days was > 5 mm. The two relationships

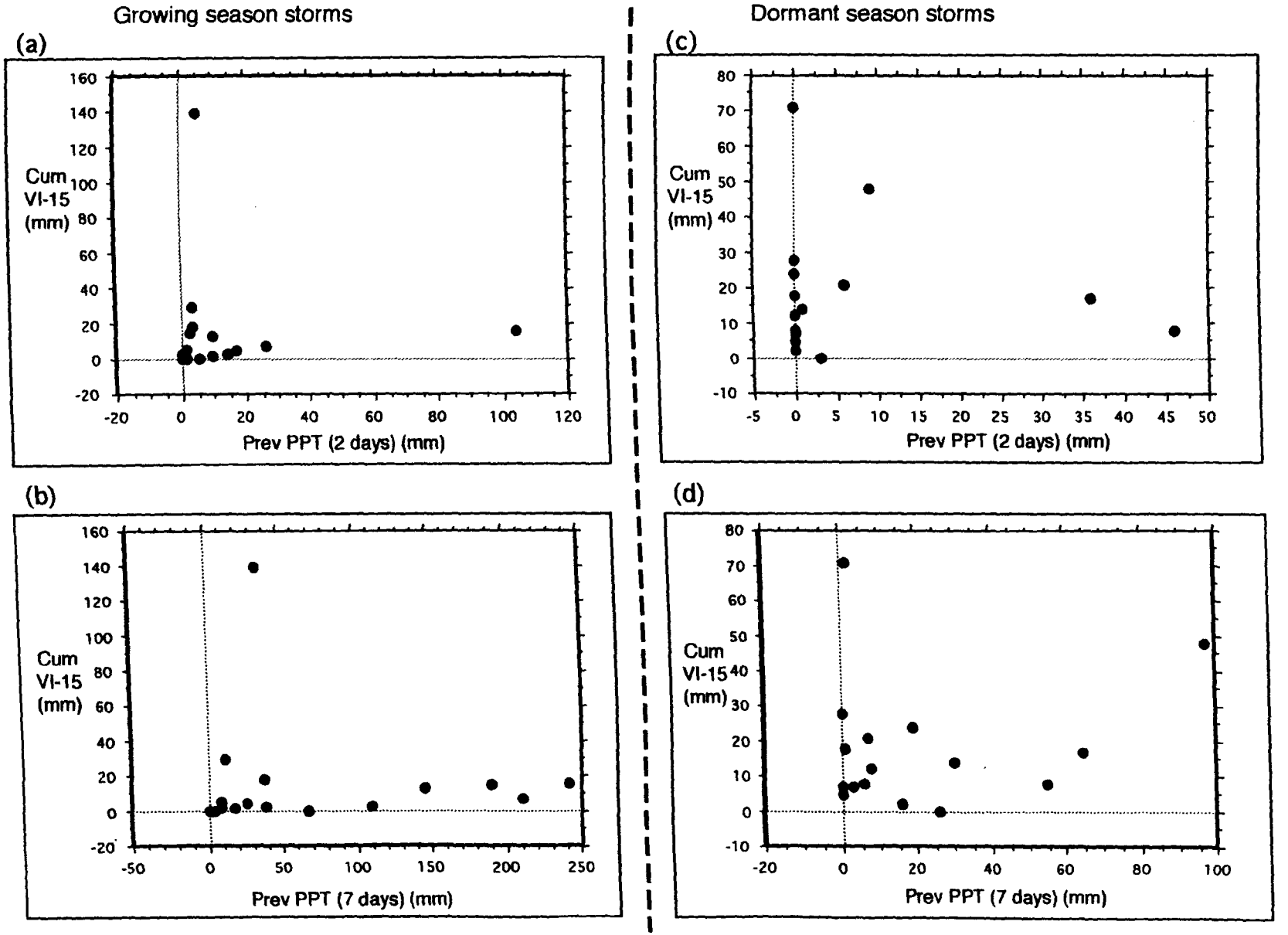

***Figure 4.19**: Plots of cumulative flow through 15 cm (Cum VI-15) and total rainfall in the previous two and seven days for growing season and dormant season storms*

between flow and antecedent conditions may be explained by the moisture content of the soil. When the moisture content of the soil is low, following dry antecedent conditions, it is only the smallest pores that are filled and these transmit water much less efficiently in relation to their cross-sectional area than do the larger pores (Atkinson, 1980). The high flow after low previous rainfall may also be due to transport of water via macropores. Dewalle *et al* (1988) found that the relative amount of soil water observed during an event appeared to be related to the basin soil moisture content prior to the event. When the basin soils are relatively dry, soil water contribution will be smaller because the soil possesses greater water retention capacity. Events which occur shortly after each other will realise greater soil moisture response because the soils then possess less storage capacity. This is shown clearly in Figure 4.19b, where the storms which delivered > 100 mm in the previous seven days, all occurred after Tropical Storm Alberto. Hence, the water storage capacity of the soil was exhausted and so flow was low.

In Figure 4.19c and d, a less obvious trend is noted in the relationship between total flow at 15 cm and rainfall in the previous two and seven days. In Figure 4.19c, the major trend observed is that flow occurs for the majority of storms when negligible rainfall occurred during the previous two days. Also, for storms with < 10 mm rainfall in the previous 48 hr, flow was high, but for greater rainfall volumes, flow became lower, suggesting that the soil may have become saturated and hence 'new' water was prevented from entering the profile. The relationship between total flow at 15 cm and rainfall in the previous seven days was random (Figure 4.19d).

50 cm soil water flow

If the plots of 50 cm flow vs. rainfall in the previous two and seven days (Figure 4.20) are compared with those for 15 cm flow (Figure 4.20), a high degree of similarity is observed, suggesting that 50 cm flow is controlled to a similar extent by antecedent moisture conditions as 15 cm flow is.

RAINFALL/THROUGHFALL CHARACTERISTICS

Throughfall magnitude has a major control on the amount of flow at 15 cm, which in turn, controls the amount of flow at 50 cm. For flow at 15 cm to be noted, throughfall must exceed 10 mm. This control is observed for growing season and dormant season storms. This must affect the relationship between 15 and 50 cm flow, where flow must exceed 5 mm at 15 cm for flow to occur at 50 cm depth.

The timing between rainfall/throughfall was also found to affect flow. Flow at 15 cm depth was relatively higher during storms that followed shortly after other storms, since the soil moisture content had been raised, and meant that 'new' water could flow through larger pores, rather than having to fill smaller pores had the soil been able to 'dry' out.

SITE LOCATION

Finally, the physical features of the soil are important controls on subsurface flow (Whipkey, 1967). If the texture is coarse, then vertical flow dominates. If the texture is fine, resistance to vertical flow results and lateral or shallow subsurface flow sometimes occurs quickly. Also, in fine textured soils,

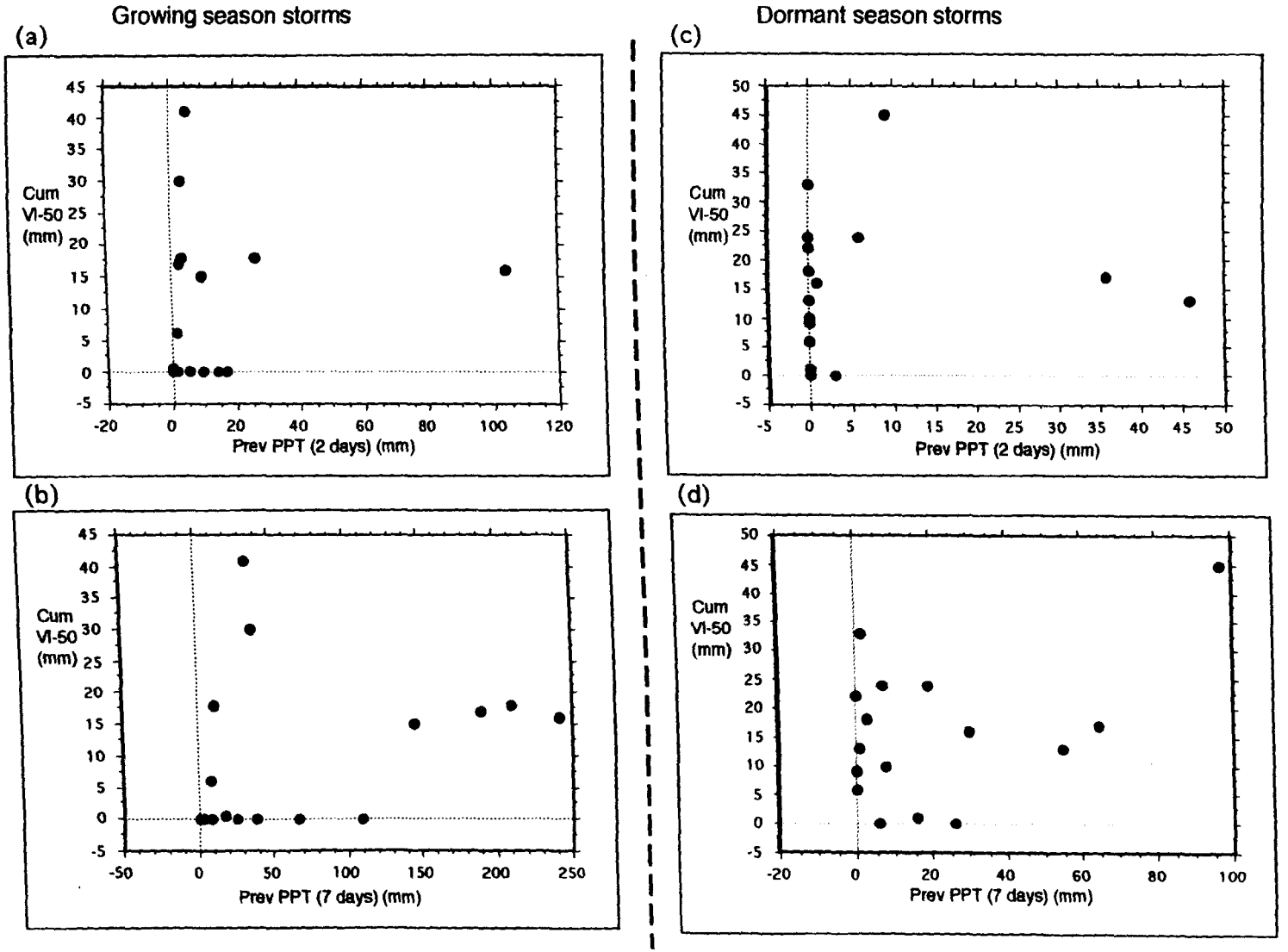

***Figure 4.20**: Plots of cumulative flow through 50 cm (Cum VI-50) and total rainfall in the previous two and seven days for growing season and dormant season storms*

cracks, fissures or channels are likely to occur, providing possible routes for flow. Quick response of instrumented plots at the lowest zone overlying impermeable strata is thought to be due to the water being routed in a pipe-like manner through otherwise slowly permeable discontinuities (Jones, 1971). The position of measurement sites on the hillslope is a major factor in determining the amount of subsurface flow that is observed. Progressing in a downslide direction, and assuming constant flow gradient and uniform soils, the accumulated subsurface flow increases more or less linearly with distance (or slope drainage area) (Whipkey, 1967). Downslope sites may thus give greater measured flow (Jamison and Peters, 1967).

(IV.4De) Summary

At all depths monitored in the unsaturated zone, flow rates compared well between those calculated from TDR equipment and those calculated from tipping bucket gages. The rate of flow was controlled at all depths by several factors, including seasonality, antecedent moisture conditions, storm duration and storm magnitude.

Figures 4.21 and 4.22 summarise the processes in operation in the unsaturated zone of the hillslope during rainstorms. There is a clear seasonal trend in the processes. Hence, each season will be considered in turn.

Growing season

During the growing season (Figure 4.21), the higher temperatures and greater plant activity reduce the soil moisture status of the soil, and hence increase the infiltration capacity of the soil. This may explain why the average 15 cm soil water cumulative flow (and 50 cm soil water cumulative flow) are lower during this season than during the dormant season.

During the growing season of the study period, the site experienced two Tropical Storms (Alberto and Beryl). Tropical Storm Alberto (4 July 1994) and the subsequent series of storms (until 15 July 1994) caused the soil to maintain a high soil moisture status, despite the high July temperatures. Hence, this 2 week period produced abnormal conditions compared with the other months in the growing season.

During all storms, throughfall magnitude must exceed 10 mm before flow is registered at 15 cm depth. In lower magnitude storms (Figure 4.21a), flow is not noted at 15 cm depth, which may be attributed to several mechanisms: The soil moisture status is low for storms that follow dry antecedent moisture conditions (especially since evaporative and plant uptake mechanisms are dominant), hence, the 'new' water can be stored in the upper 15 cm of the soil. If storms follow wet antecedent conditions, where the soil moisture status of the lower horizons (esp. 15 - 40 cm soil horizon) is high, in extreme cases, the soil may be at or near saturation. In this case, the water flows over the land surface as overland flow and flow at 15 cm is negligible. A similar mechanism will occur is the rainfall intensity is so great that it overcomes the infiltration capacity of the soil (although the soil may be unsaturated). This also leads of overland flow and no infiltration of water vertically.

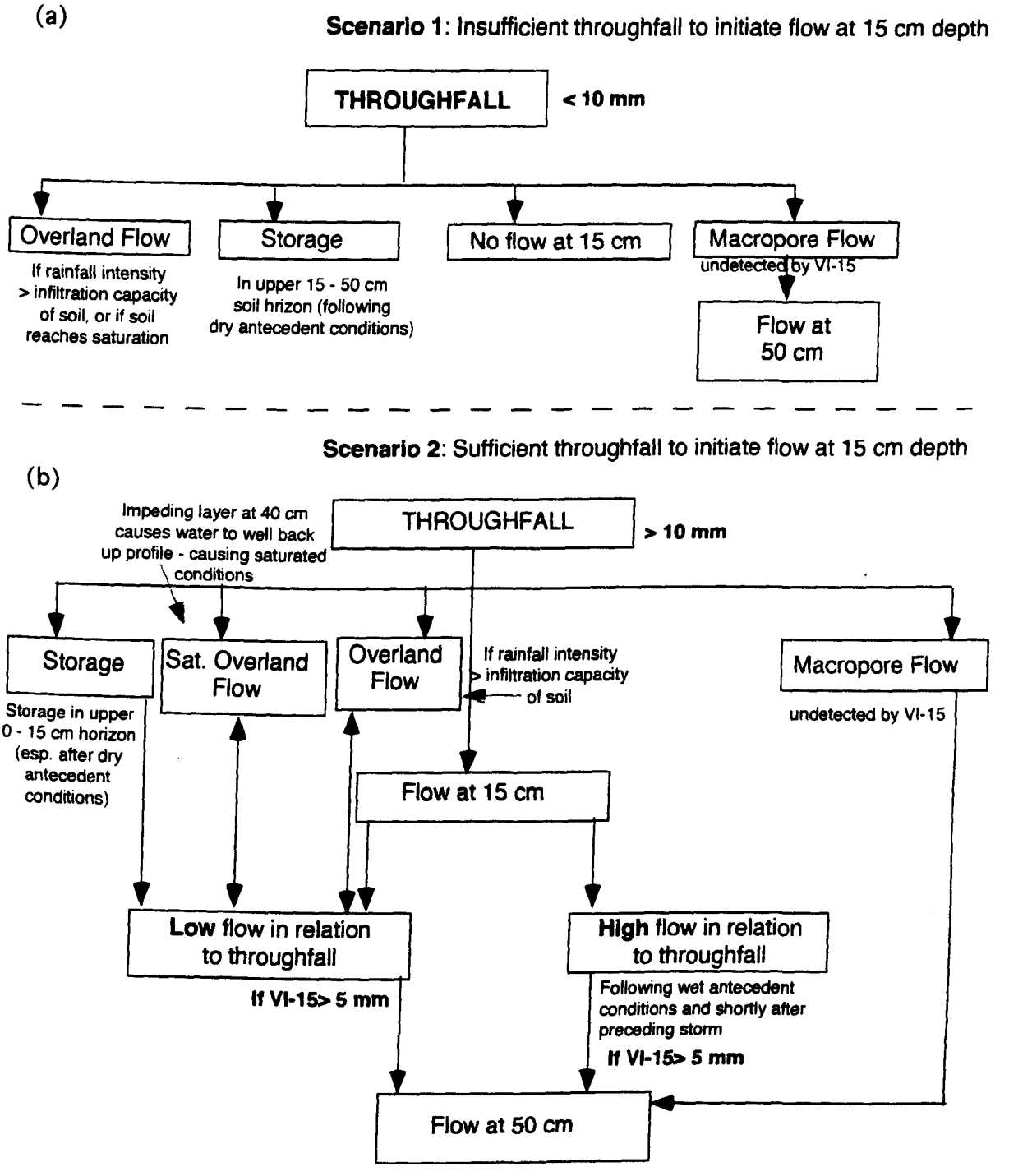

***Figure 4.21**: Representation of sub-surface flow processes during the growing season when (a) throughfall is insufficient to initiate flow at 15 cm depth; (b)throughfall is sufficient to initiate flow at 15 cm depth*

The final mechanism that may lead to negligible flow at 15 cm is if all water is routed to depth via macropores. The hydrometric analysis and results in Chapter V suggest that the VI-15 lysimeter does not intercept macropore flow. This may also explain why higher flow is measured at 50 cm depth than at 15 cm depth for many growing season storms (average flow at 15 cm depth is 7 mm and at 50 cm is 9 mm). Figure 4.21b displays the second scenario of mechanisms that operate in growing season storms. In these cases, total throughfall exceeds 10 mm, initiating flow at 15 cm depth. However, although flow is detected, it does not increase proportionally with the increase in throughfall magnitudes for all storms. The flow regimes that are noted can be divided into two broad categories:
The first category is where flow at 15 cm is low relative to throughfall. This reduction in flow can be explained by several mechanisms. The first may be due to the saturation of the soil. McIntosh *et al* (1997) describe an increase in the clay content of the soil below 40 cm. As the wetting front passes through this layer, the clay swells, reducing the overall hydraulic conductivity below that depth. Hence, the 40 cm horizon may act as an impeding layer during wet conditions. TDR data supports this hypothesis, as for many growing season storms, storm responses are noted at 40 cm depth prior to 15 cm depth. Since macropore flow is undetected by TDR, the increase in moisture at 40 cm depth prior to 15 cm depth may be explained either by lateral flow or by the backing up of water from an impeding layer (at 40 cm depth). If the water backs up as far as 15 cm, this discourages vertical subsurface flow, and water is lost via saturation overland flow.
Another explanation is that in rainfall of very high intensity (e.g. during Tropical Storm Alberto), the rate of introduction of 'new' water exceeds the infiltration capacity of the soil and leads to Hortonian overland flow.
A final explanation for the relatively low 15 cm soil water flow is that following wet antecedent conditions, the connectivity of macropores and mesopores may increase, and hence water is more efficiently channelled via these routes.
The second group of storms in this scenario are those in which flow is high compared with throughfall total. These storms all followed wet antecedent moisture conditions and followed shortly after other storms. Water is rapidly channelled to 15 cm depth, which suggests that the soil is not saturated and hydraulic conductivity is high.
During the growing season, 50 cm soil water flow is equal to or greater than 15 cm flow in most storms where 15 cm soil water flow exceeds 5 mm. This reflects the high soil moisture status (i.e. high hydraulic conductivity) of the 15 - 50 cm zone and/or the contribution of macropore flow to 50 cm depth.

Dormant season

Flow patterns during the dormant season differ markedly to those during the growing season. However, once common trend is the requirement of 10 mm throughfall for flow to be initiated at 15 cm depth (Figure 4.22a). The factors that control this trend are similar to those during the growing season (Scenario 1).

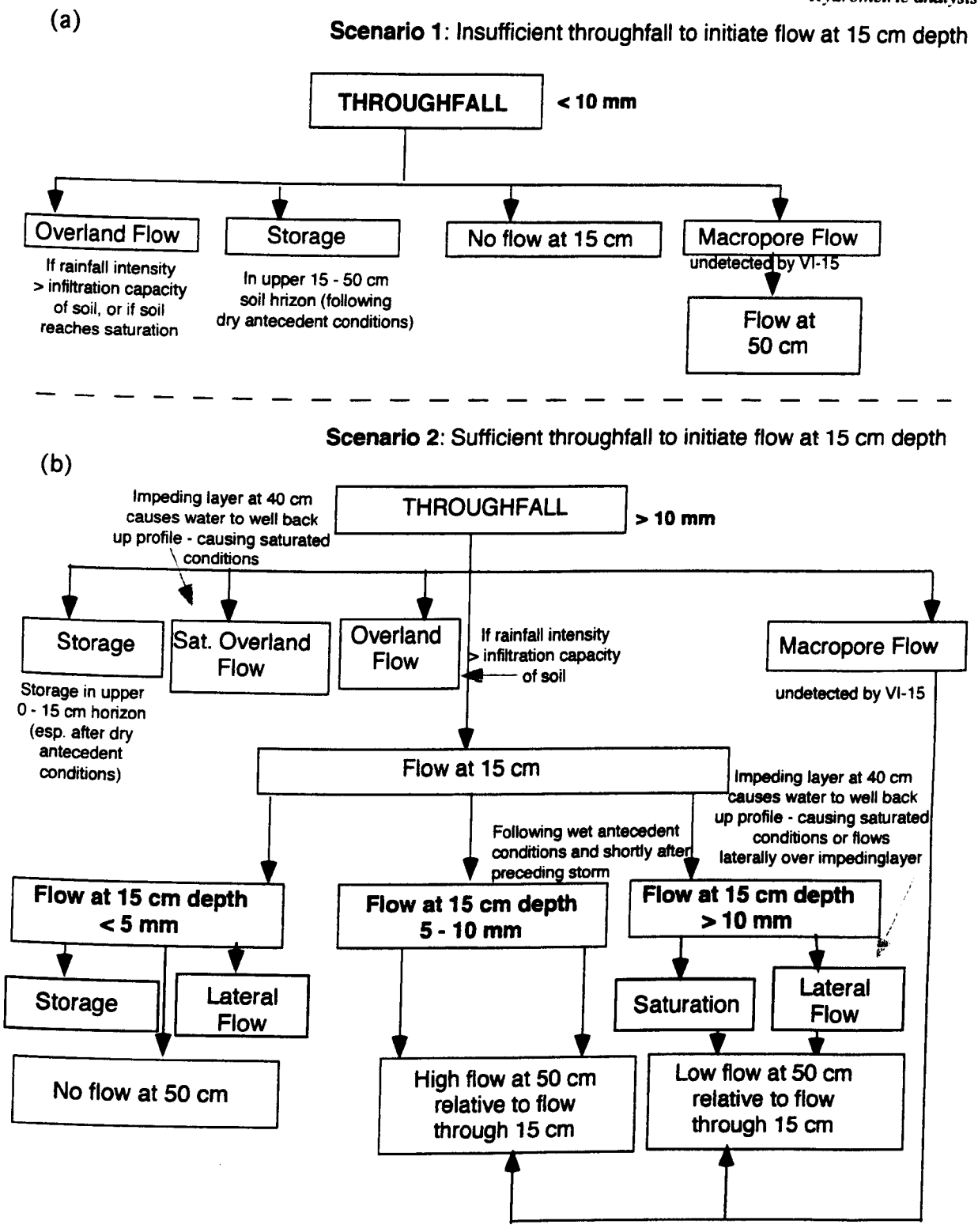

Figure 4.22: *Representation of sub-surface flow processes during the dormant season when (a) throughfall is insufficient to initiate flow at 15 cm depth; (b)throughfall is sufficient to initiate flow at 15 cm depth*

The average flow measured at 15 cm is over twice that during the growing season. The soil moisture content is typically greater during the dormant season, since plant uptake and evaporative processes are much reduced. Hence, smaller pores are already filled with water. Therefore, the storage capacity of the soil is lower, resulting in greater flow to 15 cm. The increase in flow at 15 cm is proportionate to the increase in throughfall volumes, suggesting that the processes that affected the upper 15 cm of the soil during the growing season (especially those that resulted in overland flow) are not prevalent during the dormant season. Macropore flow has been reported as prevalent during the growing season in other studies. Hence, the lack of this route for 'new' water might explain the greater matrix flow recorded at 15 cm depth.

The 50 cm soil water flow regime is more variable during the dormant season. Flow must exceed 5 mm at 15 cm depth for flow to occur at 50 cm depth. For storms where flow at 15 cm depth is between 5- 10 mm, flow is high through 50 cm, suggesting high hydraulic conductivity of the 15 - 50 cm soil horizon. However, in storms where flow exceeds 10 mm through 15 cm, the flow through 50 cm depth is relatively lower. This could be explained by the 'crusting effect'. A soil with higher clay content expands with the passage of the wetting front and hence may act as an impeding layer. If more water is introduced to this layer, it may be routed as lateral flow or may back up through the profile. In either case, this will reduce the total flow measured at 50 cm depth.

In some dormant season storms, total 50 cm flow exceeded total 15 cm flow, which suggests that macropore flow was also in operation during this season.

Hence, some generalisation can be made about sub-surface flow mechanisms at the hillslope during the dormant and growing seasons. However, many of the storms will show unique combinations of the processes outlined, since each storm 'scenario' will be controlled by a series of parameters, including rainfall magnitude and intensity, antecedent moisture conditions and season. The mechanisms of macropore and mesopore flow will be considered in greater detail in the next section.

(*IV.4E*) MACROPORE FLOW

(*IV.4Ea*) Aims and Questions

In the previous section, several observations were made which could be explained by macropore flow. In some storms, flow at 50 cm depth was higher than flow at 15 cm depth, which was attributed either to lateral or macropore flow. In the next section, the possibility that macropore flow occurs will be explored in greater detail. Chapter I discussed previous investigations into macropore flow. This section addresses the following aims and questions:

(i) Does macropore flow operate at PMRW?

(ii) Is there a seasonal control on macropore flow?

(iii) What are the controls on macropore flow?

(IV.4Eb) Hypothesised patterns

(i) Detection of macropore flow

The occurrence of macropore flow has been detected in several studies at PMRW (Shanley and Peters, 1988; 1993).

(ii) Seasonal control on macropore flow

Macropore flow occurs via voids and channels > 750 μm in diameter (Clothier and White, 1981). Desiccation cracks are caused by evaporative losses, enhanced by higher temperatures and are also due to higher solar radiation and plant growth, all of which are characteristic of growing season conditions. Thus, if more cracks occur in the growing season, then macropore flow would be greater.

(iii) Controls on macropore flow

Evidence from recent field experiments illustrate the sensitivity of macropore flow to antecedent moisture conditions (Jones, 1987; Roth *et al*, 1991). Macropore flow has been found to contribute a higher proportion of water to storm runoff following wet antecedent conditions. Rainfall intensity has also been found to influence macropore flow (Wilson and Luxmoore, 1988; Ohte *et al*, 1991).

(IV.4Ec) Equipment and Calculations

Macropore flow can be detected from lysimeter and tipping bucket gage data at 15 and 50 cm depths (VI-15 and VI-50 respectively). Any flow detected at depth in the soil soon after the onset of rainfall can be considered to be water transported by macropores. The evidence for macropore flow would be further strengthened should a tipping bucket response at 50 cm be detected before any TDR response at 15 cm (indicating matrix flow). Also, due to the spatial heterogeneity of soil characteristics, it is possible that lysimeter VI-50 (50 cm depth) intersected a macropore, whilst lysimeter, VI-15 (15 cm depth) did not. Thus, VI-50 may collect both macropore and matrix water, whereas VI-15 only collects matrix water. This is illustrated in the example provided (Figure 4.13b.). The graph shows an example of soil water flow at 15 cm and 50 cm depths. In Phase 1, rapid flow occurs at 50 cm depth, shortly after the onset of rainfall, but before the onset of flow at 15 cm depth. In Phase 2, flow ceases at 50 cm depth and shortly after this, flow is noted at 15 cm depth, signaling the passage of the wetting front through that depth. In Phase 3, flow continues at 15 cm and rapid flow occurs at 50 cm, signaling the passage of the wetting front through 50 cm depth, and thus the passage of matrix flow. Thus, storms in which a flow regime as noted in Phase 1 occurs, is considered to be evidence of macropore flow.

Thus, there are two initial steps in identifying macropore flow:
The first is to assess in which storms flow was recorded at VI-15 (15 cm) and VI-50 (50 cm) prior to the arrival of the wetting front at 15 cm and 40 cm depths, respectively (monitored from TDR).

The second step is to assess in which of those storms a response at VI-50 (50 cm depth) was noted prior to the response at VI-15 (15 cm depth).

(IVEd) Observed patterns and discussion

(i) Detection of macropore flow

33 storms were considered in this part of the analysis. In 5 of these storms, detection of macropore flow was not possible due to the continued drainage of water to depth from a previous storm.

In two of the storms, flow was recorded at VI-15 (15 cm depth) prior to the passage of the wetting front through 15 cm (according to TDR data).

In 24 storms, flow was recorded at VI-50 (50 cm depth) prior to the passage of the wetting front through 40 cm (according to TDR data). The timing at which flow occurred varied amongst storms. The most rapid response from the onset of rainfall was 5 min (23 April 1995) and the longest time was 4 hr 50 min (27 February 1995). 14 of the 24 storms exhibited flow within 1 hr of the rainfall onset. Hence, possible macropore flow was noted in 24 storms. Figure 4.23 provides examples of where macropore flow is hypothesised to occur (27 July and 16 September 1994 and 16 February 1995).

Case study storm: 27 July 1994 (Figure 4.23a)

This is an example of a storm during which macropore flow may occur. This is a growing season, high intensity storm. Rainfall begins at 5:45 on 27 July, which is intense from the onset and totals 16 mm in the first hour. Figure 4.23a shows plots of rainfall and flow at 15 and 50 cm. Macropore flow is noted at 6:00, 15 min after the onset of rainfall. Flow is rapid for the initial 100 min, totaling 0.13 mm by 7:10 on 27 July.

During this storm, flow is noted at 15 cm, before the actual passage of the wetting front. Flow occurs at 6:15, however the passage of the wetting front at 15 cm occurs at 7:15, 75 min after macropore flow is first noted past 50 cm.

Case study storm: 16 September 1994 (Figure 4.23b)

This is another growing season during which macropore flow is hypothesised to occur. The storm is of long duration, containing two periods of intense rainfall. The first intense rainfall period begins at 17:30 on 16 September. Macropore flow is noted 15 min after the onset of rainfall and lasts for 30 min, during which a total of 0.06 mm is recorded (6.1 mm rainfall had occurred). The second period of intense rainfall begins at 00:20 on 17 September, and again, macropore flow is noted at 50 cm depth, 10 min after this (00:30). In the following hour, 0.13 mm flow is recorded at 50 cm depth.

Flow at 15 cm depth is sudden and rapid, suggesting the passage of the wetting front through this depth at 1:25 on 17 September (70 min after the second period of intense rainfall).

Case study storm: 16 February 1995 (Figure 4.23c)

This storm occurred during the dormant season storm and macropore flow might occur. The passage of the wetting front past 15 and 50 cm depths is sudden and matrix flow at either depth is preceded by

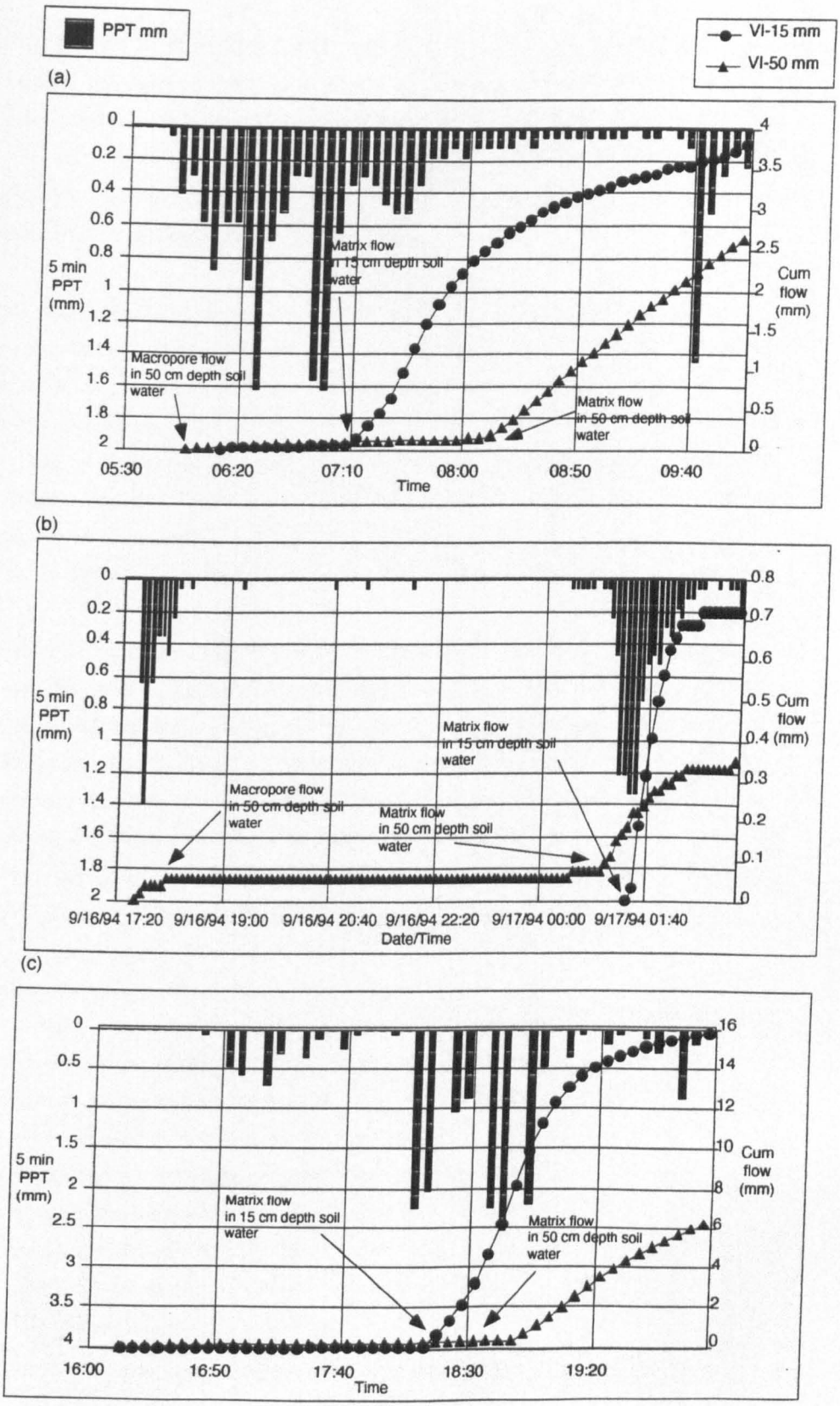

***Figure 4.23**: 5 min rainfall, 15 cm depth soil water flow and 50 cm soil water flow, showing macropore flow and/or matrix flow for storms occurring on (a) 27 July 1994; (b) 16 September 1994, (c) 16 February 1995*

drainage of water prior to the passage of the wetting front. However, the amount of 'macropore' water is very low, and in this case might be due to drainage of 'old' water rather than passage of 'new' water. This storm is 56 mm in total, and rainfall is intense in the first hour of the storm, when 21 mm fell. Rainfall becomes intense at 18:00 on 16 February, and the passage of the wetting front through 15 cm occurs at 18:10. Flow is immediately rapid at this depth. 30 min later, at 18:40, the wetting front passes through 50 cm, and again, the movement is rapid.

The storm case studies raise the issue of whether the drainage of water prior to the passage of the wetting front can be attributed to macroproe flow in all circumstances. In both the storms where drainage at 15 cm was recorded prior to the passage of the wetting front, initial flow was only equivalent to a single tip of the tipping bucket and was thus regarded as an 'old' water drainage feature. Thus, in neither case was there conclusive evidence for the detection of macropore flow. Chemical data presented in Chapter V provides evidence that the water collected by this lysimeter (VI-15) is matrix rather than macropore. The direct measurement of macropore flow is difficult due to the tremendous spatial and temporal variability involved in water movement in the field soil (Flury *et al*, 1994).

In some of the 24 storms that were found to exhibit drainage at 50 cm depth prior to the passage of the wetting front, the volume of water recorded was only equivalent to a single tip of the tipping bucket. Hence, it is possible that this water is purely from drainage of 'old' water and is not macropore flow water. Of the 24 storms in which macropore flow was originally postulated, 7 storms experienced drainage of water (prior to the passage of the wetting front) equivalent to one tip of the bucket. In these cases, the water is attributed to the drainage of 'old' water and the storms are not considered to undergo macropore flow. Hence, in the rest of this section, the only storms that will be investigated for macropore flow are the 17 storms that experienced greater initial flow.

(ii) Seasonal controls on macropore flow

Figure 4.24 displays the magnitude of all storms sampled in the study and indicated the storms in which macropore flow may have occurred (m). Nine of the storms occurred during the growing season and 8 occurred during the dormant season. Hence, the occurrence of macropore flow does not appear to be governed to a great extent by seasonality.

This does not support the hypothesis of greater macropore activity during the growing season, when desiccation cracks develop due to the higher temperatures and greater plant activity. This analysis supports the results of the sub-surface flow analysis that show that in many dormant season storms, the total flow recorded at 50 cm depth was greater than that recorded at 15 cm depth, which was attributed to contribution of water via macropores (and lateral flow).

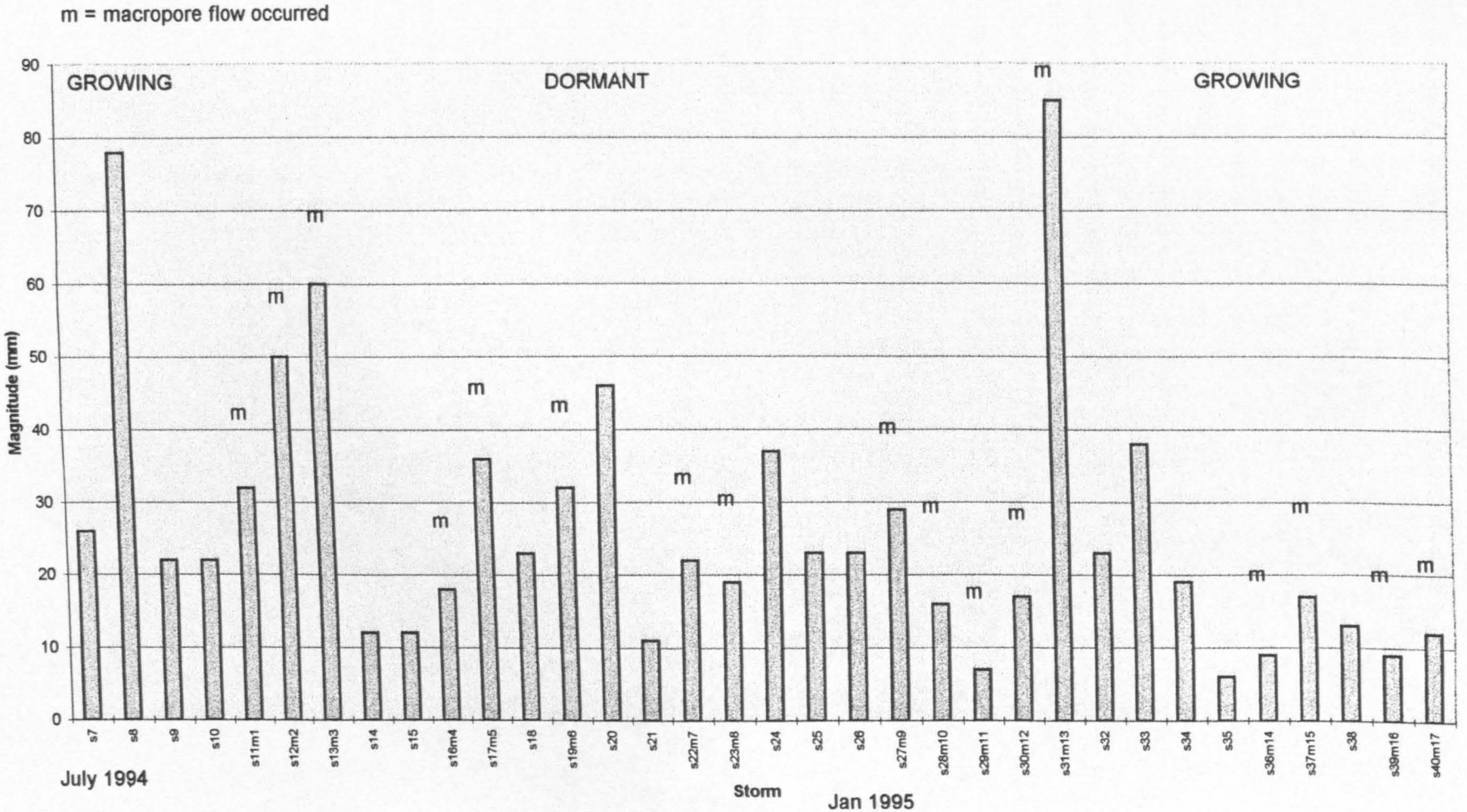

Figure 4.24: Storm magnitude and storms during which macropore flow occurred (m)

(iii) Controls on Macropore flow

STORM MAGNITUDE

In Figure 4.24, the magnitude of storms are displayed, and those during which macropore flow is postulated to have occurred at marked (m). The graph shows that macropore flow occurred during storms of all magnitudes (from 7 mm to 85 mm in magnitude). Hence, it seems that storm magnitude does not control the operation of macropore flow to any degree.

RAINFALL INTENSITY

Figure 4.25 shows a plot of storm magnitude versus storm duration. The storms in which macropore flow occurred are marked (m). The graph displays a random pattern, although there is a clustering of storms experiencing macropore flow that are between 15 to 35 mm magnitude and relatively short duration (< 750 min). The plot of duration and magnitude provides some indication of storm intensity, and the plot shows that this had little influence on the operation of macropore flow.

The assessment of the relationship between total macropore flow and rainfall intensity is difficult, since once the wetting front has passed through that depth, the flow that is recorded will be a combination of both water types. However, in two storms where significant flow was measured at 50 cm shortly after the onset of the storm (and prior to the passage of the wetting front), very intense rainfall occurred in the first hour of the storm (> 20 mm in first hour for storms occurring on 22 July and 21 October 1994). Thus, rainfall intensity does appear to have some influence on the macropore flow, especially on the initiation of the process.

Unlike overland flow, there does not appear to be a specific amount of rainfall required to initiate macropore flow. This suggests that another mechanism that may affect the amount of preferential flow that occurs is pore size. At Ryuouzan Experimental Watershed, Central Japan, low intensity throughfall infiltrated primarily the smaller pores with lower hydraulic conductivities, whereas throughfall from high intensity rainstorms likely infiltrated preferentially the larger pores with high hydraulic conductivities (Ohte et al, 1991). Mesopores are a physically realistic classification (10 - 1000 μm in diameter) (Luxmoore, 1981; Wilson and Luxmoore, 1988). The mesopore may thus contribute more to rapid infiltration than the macropores because rainfall is often insufficient to fill the mesopores and initiate preferential flow. Thus, two pore domains which hold the water at different tensions are thought to preferentially channel water through the soil profile (Wilson and Luxmoore, 1988). However, Atkinson (1980) points out that a large pipe may produce a larger volume of quick flow than many small pipes and in some cases may overshadow the small pipe flow completely. Thus, the preference of flow through larger pores (macropores) and smaller pores (mesopores) is controlled to high extent by rainfall intensity. Also, a certain amount of rainfall may be required to initiate mesopore flow and a greater volume for macropore flow (Ohte *et al*, 1991). Since the mesopores are likely to fill first, the storms that exhibit flow the shortest time after the onset of rainfall may be exhibiting mesopore flow.

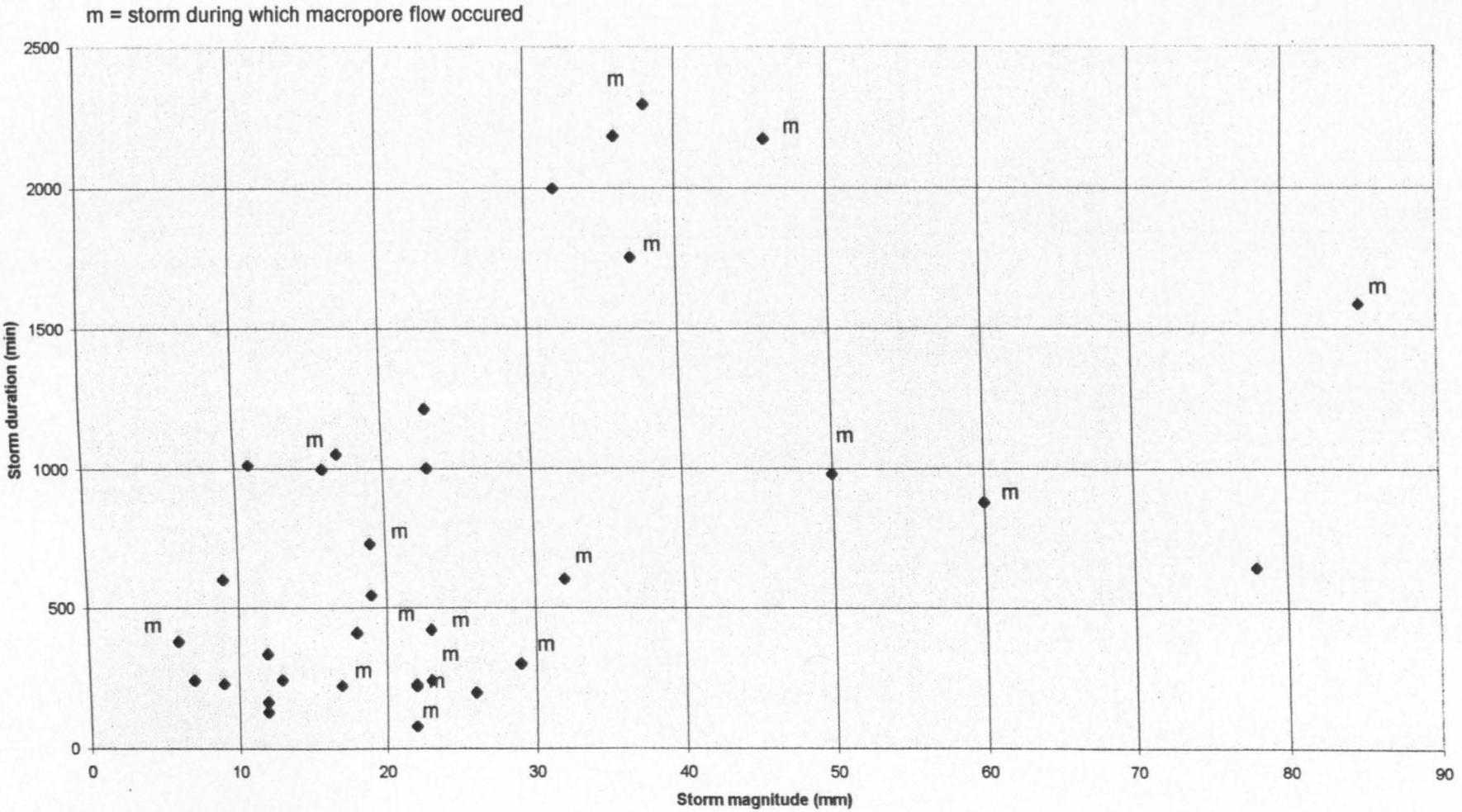

Figure 4.25: Storm magnitude and duration, and storms during which macropore flow occurred (m)

ANTECEDENT MOISTURE CONDITIONS

Total rainfall in the week prior to a storm was used as a measure of antecedent moisture conditions. Figure 4.26 displays antecedent moisture conditions for all storms, and those during which macropore occurred are marked (m). The graph clearly shows that all storms during which macropore flow occurred followed dry antecedent moisture conditions. The total rainfall in the week prior to each storm ranged from 0 to 39 mm. The majority (15) of the storms experienced below 20 mm in the previous week. Hence, antecedent moisture conditions appear to exert a strong control on the occurrence of macropore flow. Drier conditions allow for the expansion of desiccation cracks and greater macropore flow. The previous section discussed the greater clay content of the soil below 40 cm, which under wet conditions swelled and acted as an impeding layer. During wetter conditions, the clay swelling have lead to contraction of macropores and reduction in their transport efficiency.

(IV.4Ee) Summary

Flow prior to the passage of the wetting front through 50 cm depth was observed in many storms (71% in total) (Appendix 4.14). However, this observation was not regarded as robust enough for the identification of macropore flow. In storm storms, the amount of flow recorded prior to the passage of the wetting front was equivalent to a single tip of the tipping bucket. In these cases, this observation was attributed to an 'old' water drainage feature and hence, these storms were not considered to undergo macropore flow. In all, 17 of the total 33 storms were considered to experience macroproe flow (from hydrometric analysis alone).

Macropore flow occurred in growing season and dormant season storms. This was an unexpected result since previous investigations found that macropore flow was prevalent during the growing season, since higher summer temperatures caused the development of desiccation cracks in the soil. However, this analysis has shown that the main control on the operation of macropore flow is antecedent moisture conditions. The majority of storms that experienced macropore flow were preceded by less than 20 mm rainfall in the previous week. Hence, it seems that drier conditions and not necessarily higher temperatures allowed the development of macropore channels. These antecedent conditions may also have allowed drying out of the lower soil horizon with higher clay content. Under wetter conditions, the clay swells and may cause constrictions in the macropores. Dry conditions may be required for the clay to shrink again and allow macropores to channel water effectively in subsequent storms.

Thus, the hydrometric analysis has provided clear evidence that macropore flow (and mesopore flow) are important flowpaths for the rapid channelling of water to depth at the onset of storms (whether macropore flow continues during storms can not be concluded from hydrometric evidence alone). Macropore flow appears to be controlled by antecedent moisture conditions and rainfall intensity. Whether the water that follows the pipes is 'new' or 'old' water can not be determined from the analysis of hydrometric data only. The following chapter will incorporate tracer data with the data presented thus far and make an assessment of what water type is transported by macropores.

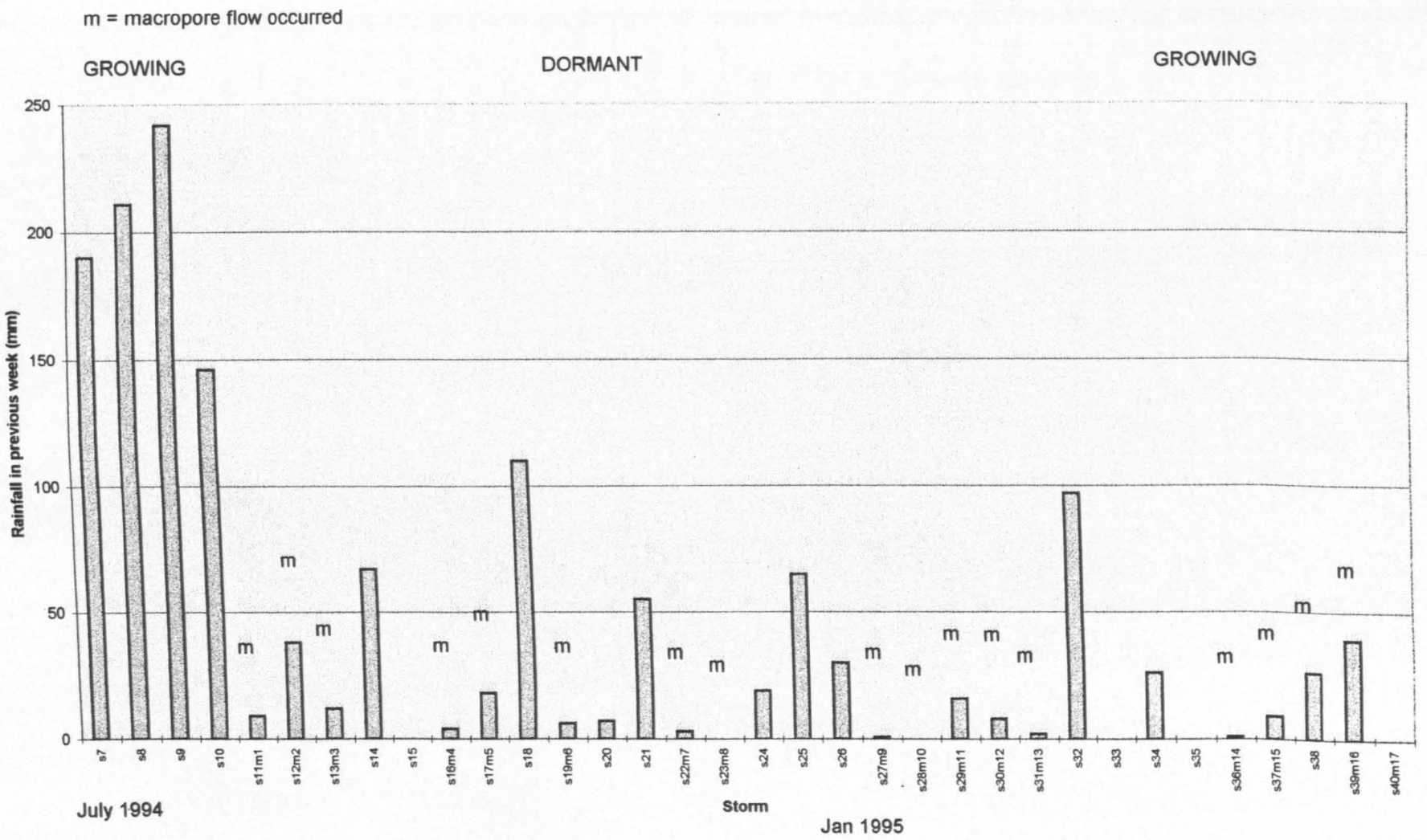

Figure 4.26: Storms during which macropore flow occurred (m)and antecedent moistureconditions (rainfall in week prior to storm)

(IV.4F) Deep Sub-Surface Flow

(IV.4Fa) Aims and Questions

Three types of groundwater flow mechanisms were identified in Chapter I; Groundwater ridging (McDonnell, 1990); groundwater displacement and an air compression effect (Todd, 1980). The occurrence and controls on each are assessed with reference to the hillslope location, and the following aims and questions are addressed:

(i) What mechanism(s) of groundwater flow operate at PMRW?

(ii) Is there a seasonal control to the operation of these mechanisms?

(iii) What are the controls on groundwater responses?

(IV.4Fb) Hypothesised patterns

(i) Mechanisms of groundwater response

The processes of groundwater response have not been addressed in previous investigations at PMRW. Groundwater levels were monitored at three positions on the hillslope. GWA was located in the riparian zone, GWB at 5 m upslope and GWC 10 m upslope. Groundwater stage data was output at 5 min intervals.

Groundwater ridging

If groundwater ridging was a major process at these locations, then the response of the well in the riparian zone (GWA) would be expected to be the most rapid and of greater magnitude than that of the other wells. The groundwater ridging phenomenon is not related to the magnitude of rainfall, but more to antecedent moisture conditions, and hence the development of saturated wedges on the lower slopes (McDonnell, 1990). Thus, the magnitude of the rise in the groundwater level may be more significantly correlated with rainfall in the week prior to storm than to the magnitude of the storm.

This mechanism is displayed in figure 4.27a. The diagram shows the field situation, whereby rainfall falling on the unsaturated zone of upper slope leads to throughflow (Qt) of water downslope. The downslope movement and rainfall falling onto the lower slopes, promotes the flow of groundwater (Qg) into the stream channel from the saturated wedges, located on the valley bottoms and lower slopes. The expected hydrometric response is illustrated in Figure 4.27aii. Base flow conditions in the groundwater prevail at time (to) and at time (t1), rainfall begins. The response of groundwater is rapid (t3), and peaks at time (t4), after which there is a slow return to base flow. This mechanism has been clearly demonstrated in lab models and mathematical models, but has not been well documented in the field (McDonnell, 1990).

Groundwater displacement

If groundwater displacement was a major mechanism, then a substantial rise in groundwater level would be expected to follow shortly after macropore flow occurs. Groundwater response prior to the

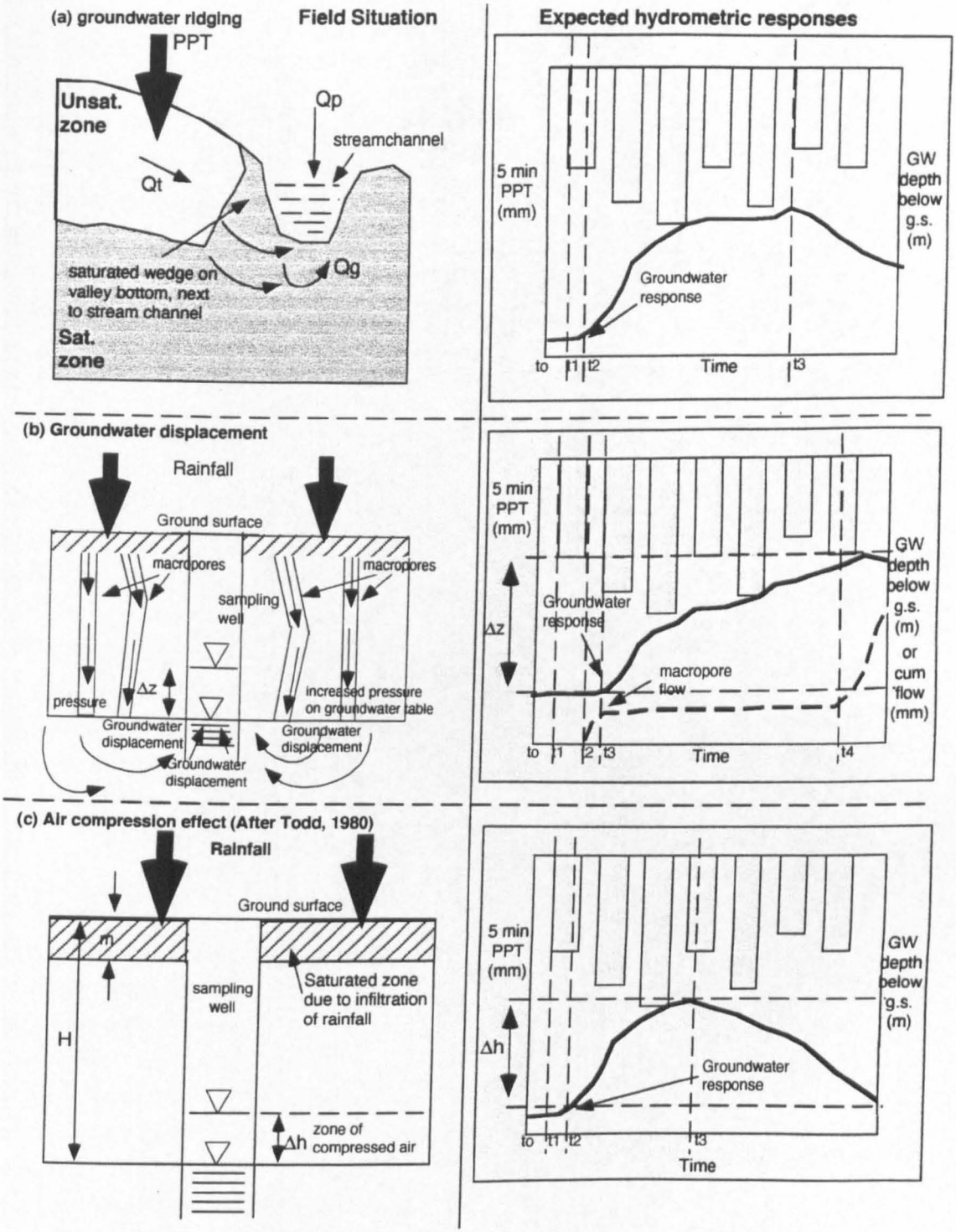

Figure 4.27: *Hypothesised groundwater response mechanisms: (a) Groundwater ridging (after Ward, 1989) where PPT = rainfall, Qt = throughflow, Qg = groundwater flow, Qp = direct channel rainfall; (b) Groundwater displacement mechanism, leading to a groundwater level rise of Δz (after McDonnell, 1990); (c) Air compression effect (after Todd, 1980), where water rise (Δh) in an observation well results from infiltration of rainfall sealing at the ground surface and compression of air above the water table. Where H = zone of interconnecting air-pores, and m = thickenss of zone of compressed air and Δh = rise in water table*

passage of the wetting front through 70 cm (or 40 cm) would reinforce evidence for the occurrence of this process.

This mechanism is displayed in Figure 4.27b. Figure 4.27bi shows the field situation, whereby macropores transport of 'new' water rapidly through the unsaturated zone. This water exerts a pressure on the saturated zone, leading to some form of displacement mechanism of groundwater from a higher position on the hillslope. This is shown in Figure 4.27bii, where baseflow conditions in groundwater prevail at time (to). Rainfall begins at time (t1) and macropore flow is noted soon after this (t2). Macropore flow promotes a rise in groundwater level at time (t3), which reaches its peak height at time (t4)

Air compression effect

If Todd's (1980) explanation for the occurrence of rapid shallow groundwater response is accepted, whereby increased pressure on the air entrapped in the soil by infiltrating water causes a shallow groundwater rise, then groundwater response would again be expected to occur prior to the time of the passage of the wetting front through 70 cm in the soil.

Figure 4.27c displays the field situation in which Todd's theory would occur. Increased pressure is exerted on the air trapped in the zone of aeration when rainfall seals surface pores and infiltrating water compresses the underlying air. If the zone containing interconnected air-filled pores (H) is compressed to a thickness (H-m), then the pressure above the water table is increased by m/(H-m) of an atmosphere, causing the water in the observation well to rise by a height, Δh:

$$\Delta h = \frac{m}{H - m}(10)m$$

Eqn 4.4a

(ii) Seasonal controls on groundwater responses

Groundwater ridging is related to antecedent moisture conditions (McDonnell, 1990). Hence, the higher temperatures in the summer, leading to lower soil moisture contents, may lead to reduction in the area of saturated wedges and hence less intense groundwater ridging.

In previous studies, macropore flow has been found to be prevalent during the growing season, and since groundwater displacement is initiated by macropore flow, the seasonal control on groundwater displacement is also expected. Hence, groundwater displacement is anticipated in the growing season, whilst groundwater ridging may be dominant during the dormant season.

(iii) Controls on groundwater responses

Seasonality has been suggested as an influence on the type and magnitude of groundwater response. However, other factors may also be important. Antecedent moisture conditions exert a control, since the wetter the conditions, then the more probable the development of saturated wedges in the riparian zone and hence the more probable the operation of groundwater ridging (McDonnell, 1990). Rainfall intensity may also influence groundwater response. Freeze (1974) indicated that recharge of

groundwater by infiltrating rainwater was likely to be greater for long duration, low intensity rainfall. However, groundwater displacement is linked with macropore flow (Beven and Germann, 1986), and hence linked to rainfall intensity. Greater macropore flow occurs following intense rainfall, and hence a higher groundwater response is anticipated following intense rainfall.

(IV.4Fc) Calculations

The identification of different mechanisms of groundwater flow require analysis of the following characteristics of the response:

- Timing of groundwater responses
- Magnitude of groundwater responses
- Rate of groundwater responses

Analysis of each is provided in the following section. Seasonal patterns to groundwater responses are also identified in each section. A summary of the major mechanisms in operation is provided at the end. Groundwater levels were monitored at three positions on the hillslope, GWA (in the riparian zone), GWB (5 m upslope) and GWC (10 m upslope). Groundwater stage data was output at 5 min intervals.

(i) Timing of groundwater response, GWt, was calculated as the time difference between when groundwater height began to rise (gt0) and the time of the onset of rainfall (t0) (Figure 4.28)

$$GWt = (gto - to)$$

Eqn 4.4b

(ii) Magnitude of groundwater rise, GWres, was the difference between the peak height (GWp) reached by the groundwater table at time (gt1) and the height of groundwater at the onset of response (GWb), at time (gt0) (Figure 4.28).

$$GWres = (GWp - GWb)$$

Eqn 4.4c

(iii) Groundwater response rate, RG, is calculated from:

$$RG = \frac{(GWp - GWb)}{(gt1 - gto)}$$

Eqn 4.4d

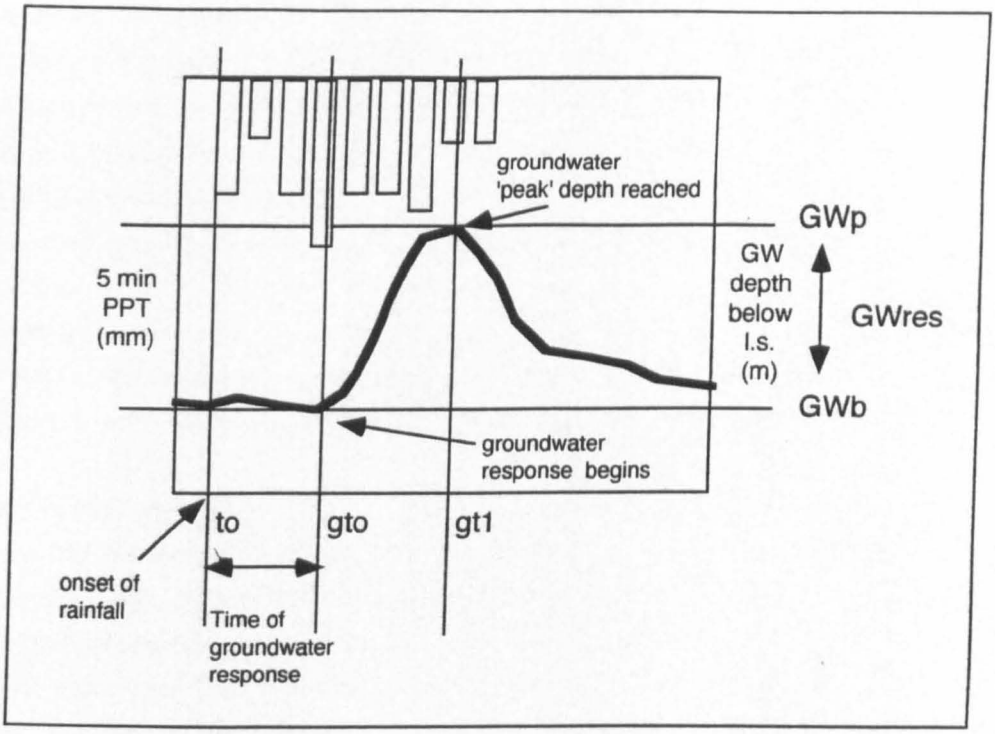

Key

GWp = peak groundwater height
GWb = baseflow groundwater height
to = time on rainfall onset
gto = time on onset of groundwater response
gt1 = time at which peak GW height is reached

***Figure 4.28**: Groundwater response for a hypothetical storm, outlining groundwater parameters used in equations (see text)*

(IV.4Gd) Observed patterns and discussion

- **Timing of groundwater responses**

Data from 37 storms were employed for this analysis. Groundwater responses were noted during 28 of these storms (Appendix 4.15). Groundwater response (i.e. the time at which an increase from base flow occurred) at GWA was the most rapid of all the wells, which supports the hypothesis that groundwater ridging may occur in the riparian zone (McDonnell, 1990).

The timing of groundwater response ranged from 45 min to 16 hr after the onset of rainfall (or 'continuous' rainfall).

- **Magnitude of groundwater rise**

GWA and GWC show large increases in water table height compared with GWB. On average, GWA water table rose 33 cm, GWC rose by 37 cm, whereas GWB only rose by 11 cm (Appendix 4.15).

- **Rate of groundwater responses**

The rates of groundwater response (from eqn 4.4c) were calculated at each site for all storms (Appendix 4.16). On average, values of 0.36 min per min, 0.05 cm per min and 0.69 cm per min were obtained for GWA, GWB and GWC, respectively. The overall rise in groundwater level was found to be similar at Sites A and C, but the average rate of increase of groundwater level at Site C was twice that at Sites A and almost 10 times that at Site B.

(ii) Seasonal controls on groundwater responses

- **Timing of groundwater responses**

The comparison of groundwater responses for storms where data is available for GWA and GWC (in 21 out of 37 storms) shows a seasonal pattern. During the growing season, the average groundwater response times are 162 min and 188 min for GWA and GWC respectively. During the dormant season, GWA is again the first to respond, but the difference between the time lag increases to 584 min and 908 min respectively. Thus, in general the groundwater response is quicker in the growing season at both sites.

- **Magnitude of groundwater responses**

A seasonal control is also evident on overall rise in water table height, where for all wells, the average rise in the growing season is twice as great as the rise in the dormant season. Average water level rises at GWA are 48 cm and 21 cm for the growing season and dormant season storms respectively. At GWB they are 13 cm and 5 cm respectively and at GWC they are 46 cm and 21 cm respectively.

The groundwater responses are converse to those of the soil water responses in terms of their magnitude. The total flow measured at depths of 15 and 50 cm in the soil (from VI-15 and VI-50 respectively) were found to be greater in the dormant season than in the growing season.

The groundwater rises at individual sites were compared for all storms, and significant correlations were obtained between all sites. The correlation of groundwater level rise at Sites A and B was 0.77, between Sites B and C was 0.96 and between Sites A and C was 0.96.

- **Groundwater response rates**

A seasonal pattern is also apparent with respect to groundwater flow rate, where, again, rates are highest in the growing season. At Sites A and C, the rate of groundwater rise was twice that calculated for all storms (0.64 cm per min and 1.03 cm per min for Sites A and C respectively). The rate at B remained the same for both seasons. During the dormant season, rates were reduced substantially, and it is interesting to note that the average flow rate at Site A was over three times that of Site C.

(iii) Mechanisms of groundwater response

Groundwater ridging

GWA was the first well to respond in the majority of storms. The timing of response was much sooner in the growing season than the dormant season. At Ruissaeu des Eaux and Hillman Creek, Canada, field observations and computer simulations suggest that very large and rapid increases in the hydraulic head of near-stream groundwater occurs soon after the onset of rainfall (Sklash and Farvolden, 1979). These responses precluded and were apparently independent of the upland area response. At the Maimai catchment, New Zealand, during the initial stages of wetting of the profile, water from storage begins to discharge into the channel, assisted by groundwater ridging along the channel margins (McDonnell, 1990). Thus, the earlier response at GWA is consistent with the theory of groundwater ridging. The greater average rise in groundwater height in the growing season at GWA (48 cm) than for the dormant season (21 cm) suggests that groundwater ridging is a more dominant mechanism in the growing season. The occurrence of Tropical Storm Alberto and the smaller storms that followed in the growing season caused abnormally wet conditions, allowing the expansion of the near-stream saturated zone. Hence, with the addition of small amounts of rainfall, very large and rapid increases in the hydraulic head of near-stream groundwater occurs. The rate and timing of groundwater response at GWA precedes that of GWC during the dormant season, hence groundwater ridging is also important during the dormant season.

Groundwater displacement

Groundwater displacement may be caused by the infiltration of 'new' water to depth via macropores, causing the saturated zone to extend upwards into the soil matrix (McDonnell, 1991). Previous studies have show that macropore flow is prevalent during the growing season, and hence groundwater displacement should be dominant during this season. At GWC, groundwater rise is twice as great during the growing season than during the dormant season, which provided evidence that groundwater displacement may be an important groundwater flow process during the growing season. This mechanism was explored further by comparison of soil water and groundwater responses for storms where macropore flow had been identified. If macropore flow was responsible for the groundwater response, then the onset of groundwater rise would be expected shortly after the occurrence of

macropore flow. In previous investigations (McDonnell, 1990), the infiltration of 'new' water to depth via macropores causes the saturated zone to extend upwards into the soil matrix. Thus, shallow groundwater is recharged rapidly during the onset of a rainstorm by 'new' water. The rapid input of 'new' water to depth causes a concurrent groundwater level rise. Hence, macropore flow may lead to groundwater displacement.

The occurrence of macropore flow has been identified in 17 storms. The responses of groundwater and soil water will be considered for a sub-set of these storms in order to assess whether macropore flow leads to the groundwater response.

Case study storm: 21 October 1994 (Figure 4.29a)

Groundwater data was only available for GWA during this storm. Response in groundwater was noted at 22:20 on 21 October, by which time the wetting front had only passed through 15 cm. Macropore flow was noted 25 min earlier, at 21:55 on 21 October. Overall groundwater rise was again substantial, at 21 cm. The occurrence of macropore flow shortly before the response of GWA might suggest groundwater displacement is in operation. This is a dormant season storm, in which, from the previous analysis, groundwater ridging in the riparian zone is believed to be responsible for groundwater flow. Hence, during this storm, it is possible that a combination of groundwater ridging and groundwater displacement occurred.

Case study storm: 20 November 1994 (Figure 4.29b)

Macropore flow was noted at 21:30 on 20 November. Response of GWA began 7 hr 55 min after this at 5:25 on 1 November This storm shows a different trend to the others since the wetting front had reached 40 cm in the soil profile by this time. Also, groundwater response was only 5 cm. Response of GWC was negligible. Hence, in this storm, macropore flow did not lead to groundwater displacement.

Case study storm: 27 July 1994 (Figure 4.29c)

This storm differs from the others, as groundwater responses at all sites were all very low and all occurred after the wetting front has passed through 70 cm. Thus, it is possible that flow through the porous media (i.e. matrix flow) may have been responsible for groundwater flow.

Macropore flow was identified in 17 storms. Groundwater response was noted prior to the passage of the wetting front past 40 cm in 10 of the these storms. For all 10 of these storms, flow was noted at 50 cm depth prior to the passage of the wetting front through this depth. This observation is attributed to macropore or mesopore flow.

Thus, in ten storms, mesopore/macropore flow may have preceded groundwater response. Three of these storms occurred in the growing season and the remaining seven in the dormant season. The lag time between apparent mesopore flow and groundwater response ranges from 15 min to 15 hr (Table 4.4). In the following chapters, chloride and temperature will be employed as tracers in attempts to investigate this mechanism further.

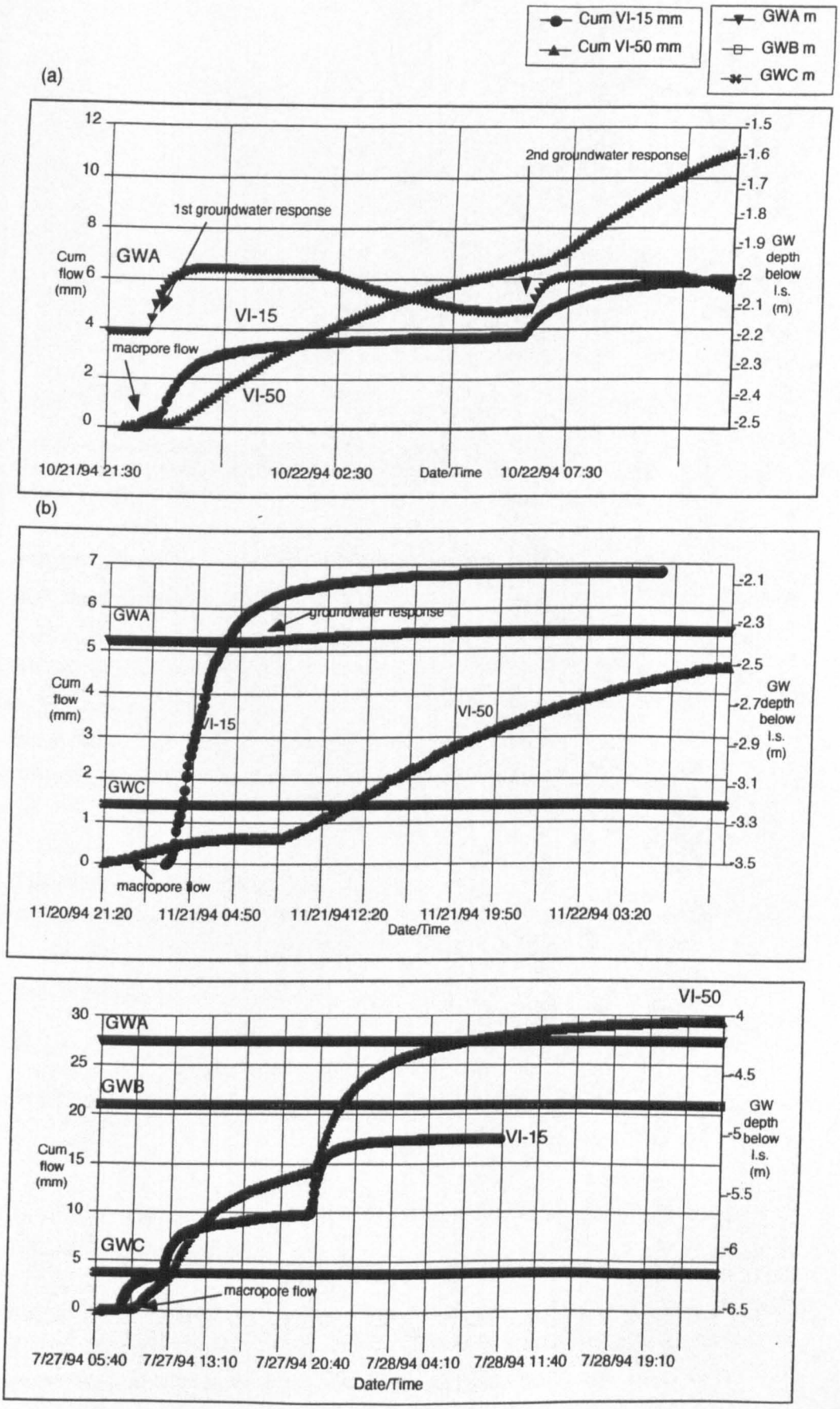

***Figure 4.29**: Groundwater responses from wells located in the riparian zone (GWA), 5 m upslope (GWB) and 10 m upslope (GWC); and soil water responses at 15 cm depth (VI-15) and 50 cm depth (VI-50) for storms occurring on (a) 21 October 1994; (b) 20 November 1994; (c) 27 July 1994*

Storm	Lag time (hr min)	'Initial 50 cm flow' cm	GW rise (cm)
16 Aug. 1994	2 hr 55 min	0.06	64
16 Sept. 1994	15 min	0.06	10
11 Oct. 1994	5 hr 30 min	0.15	32
21 Oct. 1994	8 hr 55 min	0.15	21
4 Dec. 1994	6 hr 10 min	0.04	17
19 Jan. 1994	2 hr 5 min	0.04	3
27 Jan. 1994	13 hr	0.02	21
10 Feb. 1994	14 hr 55 min	0.30	10
27 Feb. 1994	11 hr 25 min	0.02	5
19 April 1995	8 hr 10 min	0.06	2

Table 4.4: Storms experiencing flow at 50 cm before arrival of wetting front at that depth; lag time between onset of 'initial flow at 50 cm' and groundwater response at GWA, total 'initial' 50 cm flow (i.e. total flow prior to passage of wetting front through 50 cm depth) and total groundwater rise

A combination of groundwater displacement and groundwater ridging may occur at PMRW. It is possible that groundwater displacement higher on the slope may lead to the groundwater ridging mechanism. In the upslope region, the hydraulic gradient is high and hence the water is able to move laterally downslope. As the water moves downslope, the hydraulic gradient decreases and the water backs up the slope, forming a ridge. During Tropical Storm Alberto, wet antecedent moisture conditions allowed the rapid development of a groundwater ridge in the riparian zone and this explains why groundwater rise was substantially higher at GWA than GWC during the growing season.

(iv) Controls on groundwater responses

Factors that influence groundwater response have been suggested in previous studies (McDonnell, 1990). The influence of the following parameters on groundwater response were analysed in the current investigation.

- Rainfall intensity (PI)
- Rainfall total prior to onset of groundwater response (PPO)
- Rainfall magnitude (Tot PPT)
- Rainfall total in the week prior to the storm (Pwk)
- Seasonality

Regressions and correlations were conducted between the above parameters and the timing and magnitude of groundwater response.

All storms

The timing of the groundwater response from the onset of rainfall was not found to correlate significantly with any of the above parameters, apart from rainfall amount in the week prior to the rainstorm (Pwk). All correlations were negative (-0.46, -0.40 and -0.53 for Sites A, B and C respectively). This suggests that the wetter the conditions in the previous week, the more rapid the

groundwater response. The wetter the antecedent conditions, then the more probable the development of saturated ridges in the riparian zone and hence the more probable the operation of the groundwater ridging phenomenon (McDonnell, 1990).

The rate of groundwater rise was found to exhibit the strongest association with total rainfall (producing correlations of 0.64, 0.82 and 0.66 for Sites A, B and C respectively). When the correlation was performed with rainfall in the first hour of the storm, insignificant associations were obtained. However, significant correlations were obtained between rate of groundwater response and rainfall amount prior to the groundwater response (0.81, 0.40 and 0.57 for Sites A, B and C respectively).

Dormant season storms

The correlations between the time of groundwater response and total rainfall in the week prior to the storm for all sites were again significant (-0.48, -0.68 and -0.77 for Sites A, B and C respectively). These correlations provide higher coefficients than for all storms, suggesting that the control of antecedent moisture conditions are more significant in terms of the timing of the groundwater response during this season, which is consistent with conditions for groundwater ridging (Sklash and Farvolden, 1979). None of the other parameters were found to show any significant correlations with the timing of groundwater responses.

The correlations between the rate of groundwater rise and both total rainfall and rainfall total prior to the groundwater response were not found to be as high as they were for growing season storms.

Growing season storms

The correlations of the timing of groundwater response and rainfall total in the previous week were found to be significant, although not as high as for the dormant season storms (-0.46, -0.40 and -0.53 respectively). Thus, it appears that groundwater response is controlled to a greater extent by antecedent moisture conditions in the dormant season than in the growing season, which is the opposite trend to that observed for soil water responses.

However, the rate of groundwater rise was found to correlate significantly with total rainfall prior to the onset of groundwater rise during the growing season, especially at Site A (0.91, 0.51 and 0.55 for Sites A, B and C respectively). The total rainfall that is 'required' for groundwater response (i.e. total rainfall that occurs prior to groundwater response) is actually higher in the growing season (on average 19 mm, 21 mm and 23 mm for Sites A, B and C) compared to during the dormant season (on average 13 mm, 11 mm and 17 mm for Sites A, B and C), although the response is actually sooner for growing season storms.

Groundwater response via a groundwater ridging phenomenon has been found to be independent of total rainfall prior to response, since the system is primed for flow and only a small amount of rainfall will prompt a rapid and large rise in the water table height. Hence, if specific amounts of water are required for groundwater response during the growing season, some other form of groundwater flow may be in operation.

(IV.4Ge) Summary

Three possible mechanisms of groundwater flow have been outlined in previous investigations: groundwater ridging (Skalsh and Farvolden, 1984; G; McDonnell, 1990), groundwater displacement and air compression effects (Todd, 1980). From the analysis of groundwater response times and magnitudes of groundwater rise at PMRW, groundwater ridging appears to be an important process, especially following wet antecedent moisture conditions. The greater average rise in groundwater level during the growing season at GWC suggests that groundwater displacement might be in operation during this season.

Thus, two mechanisms of groundwater response appear to be in operation at PMRW, and the impact of either seems to be controlled by site position. At GWA, in the near-stream zone, groundwater ridging appears to be the major flow mechanism. Its operation is also controlled to a high extent by antecedent moisture conditions, where wet conditions allow the expansion of the near-stream unsaturated zone (Skalsh and Farvolden, 1984). With addition of small amounts of rainfall, very large and rapid increases in the hydraulic head of near-stream groundwater occurs.

In a third of storms, mesopore and macropore flow were noted prior to groundwater response, and this groundwater response preceded the movement of the matrix water past 70 cm depth. Hence, in these storms, it is possible that macropore and mesopore flow did lead to groundwater displacement.

Groundwater was found to contribute to storm flow in over half the storms. In storms where this was not true, antecedent moisture conditions were wet and rainfall was intense, and in these storms macropore flow and overland flow probably initiated storm runoff. In other storms, it is possible that inflow from the stream channel may have caused groundwater response in the near-stream zone (GWA). In general, storm runoff at PMRW has a significant groundwater contribution.

(IV.5) SUMMARY OF HYDROMETRIC ANALYSIS

The results of the previous section have been summarised and are as follows:

- Throughfall comprises 78% total rainfall on average. The proportion varies according to season, with higher throughfall in the dormant season (79% total rainfall) than during the growing season (78% total rainfall). Interception was found to vary between 2.5 mm (in the growing season) and 0.5 mm (in the dormant season). The current study found throughfall totals to be consistent with those of investigations at other locations (e.g. Ford *et al*, 1974), but significantly different to those of a previous investigation at PMRW (Cappellato, 1991). In the previous investigation, throughfall totals were found to approximate 95% total rainfall. The difference is explained as an artifact of the position and size of the throughfall collectors, and possibly due to focusing of flow to specific drip points by the canopy.

- Forest floor soil water totals were found to exceed throughfall totals in most storms. The difference is attributed to input of water via overland flow. Overland flow occurs at specific locations on the hillslope, as greatest volumes were collected when forest floor soil water was sampled in a topographic low on the hillslope. Overland flow was also found to vary according to

season, with greater flow in the growing season, which is attributed to the occurrence of two tropical storms. Operation of overland flow was associated with rainfall amount, where twice as much rainfall was required to initiate overland flow in the dormant season. This is explained by the higher frequency of high intensity rainstorms in the growing season, leaving the soil primed for overland flow

- Flow through the unsaturated zone (15 and 50 cm depths) was found to be significantly greater (two to three times) in the dormant season than in the growing season. In the growing season, water flow through 15 cm was reduced via storage and plant uptake or lateral flow. During some storms, flow at 50 cm depth was higher than total flow at 15 cm depth, indicating that lateral flow or macropore flow must occur. The quicker response of soil water during the growing season might indicate that the lysimeter collects significant macropore waters, whereas, the slower response in the dormant season suggests that the majority of soil water is matrix water.

- The timing of the initiation of matrix flow at 15 cm depth appeared to be controlled by site location. The site in the lower slope location (TDRA) was typically the first to respond, which is consistent with the continual priming of the lower slope, near-stream areas by downward drainage of water from upslope during baseflow conditions (McDonnell *et al*, 1990).

- The response of soil moisture at 15 cm depth was highly variable and no single factor was found to control it, although antecedent conditions and storm intensity were important. Thus, other factors must also contribute e.g. microtopography, soil type and plant cover (Kennedy *et al*, 1986).

- The timing of wetting front movement and increases in soil moisture status at 40 cm amongst all sites on the hillslope were found to be less variable than at 15 cm depth. However, sites lower downslope (TDRA and B) exhibited an increase in flow rates with respect to depth, whereas, at the upper slope location (TDRC), a decrease in flow rates with respect to depth were observed. This is consistent with the occurrence of wetter conditions at the lower-slope locations, allowing more rapid transport of matrix water.

- TDR data provides evidence for the occurrence of lateral flow between 15 and 40 cm, as increases in soil moisture were observed at 40 cm depth prior to those at 15 cm depth for some storms. Since TDR data is inefficient at monitoring macropore flow, the additional water must be via lateral flow.

- Macropore/ mesopore flow was found to be an important flowpath for water at PMRW. Flow was detected at 50 cm depth prior to the passage of the wetting front in over half of all storms. Its occurrence was detected in growing season and dormant season storms and was found to be controlled by antecedent moisture conditions and rainfall intensity.

- Two mechanisms of groundwater flow: groundwater ridging and groundwater displacement, are important at PMRW. The position on the hillslope determines which mechanism is dominant. In the near-stream zone, groundwater ridging is the major groundwater flow mechanism. Its

operation is controlled by antecedent moisture conditions, as expansion of the near stream unsaturated zone occurs under wet conditions, which leads to a rapid and large expansion in the hydraulic head of this zone with the addition of relatively small amounts of rainfall. This mechanism was found to be dominant in the dormant season. Groundwater displacement may contribute to groundwater ridging. Here, macropore flow introduces 'new' water to the groundwater table, promoting displacement of groundwater downslope. The water has a large hydraulic gradient and moves rapidly. However, once in the lower slope location, the hydraulic gradient is reduced, and the water begins to back-up in the soil matrix, creating groundwater ridges.

The results of the hydrometric analysis have shown that the drainage routes that develop result not only from geomorphological properties of material and relief, but also from storm runoff characteristics, including storm pathways, which are highly sensitive to antecedent conditions prior to the storm. The importance of a particular flowpath varies according to season, where flow in the unsaturated zone is typically two to three times greater in dormant season storms than in growing season storms. Hydrometric analysis has allowed identification of overland flow, macropore and mesopore flow and groundwater ridging and displacement as mechanisms that allow rapid storm runoff. In the following two chapters, chloride and temperature will be employed as conservative tracers in order to corroborate the results of this hydrometric analysis. Furthermore, they will be used in an attempt to identify the water types (i.e. 'old' or 'new' water) that follows each flowpath, which is impossible to determine from hydrometric data alone.

CHAPTER V
CHLORIDE TRACER STUDY

V.1 INTRODUCTION

(V.1A) 'Old' vs. 'New' waters

The chemistry of 'old' and 'new' waters differ significantly (Kennedy *et al*, 1986; Jenkins *et al*, 1994). 'New' waters are chemically altered mainly by processes involved with forest nutrient cycling (Eshleman *et al*, 1993). 'Old' waters have longer residence times within the system and their chemistries tend to be controlled by processes involved in chemical weathering. The most significant changes in the biogeochemistry of forested catchments occur when the system is in its most hydrologically active state, i.e. when perturbed by rainfall or snowmelt events (Kennedy *et al*, 1986; Eshleman *et al*, 1993).

Variations in the solute concentrations of event or 'new' waters in transit through a forested hillslope are due to the interaction of a series of processes, leading either to enhancement or depletion in the concentration and flux of solutes (Eshleman *et al*, 1982; Cosby *et al*, 1985; Woolhiser *et al*, 1985; Christophersen *et al*, 1990; Hooper and Christophersen, 1990; Hooper *et al*, 1993). These processes are determined by the hydrological flowpaths that are operative, as well as the source and the composition of the water. Factors affecting enhancement include leaching from vegetation or soil (Ford and Deans, 1978; Driscoll and Lichens, 1982; Adamson *et al*, 1993), release from exchange sites in the soil (Johnson, 1986; Lynch, 1989; Shanley and Peters, 1993), or evaporative concentration (Neal and Rosier, 1990). Depletion may be due to uptake by vegetation (Driscoll and Lichens, 1982), adsorption onto soil exchange sites (Johnson and Ruess, 1984; Baes and Bloom, 1988) or gaseous loss (Turner et al, 1990). Biophysical conditions of the ecosystem prior to a rainstorm may control the relative importance of these mechanisms. The magnitude of sources or sinks may also be affected by the intensity of the storm and seasonality (Pionke and Dewalle, 1992; Kennedy *et al*, 1986). The biochemical processes in operation within the system may be short term and thus chemistry must be intensively sampled along all major hydrological flowpaths to identify important mechanisms.

(V.1B) 'Old' water contributions to the storm hydrograph

Recent studies suggest that 'old', rather than 'new' water water dominates storm runoff (Thomas and Beasley, 1986; McDonnell, 1990, Luxmoore *et al*, 1993). Many tracer studies, especially those using $\delta\,^{18}O$ isotopes, have almost without exception indicated that water stored from previous rainstorms volumetrically dominates the stream flow response to storm events. McDonnell (1990) proposes that crack infiltration of rainfall to deeper soil layers leads to expansion of groundwater into the soil matrix on hillslopes and the lateral pipe flow of stored water from the soil matrix is a possible mechanism that accounts for the rapid discharge of 'old' waters from hillslopes during storms (see Chapter IV).

Luxmoore *et al* (1993) suggest that there is a major interaction between macropores, mesopores and micropores, allowing storage and/or release of water They describe this as a disconnect-connect mechanism which allows considerable storage of water in the intermediate sized pores (mesopores) between events and allows release of these waters during storm events. Thus, the relative contribution of 'old' and 'new' may vary with time within flowpaths.

(V.1C) Distinguishing between 'old' and 'new' waters: chloride as a conservative tracer

Much debate exists over the relative contribution of 'old' and 'new' water in storm runoff. This issue is addressed in the following chapter using chloride as a conservative tracer. A conservative tracer is ideally only carried by water and must not be gained or lost by the passage through matrix materials. The use of chloride as a conservative tracer of mobile storm waters assumes that the Cl^- concentration should vary minimally in the water that transits the system and is not affected by ion exchange or other rock and water interactions. Furthurmore, the Cl^- signature of the 'new' water must be distinct from that of 'old' water.

Hydrochemical tracers have been used to identify solute sources and sinks and hence whether waters are 'old' or 'new' (Pinder and Jones, 1969; Hooper and Shoemaker, 1986; Rasher *et al.*, 1987; Peters and Driscoll, 1989; Eshleman *et al*, 1993; Buttle, 1994). Chloride is highly mobile in most ecosystems because it is not readily adsorbed onto surfaces, nor readily incorporated into secondary minerals (Ohte *et al*, 1991; Peters, 1994; Reynolds and Pomeroy, 1988). Atmospheric deposition of marine aerosols is the major source of Cl^- in most ecosystems (Eriksson, 1955; Junge, 1963; Gerritse and George, 1988). Washoff of dry deposited Cl^- from canopy surfaces was reported for Hubbard Brook Experimental Forest (Juang and Johnson, 1967). Enrichment of Cl^- in throughfall and stemflow has also been observed in other investigations (Neal *et al*, 1990; Rustad *et al*, 1994 and references therein). Rainfall and washoff of dry deposition are the major short-term contributors of Cl^- to most ecosystems, and the magnitude increases with proximity to the ocean (Gerriste and George, 1988; Mazor and George, 1992).

Chloride has been widely used in the identification of hydrological flowpaths (Johnston, 1987; Williamson *et al*, 1987; Roth *et al*, 1991). Groundwater and matrix soil water (i.e. 'old' waters) are typical of longer residence-time waters (Eshleman *et al*, 1993; Jenkins *et al*, 1994) and generally have higher Cl^- concentrations than rainfall, due to evapotranspiration. Provided a sufficiently large difference exists between Cl^- concentrations of rainfall plus aerosol washoff and other end-member waters, the Cl^- concentrations of sequentially sampled soil waters during storms can help elucidate the timing and mechanisms of release and storage of solutes and water in a watershed.

V.2 AIMS AND QUESTIONS

The following chapter is broken down into three sections, each of which addresses a specific aim or question:

(A) Can chloride be used to distinguish between 'old' and 'new' waters?

(B) Can 'old' and 'new' water contributions be assessed within specific flowpaths?

(C) Can the relative contributions of 'old' and 'new' water be quantified within specific flowpaths"

(V.2A) Can chloride be used to distinguish between 'old' and 'new' waters?

The use of chloride as a conservative tracer of 'old' and 'new' water depends on significantly different concentrations in each water type. The previous section discussed how 'old' waters (i.e. matrix waters and groundwaters) typically have higher Cl^- concentrations due to evapotranspiration (Eshleman *et al*, 1993; Jenkins *et al*, 1994). The first approach will be to compare average Cl^- concentrations collected at each node and to determine whether the Cl^- concentrations of 'old' and 'new' waters are significantly different.

(V.2B) Distinguishing 'old' from 'new' waters within flowpaths

Flowpaths were identified on the basis of hydrometric data in Chapter IV. Assumptions were made about the sources of water monitored at each node. Chloride data will assist in the corroboration or the rejection of these assumptions. The Cl^- signature of complete collection sequences within flowpaths will provide information about the relative contribution of 'old' and 'new' water.

(V.2C) *Quantification of the relative contribution of 'old' and 'new' water in specific flowpaths*

Some quantification of the relative contribution of 'old' and 'new' water in specific flowpaths will be made by implementation of two-component mixing models. The flowpaths selected are:

(a) Forest floor soil water

(b) 50 cm soil water

The next section discusses data collection and calculations used in the following data analysis and discussion. The data analysis is divided into three sections, which allude to the questions discussed above. Finally, a summary of the discussion is given.

(V.3) DATA AND CALCULATIONS

Chloride determinations were performed on samples collected from 19 storms (from 4 May 1994 to 1 May 1995). Sequentially-collected samples included rainfall (PPT), throughfall (TI), forest floor soil water (VI-0 and VI-0o), 15 and 50 cm depth soil waters (VI-15 and VI-50 respectively) and streamwater (SWIg). Manually collected (or 'event') samples included rainfall (PE1), forest floor soil waters (VAo and VBo), 15 cm depth soil waters (VA_{15}, VB_{15} and VC_{15}), 40 cm depth soil waters (VA_{40}, VB_{40} and VC_{40}), 70 cm depth soil waters (VA_{70}, VB_{70} and VC_{70}), groundwaters (GQA, GQB, GQCs, GQCd and GQD) and streamwaters (SWIgm and SWug).

Sequential samples were collected via a fill-spill principle (Peters, 1994), discussed in Chapter III. Combination of sample volumes with the tipping bucket data enable the time at which each bottle filled

to be assigned to the sample. Hence, the timing of collection of sequential samples could be calculated and the Cl^- concentration variation at a specific node could be monitored with respect to time.

(V.3A) Can chloride be used to distinguish between 'old' and 'new' waters?

Cl^- concentrations at each node are compared in order to assess the concentration of 'old' and 'new' water. Average concentrations for individual storms were calculated for all manually collected samples (event rainfall, PE1; forest floor soil water samples, VAo, VBo; all tension lysimeter samples (sites VA, VB and VC), groundwaters; GQ and lower gage streamwaters, SWlg). Volume weighted means (VWM) were calculated for sequentially collected samples (rainfall, PPT; throughfall, TI; forest floor soil water, VI-0; 15 cm soil water, VI-15; 50 cm soil waters, VI-50). Volume weighted means (VWM) were calculated from:

$$VWM = \frac{(CiVi) + ... (CnVn)}{Vi + ... Vn)} \qquad \text{Eqn 5.1}$$

where

C	=	Cl^- concentration (μeq/l)
V	=	Volume collected (m)
i	=	initial sample
n	=	final sample
VWM	=	Volume weighted mean Cl^- concentration

(V.3B) Quantification of the relative contribution of 'old' and 'new' water in specific flowpaths

(a) Forest floor soil water

The contribution of 'new' water is represented by throughfall concentrations (TI), whereas, the contribution of 'old' water is represented by 15 cm soil water concentrations (VI-15) (since, the hydrometric analysis has shown that the water collected in the 15 cm pan lysimeter (VI-15) is matrix water, and hence is 'old' water). The following series of equations are used:

$$C_{ff}V_{ff} = C_{TI}V_{TI} + C_{VI\text{-}15}V_{VI\text{-}15} \qquad \text{Eqn 5.2}$$

$$V_{ff} = V_{TI} + V_{VI\text{-}15} \qquad \text{Eqn 5.3}$$

Sub 5.3 into 5.2:

$$V_{TI} = \frac{V_{ff}(C_{ff} - C_{V\text{-}15})}{(C_{TI} - C_{V\text{-}15})} \qquad \text{Eqn 5.4}$$

where

C_{ff} = Volume weighted mean Cl^- concentration in forest floor soil water (μeq/l)
C_{TI} = Volume weighted mean Cl^- concentration in throughfall (μeq/l)
$C_{VI\text{-}15}$ = Volume weighted mean Cl^- concentration in 15 cm soil water (μeq/l)
V_{ff} = Total volume of flow through forest floor (m)
V_{TI} = Total volume of throughfall (m) (i.e. 'new' water)
$V_{VI\text{-}15}$ = Total volume of 15 cm soil water flow (m) (i.e. 'old' water)

(b) 50 cm water

The contribution of 'new' water is represented by throughfall concentrations (TI), whereas, the contribution of 'old' water is represented by 40 cm soil water concentrations (the average of VA_{40}, VB_{40} and VC_{40}). Collection of soil water samples from 50 cm depth was conducted using pan lysimeter VI-50. The hydrometric analysis has shown that during the growing season, much of this water is derived from macropore flow. Tension lysimeters were employed to collect soil water samples at depths of 15, 40 and 70 cm. These soil waters are more representative of matrix soil waters (hence 'old' waters). Thus, the 40 cm soil water samples were used in this analysis to provide the chemical input (i.e. C_{V40}) for 'old' soil water, since they were sampled at the closest depth to 50 cm.

The following series of equations are used:

$$C_{VI\text{-}50}V_{VI\text{-}50} = C_{TI}V_{TI} + C_{V40}V_{V40} \qquad \text{Eqn 5.5}$$

$$V_{VI\text{-}50} = V_{TI} + V_{V40} \qquad \text{Eqn 5.6}$$

Sub 5.6 into 5.5:

$$V_{V40} = V_{VI\text{-}50}\frac{(C_{VI\text{-}50} - C_{TI})}{(C_{V40} - C_{TI})} \qquad \text{Eqn 5.7}$$

where

$C_{VI\text{-}50}$ = Volume weighted mean Cl^- concentration in 50 cm soil water (μeq/l)
C_{TI} = Volume weighted mean Cl^- concentration in throughfall (μeq/l)
C_{V40} = Volume weighted mean Cl^- concentration in 40 cm soil water (μeq/l)
$V_{VI\text{-}50}$ = Total volume of flow through 50 cm (m)
V_{TI} = Total thorughfall (m) (i.e. 'new' water)
V_{V40} = Total 40 cm soil water (m) (i.e. 'old' water)

(V.4) RESULTS AND DISCUSSION

(V.4A) Distinguishing 'old' and 'new' waters using Cl- as a conservative tracer

Average total and VWM Cl^- concentrations at specific nodes were calculated in order to assess whether there were significant differences in concentration. The results are presented in Table 5.1 (also see Appendix 5.1 and 5.2).

Rainfall Cl^- concentrations (both collected sequentially; PPT, and manually; PE1) are significantly lower than at other nodes. Throughfall (TI) and sequential forest floor soil water (VI-0) samples, on average, contain twice as much Cl^-, which may be attributed to washoff mechanisms (Neal and Rossier, 1990). However, if the minimum concentrations are considered, then it is evident that low concentrations are obtained in some storms (probably following wet antecedent conditions, when available Cl^- for washoff is low). The Cl^- concentrations in these 'new' waters are less than half the concentrations found in 'old' waters, i.e. groundwaters. The variations in the concentrations of 'old' waters are also much lower. Cl^- concentrations in 15, 40 and 50 cm soil waters are much more

variable. However, on average, concentrations are above those for throughfall and forest floor soil water, i.e. > 20 μeq/l, suggesting that they comprise a mixture of 'new' and 'old' water, although it is possible that they show the chemical pattern of 'new' water that is enhanced in Cl^- due to evaporative processes.

A more detailed comparison of variations in Cl^- concentrations will be made in the following section. This will enable discussion of variation in concentrations at each node and assessment of how the water source at each node may differ.

NODE	MEAN (μeq/l)	MIN (μeq/l)	MAX (μeq/l)
PPT (vwm)	8.3	2.5	18.5
PE1	8.0	0.6	21.2
TI (vwm)	21.8	1.9	90.0
VI-0 (vwm)	22.1	1.4	75.0
VAo	31.1	2.0	62.0
VBo	38.6	3.1	73.6
VI-15 (vwm)	42.8	18.4	91.0
VA15	35.9	6.7	134.0
VB15	21.3	4.8	43.3
VC15	27.3	15.2	45.7
VI-50 (vwm)	24.9	3.8	59.6
VA40	24.7	4.5	53.9
VB40	24.0	10.2	39.8
VC40	26.9	15.2	45.7
GQA	40.8	38.0	69.4
GQB	48.3	44.2	55.0
GQCs	48.0	43.7	51.0
GQCd	46.8	44.3	58.1
GQD	43.1	33.3	59.0

***Table 5.1**: Average, min and max total and volume weighted mean Cl^- concentrations for samples collected at major nodes for all storms (see Chapter III for description and location of equipment)*

(V.4Aa) Rainfall and Throughfall

The average VWM Cl^- concentration of sequential rainfall (PPT) is 8.3 μeq/l, and the average concentration in event rainfall (PE1) is 8.0 μeq/l. Figure 5.1a displays boxplots of VWM and average Cl^- concentrations in PPT and PE1, respectively. The boxplots display the median and interquartile ranges. The diagram shows how similar concentrations are found in both sets of samples. Table 5.2 displays VWM (or average), min and max Cl^- concentrations for growing season and dormant season storms. The Cl^- content of sequentially-collected rainfall is greater in the growing season than in the dormant season. However, the event samples display the opposite trend. Higher average Cl^- concentrations are obtained during the dormant season.

The average VWM of sequential throughfall is 21.8 μeq/l, which is twice that of rainfall. In Figure 5.1b, throughfall VWM Cl^- concentrations are shown for all, growing and dormant season rainstorms. The variation in concentration is greatest in the growing season, where a maximum VWM of 90.0 μeq/l is obtained (Table 5.2). The higher Cl^- content in the growing season is attributed to

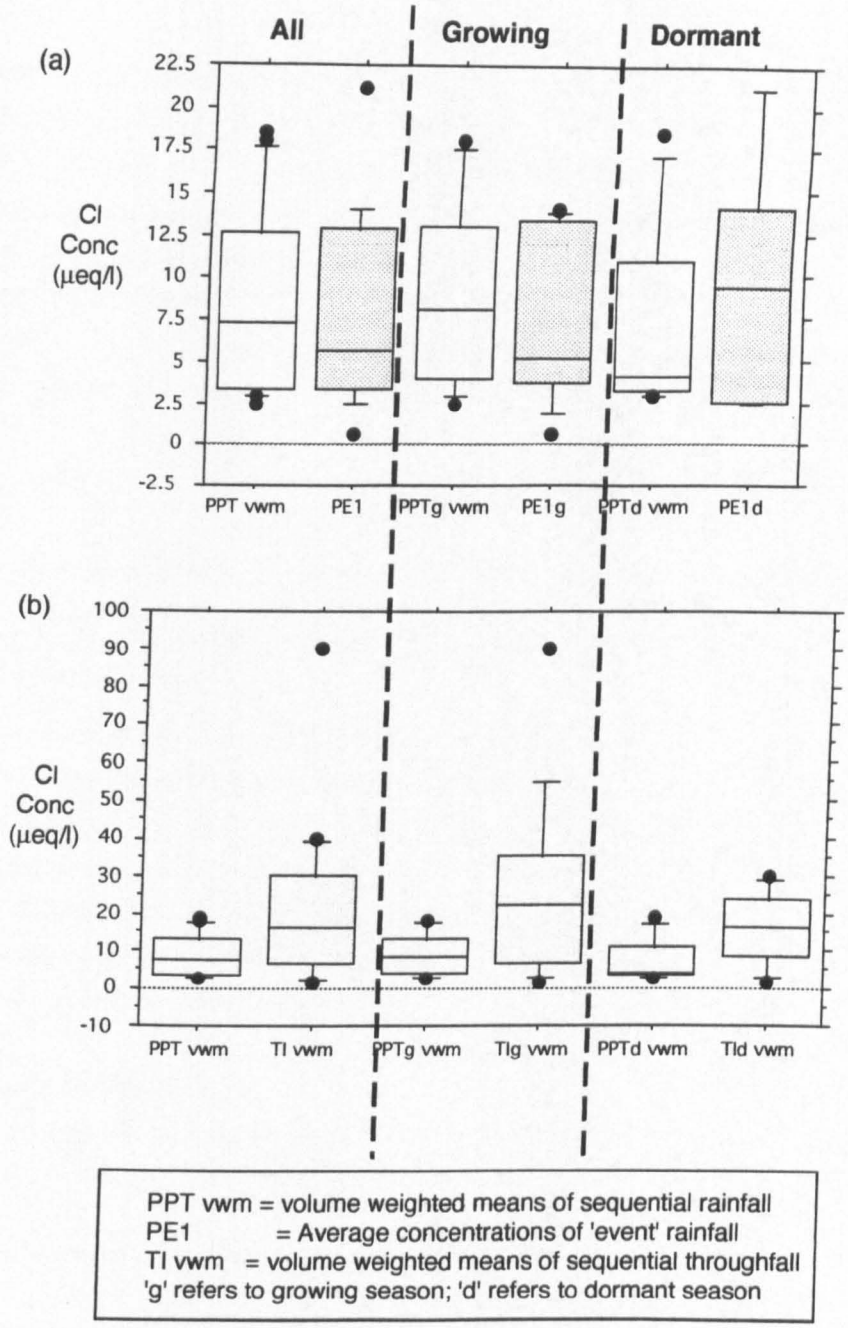

Figure 5.1: *Boxplots to show variations in volume weighted means and/or average chloride concentrations in (a) Sequential rainfall (PPT) and event rainfall (PE1); (b) Sequential rainfall and throughfall (TI)*

enrichment from washoff from the canopy (Best and Monk, 1975). The absence of leaves in the dormant season reduces the surface area for washoff and hence a lower average VWM and range in Cl^- concentrations is obtained. During the growing season, the rough surface presented by the forest, associated with high wind speeds and frequently wet surface conditions increases the capture efficiency of vegetation for particles and small droplets (Cryer, 1986).

Season	Node	Average (μeq/l)	Min (μeq/l)	Max (μeq/l)
Growing	PPT	8.9	2.5	18.0
	PE1	7.2	0.6	14.1
	TI	25.2	1.9	90.0
Dormant	PPT	7.3	2.9	18.5
	PE1	9.4	2.4	21.2
	TI	15.8	1.9	29.8

***Table 5.2**: Average volume weighted means or total, min and max Cl- concentrations in sequential rainfall (PPT), event rainfall (PE1) and sequential throughfall (TI) for storms during the growing season and the dormant season*

For all storms, VWM Cl^- concentrations in sequential rainfall are below 20 μeq/l, and in 16 of the storms are below 15 μeq/l. In sequential throughfall, concentrations are below 20 μeq/l for 11 storms, and below 15 μeq/l for 7 storms. The storms in which higher VWM Cl^- concentrations are reported occur during the dormant season, and follow dry antecedent conditions. The higher concentrations are attributed to washoff of Cl^- accumulated in the canopy from dry deposition and Cl^- retained in the canopy from the previous storm, particularly during low magnitude events in which the water evaporated before passing through the canopy.

(V.4Ab) Forest Floor Soil Water

Forest floor soil water was collected sequentially at two sites, VI-0 and VI-0o (see Chapter III). The average VWM Cl^- concentration for sequentially collected forest floor soil water is 21.8 μeq/l (Table 5.1).

Season	Node	Average (μeq/l)	Min (μeq/l)	Max (μeq/l)
Growing	VI-0	22.3	1.4	75.0
	VAo	30.8	2.0	62.0
	VBo	37.9	3.1	73.6
	TI	25.2	1.9	90.0
	PPT	8.9	2.5	18.0
Dormant	VI-0	21.8	9.3	32.3
	VAo	31.7	16.6	59.5
	VBo	40.3	32.7	45.8
	TI	15.8	1.9	29.8
	PPT	7.3	2.9	18.5

***Table 5.3**: Average volume weighted means or total, min and max Cl^- concentrations in sequential forest floor soil water (VI-0), event forest floor soil water (VAo, VBo), sequential throughfall (TI) and sequential rainfall (PPT)for storms during the growing season and the dormant season*

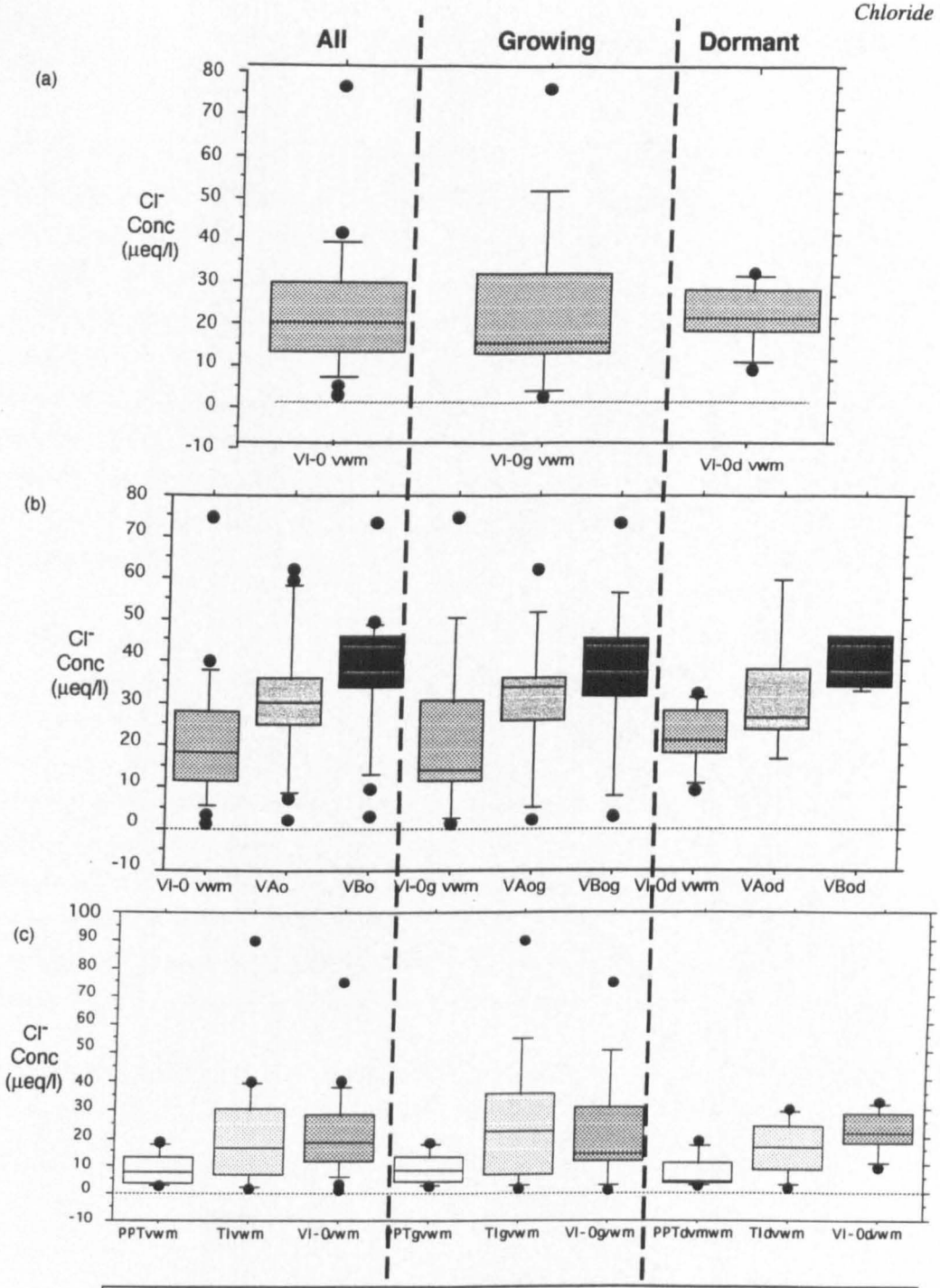

Figure 5.2 *Boxplots to show variations in volume weighted means and average chloride concentrations in (a) Sequential forest floor soil water (VI-0); (b) Sequential (VI-0) and event forest floor soil water (VAo/VBo); (c) Sequential forest floor soil water, throughfall (TI) and rainfall (PPT), for all storms, growing season and dormant season storms between May 1994 and May 1995*

Seasonal variation in Cl^- content is low, although VWMs are slightly higher in the growing season, which is again attributed to washoff (Figure 5.2a). The variation in concentration is also higher in the growing season. In 11 of the storms, VWM Cl^- concentrations are below 20 μeq/l and in 7 they are below 15 μeq/l, which mirrors variations in the Cl^- content of throughfall.

The average Cl^- concentrations in event forest floor soil water samples, VAo and VBo, are 31.1 and 38.6 μeq/l, respectively (Table 5.1). Figure 5.2b displays boxplots of VWM and average Cl^- concentrations of VI-0, VAo and VBo. The concentrations in event samples are generally higher than in sequential samples. The higher concentrations in event samples can be explained from the fact that only the initial concentrated forest floor soil water was collected, as the sample bottle was only 1000 ml in volume. Hence, the sample collected was equivalent to the 1st and 2nd of the sequential (500 ml volume) samples only.

(V.4Ac) 15 cm soil water

15 cm depth soil water (VI-15) was collected sequentially for 18 storms. The average VWM Cl^- concentration is 42.8 μeq/l, which is twice as high as that of throughfall and forest floor soil water, and five times that of rainfall (Table 5.1). In Chapter IV, the hydrometric analysis found that flow through this lysimeter was predominantly matrix water, since it was argued that macropore flow had been disrupted due to installation of sampling equipment. The high Cl^- content of the water, similar to that found in groundwater (Table 5.1), also suggests that the water is matrix soil water. Table 5.4 shows that there is no defined seasonal variation to concentrations (Figure 5.3a). However, highest VWM Cl^- concentrations are obtained in the growing season (91.0 μeq/l), although high variation is also observed in the dormant season. In only one storm is the VWM below 20 μeq/l Cl^- (27 February 1995).

Season	Node	Average (μeq/l)	Min (μeq/l)	Max (μeq/l)
Growing	VI-15	42.1	23.2	91.0
	VA_{15}	35.7	6.7	134.0
	VB_{15}	14.9	4.8	23.7
	VC_{15}	22.2	15.2	33.6
	VI-0	22.3	1.4	75.0
	TI	25.2	1.9	90.0
Dormant	VI-15	43.6	18.4	68.5
	VA_{15}	36.1	9.9	52.7
	VB_{15}	29.9	18.9	43.3
	VC_{15}	32.4	24.7	45.7
	VI-0	21.8	9.3	32.3
	TI	15.8	1.9	21.2

***Table 5.4**: Average volume weighted means or total, min and max Cl^- concentrations in sequential 15 cm soil water (VI-15), event 15 cm soil water (VA_{15},VB_{15}, VC_{15}), sequential forest floor soil water (VI-0) and sequential throughfall (TI)for storms during the growing season and the dormant season*

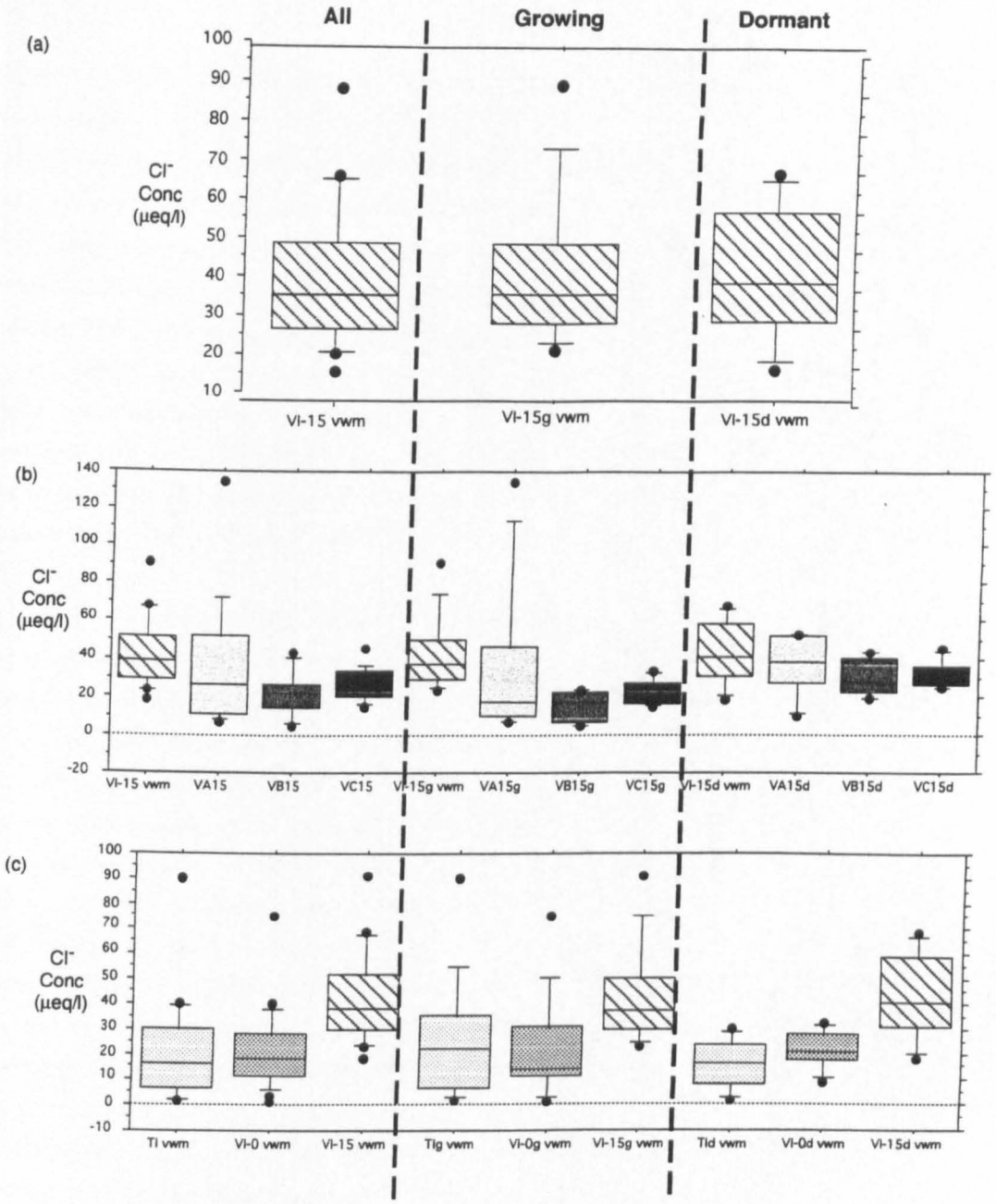

VI-15 vwm	= volume weighted means of 15 cm soil water samples
VA15/B15,VC15	= Average concentratins of 'event' 15 cm soil water samples from sites VA, VB and VC
TI vwm	= volume weighted means of sequential throughfall samples
VI-o vwm	= volume weighted means of forest floor soil water samples

'g' refers to growing season; 'd' refers to dormant season

***Figure 5.3**: Boxplots to show variations in volume weighted means and average chloride concentrations in (a) 15 cm soil water (VI-15); (b) Sequential (VI-15) and event 15 cm soil water (VA15, VB15, VC15); (c) Sequential 15 cm soil water, throughfall (TI) and forest floor soil water (VI-0) samples, for all storms, growing season and dormant season storms between May 1994 and May 1995*

Figure 5.3b displays the high variation amongst manually and sequentially collected 15 cm depth soil water samples. Manually collected samples contain lower Cl^- concentrations than sequentially collected samples. Average Cl^- concentrations are 35.9, 21.3 and 27.3 μeq/l for sites VA_{15}, VB_{15} and VC_{15}, respectively. The difference in concentrations amongst manual and sequential 15 cm depth soil water samples is greater in the growing season, where concentrations in manual samples are lowest (Table 5.4 and Figure 5.3b). Chapter IV discussed the greater abundance of macropore flow during the growing season, and thus the tension lysimeters (at Sites VA, VB or VC) might draw in macropore water. Hence, 'new' water would mix with 'old' water, resulting in lower Cl^- concentrations of samples. During the dormant season, when macropore flow is not as prevalent, the tension lysimeters have similar Cl^- contents to the sequential samples (Table 5.4). Additional evidence that macropore water may be collected in tension lysimeters is shown in the minimum concentrations collected, where some samples contained below 10 μeq/l Cl^-, which is similar to the content of rainfall, suggesting that the water is 'new'.

Figure 5.3c shows the VWM Cl^- content of throughfall, forest floor soil water and 15 cm soil water. In both seasons, the Cl^- content of 15 cm soil water is substantially higher than in the 'new' waters. The results of the hydrometric analysis (see Chapter IV) showed that the water collected by pan lysimeter, VI-15, was matrix soil water. The Cl^- concentrations of groundwaters (which are 'old' waters) have been shown to average between 40.8 and 46.8 μeq/l Cl^- (Table 5.1). For all storms, the VWM of 15 cm soil water samples typically exhibited concentrations closer to those found in groundwater and were hence regarded as 'old' waters. Tension lysimeters may contain a combination of 'old' and 'new' water, due to intersection of macropores. From the hydrometric analysis, 15 cm soil water collected at VI-15 and groundwaters collected at GQA, GQB, GQCs, GQCd and GQD were all postulated as containing 'old' waters. All groundwater samples contain > 30 μeq/l Cl-. The sequential samples of 15 cm soil water (VI-15) typically contained > 20 μeq/l Cl- (except for one storm) and the sequential samples of rainfall, throughfall and forest floor soil waters typically contained less than 20 μeq/l Cl^- (excluding the initial samples in collection sequences, which was due to enhancement from washout and washoff mechanisms). When the initial samples were removed from the analysis and the volume weighted means were calculated again, then all rainfall, throughfall and forest floor soil water VWM Cl- concentrations were below 20 μeq/l Cl-. Hence, the value of 20 μeq/l Cl- was chosen as a criteria for distinguishing 'new' from 'old' waters.

(V.4Ad) 50 cm soil water

The average VWM Cl^- concentration of 50 cm soil water (VI-50) is 24.1 μeq/l (Table 5.1). There is a distinct seasonal pattern to Cl^- concentrations in 50 cm soil water (Figure 5.4a), where high Cl^- concentrations occur in the dormant season (especially from January to March). Table 5.5 shows the average VWM Cl^- content during the growing season is 12.5 μeq/l and during the dormant season is 37.3 μeq/l. This pattern supports the hydrometric analysis which suggested that water at 50 cm during

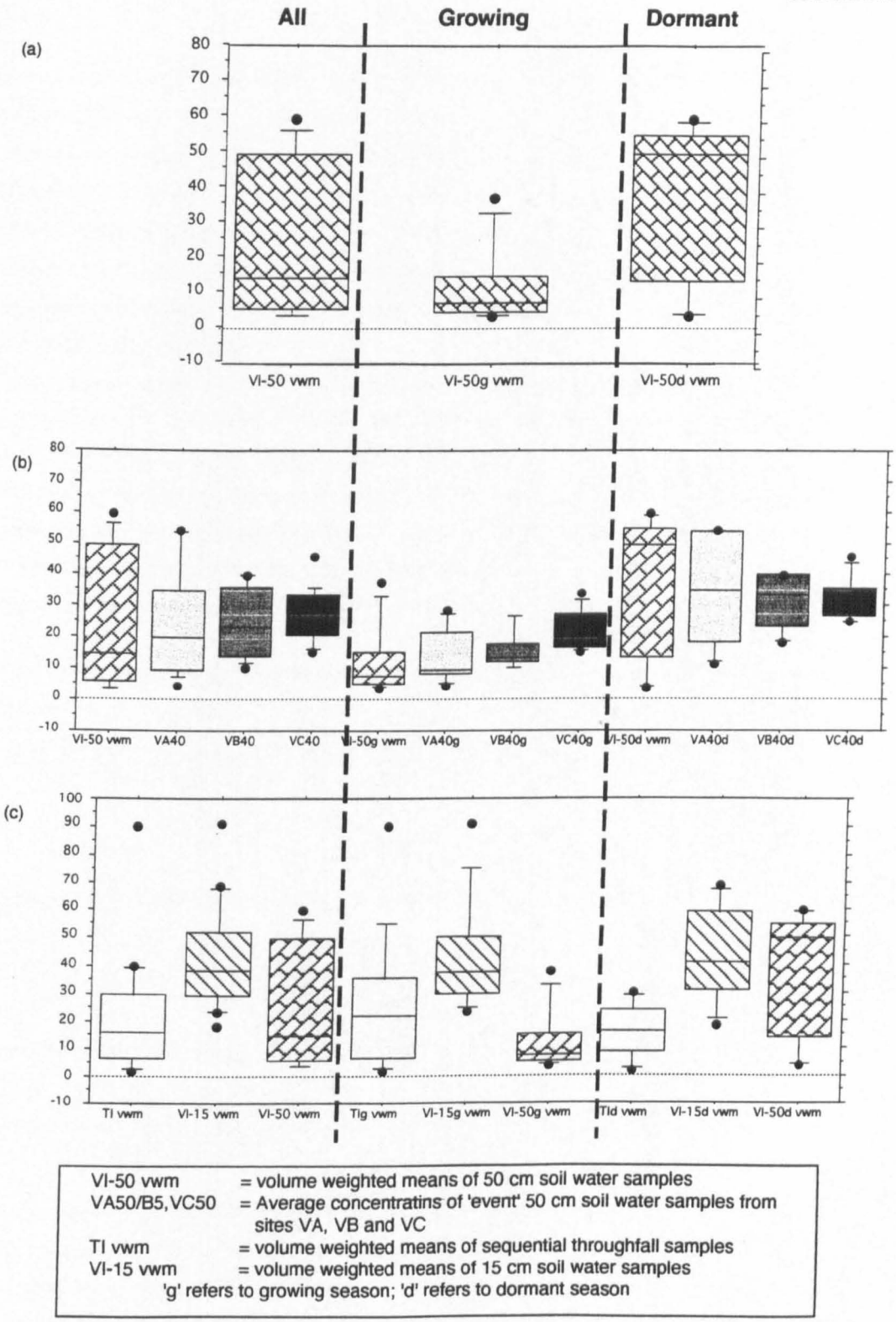

Figure 5.4. *Boxplots to show variations in volume weighted means and average chloride concentrations in (a) 50 cm soil water (VI-50); (b) Sequential (VI-50) and event 50 cm soil water (VA50, VB50, VC50); (c) Sequential 50 cm soil water, throughfall (TI) and 15 cm soil water (VI-15) samples, for all storms, growing season and dormant season storms between May 1994 and May 1995*

the growing season is macropore water (i.e. 'new' water and < 20 μeq/l Cl^-), whereas, the water collected during the dormant season is matrix water (i.e. 'old' water and > 20 μeq/l Cl^-).

Fifty cm soil water samples (VI-50) were collected for 14 storms. In eight of these storms, VWM Cl^- contents are below 15 μeq/l. The majority of these storms occur during the growing season, during which the Cl^- concentration of 50 cm soil water is similar to that of rainfall (i.e. 'new' water), and is therefore recognised as macropore water. The high concentrations in the remaining six storms, which occur during the dormant season, when the soil is generally wet (soil moisture content > 0.30) suggest a mixture of matrix and 'new' water.

Figure 5.4b compares the Cl^- content of 40 cm tension lysimeter (VA_{40}, VB_{40} and VC_{40}) and sequential 50 cm (VI-50) samples. The average Cl^- concentrations of VA_{40}, VB_{40} and VC_{40} are 24.7, 24.0 and 26.9 μeq/l, respectively, which are similar to the average VWM for 50 cm soil water (Table 5.1). Table 5.6 displays the average 40 cm soil water concentrations for growing and dormant season storms, and shows how the concentrations are lowest during the growing season. This suggests that:

(i) macropore water contributes substantially during the growing season

(ii) tension lysimeters collect a combination of 'new' and 'old' water.

Season	Node	Average (μeq/l)	Min (μeq/l)	Max (μeq/l)
Growing	VI-50	12.5	3.8	37.3
	VA_{40}	14.0	4.5	28.5
	VB_{40}	15.4	10.2	26.5
	VC_{40}	22.2	15.2	33.6
	TI	25.2	1.9	90.0
	VI-15	42.1	23.2	91.0
Dormant	VI-50	37.3	3.8	59.6
	VA_{40}	35.4	11.3	53.9
	VB_{40}	31.2	18.1	39.8
	VC_{40}	32.4	24.7	45.7
	TI	15.8	1.9	29.8
	VI-15	43.6	18.4	68.5

***Table 5.5**: Average volume weighted means or total, min and max Cl^- concentrations in sequential 50 cm soil water (VI-50), event 40 cm soil water (VA_{40}, VB_{40}, VC_{40}), sequential throughfall (VI-15) and sequential 15 cm soil water (VI-15)for storms during the growing season and the dormant season*

During the dormant season, the majority of samples contain > 20 μeq/l Cl^-, and are thus comprised 'old' water. Figure 5.4c displays the high variation in 50 cm soil water Cl^- content between the seasons. During the growing season, Cl^- concentrations in throughfall and 50 cm soil water are similar, but lower than found in the 15 cm matrix water. During the dormant season, the Cl^- concentrations in 15 cm and 50 cm soil waters are similar, and higher than found in throughfall.

(V.4Ae) Groundwaters

Average Cl^- concentrations for wells GQA, GQB, GQCs, GQCd and GQD are 44.4, 49.1, 47.5, 47.6 and 41.9 μeq/l, respectively. Table 5.6 displays average, min and max Cl^- concentrations for all wells for growing and dormant season storms. Wells GQA, GQB and GQCd display higher concentrations in the growing season, while wells GQCs and GQD display lower concentrations in the growing season. In all wells, except for GQD, Cl^- concentrations show greatest variation in the growing season, which might be attributed to groundwater displacement mechanisms (Chapter IV). Groundwater displacement involved the addition of 'new' water to the shallow saturated zone, which may then lead to displacement downslope of deeper, 'older' water. Hence, mixing of 'old' and 'new' water results.

Season	Well	Average (μeq/l)	Min (μeq/l)	Max (μeq/l)
Growing	GQA	48.5	40.6	69.4
	GQB	50.1	42.9	55.0
	GQCs	46.3	43.7	49.8
	GQCd	48.0	44.3	58.1
	GQD	40.5	33.3	51.3
Dormant	GQA	40.9	38.0	44.4
	GQB	47.7	44.2	49.1
	GQCs	49.3	46.7	51.0
	GQCd	47.0	45.0	49.2
	GQD	43.4	39.3	59.0

***Table 5.6**: Average, min and max Cl^- concentrations in groundwater samples from wells GQA, GQB, GQCs, GQCd and GQD (see Chapter 3 for location details) for storms during the growing season and the dormant season*

For all wells, Cl^- concentrations were above 30 μeq/l in all storms, which is over three times the average VWM Cl^- concentration of rainfall samples. These concentrations were higher than observed in throughfall and forest floor soil water samples. Some deeper soil water samples contained similar concentration to groundwaters, suggesting they were comprised primarily 'old' water. Soil waters containing Cl^- concentrations between those of rainfall and groundwater may comprise a mixture of 'old' and 'new' waters.

The Cl^- content of groundwater was not found to vary greatly with respect to location on slope, which has been found in other studies (e.g. O'Brien *et al*, 1996). However, high variability in Cl^- concentration was found at GQD, located at the upslope position, which is a similar finding to that for a catchment near Pullman, S.E. Washington, USA (O'Brien *et al*, 1996).

(V.4Af) Streamwaters

Average streamwater concentration at the lower gage for all storms is 37.1 μeq/l. Average concentrations are typically greater during the growing season (38.5 μeq/l) than during the dormant season (35.0 μeq/l) (see Table 5.7).

Season	Average (μeq/l)	Min (μeq/l)	Max (μeq/l)
All	37.1	26.9	48.5
Growing	38.5	26.9	46.8
Dormant	35.0	27.7	48.5

Table 5.7: *Average, min and max Cl- concentrations in lower gage streamwater for all storms, growing season and dormant season storms*

Average Cl^- concentrations at SWlg were greater than 20 μeq/l for all storms. However, in individual collection sequences, single samples contained concentrations in the order of 26 - 28 μeq/l Cl- , suggesting the contribution of 'new' water to the stream. However, for the majority of storms, it seems probable that the major contributor to storm runoff was groundwater or matrix soil waters (i.e 'old' waters).

(V.4Ag) Summary

The similarity of Cl^- concentrations in all mobile waters supports the findings of Reynolds and Pomeroy (1988) that Cl^- is relatively inert and is not affected by ion exchange or mineral equilibria processes, i.e. it is highly mobile through the system. However, the higher concentrations in matrix soil waters and groundwaters compared with rainfall or throughfall indicate that evaporative concentration has an extremely large impact. The Cl^- content of 'new' water (i.e. rainfall, throughfall, forest floor soil water and some deeper soil waters) is significantly different from that of 'old' water (i.e. matrix soil waters and groundwaters). The average VWM Cl^- concentrations of rainfall, throughfall and forest floor soil water are 8.3, 21.8 and 22.1 μeq/l respectively. The average VWM Cl^- concentration of 15 cm matrix soil water is 42.8 μeq/l. Average Cl^- concentrations of 15 and 40 cm tension lysimeter soil waters and groundwaters are 28.2, 25.2 and 46.1 μeq/l, respectively. In all storms, VWM Cl^- content of rainfall was below 20 μeq/l and in 11 of the 19 storms, for throughfall and forest floor soil waters. When initial samples of collection sequences, which are affected by washoff mechanisms, are removed from the analysis, and VWMs are recalculated, all concentrations were below 20 μeq/l Cl^- .In all storms, groundwater average Cl^- concentrations were above 20 μeq/l. Hence, 20 μeq/l Cl^- was selected as the criteria for distinguishing 'old' from 'new' water. Samples containing below 20 μeq/l Cl^- were comprised mainly of 'new' water, and those containing above 20 μeq/l Cl^- comprised mainly 'old' waters. This criteria is used in the following section for assessing the variations in the contribution of 'old' and 'new' waters within specific flowpaths throughout the duration of rainstorms.

(V.4B) Distinguishing 'old' from 'new' waters within flowpaths

Cl^- variations result from variations in the sources of water to that flowpath and variations in the compositon of the source water. The flowpaths that are considered in the next section are as follows:

(a) Rainfall and canopy mechanisms

(b) Overland flow

(c) Matrix flow

(d) Macropore flow

(e) Groundwater flow

(f) Streamwater flow

In each section, the variations in Cl^- concentration with respect to time are assessed. The influences of storm magnitude and antecedent moisture conditions on the Cl^- signatures of the water are also investigated.

(V.4Ba) Rainfall and canopy processes

(i) Concentration variation with respect to time

Although VWM Cl^- concentrations are below 20 μeq/l in sequential rainfall (Table 5.1), there is a distinct pattern to the concentrations; the first sample of the collection sequence is highest and typically is followed by progressively decreasing concentrations (Appendix 5.3). Cl^- concentrations in throughfall display similar patterns for most storms (Appendix 5.4). This pattern has been observed for most solutes in other studies (Durana *et al*, 1992; Hansen *et al*, 1994; Khare *et al*, 1996). Boxplots of the variation in Cl^- concentrations with respect to bottle sequence number are shown for all rainfall (Figure 5.5a) and all throughfall samples (Figure 5.5b). Both the boxplots show a skewed positively distribution, where the initial samples contain highest Cl^- concentrations and also the greatest degree of variance. The higher Cl^- content in the initial samples of rainfall are attributed to washout mechanisms, and the higher Cl^- content in initial samples of throughfall are attributed to washoff mechanisms. Figure 5.5c displays a case study storm, on 16 August, where the Cl^- concentrations in rainfall and throughfall collection sequences are displayed.

Case study: 16 August 1994

Figure 5.5c displays the Cl^- concentrations in rainfall and throughfall collection sequences. The initial sample of rainfall contains 12.7 μeq/l Cl^-, after which concentrations decrease with time. The initial sample of throughfall contained 38.4 μeq/l Cl^- and the second contains 18.6 μeq/l Cl^-. For the remaining samples, concentrations were all below 10 μeq/l Cl^-. In the week prior to this storm, 12 mm rainfall occurred, and hence the high concentrations in the initial two samples of throughfall are attributed to washoff, since the relatively dry antecedent conditions allowed accumulation of dry deposition on the canopy.

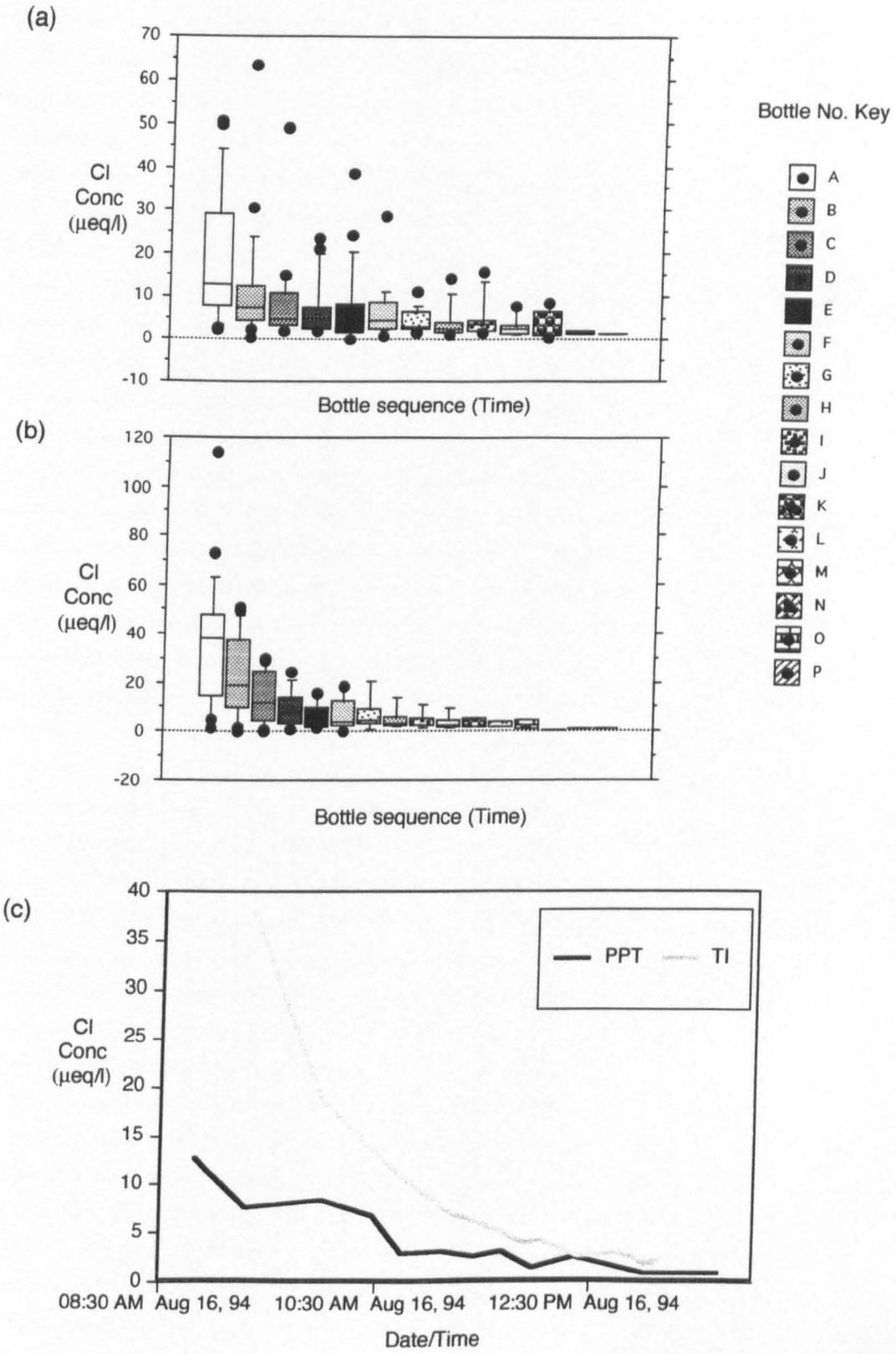

***Figure 5.5**: Chloride concentrations in bottles of sequential collection sequences of (a) rainfall (PPT); (b) Throughfall (TI); and (c) chloride variations in whole collection sequences of rainfall and throughfall for a storm on 16 August 1994*

In the previous section, the average VWM Cl^- concentrations of rainfall and throughfall were reported as 8.3 and 21.8 μeq/l, respectively. The data in Figure 5.5a-c show that the distribution of Cl^- concentrations in rainfall and throughfall are non- normal and hence, the initial samples tend to bias the VWM somewhat.

The trend of greatest Cl^- concentrations in initial samples of collection sequences of throughfall occur both in dormant and growing season storms (see Appendix 5.2). During the dormant season, water must flow over the branches and stems of the vegetation in order for the dry deposition to be mobilised. This corroborates the assumptions of the hydrometric analysis (Chapter IV) that during the dormant season, flow occurs over the branches, and might eventually lead to focusing of water at drip points in the canopy. Although the operation of drip points cannot be clarified from the Cl^- analysis, the data does provide strong evidence for the transit of water along branches.

(ii) Concentration variations with respect to storm magnitude

Figure 5.6a displays the variation in VWM Cl^- concentrations with respect to storm magnitude (i.e. total rainfall). Lower VWM Cl^- concentrations are associated with storms of higher magnitude. This pattern might be expected since a larger magnitude storm would generate a greater number of samples, the latter of which would not be affected by washout processes. Two distinct clusters exist in the data. Storms below 30 mm show the highest Cl^- contents in small magnitude storms, which decrease as the storm magnitude increases. Storms of greater magnitude (i.e. > 30 mm) tend to have similar VWM Cl^- concentrations (of between 2 and 4 μeq/l). This trend is explained by smaller storms being influenced the greatest extent by washout processes. Skartveit (1982) noted that calculated species washout ratios are not fixed, but decrease as rainfall amount increases, especially for Cl^-, which is scavenged by hydrometeors rather than incorporated via a cloud condensation nuclei pathway.

Figure 5.6b displays the variation in VWM Cl^- concentrations of throughfall with respect to storm magnitude (i.e. total rainfall). The graph shows a hyperbolic relationship, with highest Cl^- concentrations for small magnitude storms. This pattern is attributed to washoff of dry deposition from the canopy. In larger storms, more samples are generated, the latter of which are not affected by washoff of Cl^- from the canopy. Thus, the later samples in collection sequences contain lower Cl^- and cause the overall VWM Cl^- concentration to be reduced.

(iii) Concentration variation with respect to antecedent moisture conditions

The VWM Cl^- concentration of rainfall was not found to be influenced by antecedent moisture conditions (the correlation coefficient of VWM Cl^- content of rainfall on total rainfall in the week prior to the rainstorm was statistically insignificant). There was a poor relationship between VWM Cl^- content of throughfall and antecedent moisture conditions (in terms of total rainfall in the week prior to the rainstorm). The relationship showed a weak negative correlation (- 0.24). This is expected since the wetter conditions caused available dry deposition to be low, and hence the VWM Cl^- content of throughfall would also be low (Best and Marius, 1969). Thus, the wetter the antecedent conditions, the lower the Cl^- content of throughfall.

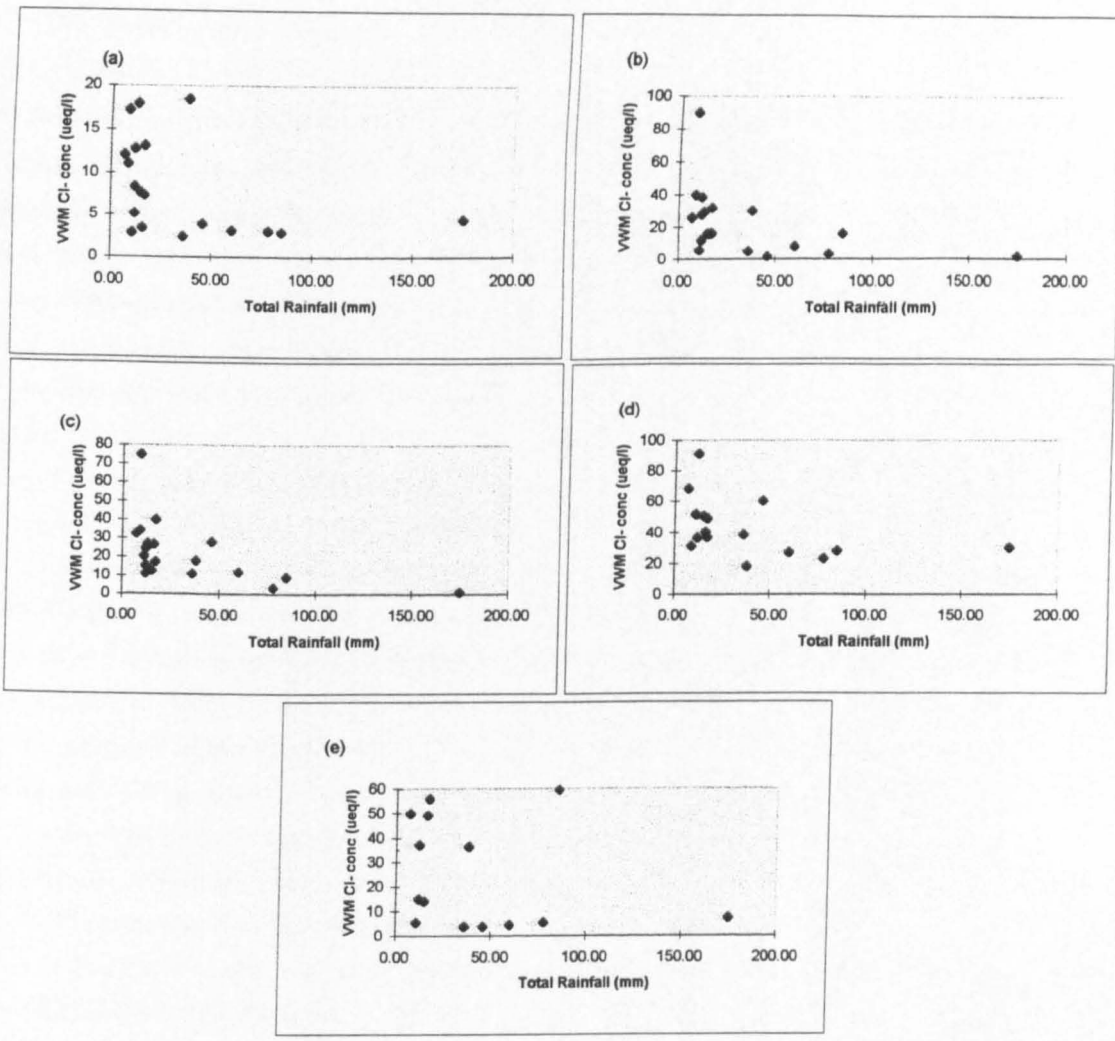

Figure 5.6: Total rainfall and VWm Cl concentrations in sequential samples of (a) rainfall; (b) throughfall; (c) forest floor soil water; (d) 15 cm soil water; (e) 50 cm soil water

(V.4Bb) Overland flow

(i) Concentration variation with respect to time

In forest floor soil water collection sequences, the first sample contains the highest Cl^- content and is typically followed by progressively decreasing concentrations (Appendix 5.5). This pattern is displayed in Figure 5.7a, where boxplots are shown of the variation in Cl^- content with respect to the bottle number in the collection sequence. The boxplots shows a skewed distribution, similar to those found in throughfall (Figure 5.5b). This pattern would be anticipated since the input water to the forest floor was throughfall, which also exhibits this pattern. However, there is a distinct seasonal pattern in forest floor soil water, when compared to throughfall. In collection sequences during the growing season, initial samples of forest floor soil water often contain higher Cl^- concentrations than throughfall, but towards the end of the sequence, similar concentrations are observed. This suggests that the forest floor soil may be comprised from throughfall and overland flow which results from return flow of matrix water (Eshleman *et al*, 1993). Hence the higher Cl^- content water at the start of storms might be attributed to washoff and saturation overland flow. The hydrometric evidence supports this hypothesis, as overland flow was found to operation soon after storm onsets during the growing season. During the dormant season, most samples of forest floor soil water contain higher Cl^- concentrations throughout the collection sequences than throughfall. This will be explored further in the following section, where a two-component mixing model is employed to calculate the contribution of 'old' and 'new' water to the forest floor. A case study storm is provided to show the variation in Cl^- contents of forest floor soil water and throughfall collection sequences (16 September 1994).

Case study storm: 16 September 1994

Figure 5.7b displays Cl^- concentrations in throughfall and forest floor soil water collection sequences. The storm occurs in the growing season. The initial sample of throughfall contains 27.0 μeq/l, and the second contains 19.2 μeq/l. There is then a decrease in concentration in the following samples to below 5 μeq/l Cl^-, followed by an increase to above 15 μeq/l Cl^-. This samples was taken following a 'gap' in rainfall. The initial sample of forest floor soil water contains 28.7 μeq/l Cl^- and the second contains 19.7 μeq/l Cl^-. After this sample, there is a general decline in Cl^- content, but the concentrations are still greater than those in throughfall. The higher Cl^- content of the water must therefore be derived from another source than throughfall, which is the return flow of matrix water in the form of saturation overland flow.

(ii) Concentration variation with respect to storm magnitude

Figure 5.6c displays the variation in VWM Cl^- concentrations of forest floor soil water with respect to storm magnitude (i.e. total rainfall). The graph shows a near-linear relationship, with highest Cl^- concentrations for smallest magnitude storms. The pattern is similar to that of throughfall, which would be expected since over half of forest floor soil water comprises of throughfall (Chapter IV).

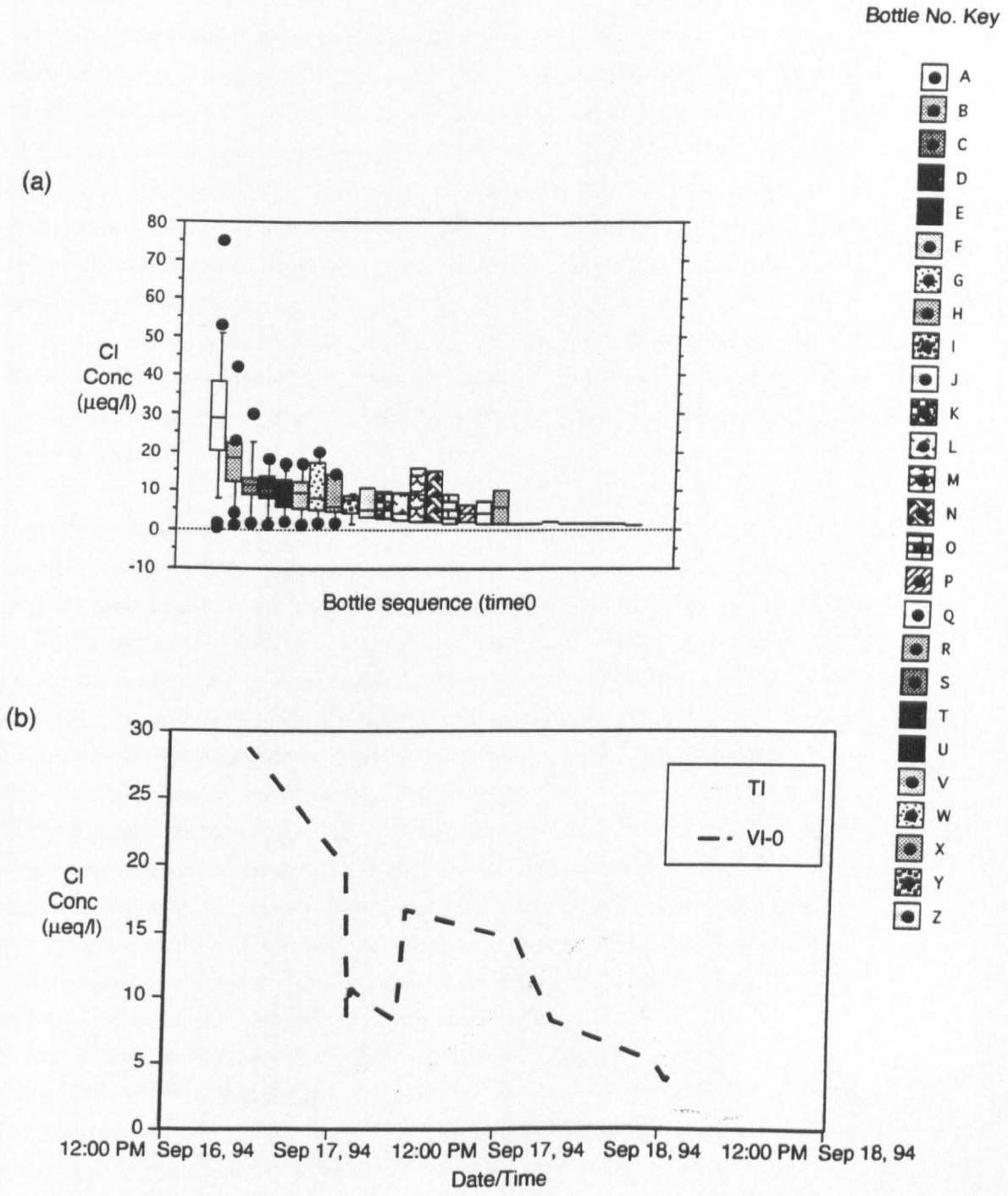

***Figure 5.7**: Chloride concentrations in (a) bottles of sequential collection sequences of forest floor soil waters, and (b) in whole collection sequences of forest floor soil water and throughfall for a storm on 16 September 1994*

(iii) Concentration variation with respect to antecedent moisture conditions

A correlation of the VWM Cl^- concentration of forest floor soil water with total rainfall in the week prior to the storm produced a negative correlation coefficient of - 0.38. A seasonal trend was evident in the relationship. A stronger correlation was obtained in the growing season (- 0.47), compared to the dormant season (- 0.21). A seasonal trend was also found in the relationship between antecedent moisture conditions (in terms of rainfall in the week prior to the storm) and the Cl^- content of the initial sample in the collection sequence. During the growing season, a negative relationship was obtained (- 0.48). Hence, the drier conditions allowed dry deposition to accumulate, both in the canopy and on the forest floor, which would be mobilised in the current rainfall. During the dormant season, a positive relationship was obtained (0.21). Hence, the wetter the conditions, the greater the Cl^- in the initial sample. This result supports the theory that saturation overland flow is important during the dormant season, since the only source of high Cl^- content water to the forest floor following wet conditions, when washoff is negligible, must be the return flow of matrix soil water. This will be explored further in a following section.

(V.4Bc) Matrix soil water

(i) Concentration variation with respect to time

There is a slight pattern in Cl^- concentration of sequential 15 cm soil water with time; where inital samples in collection sequences contain higher Cl^- concentrations. This is shown in Figure 5.8a, where boxplots are shown of the Cl^- concentration variations with respect to bottle number in collection sequences. The variation is lower than found in rainfall or throughfall (Figure 5.5a and b). All samples in the collection sequences contain > 20 μeq/l and hence must comprise 'old' water.

(ii) Concentration variation with respect to storm magnitude

Figure 5.6d displays the variation in VWM Cl^- concentrations in 15 cm soil water (V1-15) with respect to storm magnitude (i.e. total rainfall). The correlation coefficient of the relationship is - 0.43, which suggests that the greater the magnitude of the storm, the less is the Cl^- content of 15 cm soil water. The graph displays a near-linear relationship, which is suprising since the 15 cm sequential soil water was hypothesised to be matrix water. Some contribution of 'new' water at 15 cm must occur in order for this dilution effect by higher magnitude storms to be experienced.

(iii) Concentration variation with respect to antecedent moisture conditions

The correlation of VWM Cl^- concentration of 15 cm matrix water with total rainfall in the week prior to the storm shows a significant negative relationship (- 0.45). This indicates that the drier the antecedent conditions, then the greater the Cl^- content of 15 cm soil water. This supports the theory that the 15 cm soil water is matrix, and its higher Cl^- content is probably a result of evaporative mechanisms.

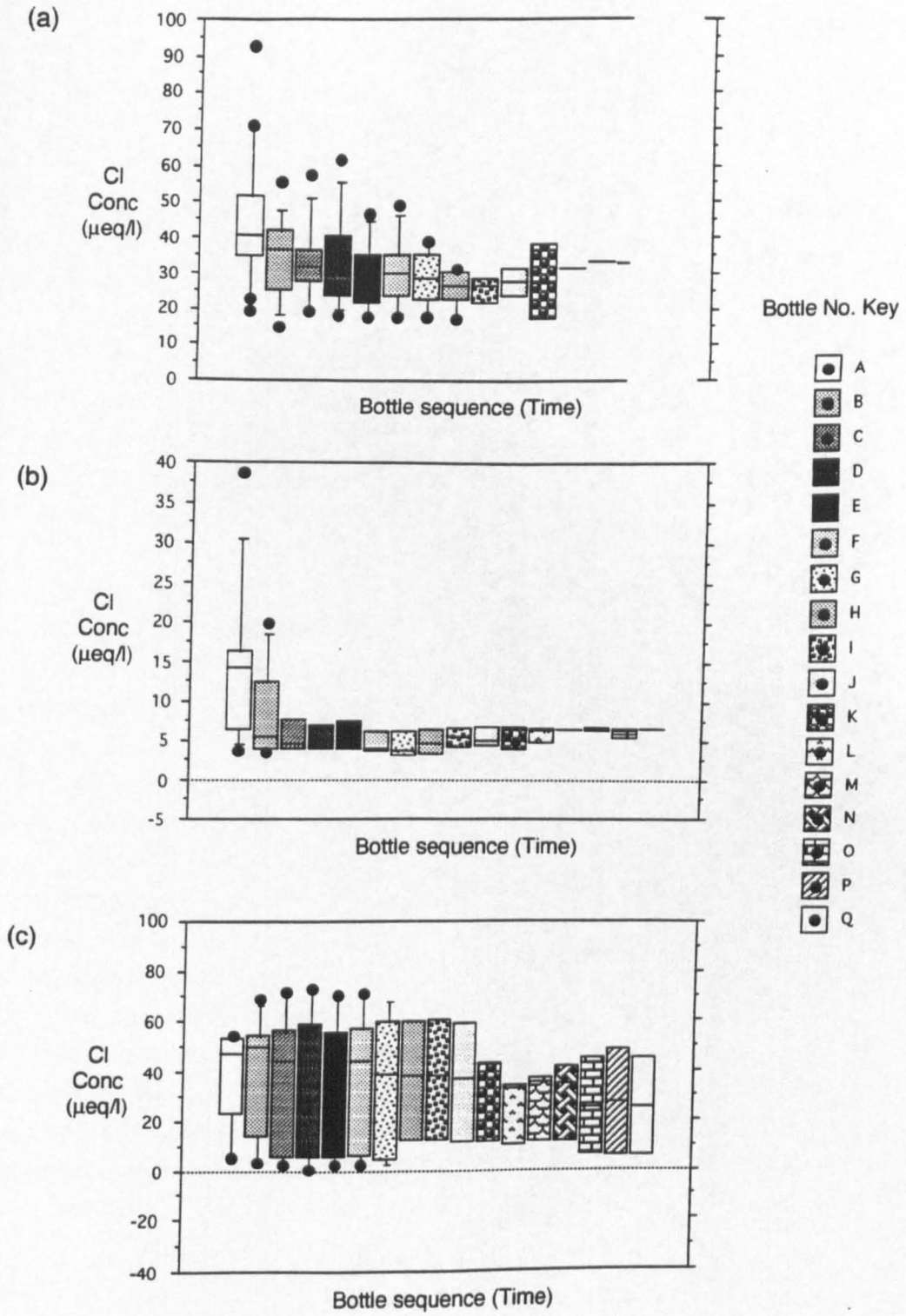

***Figure 5.8**: Chloride concentrations in bottles of sequential collectin sequences of (a) 15 cm soil water (VI-15); (b) 50 cm soil water (VI-50) during the growing season; (c) 50 cm soil water (VI-50) during the dormant season*

(V.4Bd) Macropore flow

(i) Concentration variation with respect to time

During the dry summer and fall, Cl^- concentrations of sequential 50 cm soil water samples are highest in the first sample and then decrease, remaining relatively constant for some time and then increase slightly after considerable water passes through the lysimeter (Figure 5.8a). The Cl^- concentrations are similar to those of rainfall (or throughfall) (i.e. < 20 μeq/l Cl^-), suggesting the source to be mobile 'new' water (Appendix 5.7). The initially higher concentrations correspond with and are partly attributed to rainfall and throughfall (O'Brien *et al*, 1996). The increase in Cl^- concentrations later in the storm probably are caused by mixing with matrix waters. A case study storms is presented in Figure 5.9a, on 4 July 1994.

Case study: 4 July 1994

Figure 5.9a displays the Cl^- concentrations in a sequential collection sequence of 50 cm soil water for a storm on 4 July 1994. The initial sample in the sequence contains 14.1 μeq/l, and concentrations progressively decline in following samples, with the majority of later samples containing below 8 μeq/l Cl^-. Hence, all samples in the collection sequence contains < 20 μeq/l Cl^- and were considered to comprise 'new' water.

During the wetter winter period (Figure 5.8b), Cl^- concentrations of samples collected by the lysimeter are much more variable and generally are more concentrated than those of matrix soil water or groundwater (i.e. > 20 μeq/l Cl^-). The first sample tends to be more dilute than subsequent samples, possibly indicating the contribution of 'new' water to this sample, via macropore or mesopore flow (see Chapter IV). Likewise, if many samples are generated for a rainstorm, Cl^- concentrations of later samples were lower which likewise reflects an increasing contribution of 'new' water. A case study storm in presented in Figure 5.9b, on 27 February 1995.

Case study storm: 27 February 1995

Figure 5.9b displays the Cl^- concentration in a sequential collection sequence of 50 cm soil water for a storm on 27 February 1995. The initial sample in the sequence contains 35.2 μeq/l Cl^-, which is the lowest concentration of any sample in the sequence, which is attributed to the contribution of 'new' water via macropore or mesopore flow at the onset of the storm. Since the sample contains > 20 μeq/l Cl^-, it must contain mainly 'old' water. However, comparison with concentrations in remaining samples suggests that it must contain some 'new' water. After the initial sample, there is a general increase in the Cl^- concentration of following samples, to a peak concentration of 38.6 μeq/l. After this, concentrations begin to decline again, which is attributed to the mixing of 'old' and slower moving 'new' water.

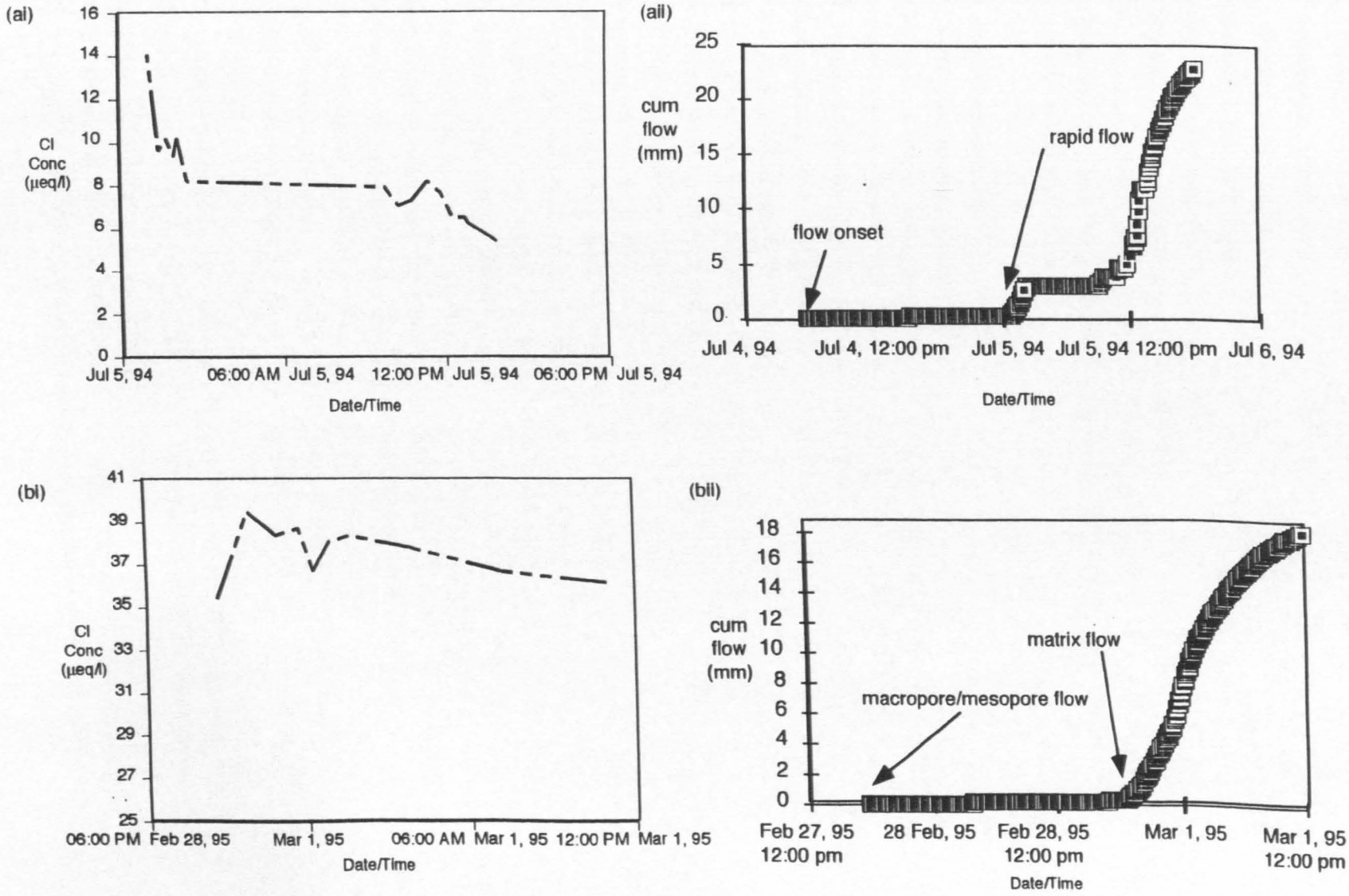

***Figure 5.9**: (ai) Chloride concentrations in 50 cm soil water, (aii) Cumulative 50 cm soil water flow, for a storm on 4 July 1994 (bi) chloride concentrations in 50 cm soil water (bii) cumulative 50 cm soil water flow, for a storm on 27 February 1995*

(ii) Concentration variations with respect to storm magnitude

Figure 5.6e displays the variation in VWM Cl^- concentrations of 50 cm soil waters with respect to storm magnitude (i.e. total rainfall). The correlation coefficient of the relationship is - 0.26. which, as for all other nodes, suggests that the greater the storm magnitude, the lower the VWM Cl^- concentration. The graph displays several outliers to this relationship, which are explained by the seasonal trend in 50 cm soil water Cl^- concentrations.

(iii) Concentration variation with respect to storm magnitude

The correlation of VWM Cl^- concentration of 50 cm soil water with total rainfall in the week prior to the storm was - 0.35. This value suggests that the wetter the antecedent moisture conditions, the lower the VWM Cl^- content of 50 cm soil water.

(V.4Be) Groundwater flow

(i) Concentration variations with respect to time

Due to the low resolution times of groundwater sampling, no quantitative assessment could be made of the variation in groundwater Cl^- concentrations with respect to time. In two storms (4 July 1994 and 28 February 1995), four groundwater samples were collected per storm. The variation in Cl^- concentrations was only by a magnitude of 2-3 μeq/l. Hence, concentration variation of groundwater with respect to time was hypothesised to be negligible.

(ii) Concentration variations with respect to antecedent moisture conditions.

Antecedent moisture conditions were calculated in terms of the lowest base flow groundwater height in the 24 hr prior to the rainstorm (24 min. baseflow height). Groundwater stage monitoring well, GWA, corresponds, in terms of location, to groundwater sampling well GQA. Groundwater stage monitoring well, GWC, corresponds, in terms of location, to groundwater sampling wells GQCs and GQCd. Correlation analyses were performed between average Cl^- concentrations in well GQA with 24 min. base flow height in GWA, and between average Cl^- concentrations in well GQCs and GQCd with 24 min. base flow height in GWC. The correlation of min 24 hr base flow height at GWA and average Cl^- content of GQA produced a value of 0.68, suggesting that the higher the base flow conditions, which in turn are related to wetter antecedent moisture conditions, the greater the Cl^- concentrations in GWA. This was inverse to the expected trend, since groundwater Cl^- concentrations were expected to be higher following dry antecedent conditions, since evapotranspiration may have been in operation, leading to concentration of Cl^-. The opposite trend might be explained by contribution of lower Cl^- concentration streamwater to groundwater in the riparian zone following wet antecedent conditions (see Chapter IV).

The correlation between min 24 hr base flow height at GWC and average Cl^- content of GQCs produced a negative correlation (- 0.23), which suggests that the drier the conditions prior to the storm, the higher the Cl^- concentration in groundwater. However, the correlation between base flow conditions at GWC and the deeper groundwater at GQCd produces a correlation of 0.29, suggesting the opposite trend. The conclusion of the analysis supports that of the hydrometric analysis (Chapter IV),

that the groundwater flow mechanisms in operation are influenced by position of the groundwater monitoring site, and also the depth of groundwater that is screened at.

(V.4Bf) Streamwater flow

(i) Concentration variations with respect to time

Figure 5.10a displays the range in Cl^- concentrations of lower gage streamwater samples in terms of their bottle number in collection sequences. The variation is high, suggesting that the particular flowpaths that contribute to storm runoff vary with respect to individual storm conditions (Appendix 5.8). The general pattern is of high Cl^- concentrations in initial samples, followed by a decrease in concentration of following samples, which is attributed to contribution of 'new' water to the stream channel. In later samples in the sequence, Cl^- concentrations rise again, which is attributed to mixing of 'old' and 'new' waters. The variability in streamwater Cl^- concentration is high, and greater than in rainfall. Many other studies find the opposite, where variations in Cl^- are high in rainfall and low in streamwaters (Kennedy *et al*, 1986; Christophersen and Neal, 1987; Reynolds and Pomeroy, 1988). Higher variation in streamwater Cl^- concentrations at PMRW are explained by distinct variations in groundwater and 'new' water contributions to the stream channel.

(ii) Concentration variations with respect to storm magnitude.

Storm magnitude was represented by the stage height (m) recorded at the time the sample of taken. The relationship between Cl^- concentration of streamwater and stage height is shown in Figure 5.10b. A near-linear negative relationship is obtained, showing that the higher the discharge, the lower the Cl^- content of the sample. This shows that in higher magnitude storms, there is greater contribution of 'new' water to the stream channel and hence the Cl^- content of that water is lower. Similar observations were made at Reedy Creek, Virginia, USA (Eshleman *et al*, 1993).

(iii) Concentration variations with respect to antecedent moisture conditions

Antecedent moisture conditions were represented in terms of the lowest base flow in the 24 hr prior to the rainstorm. A correlation of minimum 24 hr base flow with average Cl^- content of lower gage streamwater produced a value of 0.39. The positive relationship suggests that the wetter the antecedent moisture conditions, the higher the Cl^- concentration of streamwater. This was the opposite trend to that anticipated, since under drier conditions, the contribution of groundwater to streamwater might be expected to be higher and hence higher Cl^- concentrations would result. High variation in the Cl^- content of streamwater samples is observed throughout the duration of storms (Appendix 5.8), and hence, the calculation of an average value may not be of use in this calculation.

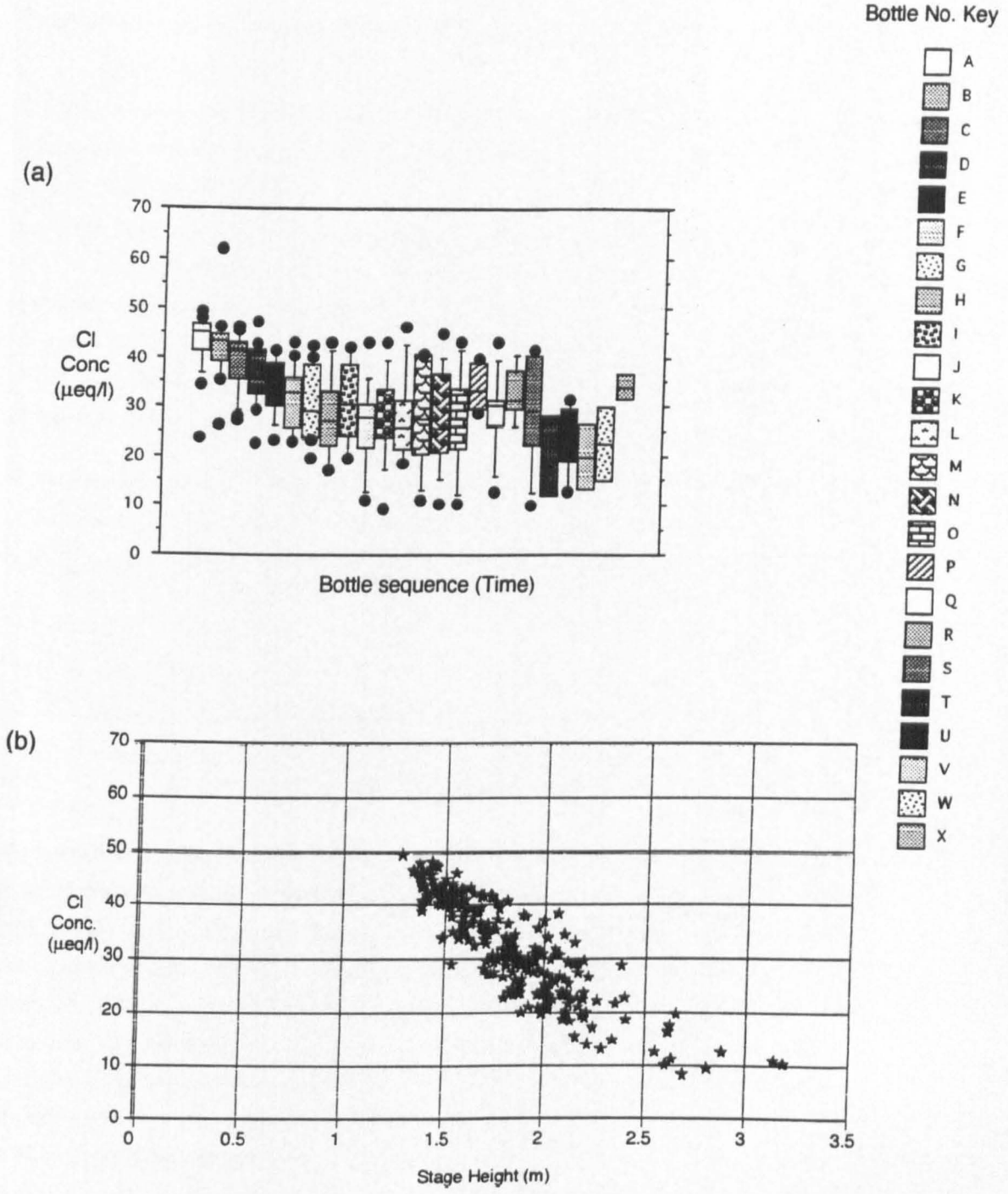

Figure 5.10: *(a) Chloride concentrations in bottles of sequential lower gage streamwater (b) Relationship between chloride concentration of samples and stage height when sample was taken*

(V.4C) Quantification of the relative contributions of 'old' and 'new' water contribution within specific flowpaths

Two-component mixing models are employed to estimate the relative contribution of 'old' and 'new' water in forest floor soil waters and in 50 cm mobile soil waters.

(V.4Ca) Forest floor soil water

Equations 5.3 and 5.4 were combined to generate two-component mixing models of water contribution to forest floor soil water. 'New' water was represented by throughfall (TI) and 'old' water was represented by 15 cm matrix water (VI-15). VWM Cl^- concentrations of forest floor soil water (VI-0), throughfall and 15 cm soil water provided values for the C_{ff}, C_{TI} and $C_{VI\text{-}15}$ term, respectively. Tipping bucket forest floor soil water volumes provided the values for the V_{ff} term. Complete datasets were available for six storms, the results of which are presented in Table 5.8.

Storm Date	V_{ff} (mm)	V_{TI} (mm)	$V_{VI\text{-}15}$ (mm)	% NEW	% OLD
17 Sept. 1994	47	38	9	81	19
11 Oct. 1994	43	23	20	53	47
13 Oct. 1994	13	9	4	69	31
19 Jan. 1995	20	17	3	85	15
19 April 1995	26	22	4	85	15
1 May 1995	16	14	2	88	12

***Table 5.8** : Results of two-component mixing model, assessing the contribution of 'old' water ($V_{VI\text{-}15}$) and 'new' water (V_{TI}), to forest floor soil water (V_{ff}). The total forest floor soil water is expressed as % of 'old' and 'new' water.*

The analysis shows that in all storms, the majority of water is 'new'. This was anticipated since 100% throughfall was collected by the forest floor soil water lysimeter, and the additional water was derived from overland flow. However, the 'old' water contribution is between 12 and 47%, which indicated that saturation overland flow is an important mechanism. Site VI-0 was located in a topographic low, where the collection of forest floor soil water as anticipated to contain a significant overland flow component. The data presented in Table 5.8 was collected from this site. The results of the analsysis have shown that overland flow contributed to forest floor soil water, and hence the Cl- analysis supports the findings of the hydrometric analysis.

(V.4Cb) 50 cm mobile soil waters

Equations 5.5 to 5.7 were combined to generate two-component mixing models to assess 'old' vs. 'new' water contribution to 50 cm mobile soil waters. 'New' water is represented by throughfall (TI) and 'old' water is represented by 40 cm soil waters (i.e. VA_{40}, VB_{40} and VC_{40}), V_{40}. VWM Cl^- concentrations of throughfall and 50 cm soil water (VI-50) provided values for the parameters C_{TI} and $C_{VI\text{-}50}$, and average Cl^- concentrations of VA_{40}, VB_{40} and VC_{40} provided the values for parameter C_{V40}. Tipping bucket 50 cm soil water data provided values for parameter $V_{VI\text{-}50}$. Complete datasets were available for five storms, the results of which are presented in Table 5.9.

Storm Date	V_{VI-50} (mm)	V_{TI} (mm)	V_{V40} (mm)	% NEW	% OLD
4 July 1994	41	21	20	51	49
11 July 1994	17	13	4	76	24
17 Sept. 1994	0.5	0.5	0	100	0
11 Oct. 1994	24	22	2	92	8
13 Oct. 1994	13	13	0	100	0

Table 5.9 : Results of two-component mixing model, assessing the contribution of 'old' water (V_{V40}) and 'new' water (V_{TI}), to 50 cm mobile water (V_{VI-50}). Total 50 cm soil water flow is expressed as % of 'old' and 'new' water.

The previous sections discussed the seasonal trends in Cl^- concentrations of 50 cm soil water. Low Cl^- concentrations were obtained during the growing season (and also for storms in October 1994). VWM Cl^- concentrations of 50 cm soil waters are low, and hence a high contribution of 'new' water is expected. This is shown in Table 5.9, where 'new' water contributes between 51 and 100% of the 50 cm soil water. Hence, the mixing model analysis supports the hydrometric (Chapter 4) and previous Cl^- analysis (section 5.IV.1), that suggests that macropore flow is an important flowpath within the system. The calculation of 100% 'new' water suggests that all water collected by the pan lysimeter is 'new' water. This supports the hydrometric analysis, which suggests that this is true, however, the calculation might give a slight overestimation, since the 40 cm soil water that is used as an estimate of the Cl- concentration of 'old' water, might actually be a combination of 'old' and 'new' water.

(V.5) SUMMARY

The following section provides a summary of the results and discussion within chapter 5.

- Cl^- is effective at distinguishing between 'old' and 'new' waters. Samples containing 20 µeq/l Cl^- are typically 'new' waters. Samples of rainfall (PPT and PE1), throughfall (TI), forest floor soil water (VI-0) and some deeper soil waters generally contain < 20 µeq/l Cl^-. Samples containing > 20 µeq/l Cl^- are typically 'old' waters. Samples of groundwater and deeper matrix waters generally contain > 20 µeq/l Cl^-.
- In all storms, VWM Cl^- concentrations of rainfall contain < 20 µeq/l Cl^-. However, in individual collection sequences, initial samples may contain higher Cl^-. This is attributed to washout mechanisms (Cryer, 1986). Samples later in collection sequences are not affected by this mechanism and hence contain Cl^- concentrations of < 20 µeq/l (Skartveit, 1982).
- In 11 out of 19 storms, VWM Cl^- concentrations of throughfall contain <20 µeq/l Cl^-. However, initial samples are enriched in Cl^- (reaching above 100 µeq/l) due to washoff of dry deposition from the canopy (Unsworth, 1980; Cryer, 1986; Eshleman *et al*, 1993). Samples later in the collection sequence typically contain < 20 µeq/l and are unaffected by the mechanism. Throughfall is influenced by washoff both during the growing and dormant seasons. When these

initial samples are removed from the analysis and the VWM Cl- concentrations are recalculated, then all storms contain VWM < 20 μeq/l Cl-.

- A two-component mixing model analysis found that between 53 and 88% of forest floor soil water is 'new' water. In 11 of 19 storms, the VWM Cl^- concentration of forest floor soil water is < 20 μeq/l, which also suggests that the majority of water is 'new'. Initial samples of forest floor soil water contain high Cl^- concentrations (up to 75 μeq/l), which is attributed either to washoff or to saturation overland flow, where high Cl^- content matrix water is collected via return flow. During the dormant season, many samples of forest floor soil water contain higher Cl^- concentrations than corresponding throughfall samples, which is again attributed to saturation overland flow.
- Cl^- is useful in distinguishing matrix from macropore soil waters. Lysimeter VI-15 collected high Cl^- content 15 cm soil water for all storms. The high Cl^- content of the water (> 20 μeq/l) and the absence of any seasonal variation supports the hydrometric analysis, which indicates that this water is matrix water. The Cl^- content of lysimeter VI-50 water varies greatly with respect to season. During the growing season (and October storms), VWM Cl^- content of 50 cm soil water is typically < 20 μeq/l , suggesting that the majority of the water is 'new'. This supports the hydrometric analysis, which found that macropore flow is dominant during the growing season, and the majority of water collected by lysimeter, VI-50, is from macropores. The application of a two-component mixing model to 50 cm soil water for growing season storms finds that that contribution of 'new' water varies between 51 and 100%. During the dormant season (excluding storms in October), VWM Cl^- content of 50 cm soil water is typically > 20 μeq/l , suggesting that the majority of the water is 'old'. However, the analysis of Cl^- concentrations in collection sequences suggests that the initial samples may contain some macropore water (which again agrees with the hydrometric analysis).
- Tension lysimeter samples contained a range of Cl^- concentrations. During the growing season, 15 cm tension lysimeter soil water is typically lower in Cl^- content that 15 cm sequential (i.e. matrix) soil water. This is attributed to the collection of macropore water by the tension lysimeters, thus diluting the Cl^- concentration of the sample. During the dormant season, when macropore flow is less dominant, Cl^- concentrations of all 15 cm soil water samples are similar. During the growing season, the Cl^- concentrations of 40 cm tension lysimeter samples are higher than 50 cm sequential samples (i.e. macropore water). Hence, tension lysimeters collect a combination of 'old' and 'new' water.
- Groundwaters all contain > 20 μeq/l Cl^- (i.e. 'old' water concentrations). They show little variation in concentration with respect to time. Greatest within storm variation is noted during the growing season, which might be attributed to rapidly changing hydrological conditions due to the occurrence of two tropical storms and the operation of groundwater ridging and/or displacement.
- Storm magnitude was found to influence Cl^- concentrations at most nodes. Negative correlations were obtained between VWM Cl^- concentrations and storm magnitudes. Hence, larger storms

typically generated lower VWM Cl^- concentrations (Skartveit, 1982). This is because many processes operating at individual nodes occur only at the beginning of storms and hence in large storms, many samples are generated, the latter of which are not affected by these processes. Latter samples thus contain lower Cl^- concentrations and hence influence the overall VWM Cl^- concentration

- Antecedent moisture conditions also influence Cl^- contents of samples at individual nodes. For rainfall, throughfall and forest floor soil waters, dry antecedent conditions lead to higher Cl^- concentrations. This is anticipated since drier conditions allow for greater concentration of dry deposition on the canopy and forest floor (Unsworth, 1982). The same relationship is true for 15 cm soil water. In this case, drier conditions allow concentration of Cl^- in the shallow soil by evaporative mechanisms. Groundwater exhibits different relationships with antecedent moisture conditions depending on the location of the monitoring site and the sampling depth.
- Streamwater average Cl^- concentrations are typically > 20 μeq/l, suggesting a major contribution of 'old' water to storm runoff (i.e. from groundwater or matrix soil water). However, individual collection sequences do show some samples containing < 20 μeq/l , indicating contribution from 'new' water. Cl^- concentrations in streamwater were greatly influenced by storm magnitude. High magnitude storms lead to low Cl^- concentrations of streamwater, suggesting addition of large quantities of 'new' water.

The Cl^- analysis has been able to corroborate may of the results of the hydrometric analysis. In the next chapter, temperature will be employed as a conservative tracer in order to provide further evidence for the occurrence of hypothesised flowpaths in Chapter IV. Temperature data will corroborate the results of the Cl^- tracer chapter, and provide further evidence for the operation of mechanisms that the Cl^- analysis was incapable of identifying due to low resolution of sampling; namely direct channel rainfall and groundwater displacement.

Chapter VI
TEMPERATURE TRACER STUDY

(VI.1) INTRODUCTION

The distinction between 'old' and 'new' water within specific flowpaths has successfully been made, using Cl^- as a conservative tracer (see Chapter V). In this chapter, a similar analysis will be performed to corroborate the results of Chapter IV, employing temperature as a conservative tracer.

The usefulness of temperature for tracing flowpaths revolves around the temporal and spatial variability and the magnitude of the difference in the temperature of source waters. Water temperatures in streams follow seasonal and diurnal cycles. Diurnal cycles are superimposed on the seasonal cycles (Sinokrot and Stefan, 1992). Diurnal stream temperature variations are related directly to diurnal changes of solar radiation and air temperature. Weather parameters such as air temperature, solar radiation, relative humidity, cloud cover and wind speed play a major role in heat exchange between the atmosphere and the stream. Thus the water temperatures of streams, especially shallow ones similar to those at PMRW, are highly dependent on atmospheric conditions (Sinokrot and Stefan, 1992).

The water temperatures of inflows from groundwater can also leave their imprint on a stream reach (Sinokrot and Stefan, 1992). Temperature is a relatively conservative property of groundwater (Ward, 1989). Thus, temperature is used widely in hydrologic analysis of groundwater flow rates. It is an easily measured property and a natural tracer of groundwater flow. Groundwater at depths of 10 - 20 m normally exceeds mean annual air temperature by 1 - 2°C (Ward, 1989). Deeper groundwater temperatures (i.e. > 20 m) tend to be relatively constant on a seasonal basis (Sakura, 1993), whereas shallow groundwaters (i.e. < 5 m depth) tend to be colder than air temperature in the summer and warmer in the winter (Shanley and Peters, 1988). Temperature of groundwater also exhibits a thermal stratification with respect to depth, where, during the summer, the water nearer the surface is warmest (Arai, 1993). This phenomenon has allowed the calculation of vertical groundwater flow rates in some studies (Stallman, 1960; Bredehoeft and Popodopulus, 1965; Sorey, 1971). Thus, not only can temperature be used to assess the contribution of different source waters to storm runoff, but it can also provide some insight into groundwater flow mechanisms.

As with air temperature, rainfall is typically warmer than groundwaters in summer and cooler in the winter. Thus, differences in temperature between rainfall ('new' water) and groundwater ('old' water) make temperature a potential tracer of water movement during certain times of the year. The use of temperature for identifying short-term flow mechanisms during storms has not been reported in the literature to date. The following investigation attempts to use temperature as a tracer of fast-flow mechanisms in the saturated and unsaturated zones and also to identify source waters to storm runoff. The results of this chapter will be used to corroborate those of Chapters IV and V.

(V1.2) AIMS AND QUESTIONS

The following questions will be considered:

(A) Can temperature be used to distinguish between 'old' and 'new' waters?

(B) Can 'old' and 'new' water contributions be assessed throughout storm durations within specific flowpaths using temperature as a tracer?

(C) Does the temperature tracer analysis corroborate the hydrometric analysis?

(V1.2A) Can temperature be used to distinguish between 'old' and 'new' waters?

The use of temperature as a conservative tracer depends on there being a significantly different thermal signature for 'old' water and 'new' water. The previous section discussed how 'old' waters (i.e. groundwaters) were typically cooler than 'new' waters (i.e. rainfall and throughfall) during the summer (or growing season). The converse is true during the winter (or dormant season) (Shanley and Peters, 1988). Both water types may show a seasonal cycle and a diurnal pattern (Sakura, 1993; Sinokrot and Stefan, 1992). The first approach is thus to compare average monthly and daily temperatures collected at each node in order to find whether the temperatures of the water types are significantly different and to assess what the degree of seasonality is in the patterns. Temperature variations at each node during storms will then be investigated. Short-term temperature variations may allude to specific hydrological mechanisms.

(V1.2B) Distinguishing 'old' from 'new' waters within specific flowpaths

Temperature data is available for air, throughfall, soil, groundwaters and streamwaters. The following flowpaths are assessed in terms of their thermal signatures to corroborate the results of the hydrometric and chloride analyses:

(a) Direct channel rainfall

(b) Matrix soil water flow

(c) Macropore flow

(d) Groundwater ridging/displacement

Temperature variations between base flow conditions and storm conditions are identified at each node. In this way, variations which are neither seasonal nor diurnal can be observed, which can be related to the occurrence of rainfall. If specific variations in temperature are noted at individual nodes for a large number of storms, then this might be related to a hydrological mechanism identified in the hydrometric analysis. Short-term increases in temperature in streamwater during the growing season would suggest the occurrence of either direct channel rainfall, or the addition of warm, 'new' water to the channel via overland flow or macropore flow. Short-term increases in temperature in the unsaturated or saturated zone during the growing season might suggest macropore flow. The opposite temperature trends during the dormant season would allude to the same processes. Temperature variations in the saturated zone may also occur due to groundwater movement, either by ridging or displacement.

In this section, temperature variations specific to individual flowpaths during storms are identified, and the controlling hydrological mechanisms are hypothesised.

(V1.2C) Combining temperature data with hydrometric data

Temperature has an advantage over Cl^- as a tracer of water movement in the current study because the temporal resolution of sampling is much more intense. In fact, the temporal resolution of temperature data is similar to that for hydrometric data (i.e. 5 min intervals). This makes the comparison of the timing of temperature and hydrological responses possible. Hence, the timing of the temperature variations during storms can be compared with the timing of responses of flowpaths outlined in Chapter IV. This allows the corroboration or rejection of the predicted hydrological mechanisms responsible for the short-term temperature variations. For example, if the timing of a rapid increase in temperature in the saturated zone is concurrent with the timing of rapid flow through lysimeter VI-50, prior to the passage of the wetting front through that depth, then this suggests the operation of macropore flow. The rapid increase in temperature indicates the passage of 'new', warm water through the unsaturated zone to the groundwater table.

(VI.3) DATA AND EQUIPMENT

Temperature was measured for air (AT), throughfall (TFT), soil at 15, 40 and 70 cm depths (VT_{15}, VT_{40}, VT_{70}, respectively), groundwater from depths of 2.2 to 4.7 m below land surface (GT1 - GT8, respectively) and streamwaters at the lower and upper gages (STlg and STug, respectively) for 35 storms between 4 July 1994 and 1 May 1995 (see Chapter 3 for full equipment descriptions). Data was output at 5 min intervals.

Throughfall was measured by installing a thermistor in a bottle, which was fed by a funnel. The temperature of throughfall was determined from the variation in the temperature of water in the bottle during storms. However, this thermistor also recorded temperatures during non-rainfall periods, when the temperature measured was that of air or any remaining water within the bottle. The 'throughfall temperatures' recorded during dry periods were removed from this analysis.

The stream monitored at the upper gage was ephemeral (see Chapter II), and for some periods of the year, the thermistor was above the water level. Hence, air temperature was recorded. Again, temperature data was removed from the analysis for these time periods.

(V1.4) RESULTS AND DISCUSSION

(V1.4A) Can temperature be used to distinguish between 'old' and 'new' waters?

In the following section, temperature variations at each node (air, throughfall, soil and groundwater) will be explored on a seasonal and storm-by-storm basis in order to assess whether the thermal signature of 'new' (i.e. AT and TFT) water is significantly different from that of 'old' (i.e. GT) water. Average monthly temperatures were used to calculate the average growing and dormant season temperatures at each node (where adequate data was available), which are presented in Table 6.1. The results of the table will be discussed in detail in the following sections.

Node	Growing Season Average Temperature (°C)	Dormant Season Average Temperature (°C)
AT	21.7	9.4
TFT	21.4	12.7
VT_{15}	23.6	11.9
VT_{40}	21.4	12.2
GT2	17.8	14.1
GT3	16.6	14.9
GT4	17.0	15.0
GT5	16.6	15.1
GT6	16.1	14.7
GT7	15.0	15.3
GT8	15.6	15.3
STlg	19.1	19.9
STug	12.5	11.4

Table 6.1: Average monthly temperatures during the growing and dormant seasons for air (AT), throughfall (TFT), soil at 15 and 40 cm depths (VT_{15} and VT_{40}), groundwaters at depths of 2.4 to 4.7 m below land surface (GT2 to GT8) and streamwaters at the lower and upper gage (STlg, STug).

(A) Seasonal Analysis

(i) Air (AT) and throughfall (TFT) temperatures

AT and TFT are higher in the growing season, 21.7 and 21.4°C, respectively, than during the dormant season, 9.4 and 12.7°C respectively. Figure 6.1a shows average daily temperatures of AT and TFT. A seasonal pattern is evident in the data. Table 6.1 displays average temperatures during the growing season and dormant season. The temperature signature of throughfall is similar to that of air temperature. Hence, during the growing season, the temperature of 'new' water is warm, and is substantially cooler during the dormant season. During the growing season, AT and TFT tend to remain above 15°C; in the dormant season, temperatures are lower, reaching a minimum in February. The range in temperature is from 0°C in February to over 20°C in July, hence > 20°C.

(ii) Soil Temperatures (VT15, VT40 and VT70)

Figure 6.1b displays average daily temperatures of soil at depths of 15, 40 and 70 cm (VT_{15}, VT_{40} and VT_{70}, respectively). A limited dataset is available for VT_{70}. A similar seasonal temperature pattern to that observed for air and throughfall is shown in the soil. Average temperatures during the growing season are highest at the surface and decrease with depth (23.6 and 21.4°C for VT_{15} and VT_{40} respectively). During the dormant season, temperatures at both depths are lower, and an apparent increase in temperature with respect to depth is noted (11.9 and 12.2°C for VT_{15} and VT_{40}, respectively). The range in temperatures is from approx. 5°C in February to over 20°C in July.

(iii) Groundwater Temperatures

Figure 6.2 displays average groundwater temperatures at the eight depths below the land surface (i.e. 2.12 (GT1) to 4.7 (GT8) m below land surface). A seasonal pattern to groundwater temperatures is

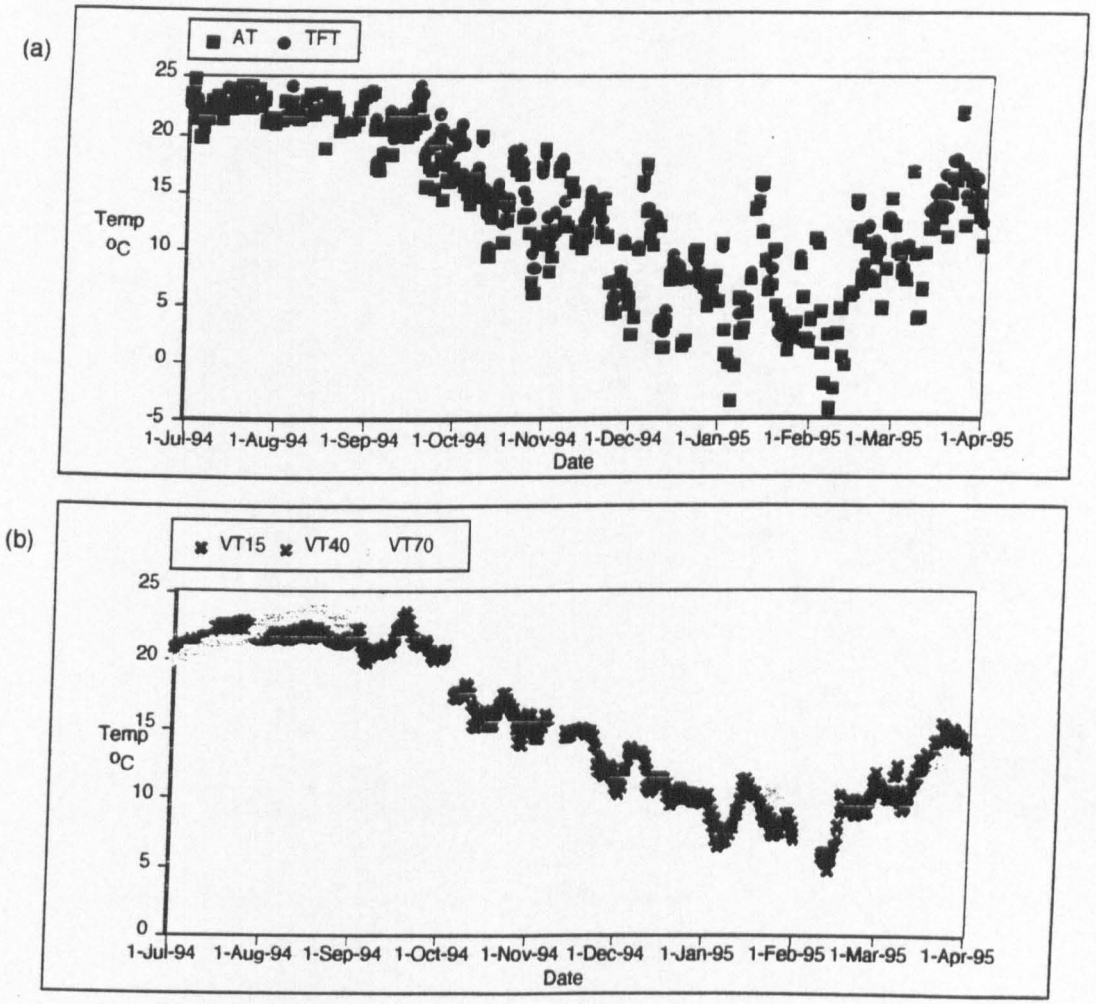

Figure 6.1 *Daily average temperatures throughout study period (July 1994 - May 1995) for (a) Air (AT), throughfall (TF); (b) 15 cm depth soil (VT15), 40 cm depth soil (VT40), 70 cm depth soil (VT70);*

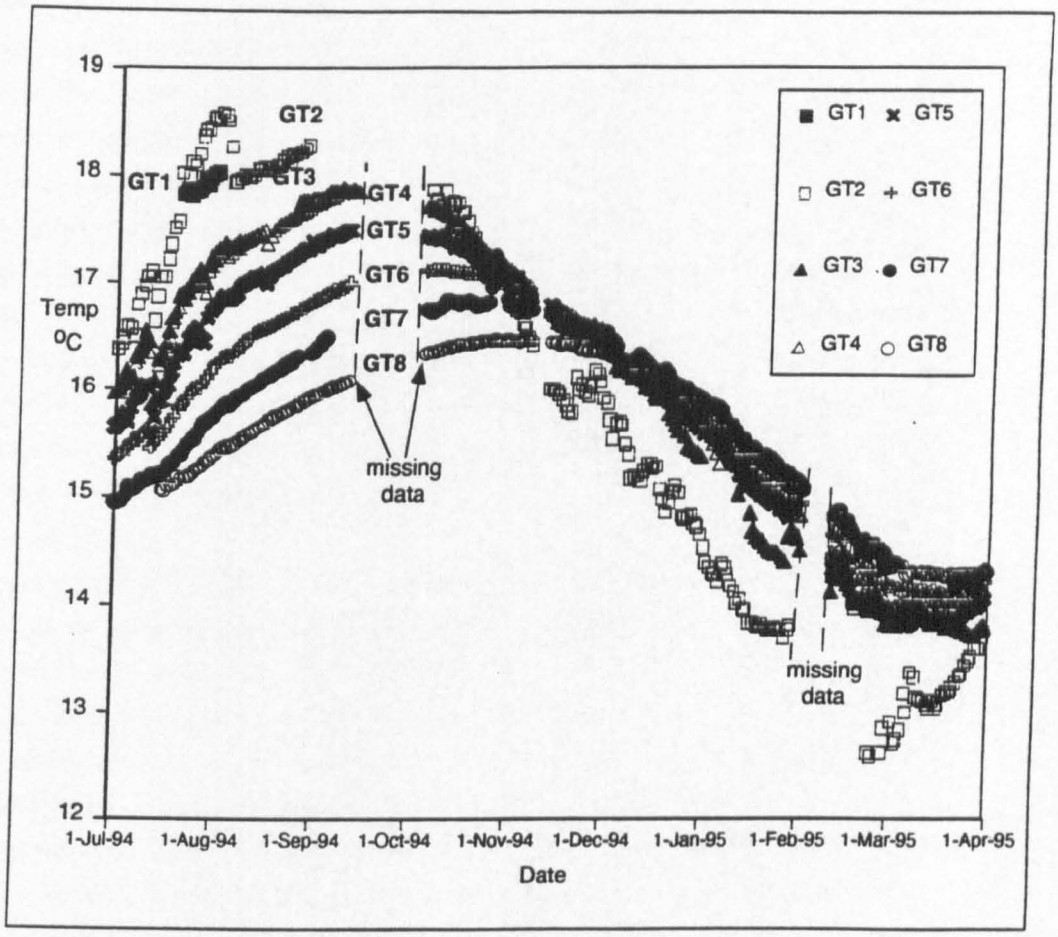

***Figure 6.2**: Daily average temperatures for groundwaters at depths of 2.13 m (GT1), 2.29 m (GT2), 2.44 m (GT3), 2.59 m (GT4), 2.74 m (GT5), 3.35 m (GT6), 3.96 m (GT7) and 4.57 m (GT8) throughout study period (July 1994 - April 1995)*

displayed, supporting the results of other investigations (Stallman, 1960; Sorey, 1971; Arai, 1993; Sinokrot and Stefan, 1992). Again, temperatures are generally higher in the growing season (e.g. 17.8°C at GT2) than during the dormant season (e.g. 14.1°C at GT2). However, the overall variation in temperature at each depth is no greater than 7°C, a lower range in temperature than for air, throughfall or soil.

A thermal stratification is apparent in the saturated zone for each season, which supports the findings of Arai (1993). In the growing season, temperature decreases with respect to depth, i.e. the temperature of the shallowest groundwater, GT2 was warmest (17.8°C) and the temperature of the deepest groundwater was coolest (15.6°C) (Table 6.1). The greatest difference in temperatures between depths occurred during August through September (Figure 6.2). During October, the difference in temperatures between depths diminished and by November, all depths displayed similar temperatures. After November, and during the dormant season, the thermal stratification reversed, whereby the shallowest groundwater (GT2) is coolest (14.1°C) and the deepest groundwater (GT8) is the warmest (15.3°C) (Table 6.1). The greatest difference between temperatures in the 'reverse' thermal stratification occurs during February. In April, the stratification begins to reverse again and returns to that of the growing season (Figure 6.2).

(iv) Summary

The analysis of average daily and monthly temperatures over the study period shows a strong seasonal influence. At all nodes, temperatures are highest during the growing season. The seasonal range of temperature decreases in the order AT>TFT>VT>GT.

During the growing season, the average temperature of 'new' water (i.e. throughfall) is 21.4°C and the average temperature of 'old' water (i.e. average of all GTs) is 16.5°C. During the dormant season, the average temperature of 'new' water is 12.7°C and that of 'old' water is 14.9°C. Thus, the difference in the average temperatures of 'old' and 'new' water during the growing season is 4.9°C and during the dormant season is 2.2°C. Thus, from the seasonal temperature analysis, the temperature of 'old' vs. 'new' water are different. However, these are only average values and a more comprehensive analysis of whether the thermal regimes of the water types are statistically different can be obtained from an analysis of temperature variations at nodes on a storm-by-storm basis

(b) Storm-by-storm Analysis

The temperature at each node at the time of the onset of rainfall is calculated for all storms (35 storms in total) (Appendix 6.1). To explore the hypothesis that 'old' and 'new' waters display distinctly different temperature profiles, the temperatures of air at the onset of rainfall are compared with the temperatures of the most shallow groundwater (i.e. the water that would be hydrologically active during the storm) at the time of onset of the storm (i.e. (AT - GT2). The temperature variations between the most shallow groundwater (GT2) and deepest groundwater (GT8) are also compared (i.e. GT2 - GT8) in order to investigate the thermal stratification phenomena further. The results are presented in Table 6.2.

Storm Date	AT - GT2 (°C)	GT2 - GT8 (°C)
4 July 1994	3.5	na
10 July 1994	10.2	na
11 July 1994	10.1	na
12 July 1994	10.8	na
14 July 1994	10.3	2.0
22 July 1994	11.4	2.9
27 July 1994	4.5	3.2
16 August 1994	2.8	2.4
21 August 1994	8.1	2.4
11 October 1994	- 7.8	1.3
13 October 1994	- 3.0	1.3
21 October 1994	- 0.6	0.6
26 November 1994	- 8.7	- 0.5
4 December 1994	- 2.8	- 0.7
6 January 1995	- 10.5	- 1.4
14 January 1995	3.7	- 1.5
19 January 1995	- 3.0	- 1.8
27 January 1995	- 4.4	- 1.4
16 February 1995	- 8.2	- 1.7
27 February 1995	- 6.0	- 1.9
8 March 1995	4.7	- 1.4
11 April 1995	9.0	- 0.2

***Table 6.2**: Differences between air temperature (AT) and shallow groundwater temperatures (GT2 at 2.4 m depth), and difference between shallow groundwater (GT2) and deep groundwater (GT8, at a depth of 4.7 m below land surface) for all storms where data is available. 'na' refers to 'no available data'.*

The thermal stratification observed in Figure 6.2 can also be noted from the results of Table 6.2. During the growing season, all storms display positive values for (GT2-GT8) (i.e. the shallow groundwater is warmer than the deeper groundwater). During the dormant season, the majority of storms display negative values (i.e. the deeper groundwater is warmer than the shallow groundwater). On average, the values of (GT2 - GT8) for growing season storms are 2.6°C and for the dormant season storms (excluding October, when the stratification is similar to that for growing season storms) are 3.3°C.

The differences between air temperature (i.e. 'new' water) and shallow groundwater (i.e. 'old' water) at the onset of rainfall are typically greater than the values calculated in the seasonal analysis. On average, during the growing season, the difference is 8°C (with many storms showing a temperature difference of > 10°C). During the dormant season, the average temperature difference is 5°C (with some storms showing a temperature difference of > 8°C). Hence, the temperature differences between 'old' and 'new' waters are substantial and are much greater than the average differences in temperature with respect to depth. Hence, it is postulated that temperature can be used as an effective tracer of 'old' and 'new' water for individual storms. Also, the thermal stratification that occurs in groundwater may be useful in providing some insight into groundwater flow phenomena, especially with reference

to groundwater displacement. In the following section, temperature will be used as a tracer in order to assess the contribution of 'old' and 'new' waters to specific flowpaths.

(VI.4B) Temperature variations within specific flowpaths during storms: an assessment of mechanisms in operation and the relative proportions of 'new' and 'old' water contributions

Short-term variations in temperature were assessed at specific nodes in order to assess the following flow mechanisms:

(a) Direct channel rainfall

(b) Matrix soil water flow

(c) Macropore flow

(d) Groundwater displacement/ridging

(a) Direct channel rainfall

During the growing season, air temperature is high and hence rainfall is warmed as it passes through the lower atmosphere. Thus, water falling directly on the stream channel is warm. Rises in streamwater temperature at the onset of storms is indicative of direct channel rainfall. This procedure has previously been adopted at PMRW to identify the source waters to storm runoff (Shanley and Peters, 1988). Temperature trends for several rainstorms in 1986 - 1987 were analysed. For a summer rainstorm (May 1986), streamwater temperature decreased and then increased. This temperature pattern was explained by the addition of cooler groundwater to the stream, followed by warmer rainfall (i.e. direct channel rainfall). In Chapter IV, detection of DCR was made difficult due to the confusion of the DCR hydrometric signal with that from other nodes. The same is true for the temperature data. Observation of streamwater temperature variations at the upper and lower gages during the growing season show rapid increases in streamwater temperature at storm onsets and the reverse temperature pattern is true during the dormant season. Since the rapid temperature response occurs shortly after the onset of rainfall, this temperature variation is attributed to DCR.

(b) Soil water flow

Temperature variations at 15, 40 and 70 cm depths in the soil were analysed during 35 storms. The temperature variations that were noted were not rapid and not great. In fact, in only two storms were temperature variations noted at all. Thus, the thermal signature of macropore flow was not monitored successfully from soil thermistors. This is not suprising since the interception of a macropore by the small surface area thermistor is unlikely. In some storms, slower variations in temperature could be explained by matrix water flow. However, the low temperature range encountered and very few storms that exhibited any variation at all suggest that in this study, temperature was unsuccessful as a tracer of macropore flow or matrix flow within the unsaturated zone.

(c) Macropore flow and groundwater flow

Distinct short-term variations in temperature in the saturated zone were observed. The variations differed on a seasonal basis, and the patterns discovered allude to macropore flow and groundwater displacement. The patterns will be discussed on a seasonal basis:

(i) Growing season thermal variations

During the growing season, rapid increases in temperature were observed in the most shallow groundwater (i.e. GT1 - GT3). These occurred shortly after the onset of rainfall and were followed by equally rapid decreases in temperature. There was then a slow increase in temperature, back to similar temperatures shown during base flow conditions. Figure 6.3 displays case study storms on 16 August 1994 and 12 July 1994 which show these patterns.

Case study storms

16 August 1994

Groundwaters are thermally stratified (Figure 6.3a). Groundwater 2.4 m below the land surface averages 18.2°C, whereas the deepest groundwater measured (GT8), remains constant at 15.7°C. Temperatures increase at the onset of the rainstorm at GT3 (2.4 m) from 18.1 to 18.4°C, followed by a marked decrease in temperature of 0.7°C. Thereafter, the temperature slowly rises to a level similar to that measured before the onset of the rainstorm. Temperature decreases markedly from 17.5 to 17.1°C at 2.6 m depth (GT4) and from 17.1 to 16.8°C at 2.7 m depth (GT5). Temperatures remain relatively constant at depths below 3.5 m (GT6 - GT8). Macropore flow was identified during this storm, according to hydrometric data (Chapter 4). Hence, the initial rise in temperature might be attributed to the introduction of 'new', warmer water to the upper saturated zone by macropore flow, which may then promote groundwater displacement, causing the groundwater level to rise and hence the rapid decrease in temperature that is observed. The combination of temperature data with hydrometric data will be made in Section VI.4.

12 July 1994

In Figure 6.3b, groundwater temperature data is presented for a storm occurring on 12 July 1994. During this storm, a similar trend in groundwater is observed. A thermal stratification is evident. Groundwaters 2.3 m below the land surface average 16.7°C, whereas the deepest groundwaters measured GT7 (4.0 m) remain relatively constant at 15.2°C. Rainfall begins at 11:45 on 12 July. Temperature increases are observed at GT2 (2.3 m), GT3 (2.4 m), GT4 (2.6 m) and GT5 (3.4 m) prior to the onset of rainfall, but continue to increase until approximately 4 hr after the onset of rainfall. After this, rapid decreases in temperature were observed; temperature decreases are 0.2, 0.3, 0.3 and 0.2°C for GT2, GT3, GT4 and GT5 respectively. Temperatures then begin to increase again to levels higher than pre-storm temperatures at 23:00 on 13 July. Following this (not shown on graph), the temperatures decline to levels similar to those prior to the rainstorm.

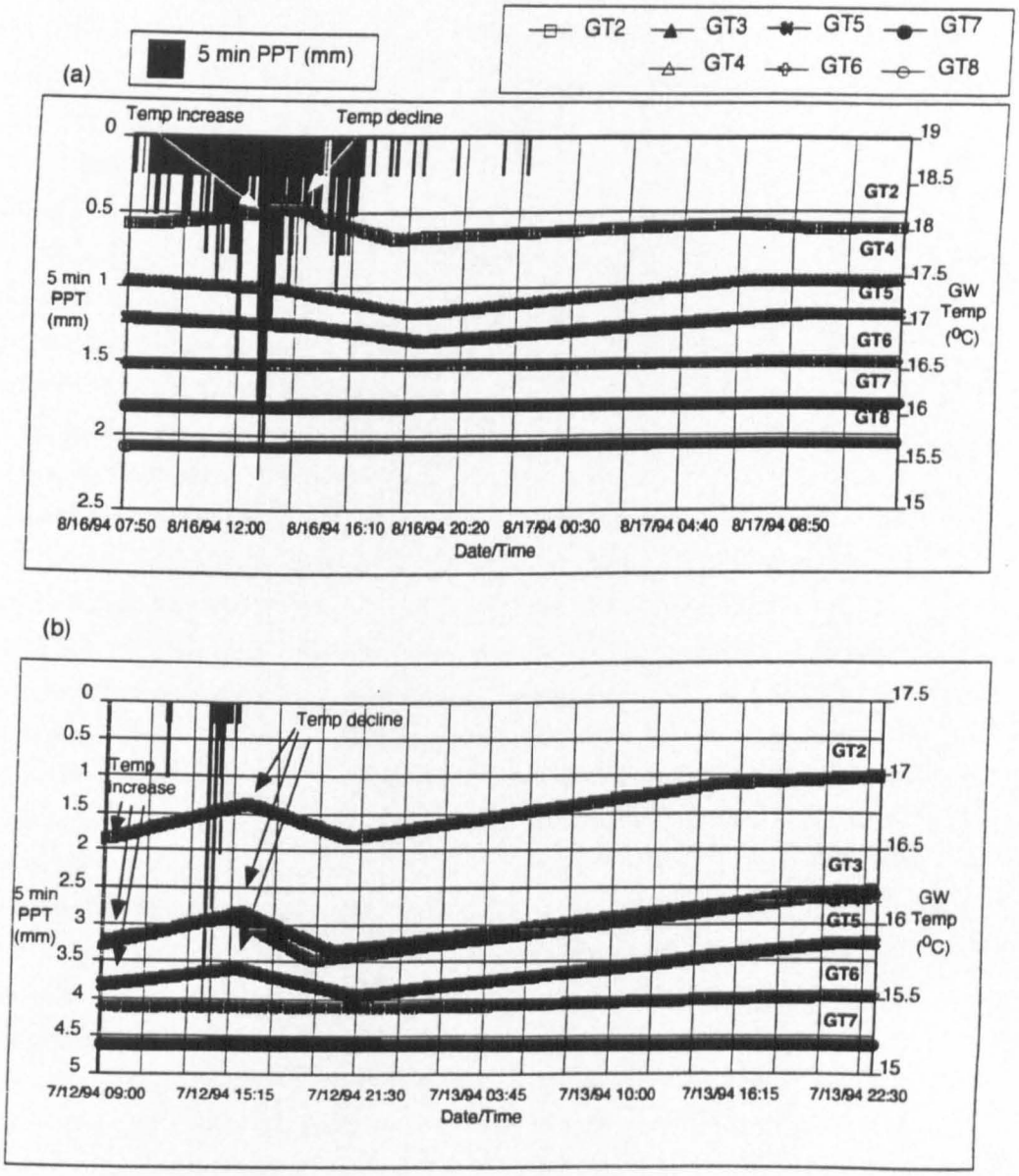

Figure 6.3: *5 min precipitation (PPT) and groundwater temperature responses at depths of 2.13 m (GT1), 2.29 m (GT2), 2.44 m (GT3), 2.59 m (GT4), 2.74 m (GT5), 3.35 m (GT6), 3.96 m (GT7) and 4.57 m (GT8) below land surface for storms during the growing season, occurring on (a) 16 August 1994; (b) 12 July 1994*

(ii) Dormant season thermal variations

During the dormant season, the reverse temperature trends are observed. Shortly after the onset of rainfall, a rapid decrease in temperature is observed, followed by an equally rapid increase in temperature. After a peak in temperature is attained, there is a gradual decline back to temperatures similar to those observed during baseflow conditions. Figure 6.4 displays two case study storms showing these patterns on 6 January and 10 February 1995.

Case study storms

6 January 1995

Figure 6.4a shows data for a storm on 6 January 1995. At the onset of rainfall, rainfall is cooler than groundwater (Appendix 6.1), air temperature is 3.8°C and GT2 (2.3 m) is 14.3°C. Groundwater exhibits a typical dormant season thermal stratification, whereby the shallowest groundwater, GT2, averages 14.3°C and the deepest groundwater, GT8 (4.6 m), remains relatively constant at 15.7°C. Prior to the onset of rainfall, water level at GWA was 2.3 m below the land surface and GWC was 3.2 m below the land surface. The reason that GT2 displays much cooler temperatures than the deeper groundwater is because it is probably above the level of the water table. This theory is supported by the temperature trend of GT2, which mimics that of AT. Rainfall begins at 13:20 on 6 January, and becomes intense after 17:50. Possible mesopore flow was identified at 18:20 on 6 January (see Chapter IV). GT5 displays a decrease in temperature at 18:15 on 6 January, concurrent with the occurrence of mesopore flow, where temperature decrease was 0.1°C. GT7 also displays a decrease in temperature at 17:50 on 6 January, which is consistent with the onset of intense rainfall. Both GT5 and GT7 exhibit a rise in temperature thereafter. However, not all GTs display this trend, as GT4 and GT6 exhibit a rise in temperature followed by a decline. GT4 exhibits a rise in temperature at 19:20 on 6 January, which is the same time at which GWA begins to rise. GWA rises by 32 cm and during this time scale, GT4 exhibited a temperature rise of 0.2°C. Thus, GT4 exhibits the largest temperature increase, which appears to be connected to groundwater response. This shall be considered in more detail in the following section.

10 February 1995

Figure 6.4b displays groundwater temperature data for a storm on 10 February 1995. Due to an electrical fault, more noise has been introduced into the data. However, the basic patterns in groundwater temperature variations can still be identified. Rainfall is cooler than groundwater (Appendix 6.1) and the dormant season thermal stratification is apparent. Groundwater temperatures at 4.6 m (GT8) remain relatively constant at 14.9°C and at 2.4 m (GT3) vary around 14.3°C. At the onset of rainfall, groundwater temperatures at GT3 decrease rapidly from 14.5 to 14.0°C and then rise gradually to 14.3°C and remain near this value. A similar pattern occurs for temperatures at 2.5 and 2.7 m (GT4 and GT5, respectively). Temperatures remain relatively constant in the deepest groundwaters.

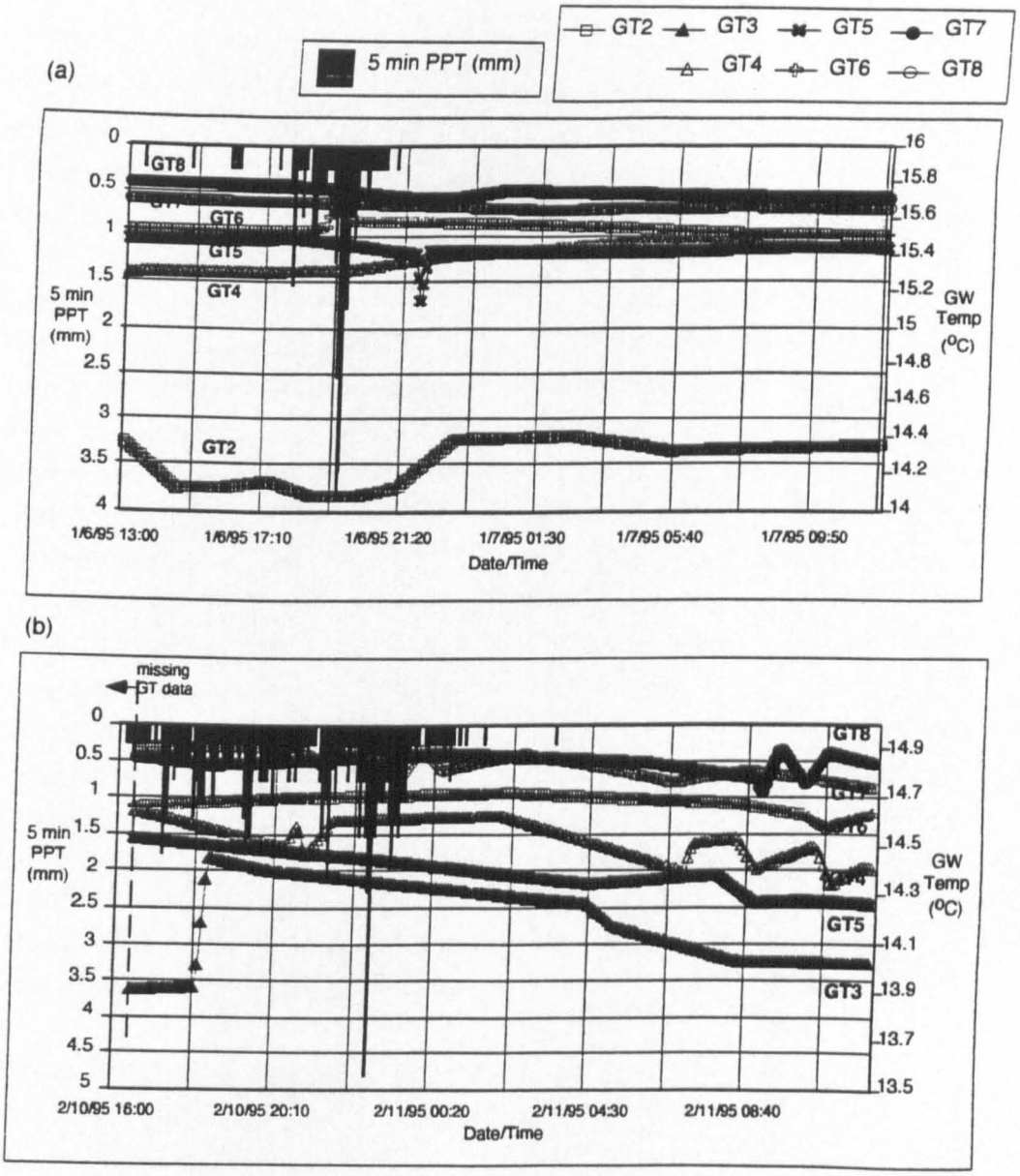

***Figure 6.4**: 5 min precipitation (PPT) and groundwater temperature variations at depths of 2.13 m (GT1), 2.29 m (GT2), 2.44 m (GT3), 2.59 m (GT4), 2.74 m (GT5), 3.35 m (GT6), 3.96 m (GT7) and 4.57 m (GT8) below land surface for storms during dormant season occurring on (a) 6 January 1995; (b) 10 February 1995*

Groundwater temperature variations were analysed in 35 storms (19 of which occurred during the growing season and 16 occurred during the dormant season) (Appendix 6.2). The patterns displayed in Figure 6.3a and b were found to occur in 14 of the growing season storms. Storms during which the patterns were not observed occurred in April and May 1995, when the thermal stratification was reversing. Hence, the variation between groundwater temperatures at different depths was minimal. The patterns displayed in Figure 6.4a and b were found in half the dormant season storms. During October, the thermal stratification was starting to reverse, but the final reversal did not complete until November (Figure 6.2). Hence, the storms in October displayed temperature variations similar to those observed for growing seasons storms.. *Temperature differences between air and shallow groundwater* were lower during the dormant season than during the growing season, which may explain why temporal variations in temperature were not as pronounced as for growing season storms

Table 6.3 presents the results of temperature variations in a sub-set of storms that exhibited the greatest temperature variations at depth. Six growing season storms and five dormant season storms are shown in the table. Temperature data is provided for the most shallow groundwaters that exhibited the temperature variations discussed above. Pre-storm temperatures are shown, the maximum temperature and minimum temperatures are presented, and the variations in temperature are calculated. The average temperature increase shortly after the onset of rainfall during growing seasons storms is 0.5°C for the most shallow groundwater that exhibit a temperature variation, whereas, the average initial temperature decrease for dormant season storms is 0.4°C. This temperature variation may seem very small, but since baseflow temperatures are stable, the variation is easily detected and must be due to addition of 'new' water to the saturated zone. The average decline in temperature (i.e. the second inc/dec in temperature) that is observed in the growing season is 0.6°C and the average increase in temperature that is observed in the dormant season is 0.5°C. The degree of variation depends on individual storm conditions. Temperature variations are as great as 2°C during some storms (e.g. GT2 on 11 July).

The patterns discussed above were observed in 3/4 of all storms and the following conceptual model was developed to explain the temperature responses:

(d) Macropore flow and groundwater displacement: A conceptual model

The temperature of 'old' and 'new' waters are significantly different and hence the two water types can be distinguished from one another. In the summer, if macropore flow occurs, the temperature response in the most shallow groundwaters should be a rapid increase if macropore flow transports 'new', warm water to the saturated zone. The expected temperature responses in a hypothetical summer storm are presented in Figure 6.5. Pre-storm temperature conditions and groundwater response at 2.3 m below are shown in Figure 6.5a.

Figure 6.5b displays the field situation at the onset of rainfall. The storm occurs during the summer and hence, rainfall is warmed as it passes through the lower atmosphere (Shanley and Peters, 1988; Arai, 1993). Hence, rainfall is warmer (>16.4°C) than groundwater. Rainfall begins at time (t1) and

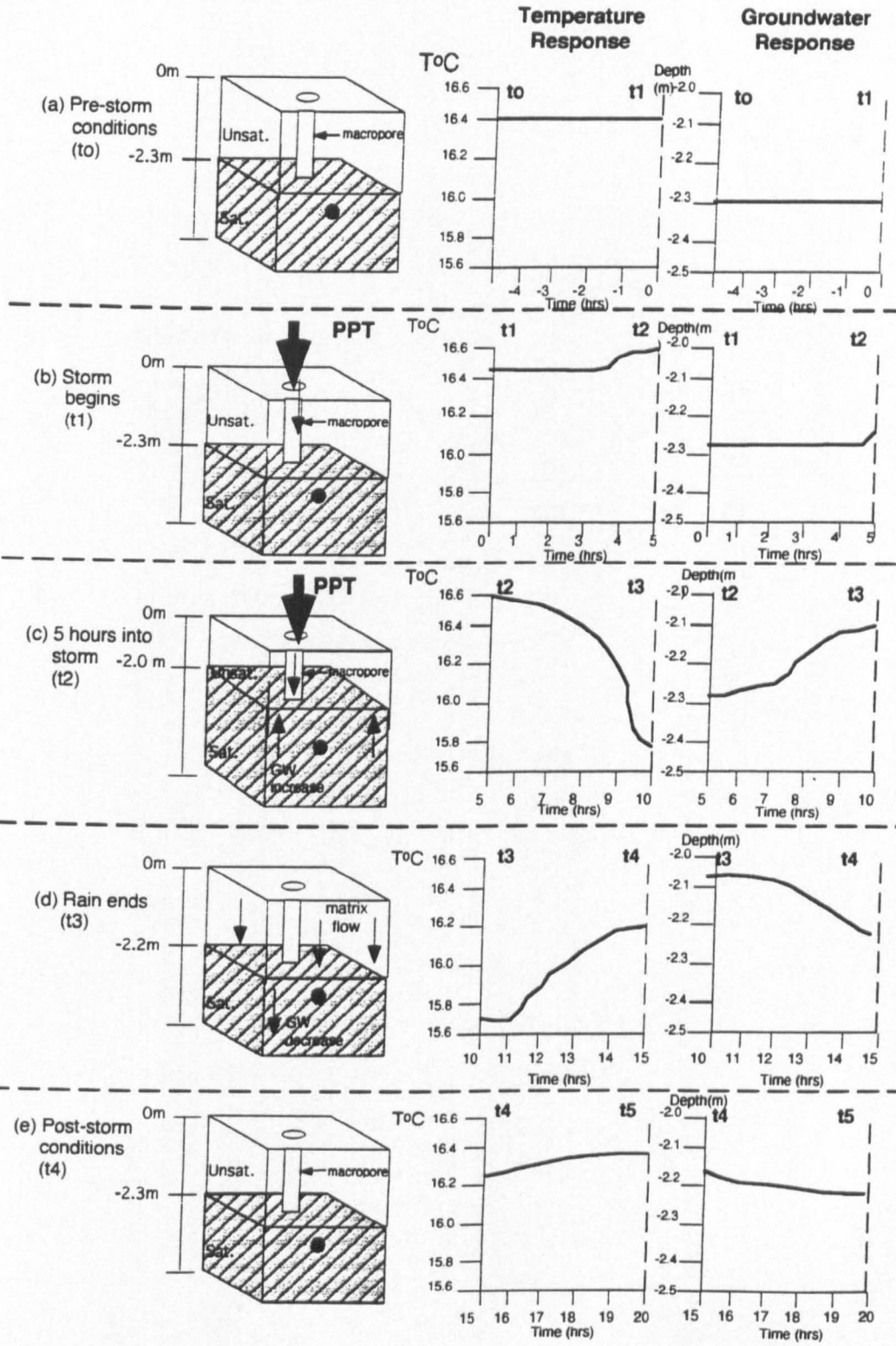

Figure 6.5: Temperaure and groundwater responses during a hypothetical summer rainstorm for (a) pre-storm conditions; (b) onset of precipitation; (c) 5 hr into rainstorm; (d) end of rainfall; (e) post-storm conditions

Storm/ Thermistor	Pre storm av temp	Date/Time	Increase or Decrease?	Maximum Temp	Maximum Date/Time	(Maximum) - Prestorm Temp	2nd Inc. or Dec	Maximum Temp.	Maximum Date/Time	(Maximum) - (Maximum 2)
Storm 3										
GT2	16.09	12:25 27 Ju	inc	16.29	10:20 27 Ju	0.20	dec	16.24	7:50 28 Ju	0.05
GT3	15.74	14:54 27 Ju	inc	16.02	10:24 27 Ju	0.28	dec	15.81	11:39 27 Ju	0.21
GT4	15.71	15:71 27 Ju	inc	16.06	10:24 27 Ju	0.35	dec	15.81	11:10 27 Ju	0.25
Storm 4										
GT2	16.39	15:35 1 Jl	inc	16.88	11:40 5 Jl	0.39	dec	16.28	14:45 5 Jl	0.59
GT3	15.96	11:50 1 Jl	inc	16.32	4:56 5 Jl	0.37	dec	15.88	21:55 5 Jl	0.43
GT4	15.96	11:10 1 Jl	inc	16.54	3:55 5 Jl	0.58	dec	15.84	11:34 5 Jl	0.70
Storm 5										
GT2	16.80	8:20 11 Jl	inc	18.31	19:24 11 Jl	1.51	dec	16.31	22:09 11 Jl	2.00
GT3	16.50	3:09 11 Jl	inc	16.69	19:24 11 Jl	0.19	dec	15.53	22:39 11 Jl	1.16
GT4	16.40	3:05 11 Jl	inc	16.50	19:09 11 Jl	0.10	dec	15.58	21:55 11 Jl	0.91
GT5	16.06	4:04 11 Jl	inc	16.09	19:09 11 Jl	0.03	dec	15.51	22:09 11 Jl	0.58
Storm 9										
GT2	18.08	2:10 18 Au	inc	18.34	13:35 18 Au	0.18	dec	17.94	17:40 18 Au	0.40
GT4			inc	17.51	17:51 18 Au		dec	17.37	13:50 18 Au	0.48
GT5			inc	17.68	17:68 18 Au		dec	16.81	16:55 18 Au	0.87
Storm 10										
GT4	15.29	00:05 12 Ja	dec	15.24	14:05 14 Ja	0.05	inc	15.29	2:10 15 Ja	0.05
Storm 11										
GT5	15.10	5:10 18 Ja	dec	14.94	17:35 19 Ja	0.16	inc	15.06	21:20 19 Ja	0.12
GT6	15.28	5:10 18 Ja	dec	15.12	19:05 19 Ja	0.16	inc	15.23	7:20 20 Ja	0.11
Storm 12										
GT2	13.73	12:20 27 Ja	dec	12.76	23:50 27 Ja	0.97	inc	13.95	11:30 28 Ja	1.19
GT3	14.40	10:05 27 Ja	dec	14.36	4:25 28 Ja	0.04	inc	14.76	6:55 28 Ja	0.40
Storm 13										
GT5	14.53	18:25 10 Fe	dec	14.22	10:10 11 Fe	0.31	inc	14.49	7:55 12 Fe	0.27
GT6	14.72	2:25 11 Fe	dec	14.57	10:45 11 Fe	0.25	inc	14.64	13:15 11 Fe	0.07
Storm 14										
GT4	14.10	00:25 27 Fe	dec	13.96	16:30 1 Ma	0.14	gen. inc			
GT5	13.94	00:45 27 Fe	dec	13.76	17:15 1 Ma	0.18	gen. inc			
Storm 15										
GT3	14.01	5:15 11 Ap	dec	14.00	13:55 11 Ap	0.01	inc	14.03	20:45 11 Ap	0.03
GT5	14.24	5:15 11 Ap	dec	14.21	13:55 11 Ap	0.03	inc	14.41	1:45 12 Ap	0.88
Storm 16										
GT3	14.38	3:00 18 Ap	dec	14.14	15:55 19 Ap	0.24	inc	14.32	00:30 20 Ap	0.18

Key; Ju = June 1994, Jl = July 1994, Au = August 1994, Ja = January 1995, Fe = February 1995, Ma = March 1995, Ap = April, 1995
GT2 (2.3 m), GT3 (2.4 m), GT4 (2.6 m), GT5 (2.7 m), GT6 (2.7 m) = thermistors (at x m below land surface)

***Figure 6.3**: Temperature variations for a sub-set of storm, from 27 June 1994 to 19 April 1995. Pre-storm temperature refers to average temperatures at specific depths prior to storm onset (i.e. baseflow conditions)). Timing of the initial increase (ic) or decrease (dec) in temperature is given and the max/min temperature is shown. The temperature difference of the min/max temperature from the baseflow temperature is provided. The timing of the secnd temperature increase or decrease is shown, with the mi/max temperature that is reached. The differences in temperature btween the initial min/max temperature and the second min/max temperature is provided. All temperatures are in oC.*

soon after this, macropore flow occurs. Macropore flow by-passes the saturated zone and introduces 'new', warm water to the shallow groundwater. This is reflected in the rise in temperature of groundwater surrounding the thermistor, which attains a peak temperature at time (t2). The introduction of 'new' water to the shallow groundwater zone then causes the displacement of groundwater.

Deeper, cooler groundwater from upslope moves down to the replace the water previously around the thermistor. Figure 6.5c illustrates the field situation 5 hr into the storm. At time (t2), the peak in groundwater temperature is attained and the decrease in temperature begins. The groundwater level continues to rise until time (t3), to a depth of 2.1 m below the land surface (Figure 6.5c) Thus, the decrease in temperature of groundwater at 2.4 m depth is due to the influx to that depth of deeper groundwater (since there is a thermal stratification to groundwater and the deeper groundwaters are coolest during the growing season).

Figure 6.5d illustrates the field situation when rainfall has ceased (at time t3). Since rainfall has stopped, no water is available to be transported via macropores and the movement of water in the unsaturated zone will be matrix flow only. After time (t3), the groundwater reaches its peak depth (Figure 6.5d) and hence, the thermistor may become surrounded by warmer, shallower groundwater again. Alternatively, 'new' and 'old' water may mix, resulting in rises in overall temperatures (Figure 6.5d).

Finally, Figure 6.5e shows post-storm conditions. Flow in the unsaturated zone has ceased and groundwater level continues to return to baseflow conditions (i.e. 2.3 m below land surface). The temperature of the groundwater at a depth of 2.4 m below the land surface also returns to the temperature observed prior to the storm occurrence (16.8°C).

During the winter period, the same mechanisms are in operation, however, the reverse temperature trends are observed, due to the cooler, 'new' waters and warmer 'old' waters during this season.

(e) Summary

Distinct variations in temperature were observed in streamwater and in shallow groundwaters during storm events. These variations were attributed to direct channel rainfall, and to macropore flow and groundwater displacement mechanisms respectively. In both cases, temperature patterns vary seasonally, but the mechanisms that were hypothesised to be responsible for those variations are believed to be the same for both seasons. A more robust analysis of these mechanisms follows in the next section, where temperature data is coupled with hydrometric data.

(VI.4C) Combination and temperature and hydrometric data

In section VI.4B, analysis of temperature variations in the saturated zone suggested that macropore flow may lead to groundwater displacement. Temperature has the advantage over Cl^- as a tracer in this study because the temporal resolution of sampling is more intense. Hence, the timings of temperature responses can be compared with the timing of hydrometric responses. This allows temperature data to

corroborate or reject the conclusions of the hydrometric analysis and visa versa. In the next section, timing of flow through the lysimeter VI-50 (i.e. macropore flow) and groundwater responses will be compared with temperature responses in the saturated zone to assess the foundation of the conceptual model that macropore flow leads to a groundwater displacement.

(a) Macropore flow

Macropore flow was identified in Chapter IV, Section VI.F, using three criteria and was detected in seven storms, five of which occurred during the growing season. The hydrometric analysis also suggested that mesopore flow may occur in other storms, where flow through lysimeter VI-50 occurred prior to the passage of the wetting front through that depth. Hence, the timing of macropore and mesopore flow are available. The conceptual model attributes the initial rise in temperature during growing season storms (or decrease during dormant season storms) to macropore flow. Thus, the timing of the temperature responses should be coincident with the timings at which macropore or mesopore flow were observed. This was investigated on a subset of storms. These storms all had strong groundwater temperature stratifications. The results are presented in Table 6.3. The groundwater temperature increase or decrease is that of the most shallow groundwater thermistor that responded.

Storm Date	Time of Temperature Response (t1)	Time of Meso-/macropore Response (t2)	Time lag (t1-t2) (min)
27 July 94	6:55	6:00	55
16 Aug 94	8:50	8:55	- 5
21 Aug 94	12:20	12:15	5
6 Jan 95	18:10	18:20	- 10
14 Jan 95	5:20	4:55	25
19 Jan 95	9:10	8:35	45

***Table 6.4**: Timings of initial temperature response in saturated zone of most shallow groundwater and of onset of macropore or mesopore flow. Time lag between the two responses is given, for a sub-set of all 35 storms*

The storms during which macropore or mesopore flow could be detected all exhibited temperature responses within an hour of the onset of flow, and in most storms within 30 min. This synchronisation between the temperature and hydrometric responses suggests that temperature variation in the saturated zone can be used to detect macropore flow.

The use of temperature as a tracer of macropore flow has not been applied in any other investigation to date, and hence, this finding is of significant importance to future hillslope hydrological research. Not only does it provide a new method for the detection of macropore flow, but the temperature variation allows the detection of the type of water transported by the macropores, which in this case is 'new' water. This result corroborates the hydrometric analysis and also the chloride tracer analysis.

(b) Groundwater displacement

The second hypothesis provided in the conceptual model of mechanisms responsible for observed temperature variations in the saturated zone was that the second rapid temperature variation (i.e. decrease in temperature during the growing season and increase in temperature during the dormant season) was due to groundwater displacement, which had been initiated by macropore flow. A similar analysis can be performed between temperature data and hydrometric data, which in this case is groundwater stage response. The well (GT) in which the thermistors were housed was located between GWA and GWC (see Chapter III), and hence the timing of responses of wells GWA, GWB or GWC was compared with the temperature response of the most shallow groundwater that responded. The results of this analysis are presented in Table 6.5.

Storm Date	Timing of Temperature Response (t1)	Timing of groundwater well (x) Response (t2)	Time lag (t1-t2) (min)
10 July 94	18:55	18:40 (A)	15
11 July 94	19:25	19:20 (AC)	5
12 July 94	15:50	15:20 (C)	30
14 July 94	17:25	17:20 (C)	5
16 Aug 94	13:30	12:15 (B)	75
21 Aug 94	12:50	13:05 (BA)	- 15
6 Jan 95	21:50	19:30 (A)	140

Table 6.5: Timings of initial temperature response in saturated zone of most shallow groundwater and of groundwater responses of GWA, GWB or GWC Time lag between the two responses is given, for a sub-set of total 35 storms

The time lag of the temperature response after the onset of groundwater response was typically within 30 min for most storms. Storms in which the lag was greatest were small magnitude events, where the groundwater response was small. The synchronisation between the timing of temperature response and groundwater response in these storms suggests that groundwater displacement occurs, which is initiated by macropore flow. Again, the use of temperature for monitoring short-term groundwater responses is not found in any previous investigations. There is also very little literature that links macropore flow to groundwater displacement (McDonnell, 1990). Hence, the use of temperature in this manner is an important result of the current investigation.

A more detailed illustration of the similarities between temperature and hydrometric responses is provided in the two case study storms on 10 July 1994 and 6 January 1995, one storm representative of the growing season responses and the other of dormant season responses.

(c) Case study storms

10 July 1994

Figure 6.6 displays hydrometric and temperature data for a storm on 10 July 1994. Figure 6.6a displays 5 min rainfall (PPT) and Figure 6.6b displays the response in the unsaturated and saturated zone. Figure 6.6c shows the temperature variations in the saturated zone. Rainfall begins at 17:25 (Figure 6.6a) and becomes intense after 18:20. The initial response in the unsaturated zone is rapid flow at 15 cm depth (VI-15) at 18:20 and 15 min later at 50 cm depth (VI-50). The groundwater is

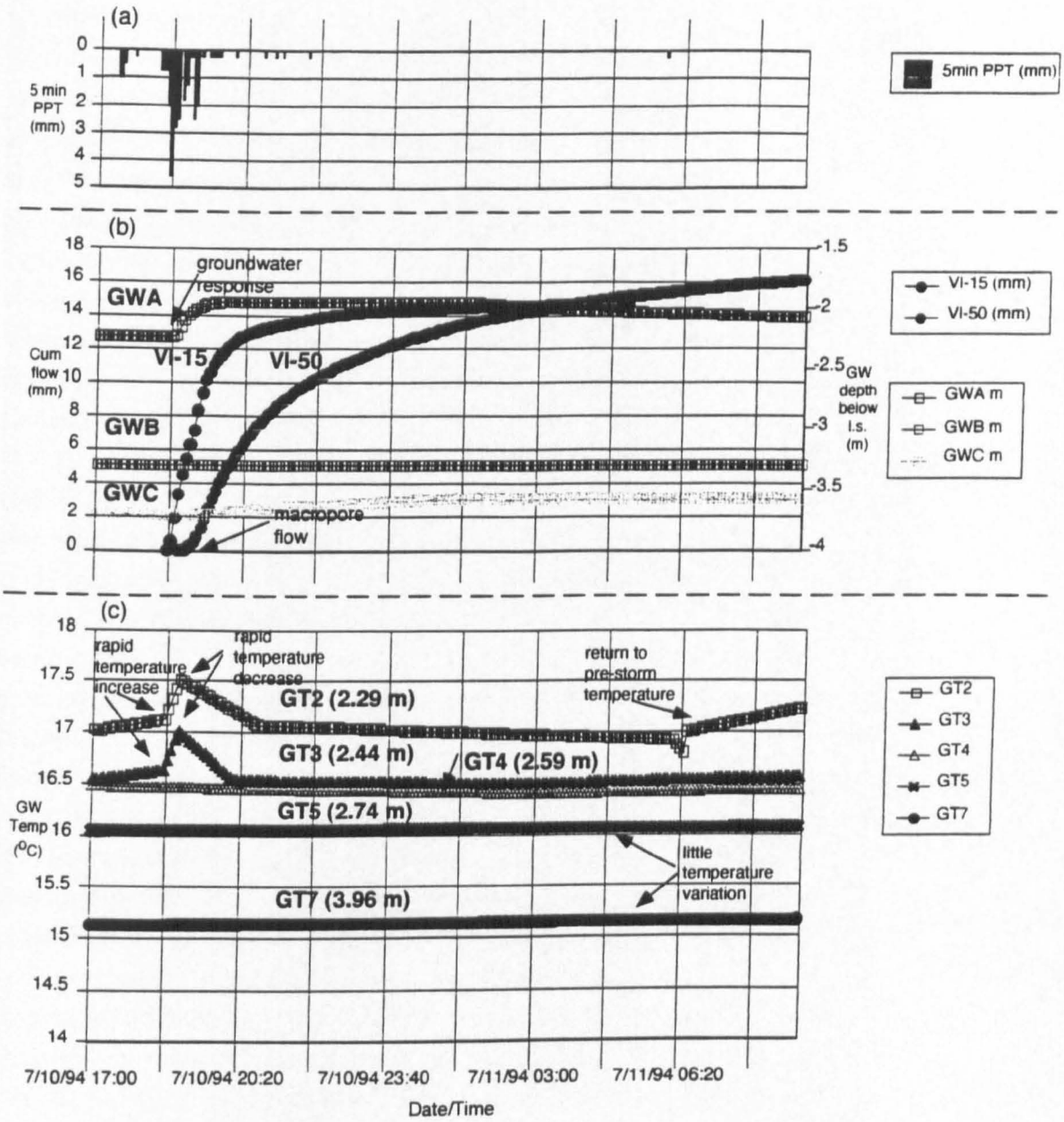

***Figure 6.6**: Hydrological and temperature responses for a storm occurring on 10 July 1994: (a) 5 min precipitation (PPT); (b) Soil water responses at 15 cm depth (VI-15) and 50 cm depth (VI-50), and groundwater responses from wells positioned in the riparian zone (GWA), 5 m upslope (GWB) and 10 m upslope (GWC); (c) Groundwater temperature responses from thermistors positioned in well GT at depths of 2.29 m (GT2), 2. 44 m (GT3), 2.59 m (GT4), 2.74 m (GT5) and 3.96 m (GT7) below land surface*

thermally stratified, with the shallowest groundwater, GT2 (2.29 m) averaging 17.0°C and the deepest groundwater measured, GT7 (3.69 m), remaining relatively constant at 15.1°C. Prior to the onset of the rainstorm, temperatures of GT2 and GT3 rise, however, the temperature increase becomes rapid at 18:30, which coincides with the period of intense rainfall and rapid flow at 15 and 50 cm depths. The peaks in temperature are attained within 25 min (18:55), where temperature increases are 0.4 and 0.5°C for GT2 and GT3 respectively. After the peaks in temperatures are reached, a trend of rapid decline in temperature is recorded. At 18:40, GWA responds and at 20:25, GWC responds. Since well GT is located mid-way between GWA and GWC, it must exhibit a rise in the groundwater level between these two times. Thus, the decline in temperature that is recorded at GT2 and GT3 must be due to groundwater response. The temperature at GT2 declines rapidly until 20:40 on 10 July, showing a decrease of 0.4°C. GT3 declines until 20:10 on 10 July, showing a decrease of 0.6°C. Temperatures continue to decline until 6:00 on 11 July, after which temperature increases are observed. GWA rises by 29 cm and groundwater height peaks at 19:50 on 10 July. GWC rises by 9 cm and reaches a peak height at 1:15 on 11 July. Rapid temperature decrease ceases at GT2 and GT3 within 30 min of the peak in GWA, which provides further evidence that the decline in temperature may be attributed to groundwater movement. GT4, GT5 and GT7 show negligible temperature variation and remain constant at 16.5, 16.1 and 15.2°C respectively.

6 January 1995

Figure 6.7 presents hydrometric and temperature data for a storm on 6 January 1995. Figure 6.7a presents 5 min rainfall (PPT) and Figure 6.7b shows responses in the unsaturated and saturated zones. Figure 6.7c shows temperature responses in the saturated zone.

Rainfall begins at 13:25 on 6 January and totals 30 mm. However, rainfall does not become 'continuous' until after 17:50 on 6 January. The initial response noted in the unsaturated zone is flow at 50 cm depth at 18:20. This may be macropore flow, although the hydrometric data does not fulfill the criteria established in Chapter 4 for the occurrence of macropore flow. Rapid flow begins at 15 cm depth (VI-15) at 19:15 and flow becomes rapid at 50 cm depth at 20:05.

The previous section displayed GT results for this storm (Figure 6.4a) and discussion explained how the temperature variations at various depths displayed different trends. GT2 was dismissed as measuring air temperature, since the probe lay above the level of the water table. It is interesting to note that GT4 and GT7 display 'rapid' temperature decreases within 30 min of the onset of possible mesopore flow. This suggests that mesopore flow may promote groundwater. However, GT4 does not show this pattern, and since this is the most shallow groundwater that was recorded, this is the probe that should respond to mesopore flow. Instead, the temperature remains constant at 15.3°C. GT3 was not in operation during this storm, which is the depth at which mesopore flow would be observed. Hence, the mechanism may have been in operation, but was not detected due to faulty equipment.

A rise in temperature of GT4 is displayed at 19:25 on 6 January. This is consistent with the response of GWA at 19:25. GWA rises from a depth of 2.72 m and reaches a maximum height of 2.00 m

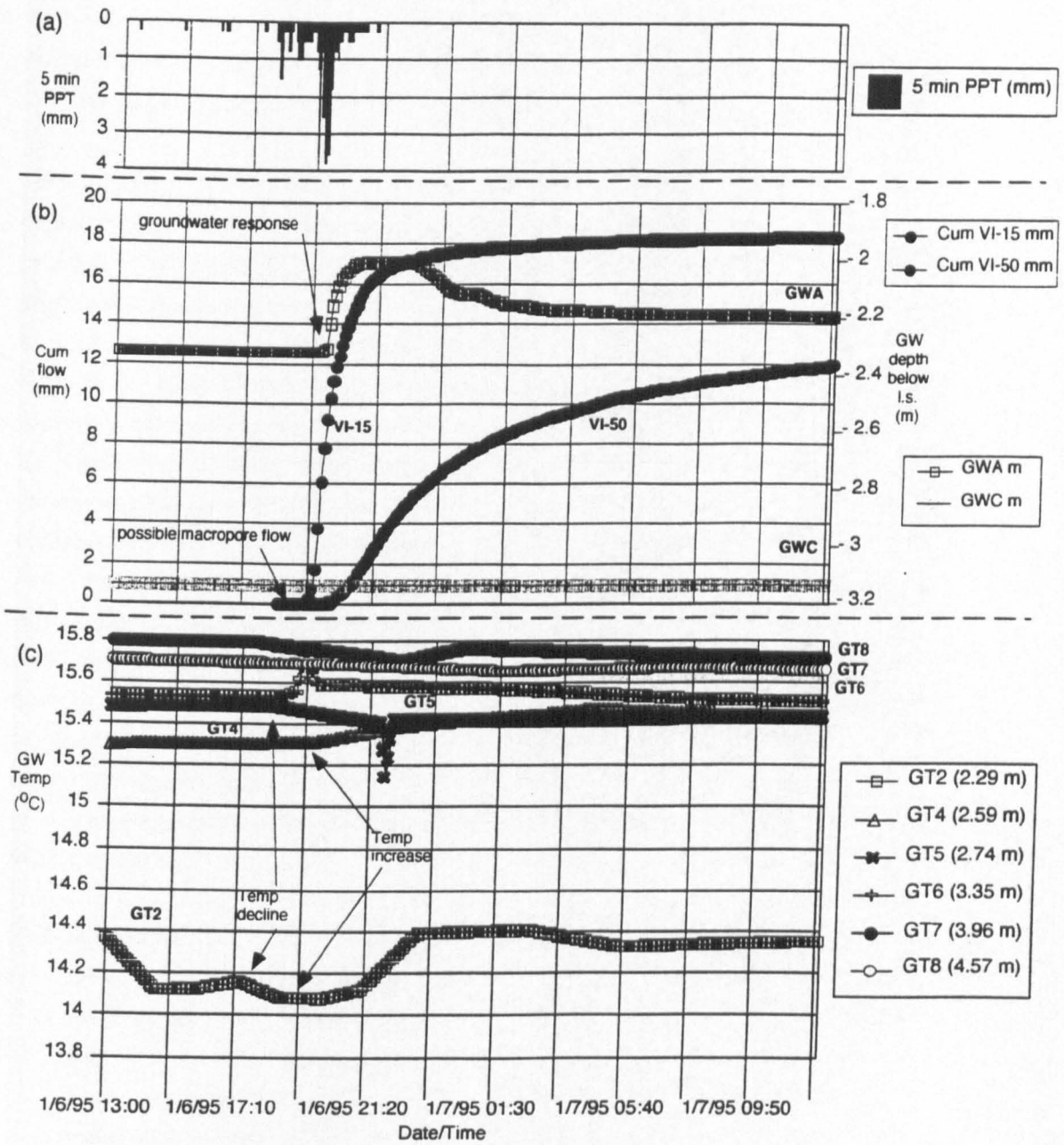

Figure 6.7 *Hydrological and temperature responses for a storm occurring on 6 January 1995: (a) 5 min precipitation (PPT); (b) Soil water responses at 15 cm depth (VI-15) and 50 cm depth (VI-50), and groundwater responses from wells positioned in the riparian zone (GWA) and 10 m upslope (GWC); (c) Groundwater temperature responses from themisors positioned in well GT at depths of 2.29 m (GT2), 2.59 m (GT4), 2.74 m (GT5), 3.35 m (GT6), 3.96 m (GT7) and 4.57 m (GT8) below land surface*

below the land surface at 22:20 on 6 January. Thus, groundwater level increases by 32 cm. GT4 continues to rise in temperature and peaks at 4:25 on 7 January, rising by 0.2°C. After this, a decline in temperature is observed, suggesting mixing of 'old' and 'new' waters.

(d) Summary

ydrometric and temperature data compliment one another and provide strong evidence for the validation of the hypothesis generated for the occurrence of macropore flow and groundwater displacement in certain storms. Similar analyses were performed on all growing season storms specified in Appendix 6.1 (although data was not available for September storms). For all storms from 4 July to 21 August (inclusive), the synchronisation in timings of temperature and hydrometric responses were very close. For the storms in April 1995, the patterns were not as obvious, nor did the hydrometric data correlate so well with the temperature data. An explanation for this is that the thermal stratification was not as intense as it was for the growing season storms in 1994. The same analysis was conducted on all dormant season storms displayed in Appendix 6.1. Only for January and February storms in 1995 are the hypothesised patterns observed. For October - December 1994, poor association exists between hydrometric and tracer data. The most reasonable explanation for this observation is that this is the period when the thermal stratification is reversing. Hence the variation in temperatures with respect to depth in the saturated zone is minimal, and also, for some of these storms, the variation between air temperature (i.e. 'new' waters) and GT2 (i.e. 'old' water) is < 3.0°C. Hence, temperature was not effective as a tracer of water movement for some storms. However, agreement between the timing of hydrometric and temperature responses was found for half the storms for which data was available.

(VI.5) SUMMARY

- The temperatures of 'new' (i.e. throughfall) and 'old' (i.e. groundwaters) waters were found to be significantly different, and hence temperature could be used as a tracer to distinguish between them. Air, throughfall, soil and groundwater temperatures were all found to vary seasonally. Temperatures at each node were highest during the growing season. The difference between the average temperatures of 'old' and 'new' waters were slightly greater during the growing season.
- Groundwater temperatures were found to be stratified with respect to depth and the stratification that was observed during the growing season was the reverse to that observed during the dormant season. During the growing season, the shallowest groundwater was warmest and there was a progressive decrease in temperature with respect to depth. During the dormant season, the shallowest groundwater was coolest and there was a progressive increase in temperature with respect to depth. The difference in temperature between the shallowest and deepest groundwater was greater during the dormant season. The growing season stratification existed from June through September, with the greatest variation in temperature occurring in August. The dormant season stratification existed from January through March, with the greatest variation in

temperature occurring in February. During October through November and in April, the thermal stratification reversed and during these time periods, the temperature variation with respect to depth was minimal.

- Distinct short-term temperature variations existed in streamwater and groundwater during storms. Soil temperatures did not vary greatly. The temperature variations in streamwater were attributed to direct channel rainfall, where rapid increases in temperature shortly after the onset of rainfall occurred in the growing season and the opposite temperature trend occurred during the dormant season. In the saturated zone, during the growing season, rapid increases in temperature were noted, followed by rapid decreases in temperature. The opposite temperature trends were noted in the dormant season.
- A conceptual model was developed to explain temperature variations in the saturated zone. This proposed that shallow groundwater is recharged rapidly during the onset of rainstorms with 'new' water, which causes an increase in temperature in summer and a decrease in the winter. The rapid input of 'new' water to depth causes a concurrent groundwater level rise and increase in temperature. After the initial transport of 'new' water and as groundwater levels fluctuate, lateral movement of groundwater from upslope displaces and mixes with the 'new' water, causing temperatures to decrease below pre-storm values, and to trend back to pre-storm levels.
- The timings of temperature responses in the saturated zone were compared with the timings of the onset of macropore flow and groundwater responses (i.e. hydrometric data). In half the storms analysed, the timings of temperature and hydrometric responses were synchronous. Hence, it is postulated that temperature is a valuable tracer of macropore flow and groundwater displacement. Both mechanisms are in operation at PMRW. Furthermore, temperature may be used to distinguish the type of water transported in macropores. The analysis suggests that during both the growing and the dormant seasons, 'new' water is transported in macropores.

Temperature and chloride have enabled more detailed investigation of flowpaths hypothesised from the hydrometric analysis. Tracer data has been able to identify the 'old' and 'new' water content of individual flowpaths. Both tracers have been instrumental in the identification of macropore flow at PMRW. In the following chapter, a conceptual hydrological model of the hillslope environment of PMRW, during rainstorms, is developed.

Chapter VII
HYDROLOGICAL MODEL OF PMRW

Development of a conceptual hydrological model of PMRW

(VII.1) Introduction

Previous studies in hillslope hydrology adopted various approaches (e.g. computer modelling, and small field investigations) in order to develop conceptual hillslope models that define all major flowpaths during storms (detailed discussion of conceptual models can be found in Chapter 1). Most results were site-specific and hence could not be applied to other geographical locations (Bishop *et al*, 1990; Kirchner, 1992; Mulholland *et al*, 1993; Robinson *et al*, 1995). However, the development of models of this type are useful for exploration of the interactions of source areas and flow processes in time and space (Mulholland *et al*, 1993). Few studies exist where hydrometric and tracer data have been collected with such a rigorous sampling program as in the present investigation, making this study unique. A hydrological model which incorporates all major flowpaths and the changes in the relative proportions of 'old' and 'new' water composition has not been developed for PMRW.

The following is an attempt to construct such a model, synthesising data presented in the previous three chapters. Firstly, a generalised conceptual model is presented which can be applied to any hillslope situation. Finally, conceptual models are presented that are specific to PMRW.

(VII.2) Generalised Conceptual Hillslope Model

Figure 7.1 illustrates a generalised conceptual model of hillslope response that can be applied to any hillslope situation. The basis of the model are the results presented in Chapters IV - VI. When rainfall begins, it can take one of five routes once it reaches the canopy: throughfall, stemflow, interception, overland flow and direct channel rainfall. The routes that have been measured directly in this investigation are shown in bold (throughfall and overland flow).

If the rainfall is intercepted by the canopy, it is either lost to interception; flows along branches and trunks as stemflow, or takes the route of throughfall. Which of these processes the water takes in controlled by a series of factors. The season in which the storm occurs will affect % canopy cover and air temperature. The total throughfall is typically lower in the growing season, as greater interception by the canopy occurs. Also, under higher summer temperatures, evapotranspiration is efficient, increasing water loss through this process. Hence, interception is a greater sink for rainfall during the growing season.

Water that is not intercepted by the canopy may contribute directly to the stream channel as direct channel rainfall. Lack of canopy overhanging the stream channel in the dormant season may result in greater contribution of water by this process in this season. Rainfall may also contribute directly to forest floor soil water in areas where canopy coverage is sparse. This may take the form of overland

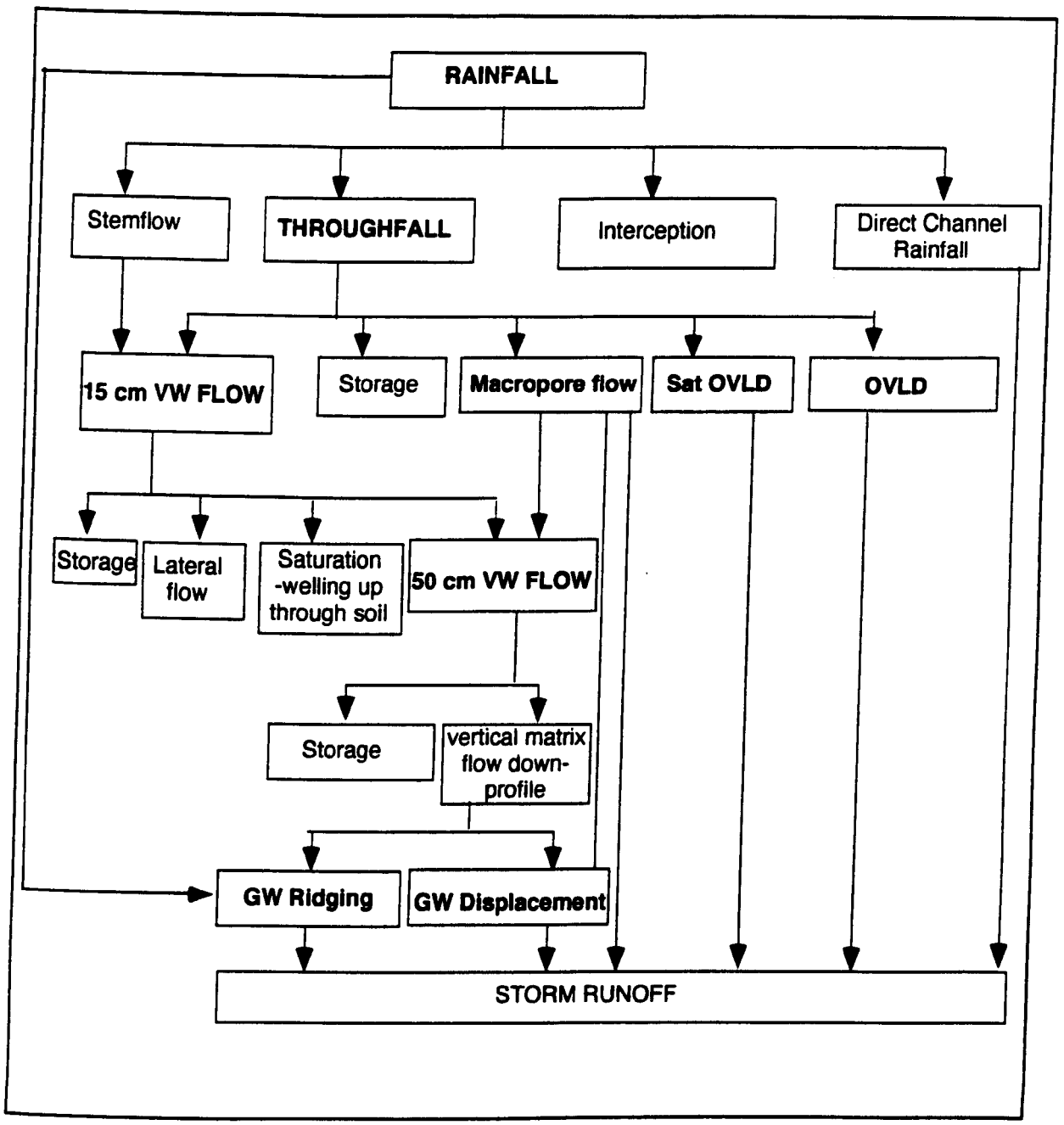

Figure 7.1: Conceptual model of hydrological responses of a hillslope (NB: Sat OVLD = saturation overland flow; OVLD = Hortonian overland flow; 15 cm vw flow = 15 cm soil water flow; 50 cm VW flow = 50 cm soil water flow

flow under high rainfall intensity conditions or if the upper soil horizon is saturated. This process is affected by a series of other parameters which are discussed below.

Water that passes through the canopy, as throughfall and stemflow will then transit the soil surface by a series of new mechanisms. Following dry antecedent conditions, the storage capacity of the soil may be sufficient to store all incoming water. Hence, flow may be recorded through the forest floor, but may not be transported to depth. If the soil moisture status of the soil is high, after wetter conditions, or during the dormant season when temperatures and plant uptake are lower, sub-surface flow occurs. Sub-surface flow will occur once smaller pores in the soil are filled and water is transported via larger pores (which can transport water more efficiently). Hence, if storms are of high enough magnitude to overcome potential storage, or follow wet antecedent conditions, flow at 15 cm may be registered.

These processes refer to matrix flow, however macropore flow also occurs in well drained soils that have abundant animal activity and concentration of roots in the upper horizons which allow pipes and channels to develop. Macropore flow occurs in the dormant and growing seasons, although it is more important during the growing season. Its occurrence is controlled to a high extent by antecedent moisture conditions, whereby drier conditions promote greater macropore flow. Macropore flow can be vertical and lateral, and water that is transported is predominantly 'new' water. Macropores are capable of transporting water to the groundwater table.

During storms that follow very wet antecedent conditions, storm water may be unable to penetrate to depth due to the saturation of the profile, and is routed over the land surface as overland flow. In some situations, especially in the growing season, deeper soil horizons may have greater soil moisture status than shallower horizons, which may have been depleted of moisture under the high temperatures by evapotranspiration. Typically, the porosity of the soils decrease with depth due to overburden pressure, which causes a decrease in hydraulic conductivity with depth. In some cases, if the clay content of the soil increases with depth, this may act as an impeding layer following wet conditions, as the clay swells. In both circumstances (i.e. either due to saturation of a lower horizon or due to the development of an impeding layer), water infiltrating from above in the profile may not be able to penetrate any deeper and will either flow laterally, parallel to the impeding layer or will back up through the soil profile. In the latter case, if water wells up to the surface, it will then be transformed into saturation overland flow and flow over the land surface. This process will be encouraged if there is an irregularity in the land surface, e.g. a topographic low.

In situations where the rainfall is very intense, water may run over the land surface if the infiltration capacity of the soil is overcome (Hortonian overland flow). Some positions on the hillslope may be in a permanent state of near-saturation, e.g. foot slope and valley bottoms adjacent to stream channels, inputs of small amounts of rainfall may promote overland flow (partial area overland flow).

Sub-surface flow may take one of three main routes: matrix, macropore or lateral. Depending on antecedent conditions, water may be stored in the soil (especially following dry antecedent conditions) or may move laterally if an impeding layer exists in the profile. Water may move laterally or well up in the profile if the lower soil horizon is near saturation (following wet antecedent conditions). Flow

that is measured at depth in the profile will be a combination of matrix and macropore flow (and hence a mixture of 'old' and 'new' water).

Matrix flow will continue through the profile to the groundwater table. Macropore flow may also reach the groundwater zone. Its operation depends on the penetration of roots and animals burrows, and also on the textural composition of the soil. However, since root abundance and animal activity dominate in the upper horizons, this is where macropore flow is expected to be dominant.

The transport of 'new' water to the groundwater table has been found to cause a groundwater displacement mechanism, and hence rapid groundwater response following the initiation of rainfall. The transport of 'new' water to depth causes a pressure mechanism on the water table which forces groundwater from higher upslope to move down and replace groundwater down profile, which, in turn, causes a rise in the groundwater table. This mechanism occurs during the dormant and growing season, when macropore flow is also in operation.

Another mechanism of rapid groundwater response shortly after rainfall onset is groundwater ridging. The operation of this process is confined to specific areas on the hillslope, namely foot slope and valley bottoms. In these locations, saturated wedges exist (especially following wet antecedent moisture conditions) from which groundwater flow is promoted by rainfall falling on lower slopes. The groundwater ridging process is promoted by drainage of matrix water, wet antecedent conditions and the direct contribution of rainfall (or throughfall) onto the soil surface.

Hence, there are a series of mechanisms that quickly contribute water to the stream channel during rainstorms: direct channel rainfall, overland flow, macropore flow and groundwater ridging and displacement.

This model exemplifies the main flowpaths and mechanisms that water takes as it transits the hillslope. Many of these mechanisms were measured directly in the investigation, and others were inferred when flow patterns at adjacent nodes were compared. This is a generalised model, and the flowpaths that dominate will be specific to the catchment in which the investigation is conducted, and even the location on the hillslope where the instrumentation is located. This investigation has shown that processes that dominate on the lower slopes vary significantly from those that dominate on the upper slopes. Sub-surface flow mechanisms will be controlled to a high degree by the structure of the profile, e.g. textural changes, penetration of plant roots etc.

The investigation of PMRW also explored the controls of antecedent moisture conditions and rainfall regime on all processes. In the following section, conceptual models of the response of the hillslope to storms during the growing and dormant seasons are presented. These are specific to PMRW.

(VIII.3) Conceptual Hydrological Model of PMRW Hillslope

The following presents conceptual models of the PMRW hillslope response to storms. The analysis has shown the variation in flow mechanisms in operation during the dormant season and growing season. Ttwo models are provided, illustrating the responses in both seasons.

GROWING SEASON

Figure 7.2 displays the hydrological response of the hillslope during the growing season. 78% of rainfall is transformed into throughfall once it enters the canopy. The remaining 22% is lost to interception (on average 2.5 mm) or is routed via branches and trunks as stemflow. The temporal variability in throughfall closely follows that of rainfall. High throughfall is associated with high rainfall. However, in some storms, this relationship varied significantly, which is attributed to a series of factors including rainfall intensity variations across the study area and factors pertaining to high spatial heterogeneity in throughfall, including inherent complexities in canopy structure and tree density.

The flowpaths followed by the water once it penetrates the canopy are controlled to high degrees by antecedent moisture conditions and rainfall characteristics. Following dry antecedent conditions, the storage capacity of the soil is high and hence 'new' water may be stored in the soil. Storage enables greater residence time in the soil matrix and hence the water is able to develop the chemical signature of 'old' water. Under dry conditions (and especially when rainfall is intense), water is routed through the soil via macropores (i.e. along fissures and channels developed from plants roots and animal burrows). The water routed via this mechanism is 'new' (*Cl' signatures of VI-50 soil water are low and comparable to those of rainfall and throughfall).*

If the storm is of sufficient magnitude (TI > 10 mm), storage of the upper 15 cm soil horizon is exceeded and *matrix flow is initiated at 15 cm depth* (this is 'old' water). As rain falls on the dry soil, smaller pores are first filled before water fills larger pores which are able to transport the water more efficiently. The amount of flow, relative to throughfall volume, is controlled by a series of factors, which also affect the operation of associated flowpaths. Where low flow is measured, this could be attributed to storage deeper in the soil (following dry antecedent moisture conditions). Another scenario that generates low flow can follow wet antecedent conditions. In the growing season, higher temperatures and plant uptake may leave the upper horizons of the soil depleted in soil moisture, where lower soil horizons may be close to saturation, as water is held from previous storms. The onset of a new storm may allow penetration of water down profile as far as the zone of saturation. At this point, the water is unable to filtrate vertically and may either flow laterally (especially if this is generated by an impeding layer) or will back up through the soil. If this mechanisms continues until the return flow reaches the surface, the water will then flow over the land surface as saturation overland flow. The increase in clay content at 40 cm in the profile may create an impeding layer, since the clay will swell after the passage of the wetting front, and similar flow processes may be initiated as if the soil was saturated. The hydrometric analysis suggests that overland flow operates on the hillslope plot (on average, overland flow is equivalent to 140% throughfall in this season). The

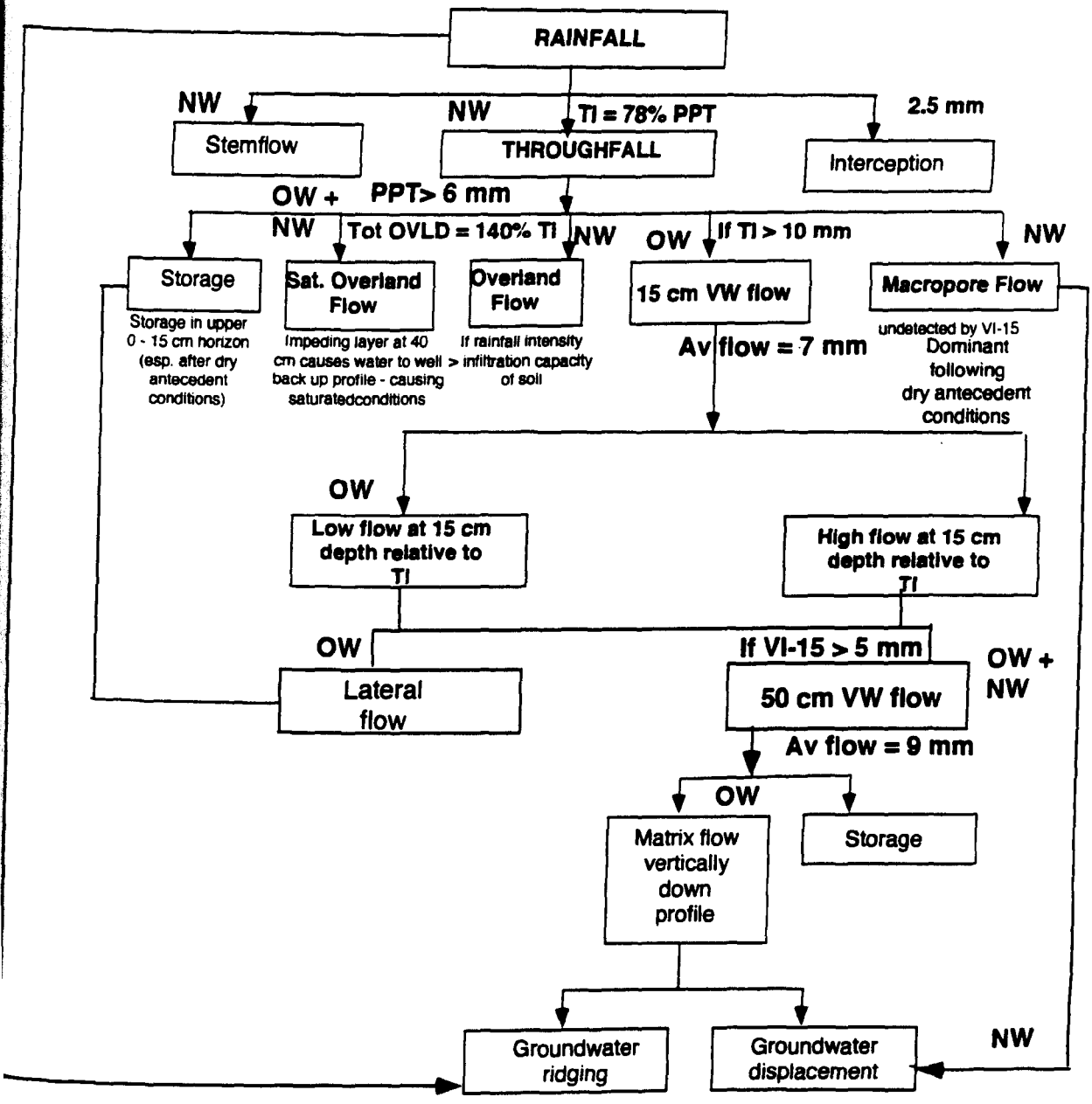

***Figure 7.2**: Conceptual model of short term hydrological response of hillslope during growing season storms*

measurement of overland flow (i.e. forest floor soil water) was conducted in a topographic flow, which is a favourable location for the operation of saturation overland flow. The operation of this form of overland flow can not be concluded from the hydrometric data alone. However, results of the Cl^- analysis of forest floor soil water samples show that Cl^- content of the initial samples are higher than corresponding samples of throughfall. This suggests that saturation overland flow (that would comprise a Cl^- signature similar to 'old' water) may occur at the onset of storms in the growing season. This is corroborated by hydrometric data that shows that overland flow occurs shortly after the onset of storms (on average after 67 min) and only 6 mm rainfall is required for the process to occur. As stated earlier, the results of the growing season analysis are atypical for PMRW, due to the occurrence of Tropical Storm Alberto and subsequent storms. The series of storms (4 - 14 July 1994) which followed shortly after one another caused extremely wet conditions. However, high July temperatures enabled upper soil horizons to become depleted of moisture 'between storms'. Hence, lower horizons may have been close to saturation (TDR data shows that lower horizons were 'wetter' than upper horizons), and only relatively small amounts of rainfall (> 7 mm) were required to generate saturation conditions, which lead to saturation overland flow. The Cl^- analysis shows that towards the end of storms, the Cl^- content of samples of forest floor soil water became similar to those of throughfall. This suggests that the form of overland flow may change during the storm, since the surface horizons eventually become saturated, resulting in no water being able to penetrate the soil surface, and flowing over the surface as partial area overland flow (or Hortonian overland flow where extremely high rainfall intensities were experienced). The dominance of overland flow in the growing season following wet antecedent conditions and the high storage capacity of the soil following dry antecedent moisture conditions may explain why flow was flow during this season compared to the dormant season (7 mm on average through 15 cm depth, and 9 mm on average through 50 cm depth).

Flow processes down profile where similar to those described above. The hypothesised impeding layer existed at 40cm depth, and hence lateral flow was hypothesised to be dominant along this interface.

For flow to be initiated at 50 cm depth, flow through 15 cm had to exceed 5 mm (flow less than this was lost to storage). Significant contribution from macropore flow or lateral flow is hypothesised at 50 cm depth, since average flow (9 mm) was greater than at 15 cm depth (7 mm). Most water collected at VI-50 was 'new' water (low Cl^- content of the water), which also provides evidence for the dominance of macropore flow. Matrix flow was found to become more important towards the end of the storm (Cl^- content increased in final samples).

Matrix flow continues down profile, although the rapidity of flow is reduced (due to decreasing pore size). Macropore flow is believed to extend to the groundwater table, and is responsible for the groundwater displacement mechanism that is observed (according to hydrometric and temperature data). 'New' water is introduced to the water table by macropores, causing a pressure difference which results in the displacement of groundwater from upslope to a lower slope position, resulting in a rapid increase in groundwater level.

Groundwater ridging is also in operation where saturation wedges exist on valley bottoms, adjacent to the stream channel. The introduction of 'new' water (i.e. rainfall) causes groundwater to flow into the stream channel. If the surface horizons are close to saturation, the addition of small amounts of rainfall may also cause partial area overland flow (comprising 'new' water).

DORMANT SEASON

Figure 7.3 displays the conceptual model of the hydrological response of the hillslope during dormant season storms. Canopy mechanisms are similar, although interception is significantly less (only 0.5 mm on average). Throughfall is slightly higher (98% PPT) than in the growing season. This was expected since the absence of leaves allows greater penetration of the canopy by rainwater.

Within the unsaturated zone, similar processes are in operation, although their magnitude or dominance differ to those during the growing season. Throughfall must exceed 10 mm for flow to occur at 15 cm, which suggests that this is the threshold at which storage is overcome. The average flow that is monitored at 15 cm depth is over twice that monitored during the growing season (although the average throughfall is similar for both seasons). This observation is coupled with the significantly lower overland flow during the dormant season (on average equivalent to 92% throughfall). Cl^- data suggests that the contribution of saturation overland flow is significant in the dormant season (as great as 46% on one storm, according to a mixing model). However, greater rainfall must occur (> 12 mm) before overland flow is initiated, suggesting that overland flow is more dominant towards the end of storms. It must also be remembered that saturation overland flow is probably confined to topographic lows in the hillslope, and hence the process may not affect sub-surface flow in other locations.

The flow regime at 50 cm in the profile appears to be controlled to a greater extent by the flow regime at 15 cm depth during this season. High flow through 15 cm depth (10 mm) often leads to no flow at 50 cm depth. This is attributed to the saturation or impeding layer, described in the previous section. Low flow through 15 cm promotes low flow through 50 cm depth (which is self-explanatory, but may also be influenced by high storage in the 15 - 50 cm zone following dry antecedent conditions).

Medium flow through 15 cm depth (5- 10 mm) promotes relatively high flow through 50 cm depth. Flow is also contributed to 50 cm depth via macropores. However, the Cl^- analysis suggests that contribution of 'new' water via macropores is not as prevalent during this season. However, hydrometric, Cl^- and temperature data all suggest that macropore flow occurs at the onset of dormant season storms. Average flow at 50 cm was 16 mm during this season, which is similar to average flow through 15 cm depth (16 mm). This provides evidence that macropore flow is not as important as in the growing season. The temperature analysis shows that macropore flow initiates groundwater displacement.

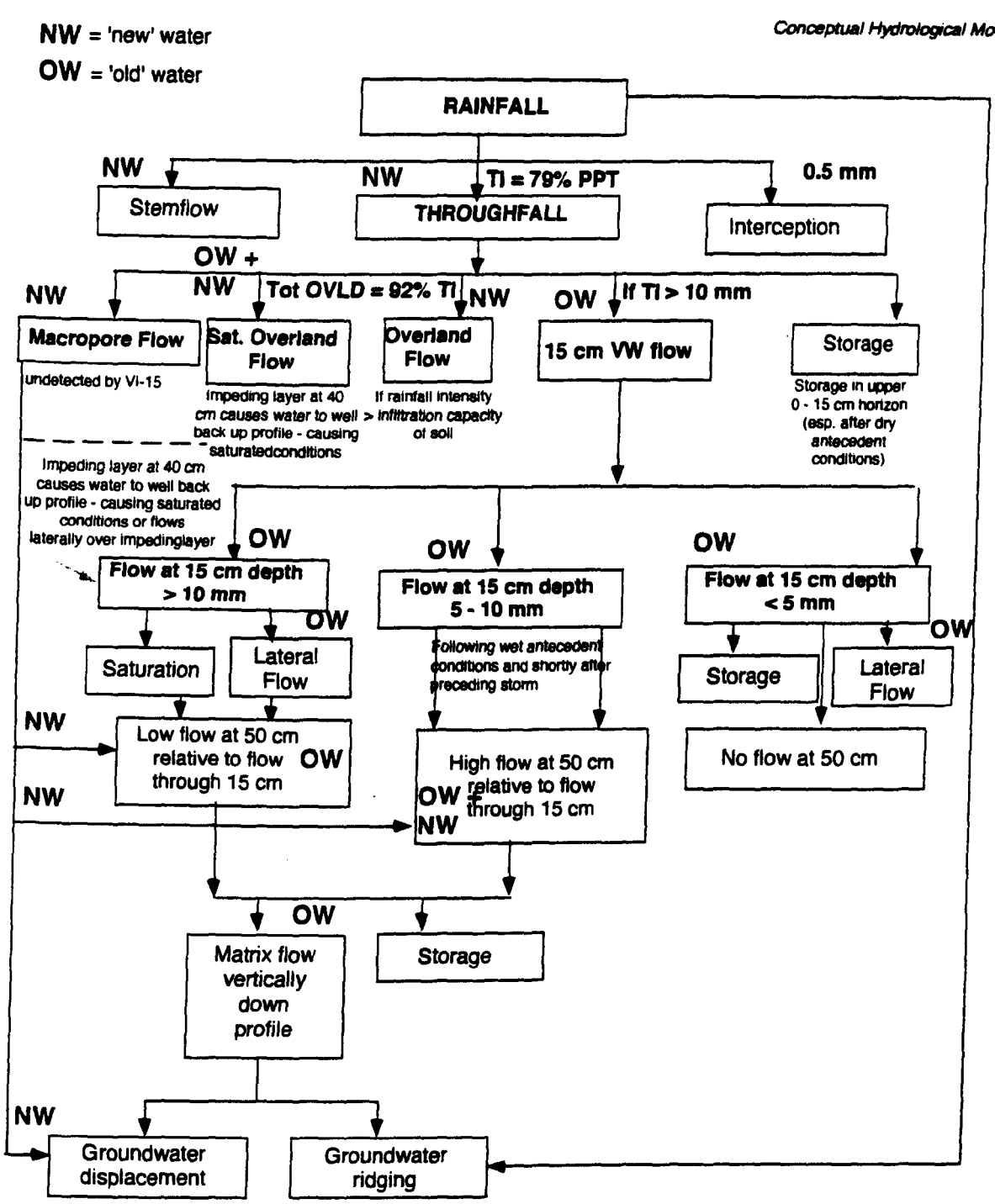

***Figure 7.3**: Conceptual model of short term hydrological response of hillslope during dormant season storms*

Groundwater ridging is also in operation during this season in the lower slopes and valley bottom zones, and is especially significant following wet antecedent conditions.

(VII.4) Summary

- The development of conceptual hydrological models of the hillslope response to rainstorms at PMRW has elucidated the major flowpaths followed by rainfall. Within this system, the dominant flowpaths responsible for the transport of 'new' water during storms are direct channel rainfall, overland flow and macropore flow. Macropore flow is a more important flowpath during the growing season than during the dormant season. Saturation overland flow is an important mechanism within topographic hollows on the hillslope, which contributes a mixture of 'old' and 'new' water downslope. Matrix soil water flow and groundwater displacement are responsible for the transport of 'old' water. Matrix flow becomes the more dominant soil water transport mechanism during the dormant season. Groundwater displacement is initiated by macropore flow, and hence, although macropore flow causes the rapid transport of 'new' water to the saturated zone, it prompts the response of groundwater, which ultimately contributes 'old' water to storm runoff.
- The operation of flowpaths vary seasonally, and are also controlled to high extents by antecedent moisture conditions, storm magnitude, rainfall intensity and timing between storms.
- The occurrence of two tropical storms (Tropical Storms Alberto and Beryl) during the growing season altered the typical hydrological response of the hillslope. This assumption is based on analysis of previous studies at PMRW and elsewhere. Many of the mechanisms that have been found to be dominant in the dormant season, when the soil moisture content of the soil is typically high, were found to occur during the growing season, since the tropical storms caused the hillslope to be in a state of continual near-saturation.

Chapter VIII
CONCLUSIONS

VIII.1 REVIEW OF AIMS

In Chapter I, the purpose of this study is stated as the examination of the major flowpaths followed by water in a hillslope during rainstorms. The study has attempted to examine the variation in quantity, quality and routing of rainfall as it passes through the hillslope system. The relative contribution of 'old' and 'new' waters to each flowpath have been examined. The methods employed have largely examined the flow rates and hydrological responses from several nodes through a one-dimensional transect; namely rainfall, throughfall, forest floor soil water, soil water, groundwaters and streamwaters. Evidence from investigations of chloride and temperature variations in water passing through these nodes has been used to support the interpretations of the hydrometric data and in assessing the 'new' and 'old' water contributions.

Hydrological responses were monitored by implementing a rigorous sampling methodology. Data concerning flow rates and responses from various flowpaths was collected from tipping bucket gages, TDR equipment and stage monitoring equipment, all of which were monitored using Campbell Scientific Model CR21X and CR10 dataloggers (Section III.3). Analysis of this data allowed the identification of specific flowpaths. The relative contribution of 'old' and 'new' waters to each flowpath was determined using chloride and temperature as conservative tracers. Samples were collected sequentially and manually from each node (Section III.3) and chloride determinations were performed on all samples (Section III.4). Air, throughfall, soil water, groundwater and streamwater temperatures were monitored using BETATHERM Model 5K3D39 thermistors (Section III.3).

The aim of the hydrometric analysis was to identify which flowpaths were in operation at the hillslope plot. Some assessment as to the spatial and temporal heterogeneity of those flowpaths was made. The controls on flow through each node were also assessed, namely seasonality, antecedent moisture conditions, rainfall intensity, and magnitude and storm duration.

The aim of the chloride tracer study was to investigate whether chloride could be used to distinguish between 'old' and 'new' waters within this environment (Section V.4A). Combination of the Cl^- data with hydrometric data enabled as assessment to be made of the relative contribution of 'old' and 'new' water within flowpaths (Section V.4B). The development of two-component mixing models allowed some quantification of the relative contribution of 'old' and 'new' water to specific flowpaths.

The aim of the temperature tracer study was to investigate whether temperature could be used to distinguish between 'old' and 'new' waters (Section VI.4A). Combination of the temperature data with hydrometric data enabled an assessment to be made of the relative contribution of 'old' and 'new' waters to specific flowpaths (Sections VI.4B and C).

The results of the above studies have been drawn together in Chapter VII, which presents a compilation of conceptual models of the hydrological response of the hillslope to rainstorms.

VIII.2 SUMMARY OF RESULTS

VIII.2A Hydrometric Analysis

Overland flow, macropore flow, groundwater displacement and groundwater ridging have all been observed at the hillslope plot during storms. Each mechanism was found to vary in its operation according to a series of 'controls', namely seasonality, antecedent moisture conditions, storms magnitude and duration, rainfall intensity and timing between individual rainstorms.

Throughfall varied slightly on a seasonal basis, with slightly greater volumes in the dormant season (equivalent to 79% PPT) than in the growing season (equivalent to 78% PPT). This is explained by the absence of the canopy during the dormant season, resulting in greater penetration by rainfall. Also, lower temperatures in the dormant season, together with lower canopy cover, resulted in lower (5 times less) interception during this season (on average 0.5 mm) compared with the growing season (on average 2.5 mm). Stemflow occurred during both seasons (although this was not measured directly in this study). In a previous investigation (Cappellato, 1991), stemflow averaged 5% PPT. Comparison of data collected in the current investigation with that collected in a previous study at PMRW (Cappellato, 1991) shows a high degree of spatial heterogeneity in throughfall, which is explained by the same factors mentioned above, and also rainfall intensity (Ford and Deans, 1978), distance from the trunk (Robson *et al*, 1994), tree type and density, and wind speed.

Measurement of higher volumes of forest floor soil water than throughfall provided evidence for the operation of overland flow. Forest floor soil water flow was monitored at two locations. In one location (VI-0), equipment was located in a topographic low, the difference between total forest floor soil water and total throughfall was significantly greater than then forest floor soil water was collected at the other site (VI-0o). This suggests that overland flow may operation preferentially in topographic lows on the hillslope.

The relative total overland flow (calculated as the difference between total forest floor soil water flow and total throughfall) varied seasonally. Higher volumes were recorded in the growing season (equivalent to 140% TI) than in the dormant season (on average 92% TI). High overland flow in the growing season is attributed to the occurrence of Tropical Storm Alberto and subsequent storms (4 - 15 July 1994). The series of storms produced very wet conditions. It is possible that between storms, the lower horizons remained near saturation, whilst upper horizons were depleted of moisture under higher temperatures through evaporation and evapotranspiration. Hence, the addition of 'new' water may have caused the lower horizons to reach saturation. Water would then be forced to flow laterally or to well back up the soil profile. If the water was able to reach the soil surface, then the water would flow over the land surface as saturation overland flow.

Flow through the unsaturated zone was greatest during the dormant season. The lower flow during the growing season was attributed to loss from storage, plant uptake and greater overland flow. The response time was affected by the position on the slope where flow was monitored. Sites in the

riparian zone exhibited the most rapid movement of the wetting front, which is consistent with the continual priming of the lower slope, near-stream areas by downward drainage of water (McDonnell, 1990).

Macropore flow was detected, and its operation was controlled by antecedent moisture conditions and rainfall intensity. Mesopore flow was also detected. Although macropore flow was detected at the onset of storms, Cl^- data suggests that it may operate throughout storms in the growing season, but only at the onset of storms in the dormant season. Hence, it is a more dominant mechanism during the growing season. Macropore flow may lead to groundwater displacement, where the rapid transport of water to the saturated zone, via macropores, leads to the displacement of groundwater in a downslope direction. Groundwater ridging occurs in the near-stream zone. Its operation is controlled by antecedent moisture conditions, as expansion of the near-stream unsaturated zone occurs under wet conditions.

VIII.2B Chloride Tracer Analysis

Chloride was an effective tracer for distinguishing between 'old' and 'new' waters. Samples of rainfall, throughfall and forest floor soil water typically contained < 20 μeq/l Cl^-. The initial samples in collection sequences from these nodes contained higher Cl^- concentrations than in following samples in sequences. This is attributed to enhancement due to washout mechanisms in the case of rainfall, and washoff mechanisms in the case of throughfall and forest floor soil waters (Unsworth, 1980; Cryer, 1986; Eshleman *et al*, 1993). However, when these initial samples are removed from the analysis, then the VWM Cl^- concentration at each of these nodes for all storms are below 20 μeq/l Cl-. The VWM Cl^- concentrations of 15 cm soil waters and average groundwater Cl^- concentrations were all above 20 μeq/l Cl^-. Thus 20 μeq/l Cl^-, was chosen as a criteria for distinguishing between the water types.

Cl^- data corroborated the hydrometric data, illustrating the macropore flow occurred at this site. The Cl^- content of 50 cm soil waters (VI-50) during the growing season all contained < 20 μeq/l Cl^-, and was hence 'new' water. Thus, macropores allow the rapid transit of 'new' water to depth during these storms. The high Cl^- content of 15 cm (VI-15) soil water samples also supports the findings of the hydrometric analysis, which suggest that this lysimeter collects matrix soil water only. Tension lysimeter soil water samples contain a range of Cl^- concentrations and are thus hypothesised to collect a combination of 'old' and 'new' water.

Two-component mixing models, based on Cl^- concentrations allowed the quantification of the relative contribution of 'old' and 'new' water to forest floor soil water and to 50 cm soil water for some storms. Between 53 and 83% of forest floor soil water was found to comprise 'new' water. This indicates that some water must be 'old' and hence suggests that saturation overland flow occurs. Between 51 and 100% of 50 cm soil water was found to be 'new' water for storms occurring between July and October 1994. Hydrometric data for these storms suggests that macropore flow occurs and hence the Cl^- data corroborates this.

Streamwater average Cl^- concentrations were typically > 20 μeq/l Cl-, although streamwater samples collected for some storms contained < 26 μeq/l Cl^-. High magnitude storms led to lower Cl^- concentrations in streamwater, suggesting the addition of large quantities of 'new' water.

VIII.2C Temperature Tracer Analysis

Temperature was found to be an effective tracer in distinguishing between 'old' and 'new' waters. Temperatures of air, throughfall, soil, groundwater and streamwater were found to vary seasonally, with highest temperatures occurring during the growing season. Groundwater temperatures showed a thermal stratification with respect to depth. During the growing season, temperatures of the most shallow groundwaters were highest and decreased with depth; during the dormant season, the temperature of the most shallow groundwaters were coolest and increased with respect to depth.

The temperature of 'new' water (i.e. throughfall) was significantly different to that of 'old' water (i.e. groundwater). During the growing season, the temperature of 'new' waters were higher than those of 'old' waters. During the dormant season, the reverse was true. Hence, the water types could be distinguished from each other on the basis of their thermal regime.

Distinct short-term variations existed in groundwaters during storms. During the growing season, rapid temperature increases shortly after rainfall onset were attributed to macropore flow. The rapid decline in temperature that followed was attributed to groundwater displacement. The reverse temperature variations were observed during the dormant season, which were attributed to the same mechanisms. A conceptual model was developed to explain the temperature variations in the saturated zone during storms (Section VI.4Bd).

Thus, this small-scale investigation, employing intensive hydrometric and chemical sampling along a one-dimensional profile has allowed the elucidation of important flowpaths for water transport during rainstorms. The combination of tipping bucket gages with sequential collection equipment allows both the monitoring of flow rates through a specific node and the chemical variations in the water with time. This has been critical in the observation of macropore flow. Although hydrometric data alone might suggest the operation of macropore flow, the coupling of this data with chloride tracer data provides more solid evidence for its operation. The occurrence of macropore flow at PMRW has been postulated previously (Shanley and Peters, 1993), but no study has actually monitored the flowpath before.

The use of temperature as a conservative tracer of water movement in the saturated zone has not been reported in the literature (excluding results from the current investigation in Ratcliffe *et al*, 1996). Short-term temperature variations in the saturated zone allowed both the identification of macropore flow and groundwater displacement.

VIII.3 RECOMMENDATIONS FOR FUTURE WORK

This study has been instrumental in the identification of important flowpaths at PMRW. However the findings of this report are derived from the analysis of data collected from a 20 m by 20 m field plot. It is anticipated that this plot is representative of the deciduous hillslope area of PMRW as a whole. However, similar studies to the current study should be conducted at various locations throughout the watershed to ensure that the results are representative of the whole area.

The field configuration in this investigation was designed to investigate vertical water movement through the profile. Hence, installation of pan lysimeters had been intended to measure forest floor soil water. However, the operation of overland flow was inferred from this data. Overland flow was hence monitored at two sites in the watershed. The volumes of overland flow collected at each sits varied, which greatest volumes recorded at the hillslope site, where the pan lysimeter had been installed in a topographic low. This suggests that the mechanisms of overland flow differed between locations. The form of overland flow that is hypothesied to dominate is saturation overland flow (which is thought to have been collected from site VI-0). In order to investigate the phenomenon of overland flow at PMRW, a carefully designed separate investigation needs to be conducted. TDR rods could be callibrated, and porosity measurements should be taken from the various horizons in the soil. Hypotheses can then be made as to whether the soil is saturated or not. This will allow the identification of the type of overland flow that occurs. Also, in order to assess whether overland flow is confined to topographic lows, the monitoring of forest floor soil water should be conducted at a series of sites on a transect from upslope to the stream. This will enable assessment of the hypothesis made in this study, that saturation overland flow is the dominant form of this process at PMRW. It would also provide information as to whether the overland flow that is generated within the topographic low is transported over the land surface, downslope to the stream channel or whether the water is able to enter the soil again, and hence does not contribute to storm runoff. If a study of this kind is performed, it should allow some quantification of the contribution of overland flow to storm runoff, which the current investigation was unable to do.

Macropore flow has been observed in the hillslope during storms. A dye-tracing experiment (Mosley, 1979, 1982) over a small area would be an expansion of the current investigation and would allow some assessment of the distribution of macropores on the hillslope. Problems with monitoring macropore flow with lysimeters have been shown in the current study, where the installation of new equipment might lead to the obliteration of current macropores.

The present investigation has developed a hydrological model of the responses of the hillslope to rainstorms. In this investigation, some 2000 samples were collected, on which full chemical analyses were performed. Hence, a large database exists that will enable the development of conceptual hydrochemical models of the response of the hillslope to rainstorms. Two-component mixing models presented in this report, based on Cl^- concentrations can be corroborated with those using silica and dissolved organic carbon. These and other solutes can be used in investigating soil water flow

dynamics further. For example, concentration of specific solutes in the upper soil horizons might enable storage mechanisms to be distinguished from evaporative mechanisms, which lead to reduced flow through the soil.

This investigation has outlined major flowpaths that water takes as it passes through the hillslope system. The field program that was implemented has led to the collection of a large hydrometric and chemical database. The study provides many 'starting blocks' for other process- and flowpath-specific investigations. The analysis has shown the interaction between the various flowpaths and supports the finding of other small-scale investigations, which conclude that without studies of this sort, reliable process-based predictive models of the hydrology of watersheds cannot be achieved (Jenkins *et al.* 1994).

REFERENCES

Adamson, J.K., Page, W.P., Kennedy, M., Noins, N.H., Paterson, I.S., and Stevens, P.A., 1993, Soil solution chemistry and throughfall under adjacent stands of Japanese larch and Sitka Spruce at three contrasting locations in Britain: *Forestry*, v. **66**, no. 1, p. 51 - 68.

Alban, 1982, Effects of nutrient accumulation by aspen, spruce and pine on soil properties.: *Soil Science Society of America*, v. **46**, p. 853 - 861.

Alexander, M., 1977, *Introduction to soil microbiology*: New York, John Wiley and Sons.

Ambramsen, G., 1984, Effects of acid deposition on forest and vegetation: *Phil. Trans. R. Soc. Lon. B.*, v. **305**, p. 369 - 382.

Amer, S.A., Keefer, T.O., Weltz, M.A., Goodrich, D.C., and Bach, L.B., 1994: Soil moisture sensors for continuous monitoring: *Water Resources Bulletin*, v. **30**, no. 1, p. 69 - 83.

Arai, T., 1993, Estimation of groundwater flow from temperature distributions, *in*, '*Tracers in Hydrology*', ed., Peters, N.E.: Washington, D.C., IAHS Publication, p. 101 - 107.

Armstrong, C.L., and Mitchell, J.K., 1988, Plant canopy characteristics and processes which affect transformation of rainfall properties: *Transactions of the ASAE*, v. **31**, no. 5, p. 1400 - 1409.

Atkins, R.L., and Griffin, M.M., 1977, *Geologic guide to Panola Mountain State Park : Watershed Trail*: Geologic Guide, 8 p.

Atkins, R.L., and Griffin, M.M., 1977, *Geologic guide to Panola Mountain State Park : Rock outcrop trail*: Geologic Guide, 12 p.

Atkinson, T.C., 1980, Techniques for measuring subsurface flow in hillslopes, *in* '*Hillslope hydrology*' (3 ed.), ed., Kirkby, M.J., Wiley and Sons, p. 389.

Aulenbach, B.T., 1992, Streamflow generation and episodic acidification during hydrological events at Woods Lake, Adirondack Mountains, New York, USA, Syracuse University, Ms.c.

Baes, A.U., and Bloom, P.R., 1988, Effect of parent material and soil development on nutrient cycling in temperate ecosystems: *Soil Science*, v. **146**, no. 2, p. 67 - 72.

Baes, A.U., and Bloom, P.R., 1988, Exchange of alkaline earth cations in soil organic matter: *Soil Science*, v. **146**, no. 1, p. 6 - 14.

Ball, J.E., 1994, The influence of storm temporal patterns on catchment response: *Journal of Hydrology*, v. **158**, p. 285 - 303.

Barbee, G.C., and Brown, K.W., 1986, Comparison between suction and free- drainage soil solution samplers: *Soil Science*, v. **141**, no. 2, p. 149-154.

Barnes, C.J., and Allison, G.B., 1988, Tracing of water movement in the unsaturated zone using isotopes of hydrogen and oxygen: *Journal of Hydrology*, v. **100**, p. 143 - 176.

Best, G.R. and Monk, C.D., 1975, Cation flux in hardwood and white pine watershed in '*Mineral cycling in S.E. ecosystems*', Ed F.G. Howell, J.B. Gentry, M.H. Smith, US Energy R and D Acid precipitation: effects in ecological systems, H26

Betson, R.P. and Marius, J.B., 1969, Source area to storm runoff, *Water Resources Research*, **5**, p 574 - 572

Betson, R.P., and Mc Master, W.M., 1975, Nonpoint source mineral water quality model: *Water Pollution Control Federation Journal*, v. **47**, no. 10, p. 2461 - 2473.

Beven, J.J., 1989, Changing ideas in hydrology: The case of physically based models: *Journal of Hydrology*, v. **105**, p. 157 - 172.

Beven, K., and Germann, P., 1981, Water flow in soil macropores : II: A combined flow model: *Journal of Soil Science*, v. **32**, p. 15 - 29.

Beven, K.J., and Germann, P., 1982, Macropores and water flow in soils: *Water Resources Research*, v. **18**, no. 5, p. 1311 - 1325.

Billet, M.F., and Cresser, M.S., 1992, Predicting stream-water quality using catchment and soil chemical characteristics: *Environmental Pollution*, v. **77**, p. 263 - 268.

Bishop, K.H., Grip, H., O;Neil, A, 1990, The origins of acid runoff in a hillslope during storm events, *Journal of Hydrology*, **116**, p 35 - 61

Bonta, J.V., and Rao, A.R., 1994, Seasonal distributions of peak flows from small agricultural watersheds: *Journal of Irrigation and Drainage Engineering*, v. **120**, no. 2, p. 422 - 439.

Bouma, J., 1981, Soil morphology and preferential flow along macropores: *Agric. water monalogue*, v. **3**, p. 235 - 250.

Bredhoeft, J.D. and Papadopulus, I.S., 1965, Rates of vertical groundwater movement estimates from the earths thermal profile: *Water Resources Research*, v. 1, no. 12, p. 325 - 328.

Bren, L.J., and Turner, A.K., 1985, Hydrologic behaviour of a small forested catchment: *Journal of Hydrology*, v. 76, p. 333 - 350.

Brown, G.W., 1969, Predicting temperatures of small streams: *Water Resources Research*, v. 5, no. 1, p. 68 - 75.

Burgess, R.L., 1984, Effects of acidic deposition on forest ecosystems in the Northeastern United States: An evaluation of current evidence: College of Environmental Science and Forestry; State University of New York ESF 84-016.

Burykin, A.M., 1957, Seepage of water from soils in mountainous regions of the humid sub-tropics: *Pochvovedine*, v. 12, p. 90 - 97.

Buttle, J.M., 1994, Isotope hydrograph separations and rapid delivery of pre-event water from drainage basins: *Progress in Physical Geography*, v. 18, p. 16 - 41.

Cantrell, K.J., 1989, Role of Soil organic and carbonic acids in the acidification of forest streams and soils, Georgia Institute of Technology. Ph.D Thesis

Cappellato, R., 1991, Atmospheric deposition, canopy interactions and nutrient cycling in adjacent deciduous and coniferous forests of the Georgia Piedmont, Emory University, Atlanta, Georgia.

Cappellato, R., Peters, N.E., and Ragsdale, H.L., 1993, Atmospheric deposition, canopy interactions and nutrient cycling in adjacent deciduous and coniferous forests in the Georgia Piedmont: *Canadian Journal of Forest Research*, v. 23. P 47 - 58

Carter, M.E.B., 1978, A community analysis of the Piedmont deciduous forest of Panola Mountain State Conservation Park., Emory University, Atlanta, Georgia, Masters.

Cartwright, K., 1970, Groundwater discharge in the Illinois Basin as suggested by temperature anomalies: *Water Resources Research*, v. 6, no. 3, p. 912 - 918.

Casey, H., and Neal, C., 1984: Abiological controls on silica on chalk streams and groundwaters, *in* *The Third International Symposium on Interactions between Sediments and Water*, Geneva, Switzerland, Springer-Verlag, p. 327 - 338.

Cerny, J., and Kacura, G., 1989, Groundwater contribution to surface runoff form the small forested catchment - Mlynaruv Luh (Czechoslovakia), *in 'Water-Rock Interaction'*, ed. Miles, : Rotterdam, Balkema, p. 145 - 148.

Chapman, J.B., Ingraham, N.C., and Hess, J.W., 1992, Isotopic investigation of infiltration and unsaturated zone flow processes at Carlsbad Cavern, New Mexico: *Journal of Hydrology*, v. **133**, p. 343 - 363.

Childs, E.C., and Bybordi, M., 1969, The vertical movement of water in stratified porous material : 1 infiltration: *Water Resources Research*, v. **5**, no. 2, p. 446 - 459.

Chorley, M.J.K., 1967, Throughflow, overland flow and erosion: *Bull. IASH*, v. **12**, no. 3, p. 5 - 21.

Christophersen, N., Neal, C., Hooper, R.P., Vogt, R.D., Andersen, S., 1990, Modelling streamwater chemistry as a mixture of soil water end-members - a step towards second generation acidification models: *Journal of Hydrology*, v. **116**, p. 307 - 320.

Christophersen, N., and Neal, C., 1990, Linking hydrological, geochemical and soil chemical processes on the catchment scale: An interplay between modelling and field work: *Water Resources Research*, v. **26**, no. 12, p. 3077 - 3086.

Christophersen, N., and Wright, R.F., 1981, Sulphate budget and a model for sulphate concentrations in stream water at Birkenes, a small forested catchment in Southernmost Norway: *Water Resources Research*, v. **17**, no. 2, p. 377 - 389.

Clothier, B.E., and White, I., 1981, Measurement of sorptivity and soil diffusivity in the field: *Soil Science Society of America Journal*, v. **45**, p. 241 - 245.

Cole, D.W., and Rapp, M., 1981, Elemental cycling in forest ecosystems, *in 'Dynamic properties of forest ecosystems'*, ed. Reichle, D.E.: London, Cambridge University Press, p. 341 - 409.

Cosby, B.J., Wright., R.F., Hornberger, G.M., Galloway, J.N., 1985, Modeling the effects of acidic deposition : assessment of a lumped parameter model of soil water and streamwater chemistry: *Water Resources Research*, v. **21**, no. 1, p. 51 - 63.

Cosby, B.J., 1986, Modeling the effects of acidic deposition : Control of long term sulphur dynamics by soil sulphate adsorption: *Water Resources Research*, v. **22**, no. 8, p. 1283 - 1291.

Cosby, B.J., Wright, R.F., Hornberger, G.M., Galloway, J.N, 1985, Modeling the effects of acidic deposition : estimation of long term water quality responses in a small forested catchment: *Water Resources Research*, v. **21**, no. 11, p. 1591 - 1601.

Crockford, R.H., Richardson, D.P., Sageman, R., 1996, Chemistry of rainfall, throughfall and stemflow in a eucalypt forest and a pine plantation in S.E. Australia: I Rainfall: *Hydrological Processes*, v. **10**, p. 1 - 11.

Crockford, R.H., Richardson, D.P. Sageman, R., 1996, Chemistry of rainfall, throughfall and stemflow in a eucalypt forest and a pine plantation in S.E. Australia: II: Throughfall: *Hydrological Processes*, v. **10**, p. 13 - 24.

Crockford, R.H., Richardson, D.P., Sageman, R., 1996, Chemistry of rainfall, throughfall and stemflow in a eucalypt forest and a pine plantation in S.E. Australia: III Stemflow and total inputs: *Hydrological Processes*, v. **10**, p. 25 - 42.

Cronan, C.S.. 1985, Biochemical influences of vegetation and soil on ILWAS: *Water, Air and Soil Pollution*, v. **26**, p. 355 - 371.

Cronan, C.S., 1985, Chemical weathering and solution chemistry in acid forest soils : Differential influence of soil type, biotic processes and H deposition, *in 'The Chemistry of Weathering'*, ed. Drever, J.I., D. Reidel Publishing Company, p. 175 - 195.

Cronan, C.S., 1985, Comparative effects of precipitation acidity on three forest soils: carbon cycling processes: *Plant and Soil*, v. **88**, p. 101 - 112.

Cronan, C.S., and Aiken, G.R., 1985, Chemistry and transport of soluble humic substances in forested watersheds of the Adirondack Park, New York: *Geochimica et Cosmochimica Acta*, v. **49**, p. 1697 - 1705.

Cryer, 1986, Atmospheric solute inputs, *in 'Solute Processes'*, ed. Trudgil, S.T., : New York, Wileys, p. 15 - 34.

Dansgaard, W., 1964, The abundance of O^{18} in atmospheric water and water vapour: *Tellus*, v. **4**, p. 461 - 469.

David, M., Vance, G., and Kahl, J., 1992, Chemistry of dissolved organic carbon and organic acids in 2 streams draining forested watersheds: *Water Resources Research*, v. **28**, p. 389 - 396.

David, M.B., Fasth, W.J., and Vance, G.F., 1991, Forest soil response to acid and salt additions of sulphate : I : Sulphur constituents and net retention: *Soil Science*, v. **151**, no. 2, p. 136 - 145.

David, M.B., and Gertner, G.Z., 1987, Sources of variation in soil solution collected by tension plate lysimeters: *Canadian Journal of Forest Research*, v. **17**, p. 190 - 193.

Davis, S.N., 1964, Silica in streams and ground water: *American Journal of Science*, v. **262**, p. 870 - 891.

Destouni, G., Sassner, M., and Jensen, K.H., 1994, Chloride migration in heterogeneous soil 2: Stochastic modeling: *Water Resources Research*, v. **30**, no. 3, p. 747 - 758.

Dethier, D.P., Jones, S.B., Feist, T.P., and Ricker, J.E., 1988, Relations among sulphate, aluminium, iron, dissolved organic carbon, and pH in upland forest soils of Northernmost Massachusetts: *Soil Science Society of America Journal*, v. **52**, no. 2, p. 506 - 512.

Dewalle, D.R., and Sharpe, W.E., 1988, Biogeochemistry of two Appalachian deciduous forest sites in relation to episodic stream acidification: *Water, Air and Soil Pollution*, v. **40**, p. 143 - 156.

DeWalle, D.R., and Swistock, B.R., 1994, Differences in O-18 content of throughfall and rainfall in hardwood and coniferous forests: *Hydrological Processes*, v. **8**, p. 75 - 82.

Dewalle, D.R., Swistock, B.R., and Sharpe, W.E., 1988, Three-component tracer model for stormflow on a small Appalachian forested catchment: *Journal of Hydrology*, v. **104**, p. 301 - 310.

Dincer, T., Payne, B.R., Florkowski, T., Martinec, J., and Tongiorgi, E., 1970, Snowmelt runoff from measurements of tritium and O-18: *Water Resources Research*, v. **6**, no. 1, p. 110 - 124.

Driscoll, C.T., Fuller, R.D., and Schecher, W.D., 1989, The role of organic acids in the acidification of surface waters in the Eastern U.S.: *Water, Air and Soil Pollution*, v. **43**, p. 21- 40.

Driscoll, C.T., and Lickens, G.E., 1982, Hydrogen ion budget of an aggrading forested ecosystem: *Tellus*, v. **34**, p. 382 - 292.

Dunne, T.; Black, R.D., 1970, Partial area contributions to storm runoff in a small New England watershed: *Water Resources Research*, v. **6**, p. 1296 - 1311.

Durand, P., Neal, C., Lelong, F., and Didon-Lescott, J.F., 1992, Effects of land-use and atmospheric input on stream and soil chemistry : field results and long-term simuation at Mont Lozere

(Cevennes National Park, Southern France): *The Science of the Total Environment*, v. **119**, p. 191 - 209.

Durand, P., Neal, M., and Neal, C., 1993, Variations in stable oxygen isotope and solute concentrations in small submediterranean montane streams: *Journal of Hydrology*, v. **144**, p. 283 - 290.

Durand, P., Robson, A., and Neal, C., 1992, Modelling the hydrology of submediterranean montane catchments (Mont - Lozere, France) using TOPMODEL : inital results: *Journal of Hydrology*, v. **139**, p. 1 - 14.

Easthouse, K.B., Mulder, J., Christophersen, N., and Seip, H.M., 1992, Dissolved organic carbon fluctuations in soil and stream water during hydrological conditions at Birkenes, Southern Norway: *Water Resources Research*, v. **28**, no. 6, p. 1585 - 1596.

Eckhardt, B.W., and Moore, T.R., 1990, Controls on dissolved carbon concentrations in streams, Southern Quebec: *Canadian Journal of Fisheries and Aquatic Science*, v. **47**, p. 1537 - 1544.

Edwards, W.M.Shipitalo, M.J; Owens, L.B; Norton, L.D., 1989, Water and nitrate movement in earthworm burrows within long-term non-tilll corn fields: *Journal of soil water conservation*, v. **44**, p. 240 - 243.

England, C.B., 1974, A technique using porous cups for water sampling at any depth in the unsaturated zone: *Water Resources Research*, v. **10**, no. 6, p. 1049.

Eriksson, E., 1955, Airborne salts and the chemical composition of new waters: *TELLUS*, v. **7**, p. 243 - 250.

Eshleman, K.N., 1988, Prediciting regional episodic acidification of surface waters using empirical models: *Water Resources Research*, v. **24**, no. 7, p. 1118 - 1126.

Eshleman, K.N; Pollard, J.S; O'Brien, A.K, 1993, Determination of contributing areas of saturation overland flow from chemical hydrograph separations, *Water Resources Research*, **29**, p 3577 - 3587

Farrell, J.D., and Ware, S., 1991, Edaphic factors and forest vegetation in the Piedmont of Virginia: *Bulletin of the Torrey Botanical Club*, v. **118**, no. 2, p. 161 - 169.

Fernandez, I.J., 1987, Vertical trends in the chemistry of forest soil microcosms following

experimental acidification: *Maine Agricultural Experiment Station Technical Bulletin*, v. **126**, p. 1 - 19.

Flury, M., Fluhler, H., Jury, W.A., and Leuenberger, J., 1994, Susceptibility of soils to preferential flow of water: A field study, *Water Resources Research*, v. **30**, no. 7, p. 1945 - 1954.

Ford, E.M., and Deans, J.D., 1978, The effects of canopy structure on stemflow, throughfall and interception loss in a young Sitka Spruce plantation: *Journal of Applied Ecology*, v. **15**, p. 906 - 917.

Ford, T.E., and Naiman, R.J., 1989, Groundwater: surface water relationships in boreal forest watersheds : Dissolved organic carbon and inorganic nutrient dynamics: *Canadian Journal of Fish and Aquatic Sciences*, v. **46**, no. 1, p. 41 - 49.

Fowler, D, 1984 Transfer of terrestrial surface, *Phils Trans R. Soc. Lond. B* V **305**, p 281 - 297

Freeze, R.A., 1974, Streamflow generation: *Review of Goephysical Space Physics*, v. **12**, p. 627 - 647.

Fritz, P., Cherry, J.A., Weyer, K.U., and Sharpe, W.E., 1976, Storm runoff analyses using environmental isotopes and major ions, *in 'Interpretation of Environmental Isotope and Hydrochemical data in Groundwater Hydrology'*, ed., IAEA: Vienna, p. 111 - 131.

Gash, J.H.C. 1979, An analytical model of rainfall interception in forests, *Q.J.R. Meteorol. Soc*, v **105**, p 43 - 55

Gash, J.H.C., Wright, I.R.; Lloyd, C.R., 1980, Comparative estimates of interception loss from three coniferous forests in Great Britain: *Journal of Hydrology*, v. **48**, p. 89 - 105.

Gaskin, J.W., Dowd, J.F., Nutter, W.L., and Swank, W.T., 1989, Vertical and lateral components of soil nutrient flux in a hillslope: *Journal of Environmental Quality*, v. **18**, no. 4, p. 403 - 410.

Germann, P., and Beven, K., 1981, Water flow in soil macropores : I : An experimental approach: *Journal of Soil Science*, v. **32**, p. 1 - 13.

Germann, P., and Beven, K., 1981, Water flow in soil macropores : III: A statistical approach: *Journal of Soil Science*, v. **32**, p. 31 - 39.

Germann, P., and Beven, K.J., 1986, A distribution function approach to water flow in soil macropores based on kinematic wave theory: *Journal of Hydrology*, v. **83**, p. 173 - 183.

Germann, P.F., 1985, Kinematic wave approach to infiltration and drainage into and from soil macropores: *Transactions of the ASAE*, v. *28*, no. 3, p. 745 - 749.

Germann, P.F., 1990, Preferential flow and the generation of runoff: 1. Boundary layer flow theory: *Water Resources Research*, v. **26**. no. 12, p. 3055 - 3063.

Gerritse, R.G., and George, R.J., 1988, The role of soil organic matter in the geochemical cycling of chloride and bromide: *Journal of Hydrology*, v. **101**, p. 83 - 95.

Gilliam, F.S., and Richter, D., 1991, Transport of metal cations through a nutrient poor forest ecosystem: *Water, Air and Soil Pollution*, v. **57 - 58**, p. 279 - 287.

Goudie, A., Atkinson, .B.W., Gregory, K.J., Simmons, I.G., Stoddard, .D.R., Sugden,D., 1985, *The encyclopaedic dictionary of physical geography* (1 ed.): New York, Blackwells, v. 1, 528 p.

Greenland, P.C., 1971, Dilution gauging in the Nant Gevig: *Subsurface Hydology* Report No 27.Institute of Hydrology, Wallingford, England

Harr, R.D., 1977, Water flux in soil and sub-soil on a steep forested slope: *Journal of Hydrology*, v. 33, p. 37 - 58.

Harrow, A.J., 1994, Spatial variations in throughfall chemistry at the small plot scale: *Journal of Hydrology*, v. **158**, p. 107 - 122.

Heimovaara, T.J., 1994, Frequency domain analysis of time domain reflectometry waveforms : 1 : Measurement of the complex dielectric permittivity of soils: *Water Resources Research*, v. 30, no. 2, p. 189 - 199.

Heimovaara, T.J., Bouten, W., and Verstraten, J.M., 1994, Frequency domain analysis of time domain reflectometry waveforms : 2 : A four-component complex dielectric mixing model for soils: *Water Resources Research*, v. **30**, no. 2, p. 201- 209.

Henkelrath, W.N., Hamburg, S.P., and Murphy, F., 1991, Automatic, real-time monitoring of soil moisture in a remote field area with Time Domain Reflectometry: *Water Resources Research*, v. **27**, no. 5, p. 857 - 864.

Herlihy, A.T., Kaufman, P.R., Church, M.R., Winginton, P.S., Webb, J.R., and Sale, M.J., 1993, The effects of acidic deposition on streams in the Appalachian Mountains and Piedmont region of Mid - Atlantic USA: *Water Resources Research*, v. **29**, no. 8, p. 2687 - 2703.

Herwitz, S.R., 1987, Raindrop impact and water flow on the vegetative surfaces of trees and effects on stemflow and throughfall generation: *Earth Surface Processes and Landforms*, v. **12**, p. 425 - 432.

Hewlett, J.D., and Hibbert, A.R., 1967, Factors affecting the response of small watersheds to precipitation in humid areas, *in 'Forest Hydrology Proceedings of the International Symposium on Forest Hydrology'* eds., Sopper, W.E., and Hull, H.W.: Pennsylvania.

Hicks, D.J., and Chabot, B.F., 1985, Deciduous Forests: Physiological ecology of North American Plant communities.

Higgins, M.W., Atkins, R.L., Crawfrd, T.J., Brooks, R., Cook, R.B, 1988, The structure , stratigraphy and technostratigraphy, and evolution of the southernmost part of the Appalachian Oregon: *U.S. Geological Survey Professional Paper*, v. **1475**, p. pp 173.

Hoefs, J., 1973, *Stable Isotope Chemistry: Minerals, Rocks and Inorganic Materials*: Berlin/New York, Springer-Verlag, p. 142.

Hooper, A.P., and Christophersen, N., 1992, Predicting episodic stream acidification in the South East USA, combining a long term acidification model and the end member mixing concept: *Water Resources Research*, v. **28**, no. 7, p. 1983 - 1990.

Hooper, R., Christopherson, and Peters, N.E., 1990, Modeling streamwater chemistry as a mixture of soil water end members - an application to the Panola Mountain Catchment, Georgia, USA: *Journal of Hydrology*, v. **116**, p. 321 - 343.

Hooper, R.P., and Shoemaker, C.A., 1986, A comparison of chemical and isotopic hydrograph separation: *Water Resources Research*, v. **22**, no. 10, p. 1444 - 1454.

Hornberger, G.M., Beven, K.J., Cosby, B.J., and Sappington, D.E., 1985, Shenandoah Watershed Study : Calibration of a topography-based, variable contributing area hydrological model to a small forested catchment: *Water Resources Research*, v. **21**, no. 12, p. 1841 - 1850.

Hornberger, G.M., Beven, K.J., and Germann, P.F., 1990, Inferences about solute transport in macroporous forest soils from time series models: *Geoderma*, v. **46**, p. 249 - 262.

Hornberger, G.M., Germann, P.F., and Beven, K.J., 1991, Throughflow and solute transport in an isolated sloping soil block in a forested catchment: *Journal of Hydrology*, v. **124**, p. 81 - 99.

Horst, 1989, Bulk precipitation deposition of inorganic chemicals in forest areas and its influence on water quality in Germany: *IHAS Publication*, v. 179.

Horton, R.E., 1933, The role of infiltration in the hydrological cycle: *American Geophysical Union Transactions*, v. **14**, p. 446 - 460.

Huntington, T.G., Hooper, R.P., and Aulenbach, B.T., 1994, Hydrologic processes controlling sulphate mobility in a small forested catchment: *Water Resources Research*, v. **30**, no. 2, p. 283 - 295.

Huntington, T.G., Hooper, R.P., Peters, N.E., Bullen, T.D., Kendall, C, 1993. Water, Energy and Biogeochemical Budgets Investigation at Panola Mountain Research Watershed, Stockbridge. Georgia - A Research Plan. *U.S. Geological Survey Open File Report* **93 - 55**

Hursh, C.R., 1936, Storm water and adsorption, *in 'Report of the comittee on adsorption and transpiration'*, American Geophyiscal Union., p. 296 - 302.

Hursh, C.R., 1944, *Report of the subcommittee on subsurface flow*: American Geophysical Union Transactions, v. **5**, p. 743 - 746.

Jabro, J.D., Lotse, E.G., Fritton, D.D., and Baker, D.E., 1994, Estimation of preferential movement of bromide tracer under field conditions: *Journal of Hydrology*, v. **156**, p. 61 - 71.

Jakeman, A.J., and Hornberger, G.M., 1993, How much complexity is warrented in a rainfall - runoff model?: *Water Resources Research*, v. **29**, no. 8, p. 2637 - 2649.

Jamison, V.C., Peters, D.B., 1967, Slope length of claypan soil effects runoff: *Water Resources Research*, v. **3**, no. 2, p. 471 - 480.

Jardine, P.M., Weber, N.L., and McCarthy, J.F., 1989, Mechanisms of dissolved organic carbon adsorption on soil: *Soil Science Society of America*, v. **53**, p. 1378 - 1385.

Jardine, P.M., Wilson, G.V., and Luxmoore, R.J., 1990, Unsaturated solute transport through a forest soil during rain storm events: *Geoderma*, v. **46**, p. 103 - 118.

Jemison Jr, J.M., and Ford, R.H., 1992, Estimation of zero - tension pan lysimeter colllection efficiency: *Soil Science*, v. **154**, no. 2, p. 85 - 94.

Jenkins, A., Ferrier, R.C., Harriman, R., and Ogunkoya, Y.O., 1994, A case study in catchment

hydrochemsitry: Conflicting interpretations from hydrological and chemical observations: *Hydrological Processes*, v. **8**, p. 335 - 349.

Johnson, D.W., 1969, A working model for the variation in stream water chemistry at the Hubbard Brook Experimental Forest, New Hampshire: *Water Resources Research*, v. **5**, no. 6, p. 1353 - 1363.

Johnson, D.W., 1986, Sulphur cycling in five forested ecosystems: *Water, Air and Soil Pollution*, v. **30**, p. 965 - 979.

Johnson, D.W., 1991, Soil changes in forest ecosystems : evidence for and probable causes: *Proceedings of the Royal Society of Edinburgh*, v. **97B**, p. 81 - 116.

Johnson, D.W., 1989, Site Description, *in 'Analysis of biochemical cycling processes in Walker Branch Watershed'*, ed., Johnson, D.W.: New York, Springer-Verlag, p. 233 - 300.

Johnson, D.W., Richter, D.D., Lovett, G.M., and Lindberg, S.E., 1985, The effects of acidic deposition on potassium, calcium, magnesium cycling in two deciduous forests: *Canadian Journal of forest research*, v. **15**, p. 773 - 782.

Johnson, D.W., Richter, D.D., Van Miegroet, H., and D.W., C., 1983, Contributions of acid deposition and natural processes to cation leaching from forest soils : A review: *APCA Journal*, v. **33**, no. 11.

Johnson, D.W., and Todd, D.E., 1984, Relationships among Fe, Al, C and SO_4 in a variety of forest soils: *Soil Science Society of America*, v. **47**, p. 792 - 800.

Johnson, J.O., and Reuss, D.W., 1984, Soil mediated effects of atmospherically deposited sulphur and nitrogen: *Philosophical transactions of the Royal Society, London*, v. **305**, p. 383 - 392.

Johnson, R.C., 1990, Interception, throughfall and stemflow in a forest in highland Scotland and the comparison with other upland forests in UK: *Journal of Hydrology*, v. **118**, p. 281 - 287.

Johnston, C.D., 1987, Distribution of environmental chloride in relation to subsurface hydrology: *Journal of Hydrology*, v. **94**, p. 67 - 88.

Jones, A., 1971, Soil piping and channel initiation: *Water Resources Research*, v. 7, p. 602 - 610.

Jones, G.F, 1969, Determination of the groundwater component of peak discharge from the chemistry

of total runoff: *Water Resources Research*, v. **5**, p. 438 - 445.

Jones, J.J., 1987, The initiation of natural drainage networks: *VET*, v. **2**, p. 207 - 245.

Jordan, J.P., 1994, Spatial and temporal variability of stormflow generation processes on a Swiss catchment: *Journal of Hydrology*, v. **153**, p. 357 - 382.

Juang, C.E., 1963, Air chemistry and radioactivity: *International Geophysics Series*: New York. Academic Press, v. **4**, 365 p.

Juang, F.H.T., and Johnson, N.M., 1967, Cycling of chloride through a forested watershed in New England: *Journal of Geophysical Research*, v. **72**, no. 22, p. 5641 - 5646.

Kayane, I., and Kaihotsu, I., 1988, Some experimental results concerning rapid water table responses to surface phenomena: *Journal of Hydrology*, v. **102**, p. 215 - 234.

Kennedy, V.C., Kendall, C., Zellweger, G.W., Wyerman, T.A., and Avanzino, R.J., 1986, Determination of the components of stormflow using water chemistry and environmental isotopes, Mattole River Basin, California`: *Journal of Hydrology*, v. **84**, p. 107 - 140.

Kerekes, 1986, Effects of forest canopy on throughfall precipitation chemistry: *IAHS* publications, v. **179**.

Kerekes, 1986, Organic vs anthropogenic acidity of tributaries of the Kejimkjik watersheds in Western Nova Scotia: *Water, Air and Soil Pollution*, v. **31**, p. 165 - 173.

Kerekes, 1986, Sources of acidity and sulphate in wetlands and lakes in Nova Scotia: *Water, Air and Soil Pollution*, v. **31**, p. 207 - 214.

Kirchner, J.W., 1992, Heterogeneous geochemistry of catchment acidification: *Geochimica et Cosmochimica Acta*, v. **56**, p. 2311 - 2327.

Kirkby, M.K., Chorley, R.Y., 1967, Throughflow, overland flow and erosion, *Bull. IASH* **12** (3) p 5 - 21

Kloeti, 1989, Effects of forest canopy on throughfall precipitation chemistry: *IHAS Publication*, v. **179**.

Komor, S.C., Emerson, D.G., 1994, Movement of water, solutes and stable isopotes in the unsaturated

zones of two sand plains in the upper Mid West, *Water Resources Research*, v **30**, no 2, p 253 - 257

Knapp, B.J., 1980, Infiltration and storage of soil water, *in 'Hillslope Hydrology'*., ed., Kirkby, M.J, John Wiley and Sons, p. 43 - 72.

Knight, J.H., 1992, Sensitivity to Time Domain Reflectometry measurements to lateral variations in soil water content: *Water Resources Research*, v. **28**, no. 9, p. 2345 - 2352.

Knoepp, J.D., and Swank, W.T., 1994, Long term soil chemistry changes in aggrading forest ecosystems: *Soil Science Society of America Journal*, v. **58**, p. 325 - 331.

Langdale, G.W., Leonard, R.A., Fleming, W.G., and Jackson, W.A., 1979, Nitrogen and Chloride movement in small upland Piedmont Watersheds : II : Nitrogen and Chloride transport in runoff: *Journal of Environmental Quality*, v. **8**, no. 1, p. 57 - 63.

Lawrence, G.B., and Fernandez, I.J., 1993, A reassessment of areal variability of throughfall deposition measurements: *Ecological applications*, v. **3**, no. 3, p. 473 - 480.

Lawrence, J.R., 1987, Use of contrasting D/H ratios of snows and groundwaters of Eastern New York State in watershed evaluation: *Water Resources Research*, v. **23**, no. 3, p. 519 - 521.

Leaney, F.W., Smettem, K.R.J., and Chittleborough, D.J., 1993, Estimating the contribution of preferential flow to subsurface runoff from a hillslope using deuterium and chloride: *Journal of Hydrology*, v. **147**, p. 83 - 103.

Ledieu, J., De Riddler, P., De Clerck, P., and Dautrebande, S., 1986, A method of measuring soil moisture by time-domain reflectometry: *Journal of Hydrology*, v. **88**, p. 319 - 328.

Lindberg, J.E., Lovett, G.M., Richter, D.D., and Johnson, D.W., 1986, Atmospheric deposition and canopy interactions of major ions in a forest: *Science*, v. **231**, p. 141 - 145.

Lindberg, S.E., and Lovett, G.M., 1983, Application of surrogate surface and leaf extraction methods to estimation of dry deposition to plant canopies, *in 'Precipitation scavenging, dry deposition, resuspension'* , eds Prippacher, H.R., Semonin, R.G., and Slinn, W.G.N: New York, Elsevier, p. 837 - 848.

Lindberg, S.E., Page, A.L., Norton, S.A., 1990, Acidic precipitation : Volume 3 : sources, deposition and canopy interactions, *Advances in Environmental Sciences*, Springer - Verlag,

p. 332.

Lindstrum, G., and Rodhe, A., 1986, Modelling water exchange and transit times in till basins using O-18: *Nordic Hydrology*, v. **17**, p. 325 - 334.

Loustau, D., Begigier, P, Granier, A., Hadj Moussa, F. El, 1992, Interception loss, throughfall and stemflow in a maritime pine stand: I: Variability of throughfall and stemflow beneath the pine canopy, *Journal of Hydrology*, v **138**, p 469 - 485

Loustau, D., Bergigier, , Granier, A, 1992: Interception loss, throughfall and stemflow in a maritime pine stand: II: An application of Gash's analytical model of interception, *Journal of Hydrology*, v **132**, p 425 - 432

Lundstrum, V.S., 1993, The role of organic acids in the solution chemistry of a podzolised soil: *Journal of Soil Science*, v. **44**, p. 121 - 133.

Luxmoore, R.J., 1981, Micro-, meso-, and macroporosity of soil: *Soil Science Society of America Journal*, v. **45**, p. 671.

Luxmoore, R.J., Wullschleger, S.D., and Hanson, P.J., 1993, Forest responses to CO_2 enrichment and climate warming: *Water, Air and Soil Pollution*, v. **70**, p. 309 - 323.

Lynch, J.A., 1989, Hydrologic controls on sulphate mobility in a forested watershed: *Water Resources Research*, v. **25**, no. 7, p. 1695 - 1703.

MacDonald, N.W., Witter, J.A., Burton, A.J., Pregitzer, K.S., and Richter, D.D., 1993, Relationships among atmospheric deposition, throughfall and soil properties in oak forest ecosystems: *Canadian Journal of Forest Research*, v. **23**, p. 2348 - 2357.

Mahendrappa, M.K., 1990, Partioning of rainwater and chemicals into throughfall and stemflow in different forest stands: *Forest Ecology and Management*, v. **30**, p. 65 - 72.

Martinec, J., Siegenthaler, H., Oescheger, H., and Tongiorgi, E., 1974, New insight into the runoff mechanism by environmental isotopes, *in 'Proceedings of the Symposium on Isotope techniques in Groundwater hydrology'*, ed., IAEA: Vienna, p. 129 - 143.

Matsuo, S., and Friedman, I., 1967, Deuterium content in fractionally collected rainwater: *Journal of Geophysical Research*, v. **72**, p. 6374 - 6376.

Maule, C.P., Chanasyk, D.S., and Muenlenbachs, K., 1994, Isotopic determination of snow-water contribution to soil water and groundwater: *Journal of Hydrology*, v. **155**, p. 73 - 91.

Maule, C.P., and Stein, J., 1990, Hydrologic flow path definition and partioning of spring meltwater: *Water Resources Research*, v. **26**, no. 12, p. 2959 - 2970.

Mazor, E., George, R., 1992, Marine airborne salts applied to trace evapotranspiration, local recharge and lateral groundwater flow in western Australia: *Journal of Hydrology*, v. **139**, no. 63 - 77.

McDonnell, J.J., 1990, A rationale for old water discharge through macropores in a steep, humid catchment: *Water Resources Research*, v. **26**, no. 11, p. 2821 - 2832.

McDonnell, J.J., Bonell, M., Stewart, M.K., and Pearce, A.J., 1990, Deuterium variations in storm rainfall: Implications for stream hydrograph separation: *Water Resources Research*, v. **26**, no. 3, p. 455 - 458.

McDonnell, J.J., Stewart, M.K., and Owens, I.F., 1990, Effect of within and between storm subsurface mixing on stream episodic isotopic response: *Journal of Hydrology*, v. 00, no. 00, p. 00.

McIntosh, J., McDonnell, J.J., Peters, N.E., 1997, A tracer study of preferential flow in large undisturbed cores from the Georgia Piedmont, in prep

McLord, J.T., Stephens, D.B., 1987, Lateral moisture flow beneath a sandy hillslope without an apparent impeding layer: *Hydrological Processes*, v. **1**, p. 225 - 238.

McShane, M.C., and Carlile, W.T., 1983, The effect of collector size on forest litter - fall collection and analysis: *Canadian Journal of Forestry Research*, v. **13**, p. 1037 - 1042.

McWilliams, E.L., and Sealy, R.L., 1987, Atmospheric chloride : Its implication for foliar uptake and damage: *Atmospheric Environment*, v. **21**, no. 12, p. 2661 - 2665.

Meyer, J.L., and Lichens, G.E., 1979, Transport and transformations of phosphorus in a forest stream ecosystem: *Ecology*, v. **60**, p. 1255 - 1269.

Meyer, J.L., and Tate, C.M., 1983, The effects of watershed disturbance on dissolved organic carbon dynamics of a stream: *Ecology*, v. **64**, no. 1, p. 33 - 49.

Miegrot, 1985, Acidification sources in red alder and douglas fir stands - importance of nitrification: *Soil Science Society of America*, v. **49**, p. 1274 - 1279.

Moore, T.R., 1989, Dynamics of dissolved organic carbon in forested and disturbed catchments, Westland, New Zealand :1: Miami: *Water Resources Research*, v. **25**, no. 6, p. 1321 - 1330.

Moore, T.R., Desouza, W., and Koprivjak, J.F., 1992, Controls on the sorption of dissolved organic carbon by soils: *Soil Science*, v. **154**, p. 1290 - 129.

Moore, T.R., and Jackson, R.J., 1989, Dynamics of dissolved organic carbon in forested and disturbed catchments, Westland, New Zealand :2: Larry River: *Water Resources Research*, v. **25**, no. 6, p. 1331 - 1339.

Mosley, M.P., 1974, Experimental study of rill erosion: *Transactions of American Society of American Engineers*, v. **17**, p. 909 - 913.

Mosley, M.P., 1979, Streamflow generation in a forested watershed, New Zealand: *Transactions of American Society of American Engineers, v.* **15**, no. 795 - 806.

Mosley, M.P., 1982, Subsurface flow velocities through selected forest soils, South Island, New Zealand: *Journal of Hydrology*, v. **55**, p. 65 - 92.

Mulder, 1990, Water flow paths and hydrochemical controls on the Birkenes Catchmnet as inferred from a rainstorm high in sea salts: *Water Resources Research*, v. **26**, p. 611 - 622.

Mulder, J., Pijpers, M., and Christophersen, N., 1989, Water flow paths and the spatial distribution of soils and exchangeable cations in an acid rain - impacted and a pristine catchment in Norway: *Water Resources Research*, v. **27**, no. 11, p. 2919 - 2928.

Mulholland, P.J., Wilson, G.V., and Jardine, P.M., 1990, Hydrogeochemical response of a forested watershed to storms: Effects of preferential flow along shallow and deep pathways: *Water Resources Research*, v. **26**, no. 12, p. 3021 - 3036.

Mulholland, P.J, Wilson, G.V., Jardine, P.M, 1993, Hydrometric and stream chemical evidence of three stream flowpaths in Walker Branch Watershed, *Journal of Hydrology*, **151**, p 291 - 316

Neal, C., Neal, M., Warrington, A., Avila, A., Pinol, J., and Roda, F., 1992, Stable hydrogen and oxygen isotope studies of rainfall and streamwater for two contrasting holm oak areas of Catalonia, northeastern Spain: *Journal of Hydrology*, v. **140**, p. 163 - 178.

Neal, C., and Rossier, P.T., 1990, Chemical studies of chloride and stable oxygen isotopes in two conifer afforested and moorland sites in the British Uplands: *Journal of Hydrology*, v. **115**, p.

269 - 283.

Neal, C., Smith, C.J., Walls, J., Billingham, P., Hill, S., and Neal, M., 1990, Comments on the hydrochemical regulation of the halogen elements in rainfall, stemflow, throughfall and streamwaters at an acidic forested area in Mid Wales.: *The Science of the Total Environment*, v. **91**, p. 1 - 11.

Neilson, D.R., Van Genuchten, M.T.; Biggar, J.W., 1986, Water flow and solute transport processes in the unsaturated zone: *Water Resources Research*, v. **22**, no. 9, p. 895 - 1083.

Nilsson, L.O., 1993, Carbon sequestration in Norway Spruce in South Sweden as influenced by air pollution , water availability and fertilization: *Water, Air and Soil Pollution*, v. **70**, p. 177 - 186.

Nodvin, S.C., Driscoll, C.T., and Lichens, G.E., 1986, The effect of pH on sulphate adsorption by a forest soil: *Soil Science*, v. **142**, no. 2, p. 69 - 75.

Nodvin, S.C., Driscoll, C.T., and Likens, G.E., 1986, Simple partioning of anions and dissolved organic carbon in a forest soil: *Soil Science*, v. **142**, no. 1, p. 27 - 35.

O'Brien, K.N., 1993, Determination of contributing areas for saturation overland flow from chemical hydrograph separations: *Water Resources Research*, v. **29**, p. 3577 - 3587.

O'Brien, K.N., Helle, C.K., Smith, J.L, 1996, Multiple tracers of shallow groundwater flow and recharge in hilly loess, *Groundwater*, **34**, p 675 - 682

Ohte, N., Tokuchi, N., Suzuki, M., and Iwatsubo, G., 1991, A numerical model for water and solute movement in forest soils and its application to Cl transport in microlysimeters, *in 'Vienna Symposium, Hydrological interactions between atmosphere, soil and vegetation'*, IAHS, p. 217 - 225.

Omoti, U., and Wild, A., 1979, Use of flourescent dyes to mark the pathways of solute movement through soils under leaching conditions: 2, field experiments.: *Soil Science*, v. **128**, p. 98 - 104.

Paniconi, C., Wood, E.F., 1993, A detailed model for simulationof catchment scale subsurface hydraulic processes, *Water Resources Research*, **6** , p 1601 - 1629

Pearce, A.J., Stewart, M.K., and Sklash, M.G., 1986, Storm runoff generation in humid headwater

catchments : 1: Where does the water come from?: *Water Resources Research*, v. **22**, no. 8, p. 1263 - 1272.

Pearson, J.A., Fahey, T.J., and Knight, D.H., 1983, Biomass and leaf area in contrstaing lodegepole pine forests: *Canadian Journal of Forest Research*, v. **14**, p. 259 - 265.

Perdue, E.M., Beck, K.C., and Reuter, J.H., 1976, Organic complexes of iron and aluminium in natural waters: *Nature*, v. **260**, no. 5550, p. 418 - 420.

Peters, N.E., 1989, Atmospheric deposition of sulphur to a granite outcrop in the Piedmont of Georgia, USA: *IAHS Publication*, v. **179**, p. 173 - 181.

Peters, N.E., Driscoll, C.T., 1991, Chloride cycling in two forested lake watersheds in the West-Central Adirondack Mountains, New York, USA: *Water, Air and Soil Pollution*, v. **59**, p. 211 - 215.

Peters, N.E., 1994, Water-quality variations in a forested Piedmont catchment, Georgia, USA: *Journal of Hydrology*, v. 00, p. 000.

Peters, N.E., and Driscoll, C.T., 1987, Sources of acidity during snow melt at a forested site in the West - Central Adirondack Mountains, New York, *in* '*Forest Hydrology and watershed management*', ed. Symposium, P.o.t.V.,, p. 99 - 108.

Peters, N.E., and Driscoll, C.T., 1989, Hydrogeologic controls of surface water chemistry in the Adirondack region of New York State: *Biogeochemistry*, v. **3**, p. 163 - 180.

Peters, N.E., and Murdock, 1985, Hydrogeochemical comparisons of an acidic - lake basin with a neutral lake basin in the Western Central Adirondack Mountains, New York: *Water, Air and Soil Pollution*, v. **26**, p. 387 - 402.

Pierce, R.S., 1967, Evidence of overland flow on forest watersheds: *Water Resources Research*, v. **3**, no. 2, p. 247 - 253.

Pilgrim, D.H., Huff., D.D., Steele, T.D., 1978, A field evaluation of sub-surface and surface runoff, *Journal of Hydrology*, **38**, p 319 - 341

Pinder, G.F., and Jones, J.F., 1969, Determination of the groundwater component of peak discharge from the chemistry of total runoff: *Water Resources Research*, v. **5**, no. 2, p. 438 - 445.

Pionke, H.B., and DeWalle, D.R., 1992, Intra- and inter-storm oxygen-18 trends in selected

rainstorms in Pennsylvania: *Journal of Hydrology*, v. **138**, p. 131 - 143.

Pionke, H.B., Gburek, W.J., and Folmar, G.J., 1993, Quantifying stormflow components in a Pennsylvania watershed when oxygen-18 input and storm conditions vary: *Journal of Hydrology*, v. **148**, p. 169 - 187.

Pionke, H.B., and Lawrence, R.R., 1991, Fate of nitrate in subsurface drainage waters, Managing nitrogen for groundwater quality and farm profitability: Madison, *Soil Science Society of America*, v. **55** p. 237 - 257.

Probst, A., Fritz, B., Ambroise, B., and Vivelle, D., 1987, Forest influence on the surface water chemistry of granitic basins receiving acid precipitation in the Vosges massif, France: *IAHS-AISH Publications*, v. **167**, p. 109 - 120.

Probst, A., Vivelle, D., Fritz, B., Ambroise, B., and Dambrine, E., 1992, Hydrochemical budgets of a small forested granitic catchment ecxposed to acid deposition : the Strengbach catchment case study (Vosges Massif, France): *Water, Air and Soil Pollution*, v. **62**, p. 337 - 347.

Rasher, C.M., Driscoll, C.T., and Peters, N.E., 1987, Concentration and fluw of solutes from snow and forest floor during snowmelt in the West- Central Adirondack region of New York: *Biogeochemistry*, v. **3**, p. 209 - 224.

Ratcliffe, E.B., Peters, N.E., Tranter, M, 1996, Hydrologic responses of soil water and groundwater in a forested hillsope, in '*Advances in Hillslope Processes*', Vol 1, Eds Anderson, M.L, Brooks, S.M., Wileys and sons, 683p

Rawitz, E.E.T., Engman, E.T., Cline, G.D., 1970, Use of the mass balance method for examining the role of soils in controlling watershed performance, *Water Resources Research*,**6** p 1115 - 1123

Reiners, W.A., and Olson, P.K., 1984, Effects of canopy components on throughfall chemistry: An experimental analysis: *Oecologia*, v. **63**, p. 320 - 330.

Reuss, J.O., 1983, Implication of the Ca - Al exchnage system for the effect of acid precipitation on soils: *Journal of Environmental Quality*, v. **12**, no. 4, p. 591 - 595.

Reuss, J.O., 1987, Chemical processes governing soil and water acidification: *Nature*, v. **339**, p. 27 - 31.

Reuss, J.O., and Johnson, D.W., 1986, Acid Deposition and the acidification of soils and waters (1

ed.): *Ecological Studies*, Springer - Verlag, v. **59**, 119 p.

Reuter, J.H., and Perdue, E.M., 1977, Importance of heavy metal-organic matter interactions in natural waters: *Geochimica et Cosmochimica Acta*, v. **41**, p. 325 - 334.

Reynolds, B., Neal, C., Hornung, M.. Hughes, S., and Stevens, P.A., 1988, Impact of afforestation on the soil solution chemistry of spodosols in Mid- Wales: *Water, Air and Soil Pollution*, v. **38**, p. 55 - 70.

Reynolds, B., and Pomeroy, A.B., 1988, Hydrogeochemistry of chloride in an upland catchment in Mid-Wales: *Journal of Hydrology*, v. **99**, p. 19 - 32.

Ribolzi, O; Valles, V; Bariaci, T, 1996, Comparison of hydrogen deconvolutions using residual alkalinity, chloride and $\delta^{18}O$ as hydrochemical tracers, *Water Resources Research*, **32**, 4, p 1051 - 1059

Richter, D.D., Comer, P.J., King, K.S., Sawin, H.S., and Wright, D.S., 1988, Effects of low ionic strength solutions on pH of acid forested soils: *Soil Science Society of America Journal*, v. **52**, no. 1, p. 261 - 264.

Riesen, D., Mdaghri Alaoui, A., and Germann, P.F., 1994, Patterns of rapid seepage at capillary potentials between 0 and -0.8 [m]: *Soil Science Society of America Journal*, v. 000, no. 000, p. 1 - 12.

Robinson, J.S., Sipapalan, M., Snell, J.D., 1995, On the relative roles of hillslope processes, channel routing and network geomorphology on the hydrogeologic response of natural catchments, *Water Resources Research*, v 3, p 3089 - 2101

Robson, A.J., Whitehead, P.G., and Johnson, R.C., 1993, An application of a physically based semi-distributed model to the Balquidder catchments: *Journal of Hydrology*, v. **145**, p. 357 - 370.

Robson, A.J., Neal, c., Ryland, G.P. Harrow, M. 1994, Spatial variations in throughfall chemistry at the small plot scale, *Journal of Hydrology*, v **158**, p 107 - 122

Rodhe, A., 1981, Spring Flood: Meltwater or Groundwater?: *Nordic Hydrology*, v. **12**, p. 21 - 30.

Roth, K., Jury, W.A., Fluhler, H., and Attinger, W., 1991, Transport of chloride through an unsaturated field soil: *Water Resources Research*, v. **27**, no. 10, p. 2533 - 2541.

Russo, D., Zaidel, J., and Laufer, A., 1994, Stocastic analysis of solute transport in partially saturated heterogeneous soil: 1. Numerical experiments: *Water Resources Research*, v. **30**, no. 3, p. 769 - 779.

Russo, D., Zaidel, J., and Laufer, A., 1994, Stochastic analysis of solute transport in partially saturated heterogeneous soil: 2. Prediction of solute spreading and breakthrough: *Water Resources Research*, v. **30**, no. 3, p. 781 - 790.

Rustad, L.E., Kahl, J.S.; Norton, S.A.; Fernadez, I.J., 1994, Underestimation of dry deposition by throughfall in mixed northern hardwood forests: *Journal of Hydrology*, v. **162**, no. 3-4, p. 319 - 336.

Ryan, 1989, Changes in chemical composition of streamwaters in two catchments in the Shenendoah National Park, Virginia, in response to atmospheric deposition of sulphur: *Water Resources Research*, v. **25**, no. 10, p. 2091 - 2099.

Sakura, Y., 1993, Groundwater flow estimated from temperatures in the Yonezawa Basin, N.E. Japan, *in 'Tracers in Hydrology'*., ed., Peters, N.E: Washington, D.C., IAHS Publication, p. 161 - 170.

Salama, R.B., Farrington, P., Bartle, G.A., and Watson, G.D., 1993, Distribution of recharge and discharge areas in a first-order catchment as interpreted from water level patterns: *Journal of Hydrology*, v. **143**, p. 259 - 277.

Sassner, M., Jensen, K.H., and G., D., 1994, Chloride migration in heterogeneous soil 1: Experimental methodology and results: *Water Resources Research*, v. **30**, no. 3, p. 735 - 745.

Saxena, R.K., 1986, Estimation of canopy reservoir capacity and oxygen 18 fractionation in throughfall in a pine forest: *Nordic Hydrology*, v. **17**, p. 251 - 260.

Shanley, J.B., 1989, Field measurement of dry deposition to spruc foliage and petri dishes in the Black Forest: *Atmospheric Environment*, v. **23**, p. 403 - 414.

Shanley, J.B., 1992, Sulphur retention and release in soils at Panola Mountain, Georgia: Journal of Hydrology, v. *Soil Science*, no. **53**, p. 361 - 382.

Shanley, J.B., and Peters, N.E., 1988, Preliminary observations of streamflow generation during storms in a forested Piedmont Watershed using temperature as a tracer: *Journal of Contaminant Hydrology*, v. **3**, p. 349 - 365.

Shanley, J.B., and Peters, N.E., 1993, Variations in aqueous sulphate concentrations at Panola Mountain, Georgia: *Journal of Hydrology*, v. **146**, p. 361 - 382.

Shriner, D.S., and Henderson, G.S., 1978, Sulphur distribution and cycling in a deciduous forest watershed: *Journal of Environmental Quality*, v. 7, no. 3, p. 392 - 397.

Singh, B.R., Abrahamsen, G., and Stuanes, A., 1980, Effect of simulated acid rain on sulphate movement in acid forest soils: *Soil Science Society of America Journal*, v. **44**, p. 75 - 80.

Sinokrot, B.A. and Stefan, K.G., 1992, Deterministic modeling of streamwater temperatures: Development and applications to climatic change effects on fish habitat: *Antony Falls Hydrologic Lab Report*. No 377, Minn.

Sinokrot, B.A and Stefan, K.G., 1993, Stream temperature dynamics; Measurements and modeling: *Water Resources Research*, v. **29**, no. 7, p. 2299 - 2312.

Skartveit, A, 1982 Wet scavenging of sea-salts and acid component in a rainy coastal area, *Atmos Environ.*, v **16**, 11, p 2715 - 2724

Sklash, M.G., and Farvolden, R.N., 1979, The role of groundwater in storm runoff: *Journal of Hydrology*, v. **43**, p. 45 - 65.

Sklash, M.G., Farvolden, R.N., and Fritz, P., 1976, A conceptual model of watershed response to rainfall, developed through the use of oxygen-18 as a natural tracer: Canadian Journal of Earth Sciences, v. 13, p. 271 - 283.

Sklash, M.G., Stewart, M.K., and Pearce, A.J., 1986, Storm runoff generation in humid headwater catchments : 2 : A case study of hillslope and low-order stream responses: *Water Resources Research*, v. **22**, no. 8, p. 1273 - 1282.

Smettem, K.R.J., Trudgil, S.T., 1983, An evaluation of some flourescent and non-flourescent dyes in the identification of water transmission in soils: *Journal of Soil Science*, v. **34**, p. 45 - 56.

Smith, R.O., 1996, Multiple tracers of shallow groundwater flow and recharge in hilly Loess: *Groundwater*, p. 675 - 682.

Sorey, M.L., 1971, Measurement of vertical groundwater velocity from temperature profiles in wells: *Water Resources Research*, v. 7, no. 4, p. 963 - 970.

Stallman, R.W., 1960, Notes on the use of temperature data for computing groundwater velocity: *Societe Hydrotechnique de France* v **6**.

Starosolszky, O., 1987, *Applied surface hydrology*: Colorado, Water Resources Publications, 821 p.

Startveit, A., 1982, Wet scavenging of sea salts and acid components in a rainy coastal area: *Atmospheric Environment*, v. **16**, no. 11, p. 2715 - 2724.

Stewart, G.L., and Stetson, J.R., 1975, Tritium and deuterium as water tracers in hydrological systems: Water Resources Research Center, University of Massachusetts, Amherst FY-76-2.

Stewart, M.K., and McDonnell, J.J., 1990, Modelling water flow in soils of a steep headwater catchment traced by deuterium: *Water Resources Research*, v. 00, no. 00, p. 00.

Stewart, M.K., and McDonnell, J.J., 1991, Modeling base flow soil water residence times from deuterium concentrations: *Water Resources Research*, v. **27**, no. 10, p. 2681 - 2693.

Swistock, B.R., Yamona, J.J., Dewalle, D.R., and Sharpe, W.E., 1990, Comparison of soil water chemistry and sample size requirements for pan versus tension lysimeters: *Water, Air and Soil Pollution*, v. **50**, p. 387 - 396.

Tanaka, T., Yasuhara, M., and Atsunao, M., 1982, Pulsating flow phenomenon in soil pipe: **8**, no. 33 - 36.

Tate, C.M., and Meyer, J.L., 1983, The influence of hydrologic conditions and successional state of dissolved organic carbon export from forested watersheds: *Ecology*, v. **64**, no. 1, p. 25 - 32.

Thomas, D.L., and Beasley, D.B., 1986, A physically-based forest hydrology model I : Development and sensitivity of components: *Transactions of the American Society of Agricultural Engineers*, v. **29**, no. 4, p. 962 - 972.

Thomas, D.L., and Beasley, D.B., 1986, A physically-based forest hydrology model II : Evaluation under natural conditions: *Transactions of the American Society of Agricultural Engineers*, v. **29**, no. 4, p. 973 - 981.

Tietema, A., Warmerdam, B., Lenting, E., and Riemer, L., 1992, Abiotic factors regulating nitrogen transformations in the organic layer of acid forest soils : Moisture and pH: *Plant and Soil*, v. **147**, p. 69 - 78.

Todd, D.K., 1980, *Groundwater Hydrology*, Ed 2, John Wiley and Sons, 535p

Topp, G.C., and Davis, J.L., 1985, Measurement of soil water content using Time - Domain Reflectometry (TDR): A field evaluation: *Soil Science Society of America Journal*, v. **49**, p. 19 - 24.

Topp, G.C., Davis, J.L., and Annan, A.P., 1980, Electomagnetic determination of soil water content : Measurements in coaxial transmission lines: *Water Resources Research*, v. **16**, no. 3, p. 574 - 582.

Topp, G.C., Yanuka, M., Zebchuk, W.D., and Zegelin, S., 1988, Determination of electrical conductivity using time domain reflectometry : Soil and water experiments in coaxial lines: *Water Resources Research*, v. **24**, no. 7, p. 945 - 952.

Trudgil, S.T., 1986, *Solute Processes*, John Wiley and Sons, 512 p.

Turner, J., Lambert, M., and Holmes, G., 1992, Nutrient cycling in forsted catchments in North East New South Wales : Biomass Accumulation: *Forest Ecology and Management*, v. **55**, p. 135 - 148.

Turner, J.V., Macphersen, D.K., and Stokes, R.A., 1987, The mechanisms of catchment flow processes using natural variations in Deuterium and Oxygen-18: *Journal of Hydrology*, v. **94**, p. 143 - 162.

Unsworth, M.H., 1980, Evaluation of atmospheric inputs: dry deposition of gases and particles in # vegetation, *in 'Methods for studying acid precipitation in forest ecosystems'*:, ed., Ecology, I.o.T. Cambridge, p. 9 - 15.

Vallochi, A.J., 1990, Use of temporal moment analysis to study reactive solute transport in aggregated porous media: *Geoderma*, v. **46**, p. 233 - 247.

Van Breeman, N., 1987, Effects of redox processes on soil acidity: *Netherlands Journal of Agricultural Sciences*, v. **35**, p. 271 - 279.

Van den Berg, J.A., and Ullersma, P., 1994, Ponded infiltration as a cause of the instability of continuous macropores: *Journal of Hydrology*, v. **159**, p. 169 - 186.

Van Genuchten, M.T., 1991, Recent progress in modelling water flow and chemical transport in the unsaturated zone, *in 'Hydrological Interactions between atmosphere, soil and vegetation,*

Vienna, IAHS', p. 169 - 183.

Van Omnen, H.C., Dijksma, R., Hendrickx, J.M.H., Dekker, L.W., Hulshof, J., and Van Den Heuvel, M., 1989, Experimental assessment of preferential flow paths in a field soil: *Journal of Hydrology*, v. **105**, p. 253 - 262.

Van Stempvoort, D.R., Wills, J.J., and Fritz, P., 1990, Aboveground vegetation effects on the deposition and cycling of atmospheric sulphur : chemical and stable isotope evidence: *Water, Air and Soil Pollution*, v. **60**, p. 55 - 82.

Villhoth, I., 1993, Field and numerical investigations of macropore flow and transport processes: Series paper: *Institute of Hydrodynamics and hydraulic engineering*, v. DK-2800, p. 164.

Wagner, G.H., and Steele, K.F., 1985, Use of rain and dry deposition composition for interpreting ground-water chemistry: *Groundwater*, v. **23**, no. 5, p. 611 - 616.

Walker, C.D., and Richardson, S.B., 1994, The use of stable isotopes in water in characterising the source of water in vegetation: *Chemical Geology (Isotope Geoscience Section)*, v. **94**, p. 145 - 158.

Ward, R.C., 1989, *Priciples of Hydrology* (2 ed.), McGraw Hill, 1 v., v. 1, 367 p.

Weyman, D.R., 1970, Throughflow on hillslopes and its relation to the stream hydrograph: *Bull. Internat. Assoc. Sci. Hydrology*, v. **15**, no. 3, p. 25 - 33.

Wheather, H.S., Langan, S.J., Brown, A., Beck, M.B, 1991, Hydrological responses of the Allt A' Mharcaidt Catchment - influences from experimental plots, *Journal of Hydrology*, **123**, p 163 - 199

Whipkey, R.Z., 1965, Subsurface stormflow from forested hillslopes: *Bull. IASH*, v. **10**, no. 2, p. 74 - 85.

Whipkey, R.Z., 1967, Theory and mechanisms of sub-surface storm flow, *in 'Forest Hydrology'*, ed., Sopper, W.E. Oxford, Pergamon, p. 255 - 260.

Whipkey, R.Z., 1969, Storm runoff from forested catchments by subsurface routes: *Floods and their computation, studies and reports in hydrology*, v. **3**, p. 773 - 779.

Whipkey, R.Z., and Kirkby, M.J., 1980, Flow within the soil, *in 'Hillslope Hydrology'*, ed. Kirkby,

M.J., John Wiley and Sons, p. 121 - 144.

Wigington, P.J., Davies, T.D., Tranter, M., Eshleman, K.N. 1990, *Episodic acidificaion of surface waters due to acidic deposition*, Acidic deposition: State of Science and technology, Report 12:200 p., NAPAP

Williamson, D.R., Stokes, R.A., and Ruprecht, J.K., 1987, Response of input and output of water and chloride to clearing for agriculture: *Journal of Hydrology*, v. **94**, p. 1 - 28.

Wilson, C.M., and Smart, P., 1984, Pipes and pipe flow processes in an upland catchment, Wales: *Catena*, v. **11**, no. 2/3, p. 145 - 158.

Wilson, G.V., and Luxmoore, R.J., 1988, Infiltration, macroporosity and mesoporosity distributions on two forested watersheds: *Soil Science Society of America Journal*, v. **52**, no. 2, p. 329 - 335.

Wilson, G.V.J., P.M.; Luxmoore, R.J.; Zelazny, L.W.; Lietze, D.A.; Todd, D.E., 1991, Hydrological processes controlling subsurface transport from an upper catchment of Walker Branch Watershed during storm events: I: Hydrologic transport processes: *Journal of Hydrology*, v. **123**, p. 297 - 316.

Wilson, L.G., 1983, Monitoring in the vadose zone : Part III, *Groundwater monitoring*, p. 155 - 166.

Woolhiser, D.A., Emmerich, W.E., and Shirley, E.D., 1985, Identification of water sources using normalised chemical ion balances : A laboratory test.: *Journal of Hydrology*, v. **76**, p. 205 - 231.

Yokoyama, T., 1993, A temperature analysis of groundwater flow systems in the upper part of the Ashigara Plain, *in 'Tracers in Hydrology'*, ed., Peters, N.E.: Washington, D.C., IAHS Publication, p. 187 - 196.

Yoon, K.S., Yoo, K.H., Soileau, J.M., and Touchton, J.T., 1992, Simulation of sediment and plant nutrient losses by the Creams Water Quality Model: *Water Resources Bulletin*, v. **28**, no. 6, p. 1013 - 1021.

Zaslavsky, D., Sinai, G., 1991, Surface hydrology I: Explanation of phenomena: *Journal Hydraul. Div. Am. Soc. Civ. Eng.*, v. **107**, p. 1 - 16.

Zellweger, G.W., 1994, Testing and comparison of four ionic tracers to measure stream flow loss by

multiple tracer injection: *Hydrological Processes*, v. **8**, p. 155 - 165.

Zimmerman, U., Mumcich, K.O., Roether, W, 1967: Downward movement of soil moisture traced by means of a hydrogen isotope: *American Geophysical Union Monalogue*, V **11**, p 28 - 36

APPENDIX

Solute	Ref stand	No	Mean	St. Dev	St Dev
Conductivity					
	R18	4	11.8	0.3	2.8
	R24	163	11.9	0.7	6.1
	R26	124	7.1	0.5	7.3
	R39	252	11.7	1.0	8.3
	R45	1277	7.4	0.3	4.2
	R46	21	41.5	1.0	2.3
	R48	23	17.0	0.3	1.7
pH (H ueq/l)					
	R18	4	0.4	0.2	61.1
	R24	163	0.5	0.2	48.9
	R26	124	3.0	0.9	30.1
	R39	252	16.6	4.1	24.8
	R45	1277	2.8	1.1	37.9
	R46	21	80.8	4.7	5.8
	R48	23	2.0	0.4	20.2
Alkalinity (ueq/l)					
	R40	771	106.2	1.9	1.8
Ammonium (ppm N)					
	R42	458	0.1	0.0	15.4
	R49	73	0.2	0.0	5.0
Chloride (ppm)					
	R01	31	0.4	0.0	6.8
	R02	582	0.9	0.0	6.0
	R03	354	1.9	0.1	6.3
	R04	196	2.5	0.1	5.6
	R05	9	2.7	0.0	0.0
	R06	47	5.1	0.9	18.3
	R07	36	9.5	0.3	3.6
	R09	15	14.9	1.0	6.8
	R10	41	0.2	0.0	12.5
	R11	27	0.5	0.0	12.5
	R12	22	1.0	0.0	6.0
	R13	15	1.6	0.0	1.3
	R15	9	2.9	1.2	42.9
	R23	9	2.6	0.0	1.4
	R24	297	1.0	0.0	6.1
	R26	187	0.4	0.0	5.3
	R30	158	1.4	0.1	7.8
	R37	597	1.0	0.0	2.9
	R39	25	1.2	0.0	2.6
	R43	23	2.6	0.4	13.4
	R44	456	1.1	0.0	3.6
	R45	38	0.1	0.0	30.0
	R46	2	3.9	0.0	2.0
Nitrate (ppm)					
	R23	9	0.3	0.0	15.3
	R26	187	0.2	0.0	3.8
	R37	597	0.6	0.0	2.5
	R43	23	1.0	0.1	10.6
	R44	456	0.4	0.2	51.2
	R45	38	0.2	0.0	3.8
Sulphate (ppm)					

	R02	582	1.0	0.0	3.6
	R03	354	2.0	0.0	3.0
	R04	196	3.0	0.1	3.3
	R05	9	4.3	0.0	0.6
	R07	36	10.1	0.1	1.1
	R09	15	20.6	0.4	2.0
	R10	41	0.1	0.0	13.3
	R11	26	0.2	0.0	11.0
	R12	22	0.4	0.0	2.8
	R13	15	0.6	0.0	1.2
	R15	9	1.0	0.0	3.2
	R18	98	4.1	0.1	2.5
	R19	205	0.3	0.0	8.8
	R20	46	0.3	0.0	3.0
	R21	4	0.2	0.0	3.1
	R23	9	0.8	0.0	1.4
	R24	297	1.5	0.0	2.8
	R26	187	0.5	0.0	3.8
	R30	158	2.8	0.0	3.4
	R37	597	3.1	0.0	2.3
	R39	25	0.3	0.0	3.1
	R43	23	6.2	0.7	11.6
	R44	456	2.5	0.0	2.9
	R45	38	0.8	0.0	4.1
	R46	2	0.4		0.0
Sodium (ppm)					
	R02	14	0.4	0.0	25.0
	R03	15	0.8	0.0	2.4
	R04	10	1.2	0.0	2.6
	R23	34	1.6	0.0	1.9
	R24	253	0.8	0.0	6.2
	R25	72	0.6	0.1	17.9
	R26	295	0.3	0.0	10.7
	R27	30	0.8	0.0	6.3
	R28	55	12.1	0.6	4.9
	R29	46	19.0	1.7	8.7
	R31	3	24.7	0.7	2.7
	R36	246	7.0	0.3	3.6
	R38	697	0.4	0.0	5.0
	R43	573	3.3	0.1	3.3
	R45	25	0.2	0.0	5.6
	R46	3	0.1	0.0	9.1
	R48	6	1.7	0.0	0.6
Potassium (ppm)					
	R03	15	0.1	0.0	21.4
	R04	10	0.3	0.0	18.5
	R23	34	0.2	0.0	45.0
	R25	72	0.2	0.0	36.4
	R27	30	0.2	0.0	23.5
	R28	55	2.6	0.2	8.2
	R29	46	1.3	0.1	8.7
	R31	3	1.1	0.1	8.9
	R36	246	0.5	0.0	4.4
	R38	697	0.5	0.0	3.9

	R39	13	0.2	0.0	11.8
	R43	573	0.3	0.0	7.7
	R45	25	0.1	0.0	20.0
	R48	6	0.2	0.0	3.2
Magnesium (ppm)					
	R02	14	0.2	0.0	6.7
	R03	15	0.3	0.0	9.7
	R04	10	0.5	0.0	18.4
	R23	34	0.2	0.0	5.6
	R24	253	0.2	0.0	7.6
	R25	72	0.1	0.0	12.0
	R28	55	9.8	0.6	6.3
	R29	46	3.1	0.2	6.9
	R31	3	5.8	0.3	5.8
	R36	246	1.2	0.0	3.6
	R38	697	0.5	0.0	2.8
	R43	573	0.7	0.0	2.7
Calcium (ppm)					
	R02	14	0.5	0.0	2.7
	R03	15	1.0	0.0	1.9
	R04	10	1.4	0.0	2.8
	R23	34	3.1	0.0	2.7
	R24	253	0.9	0.0	5.9
	R25	72	0.7	0.0	9.9
	R26	295	0.3	0.0	9.0
	R27	30	0.3	0.0	7.5
	R28	55	39.9	11.3	28.2
	R29	46	11.6	1.5	12.9
	R31	3	26.1	4.3	16.3
	R36	246	5.1	0.2	3.9
	R38	697	0.4	0.0	3.0
	R39	13	0.2	0.0	4.9
	R43	573	3.3	0.0	2.8
	R45	25	0.2	0.0	3.5
	R46	3	0.5	0.0	3.7
	R48	6	0.7	0.0	1.8
Silica (ppm)					
	R29	46	4.1	0.4	10.0
	R31	3	4.9	0.3	5.8
	R36	246	2.2	0.2	7.6
	R38	697	0.3	0.0	14.4
	R43	573	0.2	0.0	21.9
	R46	3	0.1	0.0	7.0

Storm characteristics: rainfall total (PPT Tot), rainfall duration (PPT Dur), rainfall total in previous week (PPTPW), rainfall total in the initial hour of a storm (PPT1h), season in which the storm occurs (G/D), storms during which samples were collected for chemical analyses.

Date	PPT Tot (mm)	PPT Dur (hr min)	PPTPW (mm)	PPT1hr (mm)	Growing (G) Dormant (D)	Chemistry ?
15 April 1994	42	14 hr 34	7		G	*
3 May 1994	15	10 hr 31	26		G	*
9 June 1994	12	1 hr 57	2		G	*
24 June 1994	13	0 hr 47	4		G	
27June 1994	12	7 hr 02	18		G	*
4 July 1994	175	290 hr 42	35		G	*
10 July 1994	26	3 hr 17	190	3.3	G	
11 July 1994	78	10 hr 45	211	2.0	G	*
12 July 1994	22	3 hr 46	242	1.5	G	
14 July 1994	22	3 hr 40	146	20.6	G	
22 July 1994	32	10 hr 03	9	25.4	G	
27 July 1994	50	16 hr 21	38	16.3	G	
16 August 1994	60	14 hr 39	12	0.3	G	*
21 August 1994	12	5 hr 37	67	2.3	G	
1 Sept 1994	12	2 hr 10	0	7.6	G	
9 Sept 1994	18	6 hr 50	4	2.5	G	
16 Sept 1994	36	36 hr 24	18	6.4	G	*
23 Sept 1994	23	16 hr 39	110	0.5	G	
2 Oct 1994	32	33 hr 17	6	1.3	D	
11 Oct 1994	46	36 hr 13	7	1.0	D	*
13 Oct 1994	11	16 hr 51	55	1.1	D	*
21 Oct 1994	22	1 hr 19	3	50.0	D	
20 Nov 1994	19	12 hr 09	0	0.25	D	
26 Nov 1994	37	29 hr 13	19	0.51	D	
28 Nov 1994	23	4 hr 01	65	10.7	D	
4 Dec 1994	23	20 hr 13	30	0.51	D	
6 Jan 1995	29	5 hr 00	1	0.25	D	
14 Jan 1995	16	16 hr 36	0	0.33	D	*
19 Jan 1995	7	4 hr 02	16	5.80	D	*
27 Jan 1995	17	17 hr 32	8	0.51	D	*
10 Feb 1995	85	26 hr 27	2	0.05	D	*
16 Feb 1995	23	7 hr 00	97	20.8	D	
27 Feb 1995	38	38 hr 16	0	0.76	D	*
8 March 1995	19	9 hr 04	26	1.52	D	
11 April 1995	6	6 hr 21	0	4.57	G	*
19 April 1995	9	3 hr 50	1	0.87	G	*
21 April 1995	17	3 hr 44	9	0.12	G	*
22 April 1995	13	4 hr 04	26	0.87	G	*
23 April 1995	9	10 hr 00	39	0.58	G	*
1 May 1995	12	2 hr 46	0	10.3	G	*

Measure of antecedent moisture conditions: Total rainfall in (a) previous 24 hr (PPW 1d), (b) previous 48 hr (PPW 2d), (c) previous 4 days (PPW 4d), (d) previous week (PPW 7d) and (e) previous 30 days (PPW 30d)

Storm	PPW 1d (mm)	PPW 2d (mm)	PPW 4d (mm)	PPW 7d (mm)	PPW 30d (mm)
09-Jun-94	0	1	2	2	21
24-Jun-94	0	4	4	4	36
27-Jun-94	0	0	14	18	47
04-Jul-94	5	5	5	35	86
10-Jul-94	0	2	10	190	258
11-Jul-94	25	26	30	211	284
12-Jul-94	78	104	107	242	352
14-Jul-94	0	9	136	146	380
22-Jul-94	0	1	1	9	409
27-Jul-94	0	3	5	38	427
16-Aug-94	3	3	12	12	126
21-Aug-94	5	5	5	67	189
01-Sep-94	0	0	0	0	97
09-Sep-94	1	1	1	4	104
16-Sep-94	0	0	0	18	53
23-Sep-94	0	0	3	110	144
02-Oct-94	0	0	0	6	155
11-Oct-94	1	6	7	7	177
13-Oct-94	8	46	55	55	222
21-Oct-94	0	0	0	3	124
20-Nov-94	0	0	0	0	52
26-Nov-94	0	0	0	19	39
28-Nov-94	1	36	37	65	76
04-Dec-94	1	1	1	30	92
06-Jan-95	0	0	0	1	21
14-Jan-95	0	0	0	0	40
19-Jan-95	0	0	0	16	55
27-Jan-95	0	0	0	8	62
10-Feb-95	0	0	1	2	50
16-Feb-95	5	9	9	97	133
27-Feb-95	0	0	0	0	175
08-Mar-95	0	3	23	26	219
11-Apr-95	0	0	0	0	1
19-Apr-95	0	0	0	1	7
21-Apr-95	0	9	9	9	16
22-Apr-95	0	17	26	26	33
23-Apr-95	1	14	31	39	47
01-May-95	0	0	0	0	55

Maximum precipitation intensities (IP) for all storms. Timings and 5 min maximum precipitation intensities are provided for all storms. In storms where several periods of intense precipitation exist (PPTi-iv), all magnitudes and timings are shown.

Storm	No int. periods	1st IP @	5 min PPTi	2nd IP @	5 min PPTii	3rd IP @	5 min PPTiii	4th IP @	5 min PPTiv
9 Jun 94	2	9:50	5.6	11:40	1.5				
24 Jun 94	1	12:20	5.3						
27 Jun 94	2	10:05	3.3	11:40	3.3				
4 Jul 94	4	6:15	1.3	3:45 nd	2.5	9:50 nd	2.3	12:35 nd	2.5
10 Jul 94	1	18:35	4.6						
11 Jul 94	1	17:40	9.9						
12 Jul 94	2	13:50	4.1	14:15	4.3				
14 Jul 94	2	17:05	7.1	19:15	4.1				
22 Jul 94	2	11:05	8.6	14:50	2.5				
27 Jul 94	4	5:40	2.0	6:45	2.5	10:05	2.8	20:00	3.8
16 Aug 94	2	11:55	1.5	12:50	2.0				
21 Aug 94	1	12:30	1.3						
1 Sep 94	2	21:30	5.1	23:25	1.5				
9 Sep 94	3	3:05	0.8	5:40	1.8	6:50	2.8		
16 Sep 94	4	17:35	1.8	1:20 nd	2.3	4:45 nd	2.3	13:15 nd	2.8
23 Sep 94	1	13:10	0.8						
2 Oct 94	1	11:55	1.8						
11 Oct 94	1	10:00	1.3						
13 Oct 94	2	17:25	1.0	4:30 nd	1.0				
21 Oct 94	2	21:40	4.1	6:05 nd	2.3				
20 Nov 94	1	0:15 nd	0.8						
26 Nov 94	2	10:15	1.0	2:55 nd	0.8				
28 Nov 94	1	7:00	3.6						
4 Dec 94	2	9:30	1.8	11:50	2.8				
6 Jan 95	2	17:55	1.5	19:25	3.8				
14 Jan 95	1	9:20	0.8						
19 Jan 95	1	8:10	1.0						
27 Jan 95	1	5:40	1.8						
10 Feb 95	3	17:10	1.8	19:20	1.8	22:40	4.8		
16 Feb 95	2	18:10 nd	4.8	2:15 18Fe	1.0				
27 Feb 95	2	15:45 nd	1.3	22:55 nd	1.0				
8 Mar 95	2	5:25	1.8	5:35	2.5				
11 Apr 95	1	15:30	2.5						
19 Apr 95	1	17:10	1.7						
21 Apr 95	1	5:00	1.2						
22 Apr 95	1	10:50	7.6						
23 Apr 95	1	22:15	1.5						
1 May 95	1	22:05	1.9						

NB 'nd' refers to 'next day'
For storm on 4 July 1994, several periods of rainfall occur, the maximum intensity periods are only included above

STORM	HYDROMETRIC DATA	CHEMICAL DATA
9 June 1994	*	*
24 June 1994	*	
27 June 1994	*	*
4 July 1994	*	*
10 July 1994	*	
11 July 1994	*	*
12 July 1994	*	
14 July 1994	*	
22 July 1994	*	
27 July 1994	*	
16 August 1994	*	*
21 August 1994	*	
1 September 1994	*	
9 September 1994	*	
16 September 1994	*	*
23 September 1994	*	
2 October 1994	*	
11 October 1994	*	*
13 October 1994	*	*
21 October 1994	*	
20 November 1994	*	
26 November 1994	*	
28 November 1994	*	
4 December 1994	*	
6 January 1995	*	
14 January 1995	*	*
19 January 1995	*	*
27 January 1995	*	*
10 February 1995	*	*
16 February 1995	*	
27 February 1995	*	*
8 March 1995	*	
11 April 1995	*	*
19 April 1995	*	*
21 April 1995	*	*
22 April 1995	*	*
23 April 1995	*	*
1 May 1995	*	*

'*' denotes that data was collected

Precipitation and throughfall data: The timings of the onset of precipitation and throughfall are provided together with cumulative totals at both nodes for all storms (PPT Tot and TI Tot, respect.)

Date	PPT Begins@	TI begins@	PPT Tot (mm)	TI Tot (mm)
9 June 1994	9:50	8:55	12	23
24 June 1994	12:15	12:10	13	8
27 June 1994	6:20	5:10	12	23
4 July 1994	5:25	5:55	175	na
10 July 1994	17:25	17:30	26	28
11 July 1994	17:30	17:30	78	68
12 July 1994	11:45	11:50	22	20
14 July 1994	16:30	16:25	22	27
222 july 1994	10:50	10:30	32	37
27 July 1994	5:40	5:45	50	38
16 Aug 1994	7:55	18:10	60	59
21 Aug 1994	10:40	11:30	12	8
1 Sept 1994	21:30	na	12	na
9 Sept 1994	2:55	3:00	18	9
16 Sept 1994	17:30	17:35	36	24
23 Sept 1994	11:45	13:00	23	13
2 Oct 1994	7:50	8:15	32	21
11 Oct 1994	23:25	23:55	46	33
13 Oct 1994	14:25	13:35	11	10
21 Oct 1994	21:35	21:40	22	20
20 Nov 1994	20:10	21:30	19	12
26 nov 1994	4:50	5:05	37	25
28 Nov 1994	6:15	5:55	23	19
4 Dec 1994	2:50	2:25	23	16
6 Jan 1995	13:25	13:50	29	19
14 Jan 1995	5:20	5:20	16	16
19 Jan 1995	8:05	6:25	7	5
27 Jan 1995	15:40	16:00	17	17
10 Feb 1995	1:05	2:05	85	na
16 Feb 1995	18:00	16:40	23	44
27 Feb 1995	13:00	na	38	32
8 March 1995	3:05	3:05	19	12
11 April 1995	15:20	15:30	9	3
19 April 1995	14:20	14:20	9	5
21 April 1995	3:00	3:00	17	na
22 April 1995	8:45	9:15	13	12
23 April 1995	17:45	17:55	9	18
1 May 1995	21:10	21:10	12	6

Lag times between maximum 5 min flow intensites between adjacent nodes

Storm	Res No (min)	PPT-TIig (min)	TI-VI-0ig (min)	TII-15Ig (min)	VI-15-VI-50ig (min)
9 Jun 94	1	5	0	115	
24 Jun 94	1	0	35	0	
27 Jun 94	1	0	-15	5	
	2	0		5	
3 July 94	1	-50	55	170	
	2				
	3	-5	5	5	
	4	5	-10	5	50
	5	0	35	5	15
10 Jul 94	1	-5	10	15	40
	2				
11 Jul 94	1	0		10	85
	2	20			
12 Jul 94	1	5			
	2	0		5	295
14 Jul 94	1	0		10	20
22 Jul 94	1	0		5	-10
	2				
27 Jul 94	1	10		35	70
	2	5		10	35
	3	5		15	20
16 Aug 94	1	50	-50	5	
	2	10		5	
	3		-5		
21 Aug 94	1	5			
	2		0		
1 Sept 94	1		0		
	2		5		
9 Spet 94	1	0	0		
	2	-5	-5		
	3	0	0		
16 Sept 94	1	5	0	10	
	2	0	5		
	3	10	0		
	4	10	0		
23 Sept 94	1	5	0	140	-15
	2	15	-10		
2 Oct 94	1	0	0	25	385
	2	5	5		
11 Oct 94	1	10	-30	25	200
	2	0	0	10	
	3	0	-10	25	50
13 Oct 94	1	15	0	5	115
	2	15	0	60	
21 Oct 94	1	25	0	40	35
	2	20	-5	10	65
20 Nov 94	1	0	0	75	480
	2	0	-35	0	
26 Nov 94	1	15	0	30	115
	2	5	0	25	45
	3	0	5	15	45
28 Nov 94	1	0	0	10	100
4 Dec 94	1	0	0		
	2	45	15	15	50
6 Jan 95	1	0			
	2	0		10	80
14 Jan 95	1				
19 Jan 95	1	0	0	90	
27 Jan 95	1	-25		30	160
10 Fb 95	1				
	2				
	3				
16 Feb 95	1	30		5	
	2	-5			
	3	5		20	
27 Feb 95	1			30	
	2				

8 Mar 95	1	0			
11 Apr 95	1	10	0		
19 Apr 95	1	0		80	
21 Apr 95	1				
	2				
22 Apr 95	1	-25		5	
23 Apr 95	1	-5		70	
	2				
1 May 95	1	5			
	2		0		

where

PPT = rainfall
TI = throughfall
VI-0 = forest floor soil water
VI-15 = 15 cm soil water
VI-50 = 50 cm soil water
PPT-TIlg = time lag between max rainfall and max throughfall intensities
TI-VI-0lg = time lag between max throughfall and max forest floor soil water intensites
TI-VI-0lg = time lag between max forest floor and 15 cm soil water intensities
VI-15-VI-50lg = time lag between max 15 and 50 cm soil water intensities
Res No refers to the no of intense flow periods per storm

Precipitation. forest floor soil water and overland flow data: The timings of the onset of precipitation. forest floor soil water flow and overland flow (OVLF PPT) are provided. together with cumulative totals at both nodes for all storms (PPT Tot and VI-0 Tot. respect.).and total OVLF. calculated using OVLF TI = VI-0 Tot - TI Tot

Date	PPT Begins@	VI-0 begins @	OVLF begins@	PPT Tot (mm)	VI-0 Tot (mm)	OVLF PPT (mm)	OVLF TI (mm)
9 June 1994	9:50	8:20	none	12	8	none	none
24 June 1994	12:15	10:50	none	13	5	none	none
27 June 1994	6:20	8:10	na	12	na	na	na
4 July 1994	5:25	na	na	175	na	na	na
10 July 1994	17:25	15:15	18:10	26	43	17	15
11 July 1994	17:30	na	na	78	na	na	na
12 July 1994	11:45	na	na	22	na	na	na
14 July 1994	16:30	na	na	22	na	na	na
22 July 1994	10:50	na	na	32	na	na	na
27 July 1994	5:40	na	na	50	na	na	na
16 Aug 1994	7:55	na	na	60	na	na	na
21 Aug 1994	10:40	11:10	12:15	12	18	6	10
1 Sept 1994	21:30	21:30	na	12	na		0
9 Sept 1994	2:55	3:00	5:35	18	27	9	18
16 Sept 1994	17:30	17:35	18:05	36	47	11	23
23 Sept 1994	11:45	13:05	14:25	23	27	4	14
2 Oct 1994	7:50	11:10	none	32	31	none	10
11 Oct 1994	23:25	0:00 nd	3:45 nd	46	42	1	8
13 Oct 1994	14:25	14:45	18:00	11	13	1	3
21 Oct 1994	21:35	21:40	22:05	22	43	11	23
20 Nov 1994	20:10	22:45	6:50 nd	19	20	2	8
26 Nov 1994	4:50	7:15	12:20	37	46	9	21
28 Nov 1994	6:15	6:30	7:00	23	33	9	13
4 Dec 1994	2:50	4:50	12:00	23	31	7	15
6 Jan 1995	13:25	na	na	29	na	na	na
14 Jan 1995	5:20	na	na	16	na	na	na
19 Jan 1995	8:05	6:10	na	7	20	13	15
27 Jan 1995	15:40	na	na	17	na	na	na
10 Feb 1995	1:05	na	na	85	na	na	na
16 Feb 1995	18:00	16:10	na	23	na	na	na
27 Feb 1995	13:00	15:40	na	38	na	na	na
8 March 1995	3:05	na	na	19	na	na	na
11 April 1995	15:20	15:15	21:45	9	12	3	9
19 April 1995	14:20	13:20	18:00	9	26	17	21
21 April 1995	3:00	na	na	17	na	na	na
22 April 1995	8:45	7:40	na	13	na	na	na
23 April 1995	17:45	17:05	na	9	na	na	na
1 May 1995	21:10	20:40	21:15	12	16	4	10

where 'na' refers to 'not available' (i.e. missing data)
and 'nd' refers to 'next day'

Precipitation (PPT), 15 cm soil water flow (VI-15) and 50 cm soil water flow (VI-50). Timing of the onset of precipitation and the passage of the wetting front at either depth (i.e. period of rapid flow) are provided, and also any flow prior to this (perhaps macropore flow) is given. Cumulative precipitation (PPT Tot), total 15 cm depth soil water flow (VI-15 Tot) and total 50 cm depth soil water flow (VI-50 Tot) are given.

Date	PPT Begins@	Initial 15 cm flow@	rapid 15 cm flow@	Initial 50 cm flow@	Rapid 50 cm flow@	PPT Tot (mm)	VI-15 Tot (mm)	VI-50 Tot (mm)
4 July 1994	5:25	5:55	18:00	5:45	0:45nd	175	139	41
10 July 1994	17:25		18:40		18:55	26	15	17
11 July 1994	17:30		17:45	drains	17:55	78	7	18
12 July 1994	11:45		12:20	drains	14:25	22	16	16
14 July 1994	16:30		17:10		17:15	22	13	15
22 July 1994	10:50		11:05	11:00	15:05	32	5	6
27 July 1994	5:40	6:15	7:15	6:00	8:10	50	18	30
16 Aug 1994	7:55	8:55	11:45	8:55	14:55	60	30	18
21 Aug 1994	10:40	none	none	12:15	1:10 nd	12	0	0.09
1 Sept 1994	21:30	na	na	na	na	12	na	na
9 Sept 1994	2:55		none	3:40		18	0	0.1
16 Sept 1994	17:30		1:25 nd	17:40		36	2	0.5
23 Sept 1994	11:45		19:00	18:40		23	3	0.01
2 Oct 1994	7:50	na	na	na	na	32	8	0.1
11 Oct 1994	23:25		5:35 nd	0:40 nd	8:50	46	21	24
13 Oct 1994	14:25	15:40	17:20	drains	19:00	11	8	13
21 Oct 1994	21:35		22:10	21:55	22:50	22	7	18
20 Nov 1994	20:10		1:00 nd	21:30	8:15 nd	19	7	6
26 Nov 1994	4:50		10:20	5:50	12:10	37	24	24
28 Nov 1994	6:15		7:05	drains	7:55	23	17	17
4 Dec 1994	2:50		9:45	4:55	12:30	23	14	16
6 Jan 1995	13:25		19:15	18:20	20:05	29	18	13
14 Jan 1995	5:20		9:25	4:55	12:30	16	5	9
19 Jan 1995	8:05		9:25	8:35	17:00	7	2	1
27 Jan 1995	15:40		17:15	17:15	7:45 nd	17	12	10
10 Feb 1995	1:05	9:05	16:50	2:45	18:30	85	71	333
16 Feb 1995	18:00		18:10		18:40	23	48	45
27 Feb 1995	13:00		15:40	17:50	18:30	38	28	22
8 March 1995	3:05		none		none	19	0	0
11 April 1995	15:20		none	16:15		9	0	0.04
19 April 1995	14:20		17:30	16:50		9	0.1	0.06
21 April 1995	3:00		5:20	4:25		17	2	0.07
22 April 1995	8:45		10:55			13	4	0
23 April 1995	17:45		21:50	17:50		9	3	0.05
1 May 1995	21:10		22:20	21:45		12	0.1	0.13

where 'na' refers to 'not available' (i.e. missing data)
and 'nd' refers to 'next day'
and 'drains' refer to where soil waters continue to drain water from previous storms at the onset of the current storm

Lag times of soil waters measured by pan lysimeters VI-15 and VI-50, i.e. the timing between the onset of precipitation and the passage of the wetting front through either depth, and also the lah between the timing of the passage of the wetting front through 15 *cm* and 50 *cm* depths

where
to = timing of onset of precipitation
t1 = timing of the passage of the wetting front through 15 cm (from VI-15 data)
t2 = timing of the passage of the wetting front through 50 cm (from VI-50 data)

Date	(t1 - to) (hr min)	(t2 - to) (hr min)	(t2 - t1) (hr min)
4 July 1994	12 hr 35	18 hr 20	6 hr 45
10 July 1994	1 hr 15	1 hr 30	0 hr 15
11 July 1994	0 hr 15	0 hr 25	0 hr 10
12 July 1994	0 hr 35	2 hr 40	2 hr 05
14 July 1994	0 hr 40	0 hr 45	0 hr 05
22 July 1994	0 hr 15	4 hr 15	4 hr 00
27 July 1994	1 hr 35	2 hr 30	0 hr 55
16 Aug 1994	3 hr 50	7 hr 00	3 hr 10
21 Aug 1994	no flow	no flow	no flow
1 Sept 1994	na	na	na
9 Sept 1994	na	0 hr 25	na
16 Sept 1994	7 hr 55	na	na
23 Sept 1994	7 hr 15	na	na
2 Oct 1994	0 hr 10	na	na
11 Oct 1994	6 hr 10	8 hr 25	3 hr 15
13 Oct 1994	2 hr 55	4hr 35	1hr 40
21 Oct 1994	0 hr 35	1 hr 15	0 hr 40
20 Nov 1994	4 hr 50	12 hr 05	7 hr 15
26 Nov 1994	5 hr 30	7 hr 20	1 hr 50
28 nov 1994	0 hr 50	1 hr 40	0 hr 50
4 Dec 1994	7 hr 55	10 hr 40	2 hr 45
6 Jan 1994	5 hr 50	6 hr 40	0 hr 50
14 Jan 1994	4 hr 05	8 hr 35	4 hr 30
19 Jan 1994	1 hr 20	8 hr 55	7 hr 35
27 Jan 1994	1 hr 35	5 hr 30	3 hr 55
10 Feb 1995	5 hr 45	18 hr 25	2 hr 40
16 Feb 1995	0 hr 10	0 hr 40	0 hr 30
27 Feb 1995	2 hr 40	5 hr 30	2 hr 50
8 March 1995	no flow	no flow	no flow
11 Apr 1995	no flow	no flow	no flow
19 Apr 1995	na	na	na
21 Apr 1995	2 hr 20	na	na
22 Apr 1995	2 hr 10	na	na
23 Apr 1995	4 hr 05	na	na
1 May 1995	1 hr 10	na	na

where 'na' refers to 'not available' (i.e. missing data)

15 cm soil moisture variations during storms

to = timing of onset of precipitation

t1 = timing of onset of rise in soil moisture curve for TDR rods installed at 15 cm depth (i.e refers to the timing of the passage of the wetting front through 15 cm depth)

ran = range in soil moisture status during storm (i.e. ran = peak SMS - SMS at time t1)

A,B,C refer to TDR sites A,B and C (see chapter 3 for location on hillslope plot)

Date	(t1-t0)A (hr min)	(t1-to)B (hr min)	(t1 - to)C (hr min)	ranA	ranB	ranC
4 Jul 1994	1 hr 30	na	12 hr 40	0.07	na	0.03
10 Jul 1994	0 hr 55	na	1 hr 45	0.06	na	0.02
11 Jul 1994	- 0 hr 05	na	0 hr 25	0.04	na	0.032
12 Jul 1994	0 hr 30	na	4 hr 35	0.04	na	
14 Jul 1994	0 hr 35	0 hr 35	0 hr 40	0.04	0.04	0.02
22 Jul 1994	0 hr 15	0 hr 15		0.01	0.06	
27 Jul 1994	0 hr 20	0 hr 50	1 hr 05	0.08	0.05	0.02
16 Aug 1994	2 hr 40	2 hr 50	4 hr 40	0.09	0.09	0.10
11 Oct 1994	3 hr 40	0 hr 55	13 hr 10	0.04	0.04	0.04
13 Oct 1994	1 hr 05	0 hr 05	0 hr 20	0.02	0.01	0.01
21 Oct 1994	0 hr 25	0 hr 25	2 hr 35	0.06	0.03	0.03
20 Nov 1994	2 hr 50	2 hr 55	2 hr 50	0.06	0.03	0.06
26 Nov 1994	1 hr 10	1 hr 35	1 hr 23	0.05	0.03	0.04
28 Nov 1994	0 hr 20	0 hr 15	0 hr 50	0.03	0.02	0.03
4 Dec 1994	7 hr 15	7 hr 40	4 hr 20	0.04	0.03	0.04
14 Jan 1995	0 hr 10	1 hr 40	1 hr 45	0.04	0.03	0.03
19 Jan 1995	1 hr 05	1 hr 05	1 hr 05	0.02	0.01	0.02
27 Jan 1995	0 hr 35	0 hr 30	0 hr 40	0.03	0.03	0.05
10 Feb 1995	2 hr 50	- 1 hr 25	0 hr 25	0.01	0.04	0.06
16 Feb 1995	0 hr 05	0	0	0.04	0.03	0.04
27 Feb 1995	15 hr 35	14 hr 30	15 hr 05	0.04	0.03	0.03

NB storms during which TDR was not in operation have not been included in the table

Matrix soil water flow rates through 15, 40 and 70 cm depths

Flow rates were calculated by dividing the lag time of responses at respective depths by the distance between each depth. i.e. if :

to = timing of onset of precipitation

t1 = timing of the onset of the rise in soil moisture at 15 cm (from TDR data). the flow rate between 0 cm and 15 cm. FT =

$$FT = \frac{(t1 - to)}{z}$$

where z = 15 cm (distance travelled by the water)

Flow rates were calculated for 0 - 15 cm. 15 - 40 cm and 40 - 70 cm.

Where the box is blank. data was not available

'inst' - refers to responses that occur at the same time at all depths

'-ve' - means that water movement was not in a vertical direction. since a lower soil zone experienced increased soil moisture prior to an upper soil zone

A.B.C - refer to TDR sites A. B and C (see chapter 3 for location information)

VI-15, VI-50 = 15 cm and 50 cm depth pan lysimeters

Date	A (0-15)	B (0-15)	C (0-15)	VI-15 (0-15)	A (15-40)	B (15-40)	C (15-40)	VI- (15-50)	A (40-70)	B (40-70)	C (40-70)
3 Jul 1994	0.17		0.02	0.16	0.22		-ve	0.09	0.08	0.20	0.09
10 Jul 1994	0.27		0.14	0.27	1.67		-ve	1.00	0.50	3.00	-ve
11 Jul 1994			0.60	1.50	5.00		-ve	3.50	0.55	-ve	0.36
12 Jul 1994	0.50		0.10	0.43	0.23		-ve	0.28	1.00	1.00	0.19
14 Jul 1994	0.43	0.43	0.38	0.37	inst	5.0		7.00	1.00	3.00	
22 Jul 1994	0.43	1.00		1.00	inst			0.15			
27 Jul 1994	0.75	0.30	0.23	0.17	0.50	0.10	0.03	0.04	0.11	1.20	5.00
16 Aug 1994	0.09	0.11	0.05	0.07	0.25	0.24	-ve	0.18	0.17	0.35	0.08
21 Aug 1994	0.38		0.21	0.12	inst	inst	inst				
11 Oct 1994	0.07	0.27	00.02	0.04	0.08	0.06	-ve	0.18	0.09	0.16	
13 Oct 1994	0.23	3.00	0.75	0.30	0.42	-ve	-ve	0.35	0.40		
21 Oct 1994	0.60	0.60	0.10	0.43	0.71	0.42		0.88	0.04	0.07	
20 Nov 1994	0.09	0.09	0.09	0.07	0.15	0.05	-ve	0.08		0.19	
26 Nov 1994	0.21	0.16	0.19	0.08	0.18	0.29	0.11	0.32	0.33	0.46	0.26
28 Nov 1994	0.75	1.00	0.30	0.30	0.63	0.45	0.28	0.70	0.40		
4 Dec 1994	0.03	0.03	0.06	0.03	0.17	-ve	0.06	0.21	0.27	0.19	0.11
14 Jan 1995	1.50	0.15	0.14	0.06	0.07	0.14	0.05	0.11	-ve	0.46	0.08
19 Jan 1995	0.23	0.23	0.23	0.19		-ve	0.11	0.08			
27 Jan 1995	0.43	0.50	0.38	0.50	0.29	1.00	-ve	0.23	-ve	0.20	
10 Feb 1995	0.09		0.60	0.02	0.05	-ve	0.03	0.35	0.22	0.03	-ve
16 Feb 1995	3.00			1.50	0.83	0.71	1.17	1.17	1.00	inst	
27 Feb 1995	0.02	0.02	0.02	0.09	0.03	0.04	0.21	0.21	0.08	0.14	0.06

all data is in terms of $cm^{-1}min^{-1}$

40 cm soil moisture variations during storms

t1 = timing of onset of rise in soil moisture curve for TDR rods installed at 15 cm depth (i.e refers to the

t2 = timing of onset of rise in soil moisture curve for TDR rods installed at 40 cm depth (i.e refers to the timing of the passage of the wetting front through 40 cm depth)

ran = range in soil moisture status during storm (i.e. ran = peak SMS - SMS at time t2)

A,B,C refer to TDR sites A,B and C (see chapter 3 for location on hillslope plot)

Date	(t2-t1)A (hr min)	(t2-t1)B (hr min)	(t2 - t1)C (hr min)	ranA	ranB	ranC
4 Jul 1994	1 hr 55	na	- 11 hr 30	0.10	0.07	0.10
10 Jul 1994	0 hr 15	na	- 0 hr 35	0.04	0.05	0.3
11 Jul 1994	0 hr 05	na	- 0 hr 10	0.03	0.04	0.04
12 Jul 1994	1 hr 50	na	- 2 hr	0.03	0.03	0.02
14 Jul 1994	0	0 hr 05		0.03	0.04	
22 Jul 1994	0	na		0.03		
27 Jul 1994	0 hr 50	4 hr 10	12 hr 40	0.04	0.04	0.02
16 Aug 1994	1 hr 40	1 hr 45	- 2 hr 10	0.07	0.08	0.04
11 Oct 1994	5 hr 25	7 hr 25	- 0 hr 45	0.05	0.06	0.02
13 Oct 1994	1 hr	- 1 hr 25	- 1 hr 25	0.01	0.02	0.01
21 Oct 1994	0 hr 35	1 hr		0.03	0.04	
20 Nov 1994	2 hr 45	0 hr 55	- 2 hr	0.03	0.05	0.02
26 Nov 1994	2 hr 20	1 hr 25	3 hr 40	0.03	0.04	0.02
28 Nov 1994	0 hr 40	0 hr 55	1 hr 30	0.02	0.01	0.01
4 Dec 1994	2 hr 25	- 0 hr 15	7 hr 15	0.03	0.04	0.01
14 Jan 1995	6 hr 05	3 hr	8 hr 35	0.02	0.03	0.01
19 Jan 1995		- 7 hr 55	3 hr 50		0.02	
27 Jan 1995	1 hr 25	0 hr 25	- 0 hr 55	0.02	0.04	0.02
10 Feb 1995	9 hr 05	- 1 hr 45	13 hr 40	0.06	0.07	0.07
16 Feb 1995	0 hr 30	0 hr 35	1 hr	0.03	0.03	0.01
27 Feb 1995	13 hr	10 hr 40	12 hr 35	0.04	0.02	0.03

NB storms during which TDR was not in operation have not been included in the table

70 cm soil moisture variations during storms

t2 = timing of onset of rise in soil moisture curve for TDR rods installed at 40 cm depth

t3 = timing of onset of rise in soil moisture curve for TDR rods installed at 70 cm depth (i.e refers to the timing of the passage of the wetting front through 70 cm depth)

ran = range in soil moisture status during storm (i.e. ran = peak SMS - SMS at time t3)

A,B,C refer to TDR sites A,B and C (see chapter 3 for location on hillslope plot)

Date	(t3-t2)A (hr min)	(t3-t2)B (hr min)	(t3 - t2)C (hr min)	ranA	ranB	ranC
4 Jul 1994	6 hr 15	2 hr 30	4 hr 45	0.14	0.12	0.10
10 Jul 1994	1 hr	0 hr 10	- 1 hr 25	0.03	0.05	
11 Jul 1994	0 hr 55	- 0 hr 05	1 hr 10	0.06	0.06	0.02
12 Jul 1994	0 hr 30	0 hr 30	2 hr 15	0.03	0.04	0.01
14 Jul 1994	0 hr 30	0 hr 10		0.03	0.01	
22 Jul 1994						
27 Jul 1994	4 hr 25	0 hr 25	0 hr 05	0.04	0.01	0.01
16 Aug 1994	3 hr	1 hr 25	5 hr 05	0.04	0.04	0.02
11 Oct 1994	5 hr 50	3 hr 05		0.04	0.03	
13 Oct 1994	1 hr 15			0.01		
21 Oct 1994	11 hr 35	7 hr		0.02	0.02	
20 Nov 1994	no res	2 hr 35			0.02	
26 Nov 1994	1 hr 30	1 hr 05	1 hr 35	0.03	0.01	
28 Nov 1994	1 hr 15	- 2 hr		0.02	0.01	
4 Dec 1994	1 hr 50	2 hr 40	3 hr 55	0.02	0.01	
14 Jan 1995	- 6 hr 05	1 hr 05	4 hr 55	0.01	0.01	0.01
19 Jan 1995						
27 Jan 1995	- 0 hr 25	0 hr 15		0.02	0.01	
10 Feb 1995	2 hr 15	15 hr 05	- 3 hr 40	0.07	0.03	0.03
16 Feb 1995	6 hr 20	0		0.04	0.05	
27 Feb 1995	- 3 hr 20	3 hr 35	5 hr 55	0.04	0.02	0.02

Evidence for macropore flow at 50 cm depth

to = timing of onset of precipitation
t1 = timing of onset of flow at 50 cm (where flow is detected prior to arrival of wetting front)
t2 = timing of passage of wetting front through 50 cm depth
PPT1hr = total precipitation in 1st hour of the storm
Criteria class = in chapter 4. 3 classes were developed in order to identify whether macropore flow was occurring. Class 3 donated a storm where macropore flow definately occurs. whereas classes 1 and 2 exhibit some of the trends necessary for macropore flow to exist. but its presence can not be detected 100% from hydrometric evidence

Date	(t1- to) (min)	Tot. flow prior to t2 (mm)	PPT prior to t1 (mm)	PPT1hr (mm)	Criteria class
3 Jul 1994	20	0.06			2
10 Jul 1994		0		3.3	0
11 Jul 1994		drains		2.0	0
12 Jul 1994		drains		1.5	0
14 Jul 1994		0		20.6	0
22 Jul 1994	10	0.13	12	25.4	3
27 Jul 1994	15	0.18	7	16.3	3
16 Aug 1994	60	0.20	0.3	0.3	3
21 Aug 1994		0		2.3	0
1 Sept 1994		0		7.6	0
9 Sept 1994	45	0.02	2.5	2.5	3
16 Sept 1994	15	0.06	4	6.4	2
23 Sept 1994		0		0.5	0
2 Oct 1994	75	0.02	10.4	1.3	2
11 Oct 1994	65	0.45	1.5	1.0	1
13 Oct 1993		drains		1.1	0
21 Oct 1994	20	0.45	7.0	20.0	3
20 Nov 1994	80	0.76	0.8	0.3	3
26 Nov 1994	60	0.28	0.5	0.5	1
28 Nov 1994		drains		10.7	0
4 Dec 1994	185	0.04	1.3	0.5	2
6 Jan 1995	30	0.02	5.1	0.3	2
14 Jan 1995	35	0.20	0.3	0.3	2
19 Jan 1995	30	0.04	3.1	5.8	2
27 Jan 1995	95	0.02	7.4	0.5	2
10 Feb 1995	100	0.30	0.1	1.5	2
16 Feb 1995		0		0.1	0
27 Feb 1995	290	0.24	2.5	20.8	1
8 March 1995		0		0.8	0
11 April 1995	55	0.37	4.8	4.6	1
19 April 1995	150	0.06	3.5	0.9	2
21 April 1995	85	0.07	02	0.1	2
22 April 1995		0		0.9	0
23 April 1995	5	0.02	0.6	0.6	2
1 May 1995	35	0.09	3.6	10.3	3

Groundwater response timing and magnitude

to = timing of onset of precipitation

t1 = timing of groundwater response

res = rise in groundwater level (i.e. peak depth - depth at time t1)

'slight' - refers to where a very slight increase in groundwater level is noted (< 1cm)

A,B,C refers to groundwater wells GWA, GWB and GWC (see Chapter 3 for site information)

where a negative value of (t1-t0) is provided, this indicates that groundwater responded prior to precipitation, hence the groundwater still responds to the prior storm

Date	(t1-to)A (hr min)	(t1-to)B (hr min)	(t1-to)C (hr min)	resA (cm)	resB (cm)	resC (cm)
9 June 94	no res	no res	no res	0	0	0
24 June 94	no res	no res	no res	0	0	0
27 June 94	no res	no res	no res	0	0	0
3 Jul 94	3 hr 25	nw	4 hr	1.41		
10 Jul 94	1 hr 15	nw	3 hr	0.29		0.09
11 Jul 94	1 hr 45	nw	1 hr 45	2.01		3.59
12 Jul 94	- 1 hr 45	nw	- 1 hr 45			0.05
14 Jul 94	nw	1 hr 15	1 hr 10		0.03	0.06
22 Jul 94	nw	nw	nw			
27 Jul 94	11 hr 35	23 hr 35	nw	0.01	0.01	
16 Aug 94	3 hr 35	4 hr 20	4 hr 40	0.64	0.44	0.33
21 Aug 94	2 hr 25	3 hr 10	3 hr 35	0.08	0.04	0.03
1 Sept 94	- 10 hr 10	nw	1 hr 10	slight		0.01
9 Sept 94	no res	no res	no res	0	0	0
16 Sept 94	2 hr	2 hr 40	2 hr 50	0.10	0.32	0.29
23 Sept 94	4 hr 35	5 hr 10	1 hr 45	0.25		0.06
2 Oct 94	22 hr 45	nw	24 hr 15	0.29		0.09
11 Oct 94	6 hr 35	nw	7 hr 40	0.32		0.55
13 Oct 94	3 hr 15	nw	12 hr 40	0.11		slight
21 Oct 94	0 hr 45	nw	nw	0.21		
20 Nov 94	7 hr 55	7 hr 45	nw	0.05	0.01	
26 Nov 94	4 hr 15	nw	15 hr 30	0.31		slight
28 Nov 94	- 1 hr 10	nw	nw	0.19		
4 Dec 94	9 hr 15	nores	no res	0.17	0	0
6 Jan 95	6 hr 05	no res	no res	0.32	0	0
14 Jan 95	5 hr 10	nores	nw	0.05	0	
19 Jan 95	5 hr 40	2 hr 35	nw	0.01	slight	
27 Jan 95	14 hr 35	no res	15 hr 30	0.21	0	0.06
10 Feb 95	11 hr 40	nw	nw	0.73		
16 Feb 95	0 hr 25	0 hr 10	3 hr 35	0.19	0.12	0.09
27 Feb 95	16 hr 15	18 hr	26 hr 50	0.05	0.02	0.12
11 April 95	no res	no res	no res			
19 April 95	10 hr 40	no res	no res	0.02		
21 April 95	4 hr 30	no res	no res	0.17		
22 April 95	no res	no res	no res	0.30	0.08	0.10
23 April 95	no res	no res	no res			
1 May 95	no res	no res	no res			

Groundwater response rates and total precipitation prior to groundwater responses

to = timing of onset of precipitation (PPT)

t1 = timing of groundwater response

res = rise in groundwater level (i.e. peak depth - depth at time t1)

Groundwater flow rates, GWrat, is calculated from the following:

$$GWrat = \frac{res}{(t1 - to)}$$

all rates are in terms of $cm^{-1}min^{-1}$

PPP refers to total precipitation prior to (t1)

A,B, C refer to groundwater wells GWA, GWC and GWC (see chapter 3 for site locations)

Date	PPT Tot (mm)	GWratA	GWratB	GWratC	PPPA	PPPB	PPPC
9 June 94	12	no res	no res	no res			
24 June 94	13	no res	no res	no res			
27 June 94	24	no res	no res	no res			
3 Jul 94	175	0.28					
10 Jul 94	16	0.41		0.03	24.4		24.6
11 Jul 94	79	5.03		8.90	44.7		
12 Jul 94	22		0.04	0.40	0		0
14 Jul 94	22		0.01	0.01		20.8	20.6
22 Jul 94	31						
27 Jul 94	50	-ve	-ve		21.6	38.0	
16 Aug 94	60	0.16	0.14	0.07	13.6	21.4	48.5
21 Aug 94	12	0.17	0.02	0.01	9.4	10.2	10.7
1 Sept 94	12	-ve		-ve	0		8.6
9 Sept 94	18						
16 Sept 94	36	0.06	0.11	0.09	20.0	20.6	23.3
23 Sept 94	23	0.14		0.02	10.7	14.9	8.1
2 Oct 94	32	0.10		0.04	21.3		24.1
11 Oct 94	45	0.08		0.13	11.2		14.5
13 Oct 94	12	0.17			6.6		8.9
21 Oct 94	32	0.30			16.5		
20 Nov 94	18	0.01	-ve		18.5	18.5	
26 Nov 94	37	0.09		-ve	16.0		27.4
28 Nov 94	23	0.08			0		
4 Dec 94	24	0.16			7.1		
6 Jan 95	30	0.19			22.4		
14 Jan 95	7	0.02			8.3		
19 Jan 95	7	-ve	-ve		7.4	6.9	
27 Jan 95	18	0.23		0.02	12.7		16.5
10 Feb 95	85	0.19					
16 Feb 95	56	0.38	0.08	0.02	10.4	8.6	14.5
27 Feb 95	38	0.01	0.04	0.01	9.1	10.2	15.6
11 April 95	9						
19 April 95	9	0.01			9.1		
21 April 95	16	0.07			16.6		
22 April 95	13						
23 April 95	8						
1 May 95	11						

Appendix 5.1: Volume weighted mean chloride concentrations in all sequential samples

Storm Date	PPT VWM Cl^-	TI VWM Cl^-	VI-0 VWM Cl^-	VI-15 VWM Cl^-	VI-50 VWM Cl^-
3 May 1994	7.6	15.9	12.6	50.8	14.0
9 June 1994	8.3	38.4	15.4	91.0	37.3
27 June 1994	12.8	11.8	11.0	36.9	15.1
4 July 1994	4.5	1.9	1.4	30.1	7.2
11 July 1994	3.1	3.3	3.4	23.2	5.5
16 August 1994	3.2	8.1	12.1	27.2	4.6
17 September 1994	2.5	5.0	11.2	38.8	3.8
11 October 1994	4.0	1.9	27.9	60.7	3.8
13 October 1994	2.9	5.8	20.7	52.0	5.6
14 January 1995	3.5	15.8	26.8	40.5	49.4
19 January 1995	12.1	25.8	32.3	68.5	50.1
27 January 1995	7.3	16.1	17.6	37.2	56.1
10 February 1995	3.0	15.7	9.3	28.2	59.6
27 February 1995	18.5	29.8	18.2	18.4	36.6
19 April 1995	11.1	90.0	75.0		
21 April 1995	13.2	31.6	40.1	49.5	
22 April 1995	18.0	29.2	26.9		
23 April 1995	17.3	39.8	34.4	31.3	
1 May 1995	5.2	27.5	24.3		

all values reported in μeq/l
PPT = rainfall
TI = throughfall
VI-0 = forest floor soil water
VI-15 = 15 cm soil water
VI-50 = 50 cm soil water

Date	PPT	TI	VI-D	VI-15	VI-50	GQA	GQB	GQCs	GQCd	GQD	SWug	SWlg	VAo	VA15	VA40	VA70	VBo	VB15	VB40	VB70
15 Apr 94	11.1	14.9	14.9	41.5	18.9						32.2	34.2								
3 May 94	7.7	15.8	12.5	50.8	14.5	40.6	47.2	44.8	44.3	33.3	34.4	40.3		25.9	28.5	29.1	27.9	6.5	26.5	35.5
9 Jun 94	8.5	84.5	13.4	92.8	38.6		55	45.7	58.1	51.3			35.8				39.8			36.9
27 Jun 94	14	11.4	11.2	39.9	15.5	69.4						46.8	33.3	66			42.9			
4 Jul 94	4.6	1.8	1.4	29.8	8.3	46.8	48.2	46.3	45.3		6.7	26.9	2	6.7	9.2		3.1	23.7	13.4	18.5
11 Jul 94	3.6	3.4	3.4	23.5	5.5	48.1	47.4	49.8	45.3		31.4	27.6	7.6	8.5	7.5	6.2	9.6	6.2	10.2	12
16 Aug 94	4.4	8.4	12.5	27	4.5	42.6	42.9	46.5	45.1		26.8	32.4	35.3	134	4.5	9.3	34.4	4.8	14.7	10.7
16 Sept 94	2.8	5.2	11.4	38.8	3.8	43.7	52.7	46.5	46.5		35.8	31.8	24.3	15.8	9	15.1	43.4	13.8	12.3	9.9
11 Oct 94	4.4	2.4	30.8	60.8	3.8	39.2	49.1	49.4	45	41.1		48.5	59.5	27.1	11.3	27.4	45.8	29.1	39.5	13
13 Oct 94	2.9	5.8	16.9	51.9	5.6	39.5	47.4	51	47.7	40.3		35.6		52.7	15.5	29.1		18.9	18.1	13.8
4 Dec 94	3.7	16.3	26.8	38.9	39.7	43	49	46.7	46.8	41.5	35.3		25.7	48.3	53.9	44.3	45.7		37.8	36.7
14 Jan 95	10.4	22.6	31.9	70.8	50.3	44.4	48.4	49.5	49.2	42.3	40			51.9	53	42.9		43.3	39.8	38.4
19 Jan 95	7.1	16.7	16.7	37.3	56.1	42.3	48.5	48.8	46.8	40	32.6		16.6	9.9	53.7	27.6	32.7	40		37.4
10 Feb 95	3.4	16.5	9.4	27.6	56.4	38	44.2	50	46.7	39.3	29.1	27.7	30.5	26.6	34.5	20.2	43.7	22.1	29	34.1
27 Fb 95	18.1	30.9	18.6	18.5	36.9	39.6	47.2	49.5	46.7	59	30.3	31.2	26.1		25.7	19.7	33.6	25.9	22.7	33.7
11 Apr 95	19.9	194	67.7				52.7	45.7	45.7	44.6		47.1	185.8				199.7			
19 Apr 95	11	82.6	75					47.1	51.3	41.5		44.3	62				73.6			37.2
21 Apr 95	13.6	26.9	35.7	47.9			52.2	46	47.7	36.4			45.1				49.4			
22 Apr 95	17.6	29.3	25.9	35.8			53	43.7	49.1	38.4		45.6	29.9	18.3	16.4	20.9	42.3	19.5		24.8
23 Apr 95	14.8	38.3	34.4	31.3			49.9	47.1	49.4	37.8			29.9				46.8	22		
1 May 95	4.8	26	22.4									44.1	34.1	10.7	22.6		41.5	22.3		30.5

Date	VC15	VC40	VC70	PE1
15 Apr 94				6.8
3 May 94		22.3	57	3.7
9 Jun 94			66	4.5
27 Jun 94				13.3
4 Jul 94	16	16	3.3	5.6
11 Jul 94	20	20	26.4	3.8
16 Aug 94	15.2	15.2	47.9	3.1
16 Sept 94	17.1	17.1	34.4	0.6
11 Oct 94	31.9	31.9	41.2	21.2
13 Oct 94	29.6	29.6	38.6	
4 Dec 94	45.7	45.7	38.4	2.5
14 Jan 95	34	34	35	9.3
19 Jan 95	35.5	35.5	35.7	
10 Feb 95	25.1	25.1	32	2.4
27 Fb 95	24.7	24.7	32	11.6
11 Apr 95				
19 Apr 95			38.4	13.5
21 Apr 95				
22 Apr 95	25.9	25.9	37.2	
23 Apr 95	27.4	27.4		14.1
1 May 95	33.6	33.6	40	10.2

All concentrations are in μeq/l Cl^-
see thapter 3 for definiation of site equipment

Date	A	B	C	D	E	F	G	H	I	J	K	L	M
15 Apr 1994	12.7	17.2	14.9	9.9	9.3	8.7	5.1						
3 May 1994	16.7	5.1	4.8	2.5	5.6	11.3							
9 June 1994	12.7	7.1	6.8	7.3									
27 June 1994	13.8	9.9	13.5	19.2	10.7	28.5	11.3	14.4	15.8	7.9	8.7		
4 July 1994	16.1	2.5	1.9	2.3	1.1	3.9	4.2						
11 July 1994	4.3	5.9	1.9	1.9	3.4	6.7	6.5	3.1	3.9	1.2	1.2		
16 Aug 1994	12.7	7.6	8.5	6.8	2.8	3.1	2.6	3.1	1.4	2.5	0.8	0.8	
16 Sept 1994	10.4	2.8	2.8	1.9	1.2	2.5	2.3	1.9	2.5	2.5	0.8	2.3	
11 Oct 1994	2.8	5.4	4.8	4.8	5.4	5.1	2.8						
13 Oct 1994	5.4	3.4	3.1	1.9	1.9	2.6	2.5						
14 Jan 1995	11.8	3.7	2.3	1.9	1.4	2.5	1.9						
19 Jan 1995	31.0	12.9	2.5	3.1	2.3								
27 Jan 1995	2.5	9.3	9.9	6.7	8.2	8.5	6.8	5.6					
10 Feb 1995	4.2	0.6	4.5	5.1	2.6	6.2	2.3	3.4	1.9				
27 Feb 1995	49.9	63.4	49.1	23.7	38.6	0.8	1.9	1.7	1.7	1.1	0.5	1.7	1.1
11 April 1995	64.5	8.2	3.7	3.1									
19 April 1995	29.9	9.9	4.2	3.4	4.6								
21 April 1995	50.8	30.5	10.7	5.4	3.9	4.2	1.7	1.4					
22 April 1995	38.6	14.9	11.0	7.3	24.5	9.0							
23 April 1995	27.9	12.1	12.4	21.4	0								
1 May 1995	9.9	5.9	4.2	3.9	0								

all concentrations are in μeq/l Cl^-

Date	A	B	C	D	E	F	G	H	I	J	K	L	M
15 Apr 1994	38.9	19.5	15.8	13.8	14.7	18.6	20.3	13.5	11.2	9.8	8.5	4.8	4.2
3 May 1994	15.7												
9 June 1994	51.0	37.8	29.6	19.7									
27 June 1994	14.1	9.3	12.7	9.3									
4 July 1994	1.9	1.7	1.2	1.2	1.4	2.8	1.1	2.8	2.3	2.3			
11 July 1994	8.7	5.6	5.1	1.7	1.9	4.5	3.9	3.1	2.3	1.4	1.4	1.4	
16 Aug 1994	38.4	18.6	11.3	7.1	5.4	3.9	4.2	2.5	2.8	2.5	1.7	2.3	
16 Sept 1994	27.1	12.4	4.2	4.5	2.5	15.3	5.4	2.5	1.7	1.4	1.4	1.4	0.9
11 Oct 1994	5.4	0.6	0	3.7	5.6	5.7							
13 Oct 1994	6.2	5.4											
14 Jan 1995	20.0	19.5	9.3										
19 Jan 1995	38.3	14.4	14.9										
27 Jan 1995	24.5	16.6	9.0										
10 Feb 1995	50.8	37.5	3.4	1.9	3.4	2.4							
27 Feb 1995	72.8	44.3	27.0	8.2	1.9								
11 April 1995	163.3	224.7											
19 April 1995	114.2	51.0											
21 April 1995	57.0	49.4	25.1	14.4	15.8								
22 April 1995	39.1	28.8	23.7	24.8									
23 April 1995	46.5	38.1	30.2										
1 May 1995	42.0	18.6	17.5										

all concentrations are in µeq/l Cl^-

Chloride concentrations in sequential forest floor soil water (VI-0)

Date	A	B	C	D	E	F	G	H	I	J	K	L	M	N	O	P	Q	R	S	T	U	V	W	X	Y	Z
15 Apr 1994	195	54	195	161	144	144																				
3 May 1994	206	138	116	116	104	99	93																			
9 June 1994	166	124	118	138	169	169	183	141																		
27 June 1994	115	118	121	131	121	76	110	73	155	118	107	158	149	87	59	68										
4 July 1994	17	14	17	14	23	14	17	17	14	17	13	14	17	17	13	17	14	12	12	14	17	12	12	12	12	08
11 July 1994	05	42	16	19	19	17	17	17																		
16 Aug 1994	420	195	96	76	59	56	73	56	90																	
16 Sept 1994	287	197	85	107	91	82	166	143	82	51	17	19														
11 Oct 1994	510	423	298	181	107	99	200																			
13 Oct 1994	209																									
14 Jan 1995	110	226																								
19 Jan 1995	319																									
27 Jan 1995	226	158	118																							
10 Feb 1995	293	192	87	6	59	54	56	48	48	71																
27 Feb 1995	463	214	113	82	56																					
11 April 1995	677																									
19 April 1995	750																									
21 April 1995	488	226																								
22 April 1995	288	231																								
23 April 1995	344																									
1 May 1995	276	172																								

all concentrations are in mg/l Cl⁻

NB for storms from April 1994 - 11 July 1994, all samples were collected at site VI-0a, 2m downstream of hillslope plot
but for all storms occurring after 11 July 1994, all samples were collected from site VI-0, at the hillslope plot

Appendix 5.6 Chloride concentrations in sequential 50 cm soil waters (VI-50)

Date	A	B	C	D	E	F	G	H	I	J	K	L	M	N	O	P	Q
15 Apr 1994																	
3 May 1994	15 8	13 3															
9 June 1994	38 6																
27 June 1994	15 5																
4 July 1994	14 1	9 6	10 2	9 3	8 2	7 9	7 1	7 3	8 2	7 6	6 5	6 5	6 2	5 4			
11 July 1994	9 0	5 4	5 1	3 9	4 2	3 7	3 1	2 7									
16 Aug 1994	6 5	3 9	3 7	4 5	4 5	3 9	4 2	5 4	4 8	4 2	4 2						
16 Sept 1994	5 6	3 3	3 9	3 7	3 7	3 1	2 8	3 4	4 5	3 7	4 2						
11 Oct 1994	10 9	3 1	2 5	0 5	2 5	2 8	2 8	3 1	3 4	3 1	3 1	2 8	3 4	3 9	5 9	5 6	5 1
13 Oct 1994	5 1	5 6	5 6	5 6	5 9	5 4											
14 Jan 1995	51 9	51 3	49 4	49 1	47 4	49 1											
19 Jan 1995	53 2																
27 Jan 1995	54 1	55 3	56 1	58 7	55 6	56 7	56 4										
10 Feb 1995	43 9	68 8	71 6	72 7	70 5	71 1	67 8	66 5	67 1	66 0	65 9	44 3	32 1	36 4	43 5		
27 Feb 1995	35 2	39 5	38 4	38 6	36 7	38 1	38 1	37 8	37 8	36 7	36 1						

all concentrations are in μeq/l Cl^-

Date	A	B	C	D	E	F	G	H	I	J	K	L	M	N	O	P	Q	R	S	T	U
15 Apr 1994	46.8	46.3	41.5	39.2	36.4	37.2	33.6	35.3	30.7	30.7	29.6	22.3	22.9	26.3	28.8	31.0	36.1	40.6			
4 July 1994	49.4	43.7	33.8	35.5	28.2	22.8	23.7	21.1	20.0	21.4	20.3	20.6	23.7	27.4	32.4	29.2	25.9	23.2	18.9	13.3	14.9
5 July 1994	23.7	26.3	27.9	29.3	24.3	23.7	21.7	25.1	27.6	28.8	30.7										
10 July 1994	42.9	42.0	31.3	17.2	19.7	27.4	27.6														
11 July 1994	40.0	35.5	31.6	31.0	22.8	19.5	11.3	9.6	10.9	10.4	10.4	12.7	16.4	21.7							
16 Aug 1994	62.0	42.8	40.6	22.6	14.1	19.7	18.6	21.2	30.7	40.0											
16 Sept 1994	46.3	43.4	40.0	41.7	29.0	41.7	42.0	36.4	20.0	16.4	10.2	8.5	12.7	34.4	42.0						
11 Oct 1994	44.8	34.4	24.8	32.7	37.8	38.6	37.8	34.4	35.5												
10 Feb 1995	44.6	42.3	36.4	29.0	25.4	21.1	18.6	17.5	19.7	22.8	26.5	29.3	31.3								
27 Feb 1995	43.4	40.3	29.6	27.1	23.7	23.7	30.5														
21 April 1995	47.4	45.9	38.6	42.0																	
22 April 1995	47.1	42.3	45.7	47.4																	
1 May 1995	46.5	43.9	41.7																		

all concentrations are in μeq/l Cl^-

Date	Time	AT	TFT	VT15	VT40	VT70	GT1	GT2	GT3	GT4	GT5	GT6	GT7	GT8	STlg	STug
4 Jul	5 25	20 0	21 7	34 4	21 1	20 0	na	16 5	16 1	na	15 8	15 4	15 0	na	na	na
10 Jul	17 25	27 2	25 3	34 8	21 4	20 6	na	17 0	16 6	16 5	16 0	na	15 1	na	na	22 0
11 Jul	13 05	27 3	25 1	34 7	21 6	20 7	na	17 3	16 6	16 5	16 1	15 7	15 2	na	19 7	20 7
12 Jul	11 45	27 5	na	34 5	21 6	21 1	na	16 7	16 0	16 0	15 6	15 4	15 2	na	19 5	19 8
14 Jul	16 30	27 3	na	22 5	21 7	21 4	na	17 0	16 3	16 2	15 9	15 5	15 2	15 1	19 7	19 8
22 Jul	10 50	29 5	25 8	22 6	22 1	na	17 9	18 1	17 0	16 8	16 4	15 9	15 4	15 2	19 6	19 5
27 Jul	5 45	22 7	20 0	22 5	22 0	na	18 0	18 4	17 2	17 0	16 6	16 0	15 6	15 3	19 3	20 4
16 Aug	7 55	20 9	20 8	22 2	21 9	na	na	18 1	na	17 5	17 0	16 6	16 1	15 7	19 2	20 9
21 Aug	10 40	26 3	25 0	22 0	21 8	na	na	18 2	na	17 6	17 1	16 8	16 2	15 8	19 6	20 4
1 Sep	21 30	21 2	23 2	22 6	21 8	na	na	na	17 8	17 8	17 4	16 9	16 4	16 0	19 6	22 5
9 Sep	2 55	16 5	19 3	20 6	20 4	na	na	na	na	17 8	17 5	16 9	na	16 1	18 5	19 3
16 Sep	17 30	24 9	26 1	22 7	22 1	na	na	na	na	na	na	na	na	na	19 4	22 0
23 Sep	11 45	16 9	19 8	20 9	21 3	na	na	na	na	na	na	na	na	na	17 9	17 6
2 Oct	7 50	16 7	20 9	20 2	20 2	na	na	na	na	na	na	na	na	na	17 8	19 0
11 Oct	23 25	10 1	10 8	16 3	17 2	na	na	17 1	17 6	17 6	17 4	17 1	16 8	16 4	15 3	11 1
13 Oct	14 25	14 8	14 3	15 1	15 8	na	na	17 7	17 6	17 6	17 3	17 1	16 8	16 4	16 2	16 3
21 Oct	21 35	16 5	18 5	17 3	16 6	na	na	17 1	17 3	17 4	17 2	17 1	16 8	16 4	16 9	16 7
20 Nov	20 10	13 8	14 6	14 8	14 8	na	na	na	16 6	16 6	16 6	na	16 6	16 4	14 9	13 7
26 Nov	4 50	7 2	7 4	11 8	12 6	na	na	15 9	16 5	16 5	16 6	16 6	16 6	16 4	12 3	7 8
28 Nov	6 15	13 0	12 6	11 6	12 2	na	na	na	na	16 5	16 5	na	16 5	16 4	13 5	14 4
4 Dec	1 50	12 8	12 8	11 3	11 4	na	na	15 6	16 3	16 3	16 3	na	16 4	16 3	13 3	14 2
6 Jan	13 25	3 8	1 2	6 3	7 4	na	na	14 3	na	15 3	15 5	15 5	15 8	15 7	8 6	2 8
14 Jan	5 20	17 8	17 1	10 8	10 0	na	na	14 0	na	15 2	15 1	15 4	15 5	15 5	12 6	12 7
19 Jan	8 05	10 5	10 11	10 1	10 3	na	na	13 6	14 6	15 1	15 0	15 2	15 3	15 4	11 5	10 1
27 Jan	15 40	9 4	10 2	7 4	7 9	9 5	na	13 8	14 4	14 9	14 8	15 0	15 2	15 1	10 4	5 3
10 Feb	1 05					na	na									
16 Feb	18 00	21 2	19 7		na	na	na	13 0	14 2	14 4	14 2	14 5	14 7	14 8	9 8	13 1
27 Feb	13 00	18 6	18 2	9 9	9 4	na	na	12 6	14 0	14 1	13 9	14 2	14 4	14 5	10 8	13 0
8 Mar	3 05	17 4	16 5	12 7	11 5	na	na	12 9	13 8	14 0	13 8	14 1	na	14 3	13 1	13 2
11 Apr	15 20	23 2	22 4	16 7	15 6	na	na	14 2	14 0	14 1	14 2	14 4	14 4	14 5	15 8	19 1
19 Apr	14 20	24 2	24 6	16 7	15 8	14 9	na	na	14 2	14 3	14 3	14 5	14 5	14 5	16 5	20 7
21 Apr	3 00	19 7	18 9	17 3	16 4	15 2	na	na	14 3	14 4	14 4	na	14 5	14 5	15 7	18 6
22 Apr	8 45	15 5	17 3	17 1	16 6	15 5	na	14 7	14 3	14 4	14 4	na	14 5	14 6	15 5	17 6
23 Apr	17 45	20 1	na	na	na	na	na	na	na	na	na	na	na	na	15 9	17 8
1 May	21 10	na	na	na	na	na	na	na	na	na	na	na	na	na	na	na

Where

AT	= Air temperature
TFT	= Throughfall temperature
VT15	= 15 cm Soil temperature
VT40	= 40 cm Soil temperature
VT70	= 70 cm Soil temperature
GT1-8	= Groundwater temperatures at depths of 2 12, 2 29, 2 44, 2 59, 2 74, 3 35, 3 96 and 4 57 m below land surface
STlg	= Streamwater temperature at lower gage
STug	= Streamwater temperature at upper gage